U.PORTO
FEUP FACULDADE DE ENGENHARIA
UNIVERSIDADE DO PORTO

Assessing the Performance of Electric Buses: a Study on the Impacts of Different Routes

Deborah Perrotta de Andrade

Thesis submitted under the framework of the
MIT Portugal Program "Engineering Design and
Advanced Manufacturing" for the degree of
Doctor of Philosophy in Leaders for Technical Industries

Supervisor: Prof. Dr. João Luiz Afonso

Co-supervisor: Prof. Dr. Rosaldo J. F. Rossetti

January, 2015

“Wyrd biõ ful ãræd.”

Bernard Cornwell

Acknowledgements

I would like to thank my supervisors Professor João Luis Afonso and Professor Rosaldo Rossetti for their guidance throughout this thesis, not only for the great brainstorming ideas but also for the life lessons I learned from them. Their availability, interest and open-minded attitude allowed me to perform a research following my own directions. I would also say thank you to Professor Christopher Zegras, who besides welcoming me in his research group at the MIT has always supported my research and my ideas. I would thank Bernardo Ribeiro as well, from CEIIA, and José Costa, from CaetanoBus, whose advices were of great relevance in the development of this research. Moreover, I thank my colleagues from LIACC, especially José Macedo, Guilherme Soares and Zafeiris Kokkinogenis for their crucial help and support, and also Professor Jorge Freire for his partnership and share of experiences in the bus operation sector. I would also like to thank the Portuguese Foundation for Science and Technology for my 4-year granted scholarship, without it this research would never be possible.

In addition, Alexandra Monteiro undoubtedly deserves my full appreciation both for the high level of efficiency regarding administrative/bureaucratic issues and for our epic conversations ranging from French movies to Star Wars. This certainly made my trajectory easier and more pleasant to be done. I would also like to thank my dearest friend Pouya Samani for all the great time we spent together, for all the laughs, gossips and conversations we had along these years. At last but not least, I thank my friends André Camboa for his partnership along the development of this research, Miguel Vieira for his seasonal check-up Gmail chats and amazing mood and Filipe Nascimento, whose calm and wise attitude are of great value in such a turbulent period.

I want also to thank my family, which although far away from me, has always made themselves present in my life as if there was no distance between us.

Above all, I must thank Bruno Martins for the patience, caring, devotion, wisdom and great ability to make me laugh, especially during the last months, in which I was really anxious and could hardly cope with myself. More than a boyfriend, he is a life partner for the good and for the bad moments, and crucial for the accomplishment of everything in my life. Also important is to thank Morgana and Luna for the funniest and cutest moments ever.

Abstract

In order to effectively assess the potential benefits of implementing a public transport solution based on electric buses, it is imperative to assess not only the performance of their powertrain, but also their interaction with the traffic flow influencing their routes. The idea is to propose an integrated simulation framework to support the assessment of electric buses which accounts for these two perspectives.

As for the correct representation of the electric bus operation, a mathematical model of an electric bus dynamics is developed, considering its motor specifications and energy storage device (lithium-ion batteries). To model traffic interactions within different bus services, a microscopic simulator was integrated to the bus simulation model, allowing for a more realistic representation of the routes regarding network topography, number of stops, distance between stops and traffic.

Experiments were developed as a way to demonstrate the applicability of this platform. Some case studies were analyzed based on real bus routes in the city of Porto, Portugal. Others were made with routes to be implemented in Boston for the new project of Bus Rapid Transit, resorting to real data to model traffic.

Keywords: electric bus; traffic simulation; integrated simulation platform; electric vehicle simulation.

Resumo

De modo a poder avaliar os potenciais benefícios da implementação de uma solução de transporte público baseada em autocarros eléctricos, é imperativo avaliar não só o desempenho do sistema de propulsão, mas também a interação com o tráfego que acaba por influenciar as rotas. A ideia é propor uma plataforma integrada de simulação que suporta a avaliação de autocarros eléctricos e engloba ambas as perspectivas.

Quanto à correta representação da operação do autocarro eléctrico, um modelo matemático da sua dinâmica é desenvolvido, considerando as especificações do motor e do dispositivo de armazenamento de energia que utiliza (baterias de lítio). Para modelar as interacções com o tráfego para cada rota do autocarro, um simulador microscópico foi integrado ao modelo de simulação do autocarro, permitindo a representação mais realista das rotas, relativamente à topografia do terreno, ao número de paragens, à distância entre as paragens e ao tráfego circundante.

Experimentos foram executados de forma a demonstrar a aplicabilidade desta plataforma. Alguns estudos de caso foram realizados tendo como base rotas reais de autocarros na cidade do Porto, em Portugal. Outros foram realizados com rotas a serem implementadas em Boston para o novo projeto dos *Bus Rapid Transit*, sendo neste caso, considerados dados reais para modelar o tráfego.

Palavras-chave: autocarro eléctrico; simulação de tráfego; plataforma de simulação integrada; simulação de veículos eléctricos.

Table of Contents

List of Figures

List of Tables

List of Abbreviations

API	Application Programming Interface
BRT	Bus Rapid Transit
BYD	Build Your Dreams (manufacturer company of electric buses)
CEIIA	Center for Innovation and Creative Engineering
CUBE	Suite of software products for transportation planning. Citilabs©
DEIR	Draft Environmental Impact Report
DEIS	Draft Environmental Impact Statement
DLR	German Aerospace Center
DRACULA	Dynamic Route Assignment Combining User Learning and microsimulAtion
DUA	Dynamic User Assignment
EPFL	École Polytechnique Fédérale de Lausanne
EU	European Union
EV	Electric Vehicle
FEUP	Faculdade de Engenharia da Universidade do Porto
GUI	Graphical User Interface
HHI	Hyundai Heavy Industry
HLA	High Level Architecture
ICE	Internal Combustion Engine
IDE	Integrated Development Environment
IEEE	Institute of Electrical and Electronics Engineers
ITS	Intelligent Transportation Systems

LPA	Locally Preferred Alternative
Matlab	MATLAB, The Language of Technical Computing. Mathworks©
MBTA	Massachusetts Bay Transportation Authority
MIT	Massachusetts Institute of Technology
OMT	Object Model Template
RDEIR	Revised Draft Environmental Impact Report
ROW	Right-of-Way
RTI	Run-Time Infrastructure
SI	International System of Units
Simulink	Simulation and Model-Based Design. Mathworks©
SL6	Silver Line Gateway
SOC	State-of-Charge
STCP	Sociedade de Transportes Colectivos do Porto
SUMO	Simulation of Urban MObility Traffic Simulator
TAZ	Traffic Assignment Zone
TOSA	Trolleybus Optimisation du Système d'Alimentation
TraCI	*SUMO* Traffic Control Interface
V&V	Verification and Validation

Chapter 1

Introduction

1.1 Contextualization

Despite an overall reduction in emissions of greenhouse gases since the Kyoto Protocol was signed, surpassing this agreement objectives and on the track to satisfying the European Union (EU) target for 20% reduction in 2020 (from 1990), the transportation domain was the only sector that suffered an increase in greenhouse gases emissions from 1990 to 2012, with a value of 14%. Transportation share in total emissions was approximately 24% in 2012, as it can be seen in Figure 1.1 (European Comission 2014). Inside the transportation sector, road transport accounts for an astonishing 94%, urging for improvements in this source of emissions.

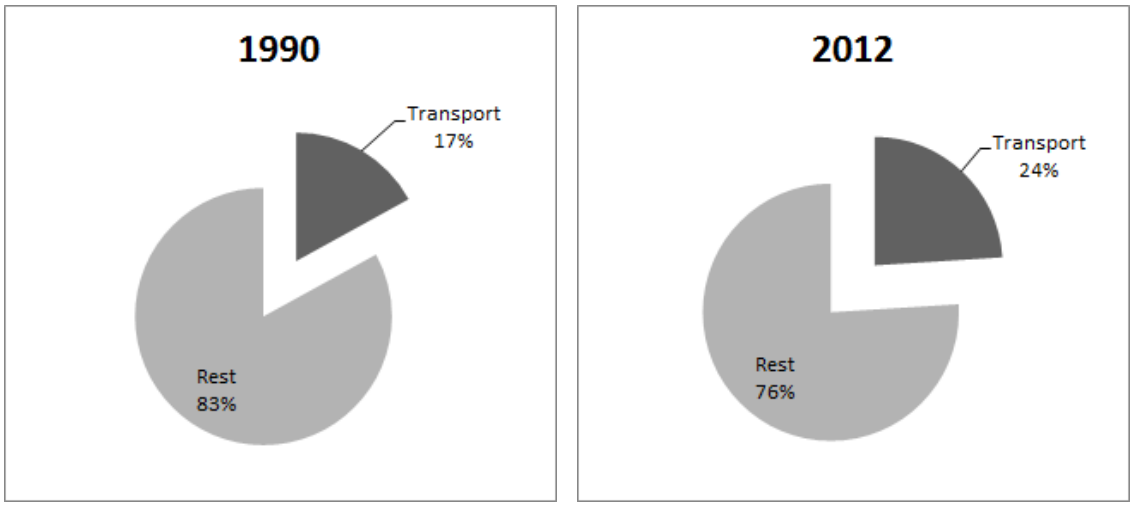

Figure 1.1 – Transportation greenhouse gases emissions share in 1990 and 2012, adapted from (Eurostat 2014)

Electric vehicles play an important role in tackling this problem, once they are characterized for having zero tailpipe emissions. However, the implementation of private electric vehicles alone, despite the obvious improvements in pollution (air and sound), does not bring advantages for the urban chaos that big cities are facing. In larger cities, travel times have suffered a high pace increase and one of the main reasons was the fast

growth of vehicle registrations until 2007. Fortunately, since then this number has been falling (The International Council of Clean Transportations 2013).

Generally speaking, if the trend prevails regarding the increase of the world population and consequently the number of trips, it is expected especially for Asian countries the increase on the number of private motorized vehicles, driven by their fast economic development. This will impact greatly on the number of trips made by this mode of transportation, expected to be almost 80% of the total number of trips by 2025. In developed countries, such as North America and Australia, most of the trips are already made by private motorized vehicles (Pourbaix 2012). In France, private cars account already for two thirds of daily journeys, specially due to the independence they bring (Pierre et al. 2011). In this sense, promoting awareness of the population and investments in public transport are of high priority.

Another factor that goes against a sustainable urban development is the impact of private cars on the consumption of land in space/time terms (land consumption in square meters per hour) (Camagni 2002). Research carried out in the Paris region showed that the private cars consume 94% of road space/ hour, whereas buses consume 2.3%; in other words, a bus in movement consumes 24 times less space per passenger than a single car (Servant 1996).

Moreover, one can say that public transportation is a crucial part of the solution to a country's economic, energy, and environmental challenges, contributing to bring a better quality of life. A correct implementation reduces emissions, provides affordable options to personal mobility alternative to driving, and reduces congestion costs. In general, public transportation is crucial for the development of high-density cities, once less land would need to be used for parking and travel lanes (Federal Transit Administration 2010). Moreover, incentives can be applied as a tool to promote the use of public transportation system (e.g. fare price decrease) and/ or discourage the use of private cars during peak hours, by rewarding commuters who goes to work at alternative times (Kokkinogenis et al. 2014).

However, incentives and investment on conventional city buses – equipped with internal combustion engine – do not seem alone to be an adequate attempt at solving all the aforementioned issues. On the other hand, electric buses emerge as a more comprehensive solution to solve both the air pollution issue — due to the absence of tailpipe emissions — as well as the "urban chaos" problem. Buses, generally speaking, are characterized for

promoting a door-to-door service, which cannot be achieved by the deployment of other transportation solutions such as trolleys, subways or trains.

Electric buses also have plenty of other positive aspects. The electric engine causes far less vibration throughout the vehicle, which increases the life and reduces maintenance requirements of the bus, making it a cost-effective option for operators. Another quality associated with electric buses is their reduced noise. They are quieter than regular internal combustion engine buses, promoting higher comfort for those onboard. Although the initial introduction of an electric transport system and fleet can be costly, as a long-term mode of public transport they are surprisingly cost-effective (Unger et al. 2010).

By taking all this into consideration, the Portuguese company *CaetanoBus* worked on two full-electric bus prototypes and launched them in 2010 for a testing phase. Taking advantage of this milestone for Portugal, the Portuguese development center *CEIIA* (Center for Innovation and Creative Engineering) has created the *MobiBus* project, whose objective is to conceive, develop and test an integrated solution for the energy management in public urban transportation. This thesis is developed under the framework of the *MobiBus* project.

1.2 Problem Statement and Research Questions

Based on the initial problem analysis promoted in the previous section, it is clear that improvements in emissions ascribed to the transportation sector, especially to road transport are imperative. Despite all efforts to reduce emissions, the transportation sector is falling behind, and electric buses seem to represent a plausible part of the solution for decreasing greenhouse gases emissions in the road transportation sector, besides the benefits stemming at traffic reduction.

The main problem that is posed to the adoption of electric buses on a large scale is to transform them into a viable solution. Although there are already electric buses in circulation in some countries, there are still concerns regarding whether they can promote the same autonomy as conventional internal combustion engine buses. Therefore, it is relevant to evaluate if there is a real need for them to provide this similar autonomy.

In this sense, the work developed in this thesis intends to answer on a first approach the following research question:

RQ1: How to transform electric buses implementation into a viable solution for cities?

The answer to this question will hopefully counteract the greatest mistrust regarding this mode of operation, in an attempt to raise awareness of buses operators for the benefits of electric buses in first place, and not for their limitations. However, the limitations should be taken into consideration as well, thus generating the second research question:

RQ2: Are there ways to simulate electric buses operation in order to extract the most of the batteries limited energy range?

By answering this second research question, it is intended to create a holistic solution for the implementation of electric buses. By working on the bus energy limitation and demonstrating what to do to get the most advantage from it, it will corroborate the important role electric buses can play in the future.

1.3 Related Work and Scientific Gap Identification

In a way to answer the proposed questions, a research was held in the existing literature to assess how other researchers have approached this topic. Firstly, in order to be able to simulate the electric bus operation, there are mathematical equations governing their behavior. Once those equations are defined, then they may be applied to a piece of software of choice to perform the calculations. The simulation of electric vehicles is an interesting and economic solution to evaluate performance of this type of vehicle, once it can predict its behavior without the need to build a physical prototype and/or put it to run in every desired scenario.

1.3.1 Electric Vehicles Mathematical and Simulation Models

Some articles focus on the mathematical equations that govern the vehicle behavior. Usually, those equations are related to the dynamics of the vehicle and are equivalent to what is used for calculating parameters for conventional internal combustion engine (ICE) vehicles. For instance, Ehsani et al. (1997) have developed an electric vehicle system design to satisfy a set of requirements, such as rated speed and the time to achieve it, and maximum speed. Because the intent was not to evaluate urban performance, no driving cycle was used as basis and all calculations are performed without the use of simulation software.

In general, the existing literature is focused on simulation models to analyze an electric vehicle behavior based on standard driving cycles (speed profile along time). Jinrui et al. (2006) have developed a simulation model in *Simulink* (Mathworks 2012) for an electric vehicle equipped with supercapacitors instead of batteries. All calculations are performed based on a driving cycle. Using a slightly different approach, Xu (2011) has proposed a

procedure for matching electric vehicle (equipped with batteries) parameters using a commercial simulator coupled with *Simulink*, being the latter responsible for the energy management control system. The calculations are also based on standard driving cycles.

Similarly, Xiaohua et al. (2008) have used a commercial simulator to access parameters matching for electric buses. Beijing standard driving cycle was used as basis to perform the simulations. Those simulation results were supposed to provide an academic foundation to be used in the development of real electric buses in China. Yu et al. (2012) have also used a commercial simulator to perform parameter matching for electric vehicles powertrain, with the objective to determine the transmission shift control design for better efficiency. Once again, standard driving cycles were used; moreover, simulation results were further tested in experiments.

Using a similar though more complete approach, Butler et al. (1999) have developed a simulator for conventional ICE, hybrid and full-electric vehicles using the *Simulink* platform. The simulation in all cases is held over standard driving cycles and results range from fuel consumption to vehicle emissions and acceleration performance accordingly.

Presenting a different approach, Maia et al. (2011) have implemented an extension in the traffic simulator *SUMO* (Krajzewicz et al. 2002) to simulate electric vehicles. The mathematical equations that govern the vehicle dynamics, together with the battery modeling were applied as one module in *SUMO*, while the altitude values were implemented in another module to transform *SUMO* in a three-dimensional simulator. By making use of a traffic simulator, they simulated the bus both in standard driving cycles and in a real route. The model also takes into consideration the regenerative braking, which is approached in the next section. This work represented the first attempt to simulate electric vehicles in real routes.

1.3.2 Regenerative Braking

At this point, it is relevant to highlight the importance of regenerative braking when simulating electric vehicles. Regenerative braking can be described as the ability of the electric motor to work as a generator whenever the vehicle is braking, allowing the energy to flow back into the batteries. This is an extremely important characteristic, once it increases the autonomy of the electric vehicle. It is easy to qualitatively describe the benefits from regenerative braking, but a much more difficult analysis is required to quantify these benefits.

Wicks and Donnelly (1997) analyze the upper limit of the benefit of regenerative braking on a municipal bus, which is a heavy hybrid vehicle with a certain driving cycle. They assume an ideal regenerative braking system in the form of a flywheel, which can be defined as having 100% charge/discharge efficiency and not representing any additional weight on the vehicle. The paper shows how the power for the cycle was calculated, but the methodology they used to quantify the potential energy to be recovered from regenerative braking was not completely revealed.

Other papers that have regenerative braking as the main subject are focused on how to obtain the optimal efficiency of energy regeneration, once this is a very difficult matter, due to complex road conditions and the high sensibility of the converter to lose power. Huang et al. (2008) state that different control strategies, such as maximum regenerative power control, maximum regenerative efficiency control and constant regenerating current control are usually put forward. However, there is the need for optimizing the control strategy so as to improve the entire vehicle efficiency. Thus they propose a solution to overcome this issue, namely the definition of a control strategy with algorithms, but the amount of energy that can be recovered on braking episodes is not calculated.

Cikanek and Bailey (2002) also propose a detailed description of the regenerative braking algorithm along with simulation results from a dynamic model of a hybrid vehicle, exhibiting the regenerative braking performance. Again, the focus is on the efficiency with which the vehicle is capable of absorbing the energy from braking, and not on the quantification of such an amount.

Lin et al. (2001) propose an integrated simulation tool of a hybrid vehicle and its further use for energy management control algorithms. They use a commercial simulator for simulating the dynamics of the vehicle and integrate it with *Simulink* to further develop the control algorithms. Hence, the focus is primarily on the energy management control algorithms, such as (Grbovi et al. 2011), who discussed modeling and control aspects of the regenerative controlled electric drive using the supercapacitor as energy storage and emergency power supply device.

After presenting this review, it could be noticed that there is a lack of evidence in the literature reporting on tools and methods to precisely evaluate the performance of electric buses in urban settings. Tools that would allow for the correct representation of the routes to be performed, possessing elements such as bus stops, traffic lights, interactions with other vehicles and topography of the field are not available as easily. In addition, a tool

that would also calculate some performance measures from the vehicles' point of view, such as the required energy to perform the route and the potential of recovering energy on braking episodes is also of paramount importance.

1.4 Research Approach

In order to effectively assess the potential benefits of implementing a public transport solution based on electric buses, it is imperative to assess not only the performance of vehicle itself for each specific route, but also its interaction with the traffic flow influencing these routes. In this sense, this thesis presents an integrated simulation framework to support the assessment of electric buses accounting for all those perspectives.

Starting with the correct representation of the electric bus operation, a mathematical model of an electric bus dynamics is developed, considering motor specifications and its energy storage device. This mathematical model was further translated to *Simulink*, so that the calculations to be performed were made in an automatic manner. To model traffic interactions, a microscopic simulator was integrated to the *Simulink* model, which allows for an appropriate model of the environment, especially regarding network topography, considering a three-dimensional model of links, number of stops and distance between stops.

By associating the electric bus simulation model with a traffic simulator, the realistic representation of any route the bus is supposed to perform can be easily done. This allows for a detailed performance analysis focused on specific routes or even a set of routes. When talking about planning routes for buses, a bus transportation company assigns routes with the aid of a decision-support system, taking into account various factors including, for instance, the maintenance state of each bus, its type (standard, articulated, double deck) and other characteristics, such as low floor, wheelchair access, and so forth. Moreover, the bus can perform the same route all day long or make different ones, either intercalated with long stops at the depot out of peak hours or working continuously.

In the specific case of electric buses, it is very important to take some other factors into consideration. One of these is the total energy of the batteries that can be provided for the buses. The energy consumption is not linear, which means that the topography profile of each route plays a huge influence on the electric bus performance and autonomy. In this sense, it is intended with this integrated platform to provide a tool for bus operators to evaluate the performance of an electric bus fleet immersed in their cities, which could not be done if the electric bus simulator would not be integrated with a traffic simulator.

Figure 1.2 shows the rationale applied to this thesis resulting in the research approach proposed, represented by an interpretation of the traditional scientific method.

1.5 Thesis Synopsis

This section intends to present the organization of this thesis work into its different chapters and a brief description of their contents.

1.5.1 Chapter 1: Introduction

This chapter starts with a brief contextualization of the environment, which originated the problem statement and the research questions. Moreover, related work research is shown and the corresponding identification of the scientific gap, leading to the development of the research approach and the dissertation synopsis.

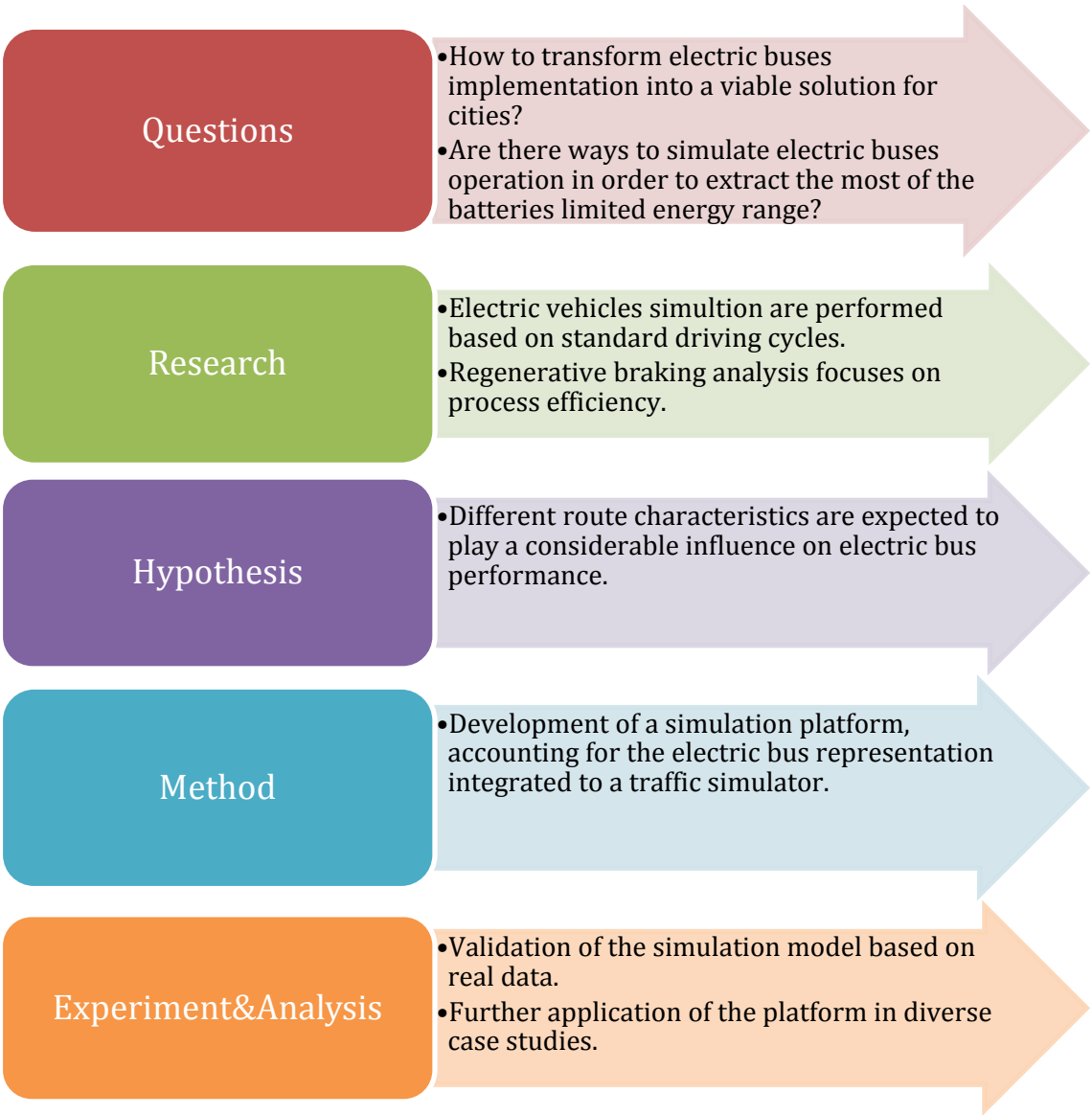

Figure 1.2 – Scientific method implementation on the research approach used in this thesis

1.5.2 Chapter 2: Electric Buses Technology

An extensive research about the state of the art of electric buses around the world is presented, especially regarding their technical specifications and implementation success. Since this is a PhD program in "Leaders for Technical Industries", it is also expected an approach considering a sense of business. Chapter 2 was developed so that this is taken into consideration, with a thorough analysis of competitors and their respective business models.

1.5.3 Chapter 3: Development of the Electric Bus Simulation Model

The simulation model for the electric bus is presented in this chapter, regarding the mathematical equations for its dynamics and the battery modeling. Moreover, the translation of these mathematical equations to *Simulink* is also presented, together with the logics associated with it.

1.5.4 Chapter 4: Development of the Simulation Integrated Platform

The chosen traffic simulator *SUMO* is presented, accounting for its characteristics and how it works. In addition, the previously developed electric bus simulation model is integrated via HLA (high-level architecture) to *SUMO*, and a brief description of this integration method is presented.

1.5.5 Chapter 5: Simulation Model Calibration and Validation

In this chapter, the electric bus simulation model is calibrated and validated based on data collected from the real bus. A sensitivity analysis is held as a way to define the validity of the simulation model for a range of the unobservable parameters.

1.5.6 Chapter 6: Case Studies

This chapter presents a set of case studies performed with the integrated simulation platform. The first set of case studies concern Portuguese scenarios, where real bus routes in Porto were simulated and analyzed regarding energy consumption and regeneration. The second set is based in the Boston scenario, where the implementation of a BRT electric bus fleet is evaluated and differences in performance according to traffic load are analyzed.

1.5.7 Chapter 7: Conclusions

Main conclusions of this PhD work, limitations, further development and future work are presented. The key contributions to the scientific community are also discussed.

Chapter 2

Electric Buses Technology

2.1 Summary

The main aim of this chapter is to present the history of buses as a public mode of transportation and their further electrification, evolution along time and the state-of-art of the current electric buses around the world. Some focus is given to the *CaetanoBus* model, its technical specifications and how the acquisition of data is performed. Moreover, a brief discussion is held on the advantages of electric buses when compared to other electric means of transportation of the same "class", like trams and trolleybuses.

2.2 The History of Public Vehicles and Their Electrification

On the seventeenth century, more specifically in 1661, Blaise Pascal invented what can be considered the first public transport in the world: a system of horse-driven cheap public transport for Paris (lately known as omnibus). Pascal had the authorization of King Louis XIV to open five routes to the Palais du Luxembourg, with fixed schedules. The use of the five lines began on March 18th, 1662 and the basic route used to cost the same as a pound of meat (Manière 2011; Blackburn 2005). However, it could not be sustainable. Parliamentarians were involved since the beginning and due to their noble privileges they could not bear the possibility of sharing the transport with less wealthy people. Thus the company collapsed after 15 years (Manière 2011).

Omnibuses only appeared again in 1826, in Nantes. A young man called Stephen Bureau envisioned transporting the employees of his grandfather, who used to be a ship-owner, from their offices in the rue Jean-Jacques Rousseau to the Customs services in the district of Salorges.

At the same time, in the same city, Stanislas Baudry, a colonel of Napoleon's army, owns a flour mill in the district of Richebourg. To make a better use of the steam plant, he decided to create a bathhouse next to it. Therefore he had the idea of opening a regular transport to bring people from the center of Nantes to his establishment. Soon he realizes that his

transmission line is being used for personal purposes of the Nantais (people from Nantes) and thus he gets the permission from the municipality of Nantes to open the first regular bus line. He expands his activity in Paris from January 30, 1828 by inaugurating the "l' Entreprise Générale des Omnibus". The success is immediate, being the omnibus much cheaper than cabs (Manière 2011). These early buses carried up to fourteen passengers. By 1836, there were 16 omnibus operators in Paris, covering 35 routes (Rodrigue 2014).

The innovation was carried to London in 1829 by George Shillibeer. He had seen this kind of operation while working in Paris in 1825 assisting the assembly of the world's first omnibus. These first buses (Figure 2.1) carried twenty-two passengers and newspapers and magazines were provided free of charge. Soon Shiilibeer was taking £100 per day, and his buses spread all around London (Knowledge of London 2014).

Figure 2.1- One of Shillibeer's first Omnibuses (Knowledge of London 2014)

The North American experience with the omnibus proceeded at a faster pace. Abraham Brower, a Manhattan stagecoach operator created the first omnibus venture in the United States. Omnibuses were oversized stagecoaches that ran along a fixed route. They could carry fifteen passengers seated, although people usually tried to get in anyway (New York Transit Museum 2014). The innovation was soon adopted elsewhere, for example, in Philadelphia and Boston in the 1830s and Baltimore in the 1840s.

In the meantime, the early nineteenth century brought technological advances regarding the development of the first form of electrochemical batteries, being the Italian Alessandro Volta responsible for demonstrating that energy could be stored chemically, in 1800. Later in 1821, Faraday used Volta's battery in his experiment for demonstrating the principles of the electric motor (and generator), improving his discovery by demonstrating in 1831 the electromagnetic induction phenomena. This has built the bridge between electric

currents and magnetism, giving the first steps into electric vehicles motor/generator requirements (Høyer 2008).

During the efforts to improve battery technology and recharging in the late 1800s, a new technology arouse: regenerative braking. It was firstly demonstrated in Paris in 1897, where the ability of the electric motor to work as a generator, charging the batteries when the vehicle would run downhill was presented. Since then, regenerative braking became standard equipment already in the first electric vehicles of the eighteenth century (Westbrook 2001).

The invention of the electric traction motor created a revolution in public urban travel, being the trams and the trolleybuses approached here. It is important to point out the difference between both of them. Trams are vehicles that run on fixed rails whereas trolleybuses are equipped with rubber tires; they are both fed by electricity through overhead wires. Tram is the term used in Europe and sometimes is confused with trolleys, which is the American term (Veasey 2014; Courtenay 2014). Their main differences can be observed in the pictures of Figure 2.2.

Figure 2.2– Examples of a tram on the left (Veasey 2014) and a trolleybus on the right (Hutchinson 2005)

In 1881, Werner von Siemens, founder of the *Siemens* company, invented the world's first electric rail-less vehicle "*Elektromote*", powered by an overhead contact line. It travelled at a speed of 30 km/h and carried a total of 20 passengers. The next years of research were dedicated to further development of the rail systems, making the rail-less vehicles implementation to be postponed to 1901 (Siemens 2014).

Meanwhile, the first electric tram line opened in 1888 in Richmond, USA, being its operating speed three times higher than that of horse-drawn vehicles. Tram corridors

attracted commercial activities and “fostered a rapid residential development” (Rodrigue 2014).

There is a third (and less widespread) type of public electric vehicle called cable cars, which were invented in 1873 to climb the hills of San Francisco, USA. Unlike trams and trolleybuses, cable cars have no motor onboard and run on steel rails with a slot between the tracks where an underground cable runs at a continuous speed (Market Street Railway 2014).

Trams and trolleybuses are since then largely used in the current world, and together with rail lines and subways, dominate the electric-traction public transportation. It was only in the end of 2010 that the first autonomous (i.e., rail-less and catenary-less) 100% electric bus was presented to the world, being the Seoul Government responsible for unveiling their innovative all-electric commercial service, surpassing other nations attempts (Singh 2010). More details about the vehicles they use and other electric buses that have been or currently are in operation around the world are presented on the next subchapter.

2.3 Electric Buses in Operation Worldwide

Electric public transportation is not a recent technological advance, as it was presented previously. However, whether not counting on rails and catenaries, then it could be considered a modern development. The most curious aspect of that is that autonomous private vehicles had their golden age in the beginning of the nineteenth century, following the advances on the battery technologies but the issue of translating this to higher-scale vehicles was not tackled. One strong reason for that can be the problems that even today are faced on battery development: to provide a long-lasting vehicle operation and fast charging.

Nowadays, batteries are getting efficient to the point that allows their use in electric buses, which are composed of a really large battery pack to provide energy for a whole day of operation, or at least to a certain point where the bus could stop for recharge. In the previous section, the Korean electric bus was mentioned as the first one in the world to be used commercially. On the other hand, shortly before that, more specifically in 2008, the Chinese bus manufacturer Ankai[1] provided full electric buses for the Beijing Olympic Games, hence becoming the first register of electric buses to be used on large scale (Yin 2007).

[1] (Anhui Ankai Automobile Company Ltd. 2014)

Another Chinese bus manufacturer, perhaps the world's largest is *BYD*[2], which first full-electric bus was developed in January, 2010, and that now manufactures buses for many cities around the globe.

China is certainly the pioneer on electric buses technology, keeping until the recent days a large share of this market. However, other large players have been having prominence, such as the American *Proterra* and their innovative fast-charge bus, and the Portuguese *CaetanoBus* that specialized in retrofitting former diesel buses to full-electric and also are one of the major players for airport buses.

On the next subsections, electric buses manufacturers and their respective models are presented.

2.3.1 *Hyundai Heavy Industry* and *Hankuk Fiber Group*

Korean *Hyundai Heavy Industry* (*HHI*)[3] and *Hankuk Fiber Group*[4] companies have united their efforts to come up with the electric bus for the Seoul Government in 2009, which model is called *e-Primus*. The bus is approximately 11 m long, low floor, and its body features a carbon-composite material, which is both lighter and resistant. It can carry 47 passengers plus the driver, and it weighs 10,720 kg. Figure 2.3 depicts the manufactured bus in its final form.

Regarding technical aspects, *e-Primus* is equipped with a 240 kW motor and can achieve a maximum speed of 100 km/h. Lithium-ion polymer batteries are its energy storage device, having a capacity of 87 kWh. The driving distance for one charge is 100 km while maintaining an average speed of 40 km/h. The batteries can be fast-charged in thirty minutes. *e-primus* has also a regenerative braking system, being able to save energy and recovering it back to the batteries when running downhill (Choi 2012).

The first five buses have started their operation in 2010 and the Seoul government intends to replace the other 14 buses of this specific fleet by electric buses soon. Investments are being made on the assembly of two other battery charging stations to provide a better service. This is part of a master plan of the Seoul government to have 50% of the whole bus fleet composed by electric buses by 2020 (Loveday 2010).

[2] (BYD - Build Your Dreams 2014)
[3] (HHI 2014)
[4] (Hankuk 2014)

Figure 2.3– *e-primus* electric bus model from *Hyundai Heavy Industry* and *Hankuk Fiber* (Loveday 2010)

2.3.2 Anhui Ankai Automobile Co., Ltd.

As previously mentioned, *Ankai* has provided a batch of six electric buses to be used at the 2008 Beijing Olympics, as those games had as motto being green. Those buses were equipped with lithium-ion batteries of a maximum power of 150 kW. These batteries provided more than 200 km autonomy after a 7-hour charge. By then, there was a great concern on producing those electric buses in high quantities, due to the bottleneck on batteries technology (Yin 2007).

In the beginning of 2012, *Ankai* has established the Chinese record of 110,000 km of continuous operation mileage for their pure electric buses, being the total mileage breaking the 8 million kilometers while transporting more than 5 million passengers. Despite their indirect relation to an electric bus (manufactured by its partner *Shanghai Leibo*) that caught fire in 2012 (Loveday 2011b), *Ankai* is seen as a trustworthy bus manufacturer, due to its large experience and lowest operation failure rate. By 2012, the bus fleet was composed of 700 units covering 20 Chinese cities (Chinabuses 2012).

In October, 2014, this company has presented its fifth generation of electric buses, bringing several technological advances. The new bus has an aluminum body structure and is equipped with the intelligent battery management system *e-control*. It has autonomy of 350 km in normal conditions but is capable of achieving 500 km. This model can save 10% of energy compared to the previous, making it one of the strongest competitors in China (Chinabuses 2014).

Ankai has three electric bus models on its product line, which basically differ on capacity of passengers carried. The smallest of those is the model *HFF6700BEV*, able of caring 16 +1 people seated (16 passengers plus the driver) and weighs 6,500 kg. It is 7 m long, equipped with lithium-ion batteries with a capacity of 200 Ah at 500 V and a drive motor manufactured by *Ruihua*[5]. The maximum speed this bus can achieve is 100 km/h. The intermediary model is the *HFF6123G03EV-2*, being 12 m long and having the ability to carry 38 + 1 people seated. The drive motor manufacture is *Siemens*, and the battery capacity is more than the double compared to the smaller bus: 480 Ah at 624 V. This model weighs 18,000 kg and can reach a maximum of 70 km/h.

The most recent model is entirely made "in-house", which means that the drive motor manufacturer is *Ankai* itself. The bus model is the *HFF6101K10EV* and it can carry 45 + 1 + 1 people seated (the extra 1 supposedly accounts for the driver companion). This bus model weighs 16,000 kg and is approximately 11 m long, a little shorter than the previous. Its lithium battery has a capacity of 585 Ah at 538 V, representing 22% more than the previous. Due to the fact that this bus is a model for long trips, its maximum speed is 100 km/h instead of 70 km/h. Figure 2.4 shows *Ankai*'s three electric bus models exterior and interior pictures (Anhui Ankai Automobile Company Ltd. 2014).

Figure 2.4– *Ankai*'s different electric bus models: exterior and interior pictures (Anhui Ankai Automobile Company Ltd. 2014)

2.3.3 *Build Your Dreams* (*BYD*)

The Chinese company *Build Your Dreams* (*BYD*) is the largest supplier of rechargeable batteries worldwide, and has the largest market share for other battery-related products.

[5] (Yueqing Ruihua Cabinet & Whole Set Equipment Co. Ltd. 2014)

Their branch *BYD Auto* (created in 2003) has become one of the most relevant electric vehicles players in China, being in specific their electric buses adopted in many countries. The company was founded in 1995 with 20 employees and has been since experiencing a major success, having nowadays 150,000 employees divided into 10 manufacturing plants across China and offices in different continents, such as Europe and North America (BYD - Build Your Dreams 2014).

In 2010, their first electric bus model called *K9* has made its way out of the factory to a test phase. Later in 2012, Shenzen has increased its already existent electric vehicle fleet (bus + taxis) from 500 to 2000, being all the 1300 electric buses bought from the *BYD K9* model; it is relevant to mention that *BYD* had (and still has) a factory there (Times 2012). Shorter before, in 2011, *BYD* expanded its activities to Europe by signing a letter of intent with the Frankfurt government to introduce three electric buses in the city, as part of their master electric mobility plan (Loveday 2011a). Also in 2012, *BYD* has signed an agreement with the Finish transportation company Veolia[6] to put in operation the *K9* for three years, as a way to access its performance on the extreme climate conditions of Finland (RealLi Research 2012).

Last year, *BYD* officially delivered 6 electric buses to the city of Schiermonnikoog, and the Netherlands' first National Park in the province of Friesland, Netherlands. The buses are 12 meters long, have an autonomy of 250 km per charge, and can accommodate 60-70 passengers, comparable to the buses already in operation there (BYD 2013b). A couple of months later, *BYD* managed to get the largest European contract for electric buses, which will be used to serve the Amsterdam Schiphol Airport, in the Netherlands. The contract comprises 35 full-electric buses and a 10-year operating support contract as well (BYD 2013a). Also in 2013, two 12-meter bus models were handed over in London to be used in the city, servicing two existing bus lines. Should the performance of those buses meet London's requirements, *BYD* could be providing more buses soon (Transport News Brief 2013).

BYD has also managed to spread its power over the United States (US), especially after Warren Buffet has invested $230 million for a 10% stake of the company in 2008 (Crippen 2008). Thenceforth, the Los Angeles headquarter was established in 2011 and already signed its first letter of intent for the American office with the major of Windsor, Ontario. This letter comprised up to 10 12-meter electric buses for using in this city, representing a milestone for Canada and the US for being the first place where long range electric buses

[6] (Veolia Transport Finland Oy 2014)

would be put in use, once Transit Windsor has the unique distinction of running between both countries through Detroit (BusinessWire 2012).

Concerning electric bus models, *BYD* has different sites according to their commercial area, being the European and the American focused in here. The European *BYD* website for their electric buses comprises five different models, basically differing on their sizes: 8 m, 10.2 m (double-deck), 10.8 m, 12 m and 18 m. The American website has only one model, which is the 12-meter size electric bus. The 12-meter model has four different sub-models, according to the number of doors and/or battery pack it carries: 2 doors/ 3 battery packs (2D3B), 3 doors/ 2 battery packs (3D2B), 3 doors/ 3 battery packs (3D3B) and 3 doors/ 3 battery packs for right-hand drive (33RH).

All models are equipped with a proprietary lithium-iron battery technology, and they allegedly declare as being the first on using it to power electric buses in the world. The general energy consumption of the buses is 130 kWh/100 km in urban conditions, being the batteries fully charged after around 5 hours. Bus autonomy is up to 250 km, which is higher than their competitors. The specifications of the different electric bus models are presented in Table 2.1.

Table 2.1– *BYD* electric bus models and their specifications

Model / **Spec**	**8 m**	**10.2 m**	**10.8 m**	**12 m**				**18 m**
Sub-model	NA	NA	NA	**2D3B**	**3D2B**	**3D3B**	**33RH**	NA
Nº Passengers	57	81	78	68	85	68	60	125
Nº Seats	22	54	26	31	27	26	29	38
Weight (kg)	13,000	19,000	18,000	19,000	19,000	19,000	18,000	30,000
Motor Power (x 2 kW)	90	150	90	90	90	90	90	150
Battery Energy (kWh)	183	320	320	324	216	324	324	480
Charging Power (x 2 kW)	40	100	40	30	30	30	40	100
Charging Time (h)	2	1.5	4	5.5	3.5	5.5	4	3
Range (km)	220	200	220	250	160	250	250	220

BYD is proud of their design and their flexibility to customize the electric bus models according to the clients' requirements. Figure 2.5 shows some pictures and conceptual designs of the different electric bus models exterior and interior appearance. The recently launched 18-meter model is considered the world's largest battery electric vehicle. It is an

articulated bus, manufactured in the *BYD* American plant at Lancaster after a 2-year development; the bus model is called *Lancaster e-bus* due to this fact (BYD 2014).

2.3.4 Proterra

Proterra is an American company founded on 2011 that produces exclusively battery electric buses. Their first generation of buses is called *EcoRide35™* and is the world's first heavy duty, fast-charge battery electric bus. This bus' batteries can be fully charged in less than 10 minutes and it is able to recover up to 90% of the available kinetic energy of braking episodes.

The *EcoRide35* is nearly 11 m long and can carry up to 60 passengers. It is powered by a *UQM PowerPhase150*[7] electric propulsion system that produces peak torque of 650 N.m and peak power of 150 kW. There is no information about the weight of this bus, although *Proterra* has mentioned that its composite structure is 20-40% lighter than the conventional steel bus. The batteries are manufactured by *Altairnano*[8] and are of lithium-titanate technology, where titanium is the material for the cathode and anode, and can tolerate high power when charging (Jandt 2010).

The prototype was tested in the beginning of 2009 at the streets of Los Angeles, California (Barz 2009). Later in 2010, *Proterra* delivered three buses to the Los Angeles County's Foothill Transit to service regular commuters. These buses were bought together with two induction fast-charge stations and could operate for 3 hours with a single charge of 10 minutes (Yoney 2010).

In 2014, *Proterra* has launched its new 40-foot (12 m) 100% electric bus called *Catalyst™*, being the other model "discontinued". This new model is lighter than other buses of this category (12 m), with a curb weight of approximately 12,500 kg. They claim this new bus is more efficient than its predecessor and it could provide a reduction of 81,600 kg of CO_2 equivalent greenhouse gases compared to a natural-gas bus. It can carry up to 77 passengers, it is also equipped with *Altairnano* lithium-titanate batteries and the body material is made of a lightweight, fiberglass balsa wood (Proterra 2014). Table 2.2 shows the specifications for each model and Figure 2.6 shows pictures of both models.

Proterra only sells to the US so far, and is really proud of using 40% of the materials from American companies as a way to foster the local economy. They have a total of 56 *EcoRide™* models and 4 *Catalyst™* running for 10 different clients. *Proterra* faces quite a hard competition from *BYD*, which as previously presented, has many of their electric

[7] (UQM Technologies 2014)
[8] (Altairnano 2014)

buses running in the US. However, they have the advantage of a 24/7 operation with their really fast-charge technology, which is pioneer in the world.

Table 2.2- *Proterra* electric bus models and their specifications

Model / Spec	EcoRide35™	Catalyst™
Size (m)	11	12
Nº Passengers	60	77
Nº Seats	NA	40
Curb Weight (kg)	NA	12,500
Gross Weight (kg)	NA	17,700
Motor Power (kW)	150	220
Charging Time (min)	10	5
Range (h)	3	3

2.3.5 Solaris Bus & Coach

Solaris Bus & Coach is a Polish company founded in 1994 that sells bus, coach, trolleybus and trams. In 2011, they launched their first bet on the electric buses world: the *Urbino 8.9 LE electric*. This model is customizable to the point of adjusting the charging system of the bus to an operator's or city's infrastructure and also the battery pack size. Due to its small structure, it can run through narrow streets. This bus can take up to 29 passengers seated, it carries lithium-ion batteries and can be equipped with a 120 kW or 160 kW motor. It comes with a standard ventilation system, being the air conditioning an extra option (Solaris Bus & Coach SA. 2014).

The 120 kW *Urbino 8.9 LE electric* version can run for 100 km without the need to recharge. The batteries can provide 120.9 kWh of energy at a nominal voltage of 600 V and regenerative braking is allowed, being the bus equipped with braking resistors in case the battery could not accept this recovered energy. Some structural materials are made of carbon fiber to allow the reduction of weight and also aluminum is used in place of steal for the rims and window frames (Solaris Bus & Coach SA. 2011).

Later, in 2012, *Solaris* developed the prototype of an electric 12-meter bus version, called *Urbino 12 electric*. This model is built over their conventional diesel *Urbino 12*, and follows all the customization characteristics of their first electric bus, i.e., battery pack size and charging system adjustable to client's requirements. Its standard version carries a 160 kW motor, with the possibility of changing it by 2 motors in the drive axle of 60 kW power each. This model can carry up to 41 passengers seated and the batteries are of lithium-ion technology as well.

8 m

10.2 m

10.8 m

12 m

18 m

Figure 2.5- *BYD*'s different electric bus models: exterior and interior pictures (BYD - Build Your Dreams 2014)

EcoRide35™

Catalyst™

Figure 2.6- *Proterra*'s different electric bus models pictures (Proterra 2014)

The *Urbino 12 electric* came with an innovation: induction charging. The prototype was equipped with the *Bombardier*[9] system *Primove*, which allows the bus to charge without cables. Therefore, the bus can go through fast-charging at stops, for example, being the stops equipped with the coils-fitted under the road surface (transportweekly 2014). It can also be standard-charged using regular external wire-chargers (plug-in), and the pantograph for charging from above is an optional addition.

In 2013, *Solaris* has launched the 18-meter electric bus version called *Urbino 18 electric*. It is an articulated bus, allowing up to 54 passengers to be transported seated. The bus can be optionally equipped with the induction-charging system, allowing it to carry only small batteries of 90 kWh on the roof, the number of cells depending on the client's requirements for energy. It also comes with the possibility of being charged from the top (pantograph) and clearly it enables plug-in standard charging. This model is equipped with a 240 kW motor and lithium-ion batteries (Solaris Bus & Coach SA. 2014).

[9] (Bombardier Transportation 2014)

Solaris electric buses have been through many tests around Europe in more than 30 cities, including Poznan, during the Euro 2012, where it ran more than 2200 km, in the Hamburg Airport, and in Montafon, an Austrian city, where the bus was tested in steep inclines (for a maximum of 13% incline), being noticed that the bus recovered 60% of the energy of the total driving cycle. The first orders for *Solaris* electric buses came from Germany and Austria. The city of Braunschweig ordered 1 *Urbino 12 electric* and 4 *Urbino 18 electric*, both with the added option of *Primove* system for induction charging, whereas Düseldorf went for 2 standard *Urbino 12 electric* (Cerqueira 2014). The Austrian city of Klagenfurt opted for one unit of the smallest of the models, the *Urbino 8.9 LE electric* (Gruber 2013).

Table 2.3 summarizes the technical characteristics of these three Solaris electric models and Figure 2.7 shows pictures of their exterior, as well as a picture of the *Urbino 12 electric* interior for reference.

Table 2.3- *Solaris* electric bus models and their specifications

Model / **Spec**	***Urbino 8.9 LE electric***	***Urbino 12 electric***	***Urbino 18 electric***
Size (m)	8.9	12	18
Nº Seats	29	41	54
Weight (kg)	NA	NA	NA
Motor Power (kW)	120	160	240
Battery Type	Lithium-ion	Lithium-ion	Lithium-ion
Charging System			
plug-in	standard	standard	standard
pantograph	optional	optional	optional
inductive	NA	optional	optional

2.3.6 Sinautec Automobile Technologies

In 2006, the American *Sinautec Automobile Technologies*[10], and its Chinese partner, *Shanghai Aowei Technology Development Company*[11] have developed the world's first full-electric supercapacitor (or ultracapacitor) bus. This type of energy storage has a much higher power density, which means they can charge really fast. However, their energy density is much smaller than those of the batteries, especially the lithium-ion type, making them not suitable for powering private electric vehicles.

[10] (Sinautec 2014)
[11] (Aowey 2014)

Urbino 8.9 LE electric

Urbino 12 electric

Urbino 12 electric (interior)

Urbino 18 electric

Figure 2.7- *Solaris*'s different electric bus models pictures (Solaris Bus & Coach SA. 2014)

In the case of public electric buses, this is different. Those buses have well-defined routes and have to stop many times along the route to the boarding or alighting of the passengers. In this sense, *Sinautec* has implemented a fleet of 17 full-powered supercapacitors buses to serve Greater Shanghai in 2006 and had no known incident or failure. However, in 2010, during the Shanghai Expo, 40 of those buses were used and some of them broke down, due to overheat of the supercapacitors (Research India 2010).

This bus model is called *Ultracap Bus*. It is 11.4 m long and can take 41 passengers seated. Its only energy source is a supercapacitor bank that can provide 5.9 kWh of energy, which is enough to run for 5.6 km when air conditioning is on or 9.7 km when off, and is able of reaching 48 km/h. The bus has to charge for 30 seconds at certain bus stops, and 5 minutes at the terminals, so that to perform a complete route. The charging is done using a pantograph, as it can be seen in Figure 2.8. The total weight of the bus is 13,000 kg.

The company states the bus is competitive with conventional buses based on fuel savings over the vehicle's 12-year life. *Sinautec* estimates that it can achieve lifetime fuel savings of $200,000. In order to increase this bus range, *Sinautec* had been in discussions back in 2009 with MIT's supercapacitor expert Joel Schindall, professor of electrical engineering and computer science at MIT about developing supercapacitors of higher energy density using vertically aligned carbon nanotube structures that give the devices more surface area for holding a charge (Hamilton 2009). However, there is no register of any developments from this partnership and there is not much information after 2010 about *Sinautec* buses.

Figure 2.8- *Sinautec*'s *Ultracap Bus* model picture at a charging station on a bus stop (Sinautec 2014)

2.3.7 CaetanoBus

CaetanoBus is a Portuguese company that manufactures bus bodies since 1946 and is able to use different manufacturers' chassis as basis. *CaetanoBus* is well-known for their airport buses, having an expertise in this matter for more than thirty years. In 1993, they made their first appearance in the market for electric buses, by delivering 8 electric models (*COBUS 200EL*) for Germany. They operated for three years and this model picture is shown in Figure 2.9. However, no longer developments were made in this sense for years, especially regarding technological limitations. Driven by the increasing need of no-pollutant vehicles and the advances in battery technology, *CaetanoBus* decided to revive their electric buses development and launched two prototypes of the new *COBUS 2500EL* in 2011 (CaetanoBus 2011a), presented in Figure 2.10 and Figure 2.11.

Figure 2.9– *CaetanoBus* first electric bus model developed in 1993: *COBUS 200EL* (CaetanoBus 2009)

Figure 2.10– *CaetanoBus* electric bus prototype *COBUS 2500EL* exterior (Delicado 2013)

Figure 2.11- *CaetanoBus* electric bus prototype *COBUS 2500EL* interior (CaetanoBus 2009)

The idea of launching two prototypes at once was to allow one of them to go through the first testing phase at the *CaetanoBus* headquarters, whereas required improvements according to the test results were directly applied to the second prototype. Therefore, this "improved" second prototype was presented at the city of Offenbach, Germany, successfully performing test routes (Velez 2011). A second testing phase was held on the streets of Vila Nova de Gaia, Portugal, where the bus was put to run at a main street as a shuttle service and planned battery recharging was done along the day. Although the bus was conceived to last for a whole day of operation, those tests had as objective to access the energy management and battery behavior of the bus (CaetanoBus 2011b).

During the operation of the bus, some data are collected automatically via CAN, which is extremely important to access the bus behavior in different conditions. Recently, *CaetanoBus* has installed GPS equipment on the bus and connected it to the CAN, allowing the geo-referenced position to be part of the CAN outcome. The collected data via CAN for different days of operation allowed the calibration and validation of the model, presented in Chapter 5; these relevant data are described below:

- Speed;
- Latitude/Longitude/Angle;
- Bat I+V (battery current and voltage);
- Bat SOC% (battery state-of-charge, in %);
- Engine state (1 for ON, 0 for OFF);
- AC (air conditioning) state (1 for ON, 0 for OFF);
- Heater state (1 for ON, 0 for OFF).

The *COBUS 2500EL* is a 12-meter long vehicle, with an aluminum body and low-floor. It can carry up to 70 passengers, being 23 seated, 45 standing and 1 wheel-chair; the maximum allowed weight is 18,000 kg. The bus is equipped with a *UQM PowerPhase150* motor (the same used by *Proterra* buses), that provides a peak power of 150 kW, a maximum torque of 650 N.m and a maximum motor speed of 5000 rpm (supplier's datasheet in Appendix A). The bus is equipped with a ventilation system instead of air conditioning, which for the Portuguese climate serves well.

The batteries are of lithium iron phosphate ($LiFePO_4$) and provide approximately 150 kWh of energy. The batteries were supplied by one of *CaetanoBus* engineering partners *Efacec*[12], and the battery pack is composed of 15,680 cells, being 140 in parallel and 112 in series. This battery type provides no-memory effect, allowing it to be re-charged anytime. The battery current is limited to 500 A either for charge or discharge, being the regenerative braking current controlled to not surpass 200 A. The operating voltage ranges from a minimum of 280 V and a maximum of 408.8 V.

CaetanoBus electric bus prototype has two ways to charge its batteries. The slow-charge takes 8 hours and is made using an onboard charger (output AC 3 x 3.2 kW), allowing it to be connected to an industrial plug of 3 x 230 V/ 16 A. The fast-charge takes 3 hours, being made through an external charger DC 62.5 kW (500 V/125 A maximum), manufactured by *Efacec*. This external charger can be upgraded to a high-power charger of 200 kW in the future; it is presented in Figure 2.12.

Figure 2.12– Battery charger developed by *Efacec* for fast-charging of the *CaetanoBus 2500EL* (CaetanoBus 2009)

[12] (Efacec 2014)

Both prototypes have run thousands of kilometers in many different European cities, such as Vila Nova de Gaia and Lisbon (Portugal), Offenbach, Wiesbaden, Frankfurt and Stuttgart (Germany), and at one of the Amsterdan airports (Netherlands). One of the prototypes was sent to Finland to engage on the same 3-year tests (ending in 2015) that the *BYD* electric bus is also participating (Delicado 2013). Those tests are of great relevance to CaetanoBus, once they will have a thorough analysis of the bus performance on a long-term basis.

CaetanoBus has recently been involved in an innovative project with Siemens Portugal[13], showing in 2013 a regular airport bus retrofitted, from internal combustion engine to electric. Together with a new design, the *eCobus* allows the extension of the bus lifetime in ten years, besides saving 75% in fuel costs. It is equipped with a full-electric driveline and lithium batteries, which can provide either 85 kWh or 116 kWh. The recharge can be made slowly (in 6 hours) with an internal charger, or faster (in 3 hours) using an external charger DC 700 V (Moura 2013). The customers though are only airports that already have a regular *Cobus* model and want to increase its lifetime, for now. The *eCobus* can be observed in Figure 2.13.

Figure 2.13– *eCobus*: the retrofitted airport diesel bus to electric (Siemens 2013)

CaetanoBus has been developing a platform for electric buses that can be powered either by batteries or fuel-cells, being on the latter case the bus equipped with hydrogen tanks on the roof. The fuel-cell prototype is intended to be presented in 2015, being a 12-meter urban bus, weighing 18,000 kg and able to carry 75 passengers. The idea is to have a standard platform to build either a battery-powered bus or equipping fuel-cells as the only power source (Moura 2014). *CaetanoBus* electric bus models are intended to be commercialized in 2015.

[13] (Siemens Portugal 2014)

2.3.8 Some Relevant Initiatives

After presenting some of the most well-known electric buses in the world, it is relevant to mention the most relevant initiatives that may result in commercial electric buses in the near future. The oldest is *Hyundai Motor*, a Korean company, which presented its full-electric bus model in 2010 and started the test phase. The *Elec-City* is equipped with three 100 kW electric motors; there is no information about the type of the energy storage device it carries. The bus can transport 51 passengers; it has an approximate autonomy of 120 km and can reach a maximum speed of 100 km/h.

Elec-City was used during the G20 Seoul Summit in 2010, being the official shuttle bus for organizers and officials. A test fleet was programmed to be operated in some metropolitan bus routes in Korea, with plans to mass produce the buses from 2013 on. However, there was no information on their website of whether any of those happened. The manufacturer states that the operating cost for this bus is only 29% of the cost of operating a natural-gas bus (Hyundai 2011). Figure 2.14 shows a picture of the *Elec-City* bus.

Figure 2.14– *Elec-City* electric bus model from *Hyundai Motor* (KoreaTimes 2010)

The more recent Swiss initiative called *TOSA* (*Trolleybus Optimisation du Système d'Alimentation*) is a fully electric articulated bus that runs without overhead lines (TOSA 2014). This bus concept was developed in a partnership of different entities, including the ABB[14] and the EPFL (*École Polytechnique Fédérale de Lausanne*)[15]. *TOSA* is a 17-meter electric bus that can carry up to 133 passengers. It uses lithium-titanate batteries. Due to the fact that it goes through fast charges along the route, it does not have to carry a lot of weight in batteries. The high power fast-charge (400 kW) happens in 15 seconds

[14] (ABB 2014b)
[15] (EPFL 2014)

(minimum) at some bus stops through a robotic arm on the roof, being the ideal time for the boarding and alighting of passengers (Campana 2014). The bus has been through a testing phase at the Geneva Airport, and there are plans that this city will adopt a *TOSA* bus line as part of its regular service by 2017 (Kooser 2014). Figure 2.15 shows a picture of the *TOSA* bus at a charging stop; the charger can be observed close to the articulation of the bus.

Another initiative comes from Australia that in 2013 launched the world's first solar-powered electric bus *Tindo*, which is the result of an eight-year development of the Adelaide City Council (Adelaide City Concil 2012). The vehicle itself does not carry solar panels but it recharges at a central station that is equipped solely with solar panels. The energy it gets when recharging is enough to serve the purpose: being a bus connector in the city center of Adelaide, supporting air conditioning and the transportation of up to 40 passengers. One charge provides the bus with autonomy for 200 km, having the regenerative braking an important role, once it recovers 30% from the total energy spent (Clean Technica 2013). The bus is equipped with 11 Swiss-made *Zebra*[16] battery modules, which use sodium/nickel chloride technology (Adelaide City Concil 2012). Figure 2.16 shows a picture of this bus circulating in Adelaide, Australia.

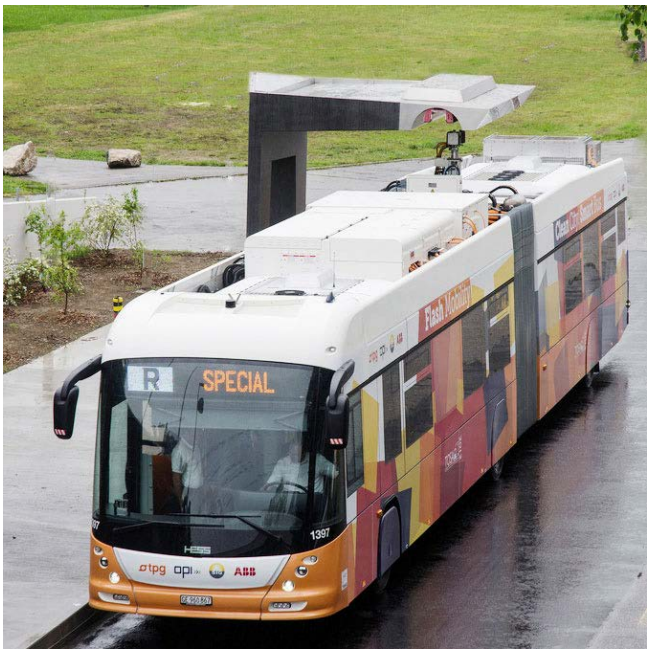

Figure 2.15– *TOSA* bus at a bus stop equipped with a charger (ABB 2013)

[16] (Zebra Technologies 2014)

Figure 2.16– *Tindo* bus in the city of Adelaide, Australia (EcoLocalizer 2013)

Volvo[17], which is a well-known and established supplier for hybrid buses, has recently announced its new modern bus service *ElectriCity*, to be launched in 2015 at Gothenburg, Sweden. The buses will be fully-powered by batteries, and these will be charged from renewable sources. Besides developing the bus itself, *Volvo* will create new bus stops solutions, traffic routing systems, among others. *Volvo* states that the main idea besides having a emissions-free bus fleet is to be able to provide a better service and to attract more people to using public transport, once the project encompasses reaching areas that nowadays are not well-served in this sense (Volvo 2013).

In 2014, *Volvo* has signed a partnership contract with *ABB* as a way to provide a standard charging solution for the Swedish hybrid and electric buses. The standards are related to the communication protocol of the infra-structure and the charging solution, the electric interface and the specification of the automatic connection system (Turbo Oficina Pesados 2014). In the end, the cooperation will create a standardized charging system for full-electric and electric hybrid buses, able of charging buses quickly through an automatic roof connection system at bus stops or through cabled charging systems overnight (ABB 2014a).

2.4 Comparing Electric Buses with Trams and Trolleybuses

Governments around the world are giving an increasing importance to cleaner means of transportation, either reducing their emissions or eliminating them. Focusing on the zero-emission vehicles, the options are narrowed to subways, trains, trolleybuses, trams and electric buses. Considering that subways and trains represent high-demand mode of transportation, being able to carry many more passengers and having the drawback of not

[17] (Volvo Group 2014)

providing a door-to-door transportation, this analysis is held in regard to the others, which somehow belong to the same "class" of public vehicles as electric buses.

As previously presented in section 2.2, trams and trolleybuses require some sort of structure to work. For the case of trams, they require rails to be built and a power cable to pass in the middle of it, besides an overhead wire to close the circuit. On the other hand, trolleybuses have the advantage of running on rubber tires but also require the overhead wire to be powered. For electric buses, no mandatory structure is required along the route, just a charging station at the terminal (at the minimum).

Regarding the required infra-structure for these modes of transportation to run, trolleybuses can be considered a more accessible option than trams, once they do not require rails to run. Besides that, trams are restricted to the route where the rail passes, not being able to make deviations or having its route changed without making major investments in structure. Trolleybuses can perform minor deviations along the path, once usually the wires on top of it are really long and flexible.

Nevertheless, both trams and trolleybuses require the overhead wires to run and they can have a really negative impact on the view, affecting the tourism sightseeing of historic venues and not allowing vertical clearance (URS 2010), as it can be observed in Figure 2.17. Moreover, the overhead wiring infra-structure has to be built, increasing the costs associated with the implementation and maintenance of those modes of transportation whereas limiting any possibility of changing the bus route.

Figure 2.17– Trolleybuses overhead wires in San Francisco (CA), USA (Hsu 2006)

On the other hand, electric buses run on rubber tires and are not subjected to any rails or wires, making them almost perfect to run on cities. Routes can be changed from night to day, or even during operation, and the electric bus will perform it accordingly with no major issues. The costs with infra-structure are related to the charging station(s) only, which are small in size and no major infra-structure construction is required. The only disadvantage of electric buses when compared to trolleybuses or trams is related to the autonomy of the vehicle. The wires provide them with "infinite" power while the electric buses rely on the energy in the batteries. This was a huge problem ten years ago but is not anymore; battery technology is evolving greatly and the electric vehicles are advancing with it.

2.5 Conclusions

This chapter presented the origins of public transportation and their electrification, focusing on urban mobility. Some of the most impacting companies commercializing electric buses were presented, together with their models technical details. The advancements in battery technology (and not only) allowed those companies to invest in research, making some of them references for others. The important point is to see that most of those products have five years old or less, which means that this is a new market with great potential, once regulations are getting harder about transportations emissions.

A brief discussion on the advantages of electric buses in relation to trams and trolleybuses (both electric-powered means of transportation at a similar scale) was held, getting to the point where electric buses actually present many advantages in relation to them, namely the lower investment cost in infra-structure and the flexibility of operation, especially regarding routes modifications.

On the next chapter, the mathematical model of the *CaetanoBus 2500EL* is developed, showing all the equations involved and describing the used parameters in each one of them. In addition, this mathematical model implementation in *Simulink* software is explained in detail, together with the logic used for composing this computerized model.

Chapter 3

Development of the Electric Bus Simulation Model

3.1 Summary

This chapter describes the whole process of creating the proposed electric bus simulation model, accounting for the mathematical model of the bus dynamics and its components and further development in a computer program.

3.2 The Electric Bus Model

In the previous chapter, electric buses from around the world were presented, concerning technologies with which they are equipped and their technical specifications. As expected, more focus was given to the Portuguese electric bus prototype, developed by the *CaetanoBus* Company. *CaetanoBus* has provided all the necessary data to make it possible to develop and validate the electric bus simulation model.

Models are largely used in many fields of knowledge: they allow for the correct representation of a specific system. By having a model that adequately mimics the real system, it is possible to create scenarios, extrapolate results and make improvements on the real system itself based on the simulation results analysis. It is common-sense that prototyping every alteration possibility in the system to evaluate the impacts would be expensive and time demanding (Gao et al. 2007).

In order to systematically develop a simulation model of the electric bus, Sargent (1984) wide-spread proposed paradigm was followed and its graphical representation can be observed in Figure 3.1. It represents a simplified yet thorough version of the traditional model development process, and its three main components account for: the problem entity, the conceptual model and the computerized model. They are interconnected by phases, namely analysis and modeling, computer programming and implementation and experimentation. Both validation and verification phases are approached in Chapter 5.

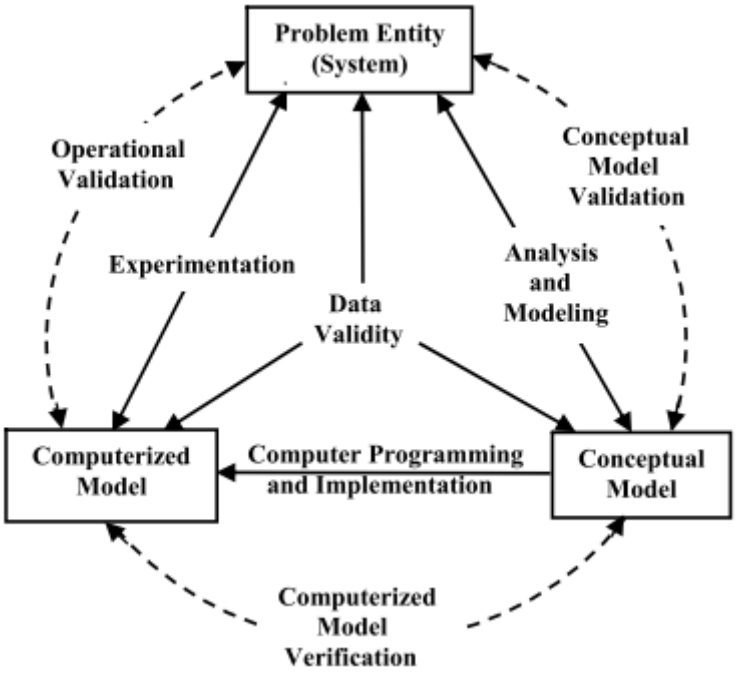

Figure 3.1– Simplified modeling process paradigm proposed by Sargent (Sargent 1984)

The problem entity represents the real system to be modeled; the conceptual model is the mathematical representation of the problem entity that is developed to mimic its behavior; and the computerized model is the translation of the conceptual model into computer software. The conceptual model is the outcome of the analysis and modeling phase while the computerized model is developed during the computer programming and implementation phase, both expressed in Figure 3.1. Moreover, an experimentation period is used to conduct as many computer experiments as possible to perform inferences on the problem entity (Sargent 2005).

Therefore, by applying this paradigm to the context of this thesis, it is clear that the problem entity is the real electric bus, more specifically the *2500EL* model from the *CaetanoBus* company. The conceptual model results from the "analysis and modeling" phases, when mathematical equations that govern the bus behavior are devised. The computerized model is the implementation of such mathematical equations in the chosen software, *Simulink*, which is a building-block diagrammatic environment integrated to the largely known *Matlab*. Due to the fact that all the bus specifications were described in detail in the previous chapter, the focus here is on the mathematical development of the conceptual model and its translation into the *Simulink* language resulting in the computerized model.

3.2.1 The Conceptual Model

The main objective in the development of the electric bus conceptual model is to mimic its behavior when in operation, in other words, to correctly represent its dynamic behavior. Vehicle dynamics is concerned with the movement of vehicles on the road and is determined by the forces imposed on the vehicle from the tires, gravity and aerodynamics. Hence these forces have to be studied and their impact over the vehicle performance evaluated (Gillespie 1992). In this sense, electric vehicles are treated like a regular internal-combustion's, and the dynamics equations are the same. The difference lies on some performance parameters and the battery modeling, described later on in this chapter.

The first step in this process is to develop an equation that accounts for the tractive effort. This is the force propelling the vehicle forward, transmitted to the wheels and necessary to allow the vehicle to leave an inertia state. This force must overcome the vehicle resistance to the movement, which is composed by the sum of the different forces that act against it. Considering the vehicle represented in Figure 3.2, which weighs m kilograms and is running up a slope of Ψ angle, it must develop a specific tractive force to allow it to actually run. Those forces are discriminated in the figure and are as follows:

- *R*olling resistance force (F_{rr}): represents the friction between the tires and the road;
- Aerodynamic drag force (F_{ad}): due to the friction of the vehicle body moving through the air;
- Hill climbing force (F_{hc}): accounts for the climbing grade of the road;
- Acceleration force (F_{ta}): stands for the necessary force besides the ones already presented to accelerate the vehicle (not represented in Figure 3.2);
- Tractive effort (F_{te}): represents the sum of all the above described forces.

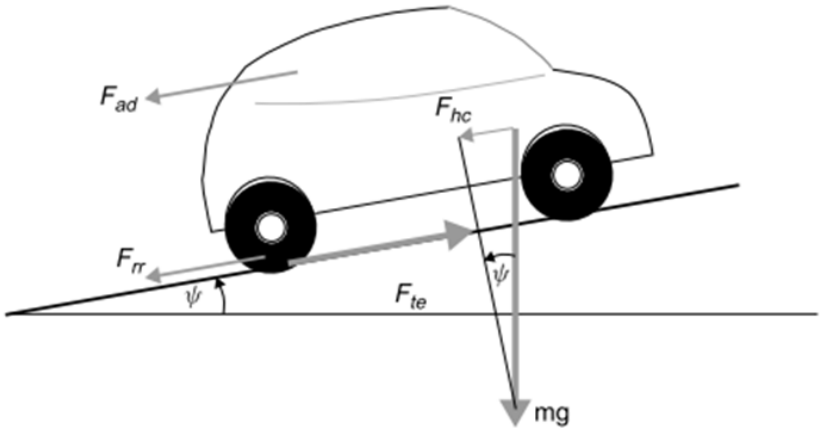

Figure 3.2– Different forces acting against a vehicle running up a slope (Larminie and Lowry 2003)

3.2.1.1 The Rolling Resistance Force

The rolling resistance force, F_{rr}, is primarily due to the friction of the vehicle tire on the road. The rolling resistance is proportional to the vehicle weight, and is represented by equation 3.1:

$$F_{rr} = f\ m\ g \tag{3.1}$$

where:

f = rolling resistance coeficient

m = mass of the vehicle (kg)

g = gravitational acceleration (m/s^2)

The rolling resistance coefficient (f) is a dimensionless factor that expresses the effects of complicated physical properties of tire and ground. It is affected by the tire temperature and inflation pressure, its material and the speed of the vehicle. Several equations to account for all these factors have been developed and are different for light and heavy duty vehicles. The chosen equation was developed by the University of Michigan Transportation Research Institute due to be specific for heavy-duty vehicles and is as follows (Gillespie 1992):

$$f = (0.0041 + 0.000041\ v\ 0.447)\ C_h \tag{3.2}$$

where:

v = linear speed (m/s)

C_h = road surface coefficient

3.2.1.2 The Aerodynamic Force

The aerodynamic force F_{ad} is due to the friction of the vehicle body moving with the air. It depends on the frontal area, shape, protrusions (such as side mirrors), among others. Its equation is presented as eq.3.3:

$$F_{ad} = 0.5\ \xi\ C_W\ A\ (v^2) \tag{3.3}$$

where:

ξ = air density (kg/m^3)

C_W = aerodynamic drag coefficient

A = vehicle frontal area (m^2)

v = vehicle speed (m/s)

3.2.1.3 The Hill Climbing Force

The hill climbing force F_{hc} is the force needed to drive the vehicle up a slope. It is simply the component of the vehicle weight that acts along the slope. It may have a negative impact on the movement of the vehicle, acting as a resistance force but also a positive impact, if the vehicle is going down a hill. Equation 3.4 represents this component bellow:

$$F_{hc} = m\ g\ \sin\Psi \tag{3.4}$$

where:

$\Psi =$ angle of inclination

3.2.1.4 The Acceleration Force

A force has to be applied in addition to the forces already mentioned if the speed of the vehicle is changing. The acceleration force F_{ta} will provide the linear acceleration of the vehicle and is represented by equation 3.5:

$$F_{ta} = m\ a \tag{3.5}$$

where:

$a =$ acceleration (m/s^2)

3.2.1.5 The Rotational Acceleration Force

There exists a fifth force that impacts on the dynamics of the vehicle, responsible for the acceleration of its rotating components called rotational acceleration force (F_{wa}). These rotating components account mainly for the electric motor/generator, driveline, and wheel/tire assemblies (Lee 2005). Larminie and Lowry (2003) have deducted an equation on their book to represent this force, presented here as equation 3.6:

$$F_{wa} = I_m\ \frac{G^2}{\eta_g\ r^2}\ a \tag{3.6}$$

where:

$I_m =$ moment of inertia of the rotating components

$G =$ gear ratio

$\eta_g =$ efficiency of the gear system

$r =$ wheel radius (m)

Due to the difficulty in knowing the I_m factor, Gillespie (1992) suggests the replacement of the rotational acceleration force component of Eq. 3.6 by a lumped mass to be further used in the equation for the acceleration force (Eq. 3.5). The combination of the equivalent mass

of the rotating components with the vehicle mass is called the "effective mass" and the ratio in relation to the vehicle mass is named "mass factor", as it can be seen in Eq. 3.7:

$$m_f = \frac{m + m_r}{m} \tag{3.7}$$

where:

m_f = mass factor

m_r = equivalent mass of the rotating components

In the absence of m_r, another approach to the mass factor can be taken, where it is dependent on the operating gear, composed by the multiplication of the gear box ratio and the differential ratio, it can be calculated using the empirical equation bellow (Wong 2008):

$$m_f = 1.04 + 0.0025\ G^2 \tag{3.8}$$

For this thesis developed model, Eq. 3.8 is applied to represent the mass factor, once the equivalent mass for all rotating components is unknown. Therefore, Eq. 3.5 had to be re-written so that the m_f factor is multiplied by the bus mass.

3.2.1.6 The Tractive Effort

After presenting all the forces that composes the tractive effort, its final value is the sum of all these forces, and is represented by equation 3.9:

$$F_{te} = F_{rr} + F_{ad} + F_{hc} + F_{ta} \tag{3.9}$$

3.2.1.7 The Performance Factors

The next step in the development of this conceptual model is to define mathematical equations to account for the main evaluation performance parameters, namely power, motor speed and torque. The power is quite simple to be extracted, being the tractive force times the linear speed (v), as in equation 3.10 below:

$$P_{te} = F_{te}\ v \tag{3.10}$$

This equation represents the necessary power on the wheels (P_{te}) to make the vehicle move. However, although electric motors are known for their high efficiency rates, usually due to their really simple gear system, they can never be considered 100% efficient, which means that the required power from the motor is higher than the calculated P_{te}. Basically, the efficiency of an electric motor is related to the motor itself and the controller and for practical reasons, they are considered together. For the case of the electric bus, the efficiency curve from the motor supplier (Appendix B) was analyzed and a mathematical

equation extracted taking as main variable the motor speed. Equation 3.11 shows the resulting equation:

$$\eta_m = -3\,x10^{-8}\,(v_m^2) + 0.0002\,v_m + 0.638 \tag{3.11}$$

where:

$\eta_m =$ motor efficiency

$v_m =$ motor speed (rpm)

It is relevant to say that the efficiency of electric motors is dependent on torque and motor speed behavior. In order to simplify the deduction of the mathematical equation, motor speed was chosen. Clearly, the next step is to define the equation for the motor speed, as it can be seen in Eq. 3.12:

$$v_m = \frac{v\ 60\ G}{2\ \pi\ r} \tag{3.12}$$

At this point, the required power from the motor can be calculated as a function of the previously defined power "on the wheels" (P_{te}) and the motor efficiency (η_m). The efficiency factor is applied differently according to the bus acceleration profile: whenever the bus is accelerating and thus power is positive, P_{te} is divided by the efficiency. Whereas whether the bus is braking and hence power is negative, the P_{te} is multiplied by the efficiency factor. The mathematical equations that represent those situations are 3.13 and 3.14, respectively:

$$if\ P_{te} > 0\text{: } P_{mot} = \frac{P_{te}}{\eta_m} \tag{3.13}$$

$$if\ P \leq 0\text{: } P_{mot} = P_{te}\,\eta_m \tag{3.14}$$

where:

$P_{mot} = required\ power\ from\ the\ motor$ (kW)

The required power from the motor is defined but especially for the case of buses, there are some other sources that require power, generically named accessories. The accessories account for air conditioning, steering pump, air compressor, lights and other smaller components. Only the first three mentioned accessories have well defined ranges of operation and account for the most part of the accessories power consumption, for they are the only to be considered. The accessories required power has to be summed up with the recently defined P_{mot}, resulting in the power required from the batteries, as follows:

$$P_{bat} = P_{mot} + P_{acc} \quad 3.15$$

where:

P_{bat} = required power from the batteries (kW)

P_{acc} = required power for accessories (kW)

At last, a torque (T) equation can be finally defined, once it depends on the motor speed and the required power from the batteries:

$$T = \frac{P_{bat}\ 60}{v_m\ 2\ \pi} \quad 3.16$$

So far, the described mathematical equations answer for the calculation of the motor performance parameters. The next step is to define the mathematical equations for modeling the battery behavior, once this is the energy source of the electric bus in analysis and of high impact on the bus performance as well. Due to the inherent electrochemical nature of batteries, their modeling is not straightforward and some really complicated physical, dynamic and electrical properties are involved in their functioning (Linden and Reddy 2002).

3.2.1.8 The Battery Modeling

The diverse properties of batteries allow their modeling to be approached from three different perspectives: electrochemical, mathematical and electrical. Electrochemical models are extremely complex and time-consuming to devise due to their sophisticated numerical algorithms, not to mention the difficulty in acquiring battery specific information of proprietary nature. Mathematical models lack information regarding either electric current or voltage behavior and usually work for very specific applications. Electric models, on the other hand, are simpler and more intuitive as they are meant to mimic battery behavior by applying a combination of capacitors, resistors and voltage sources. They usually have an accuracy residing between the electrochemical and the mathematical models (Chen et al. 2006).

Therefore electrical models were chosen to be used in this project, once they can be reliable, simple to use and perfectly applicable to the intentions herein stated: performance of electric vehicles. Despite the high amount of variations in the equivalent circuit used to mimic the battery behavior, the simple yet useful circuit of Figure 3.3 is used, also called linear model. It does not take into account the temperature impact or the self-discharge of batteries.

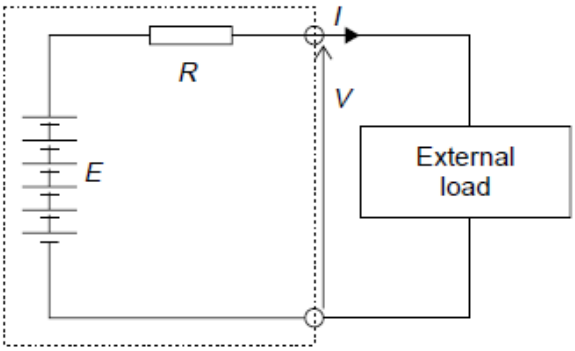

Figure 3.3– Linear equivalent circuit model of a battery

The linear equivalent circuit consists of an ideal voltage source E, a voltage in the terminals V which is different from E due to the internal resistance of the battery and the resistance itself R, represented by a resistor (Iglesias et al. 2012). If the current I is zero, the terminal voltage is equal to E and it is usually called the open-circuit voltage or nominal voltage.

This equivalent circuit representation has some limitations, as it does not mimic the dynamic behavior of the battery. For instance, if a certain load is applied, the voltage will immediately decrease, which does not happen in the real world as it would take some time for it to settle down to the new value. However, it serves really well to the purpose of the electric bus simulation, as the validation process of this simulation model shows.

The mathematical equation that represents the schematic of Figure 3.3 is 3.17 (Van Mierlo 2004):

$$V = E - I\,R \tag{3.17}$$

For simplification reasons, the battery nominal voltage (E) and the resistance (R) are both assumed to be constant values. In real battery operations, E varies with the state-of-charge (SOC) of the battery and R is influenced by either the side-reactions occurring inside the cell, causing some mass deposition on the electrode thus increasing R (Linden and Reddy 2002) or the amplitude of the applied current.

Equation 3.15 shows the amount of power to be supplied by the batteries and the important thing to be discovered is how to translate this amount into battery current and/or voltage. In other words, how much should the battery current and voltage be in order to be able to provide the required power? To start with, equation 3.18 shows the relationship between battery current, voltage and power:

$$P_{bat} = V\,I \tag{3.18}$$

Therefore by combining equations 3.17 and 3.18, a resulting quadratic equation for battery current *I* is found, and its useful solution can be observed in 3.19:

$$I = \frac{E - \sqrt{E^2 - 4\,R\,P_{bat}}}{2\,R} \tag{3.19}$$

This equation can be easily solved in *Simulink*, according to the previously calculated input power P_{bat}. By having *I*, the voltage is deducted by using equation 3.17. The next step is to define equations that would give the state-of-charge (SOC) of the battery. Basically, whenever the battery is discharged – applied current per second -, a certain capacity is removed from it. The SOC is nothing more than the percentage of capacity remaining in the battery when compared to its total capacity. Before getting to a SOC value definition, the removed capacity should be firstly calculated:

$$C_r = I\,t \tag{3.20}$$

where:

$C_r =$ charge removed from the battery (Coulomb or As)

$t =$ time (s)

The total capacity of a battery is usually given in Ampere-hour (Ah), thus creating an issue when confronted to the recently calculated C_r (Larminie and Lowry 2003). In order to solve this and making it plausible for the SOC to be calculated, the equation has to be divided by a factor of 3600, transforming the C_r from As to Ah, and thus calculating the SOC as Eq. 3.21 shows:

$$SOC(\%) = \int \frac{C_r}{3600\,C_p} 100 \tag{3.21}$$

where:

$C_p =$ battery capacity (Ah)

It is important to highlight that the battery capacity (C_p) changes according to the applied current, which is a phenomenon represented by the Peukert's Law (Linden and Reddy 2002; Larminie and Lowry 2003). Despite its relevance, lack of data from the supplier's battery datasheet did not allow for the Peukert's coefficient to be properly calculated, implying in this model assumption that battery capacity is constant.

All the equations for battery modeling presented so far, except for the C_r and *SOC*, are applicable only in case of discharging the battery, i.e., bus in motoring mode. Whenever the

bus is braking, the motor is capable of working in generator mode, which means energy can flow back into the batteries. This would cause some equations to be adapted to this new scenario, starting with 3.17 that would become:

$$V = E + I\,R \tag{3.22}$$

Consequently, by combining this previous equation with 3.18, the resulting sensible solution for this new quadratic equation would now be:

$$I = \frac{-E + \sqrt{E^2 + 4\,R\,P_{bat}}}{2\,R} \tag{3.23}$$

At this point, the battery current and voltage are known either for periods of acceleration or deceleration of the bus, as equations are different from each other for both cases. The question that arises is how much energy the bus consumes. This parameter can be found by numerically integrating 3.18, once the result from this equation is the power in W, the energy is this power along time for n steps in kWh. A factor of 1/3600000 had to be applied in order to convert the energy in Ws to kWh, as follows:

$$Energy = \frac{\int_0^n P_{bat}}{3600000} \tag{3.24}$$

After defining the equation that represent the battery behavior, it is also important to define the number of battery cells in parallel and in series that composes the battery pack. Both parameters impact on some of the variables used in the battery modeling, namely the nominal voltage (E), the battery capacity (C_p) and the battery resistance (R). Those parameters were extracted from the battery cell datasheet (Appendix C) and must be adjusted to make the calculations.

The electric bus in analysis is composed of n_p number of battery cells in parallel and n_s number of battery cells in series. In order to define the values to be used in the calculations for E, C_p and R, the following mathematical equations should be performed:

$$E = E_c\,n_s \tag{3.25}$$

$$C_p = C_{p_c}\,n_p \tag{3.26}$$

$$R = R_c\,\frac{n_s}{n_p} \tag{3.27}$$

where:

$E_c =$ nominal voltage for one battery cell (V)

$C_{p_c} =$ capacity for one battery cell (Ah)

R_c = internal resistance for one battery cell (Ω)

Therefore battery modeling equations are defined and represent the end of the electric bus conceptual model development. If it was not for the advancements on the computer simulation programs, some of those equations would be really hard to be solved manually, especially for larger time-series. In this sense, the next subchapter is about translating this conceptual model into a computerized model.

3.2.2 The Computerized Model

As previously mentioned in this chapter, *Simulink* is the chosen software to be used in this project, which in essence is a *Matlab* toolbox. *Matlab* allows the development of applications, numerical computation and also provides 2D and 3D visual representations of functions outcome. In turn, *Simulink* has *Matlab* functions contained inside boxes and the simulation model can be composed by as many boxes as required[18]. *Simulink*'s close integration with *Matlab* enables it to receive the simulation results in order to be further accessed and analyzed.

The computerized model of the electric bus in *Simulink* is divided in seven main subsystems, namely (Figure 3.4):

1. Speed/acceleration: speed profile is introduced in the model and acceleration is derived from it;
2. Tractive force: all forces composing the tractive effort are calculated;
3. Gear: speed-regulated gear control is made;
4. RPM/Efficiency: calculates motor speed and motor/controller efficiency;
5. Power: calculates required power from the batteries (P_{bat})
6. Torque: torque is calculated and exported to the Performance Scope, together with motor speed and power;
7. Battery: battery current, voltage, energy consumption and state-of-charge are calculated and further exported to the Battery Scope.

[18] (Mathworks 2012)

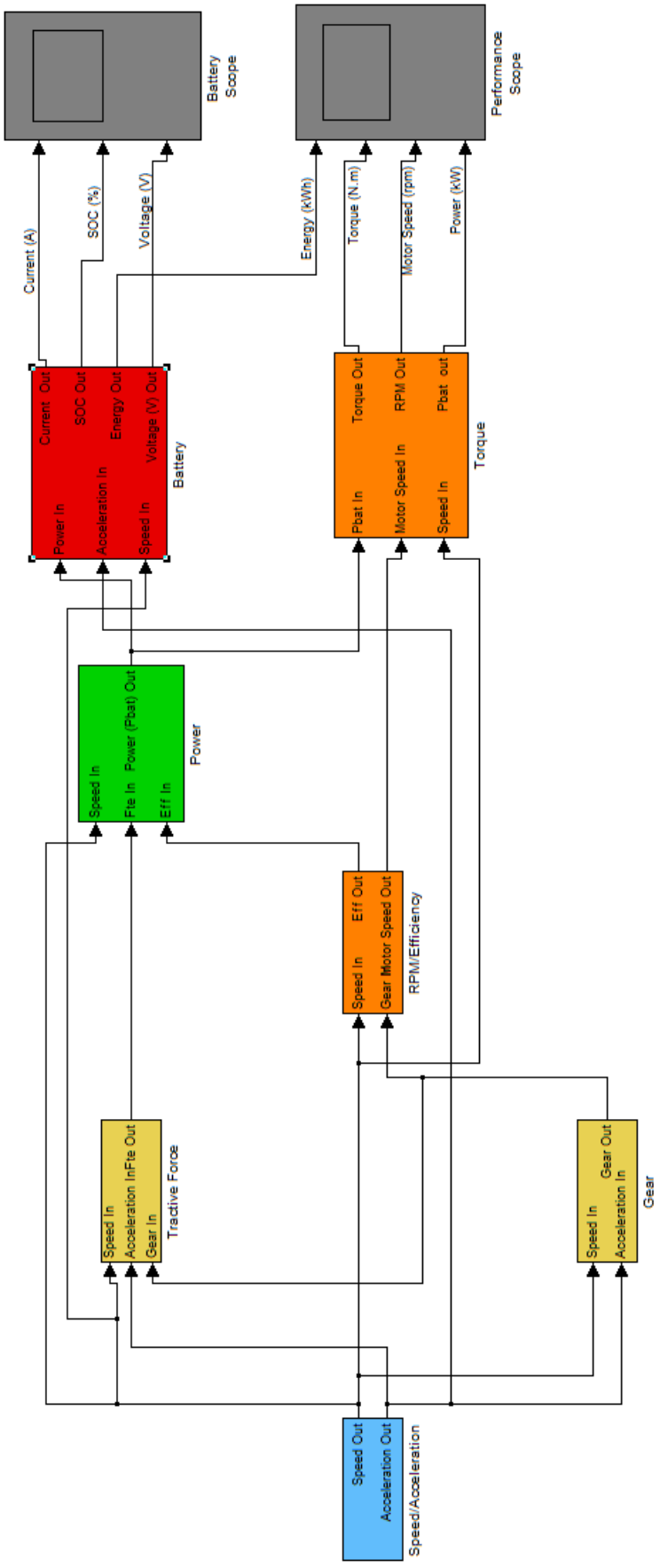

Figure 3.4– *Simulink* main model composition: seven calculation blocks and two scope blocks

3.2.2.1 Subsystem 1: Speed and Acceleration

The main function of this subsystem is to introduce the speed into the model and calculate the acceleration derived from it; this subsystem schematic is presented in Figure 3.5. It is composed of many blocks, each of which having a specific function to be accomplished, either mathematical or presentational. Along this subchapter, each of those blocks is presented and their function described.

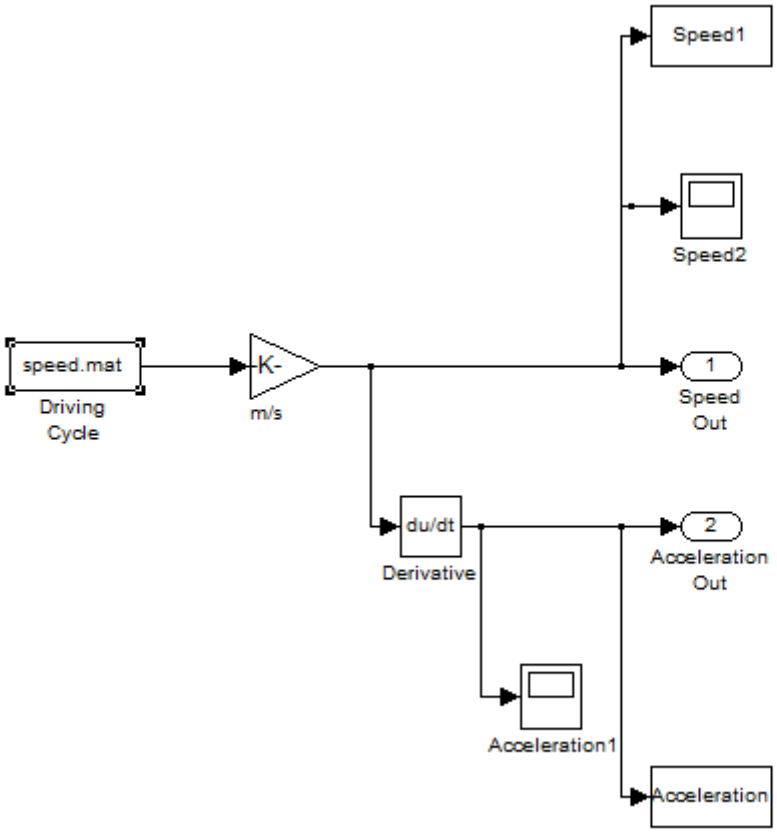

Figure 3.5– Subsystem 1 (speed and acceleration) schematic in *Simulink*

One critical component of the simulation is the driving cycle on which all the vehicle calculations are based. In this model, it is represented by a *.mat* file (*Matlab* matrix format) containing the speed profile along time, in intervals of one second. This file is introduced into the model by using the *Simulink* box "From file", as shown in Figure 3.6. Basically, the *.mat* file containing the speed profile for a specific scenario must be provided in the field "File name", enabling *Simulink* to read this file and run the simulation.

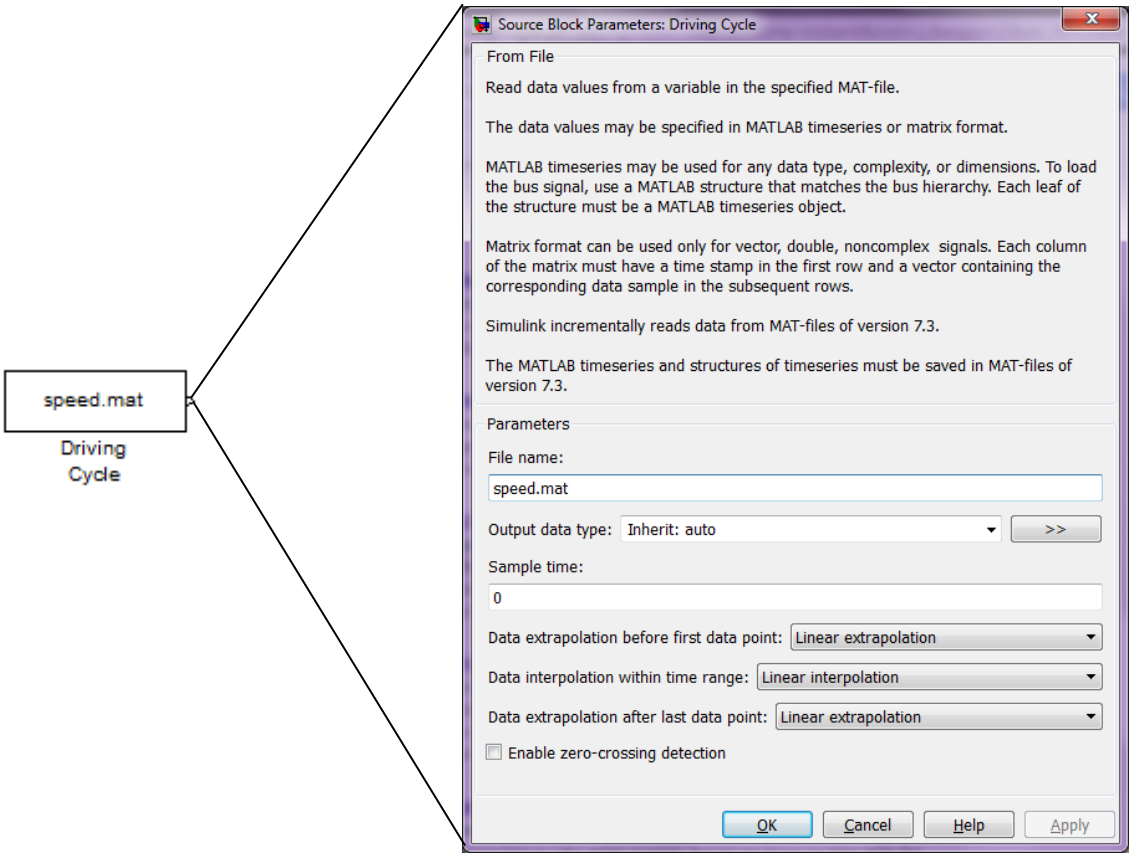

Figure 3.6– "Driving Cycle" block expanded into the "From file" function box from *Simulink* used to introduce the speed profile into the simulation

Usually, driving cycles come in km/h units, which is a problem once every calculation in the model is performed in the International System of Units (SI). In order to solve this issue, the block "m/s" is introduced, representing the *Simulink* function box called "Gain" to make the conversion from km/h to m/s, by applying a factor of "1/3.6" on the speed profile, as shown in Figure 3.7.

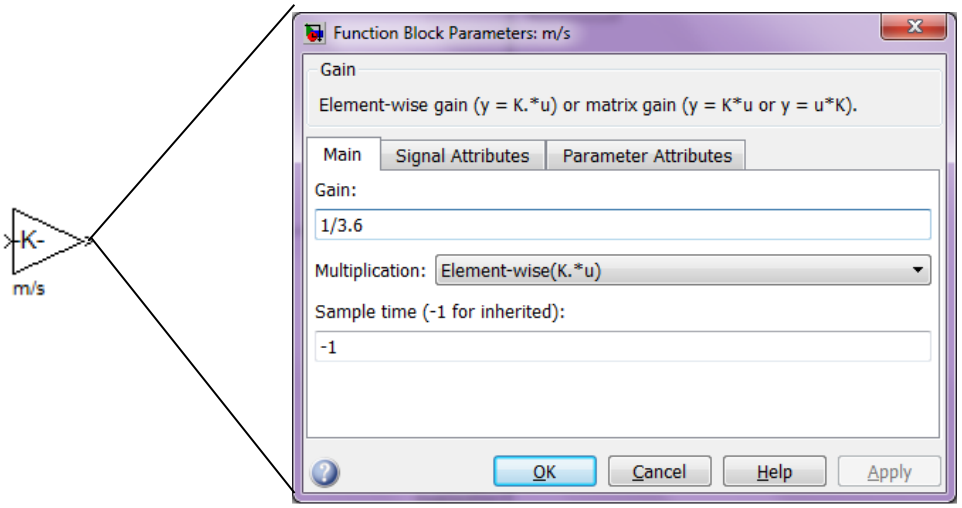

Figure 3.7– "m/s" block expanded into the "Gain" function box from *Simulink* used convert units of the speed profile

The next block related to the driving cycle does not perform any specific mathematical function, being responsible for sending the speed data in a "Structure with Time" format to the *Matlab* workspace to allow further treatment. This box appears many times in the whole model, for its graphical representation is only presented here in Figure 3.8.

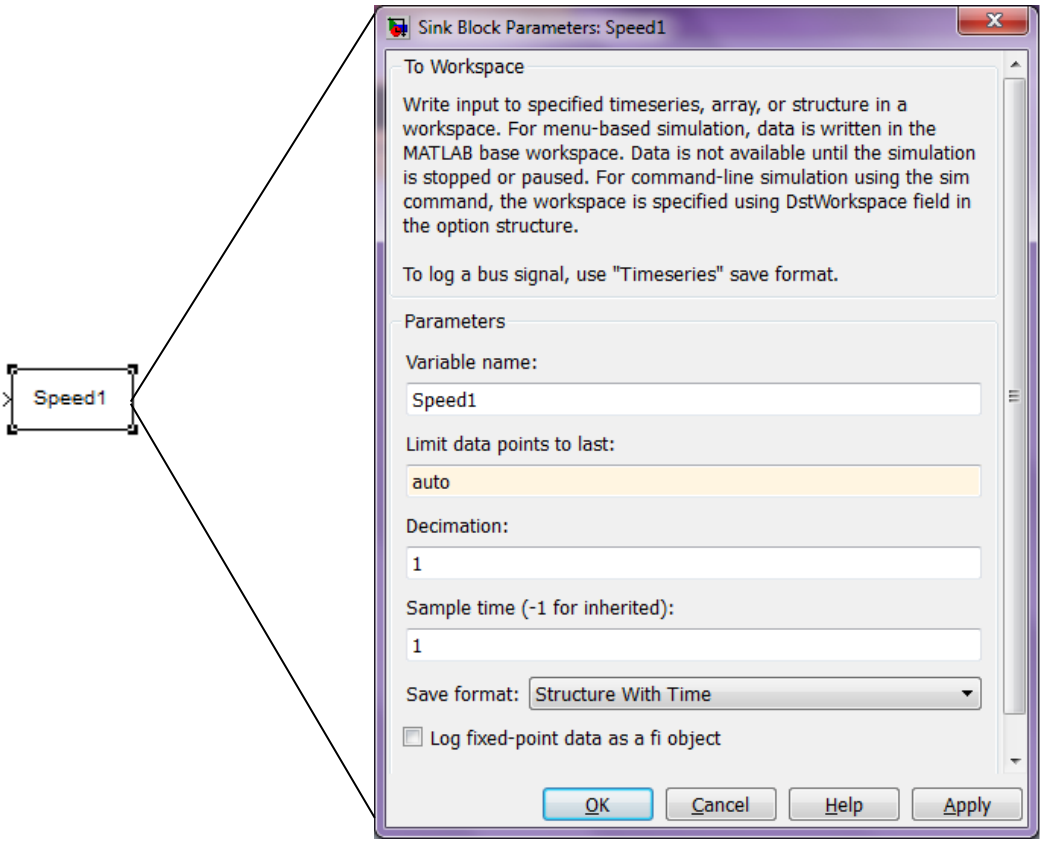

Figure 3.8- "Speed1" block expanded into the "To Workspace" function box from *Simulink* used to send data regarding the speed profile to *Matlab*

Similarly, there is another block called "Speed Out" representing the *Simulink* "Outport" function box, responsible for transferring the speed data out of this block and allowing it to serve as input for other blocks. This box also appears many times in the model and is only represented graphically in Figure 3.9.

The last block related to the driving cycle is "Speed2", which is basically a visual representation of the data to which it is attached, in this case, the speed profile. Again, this block appears many times in the model as it is a great way to follow the input signal behavior, and as such it is only represented graphically in Figure 3.10.

The driving cycle subsystem is also responsible for calculating the acceleration of the vehicle, which can be easily done by applying the time derivative on the speed. In *Simulink*, there is a specific function box for that called "Derivative" and is shown in Figure 3.11.

Acceleration also contains an "Outport", a "Scope" and a "To Workspace" blocks, such as the speed does.

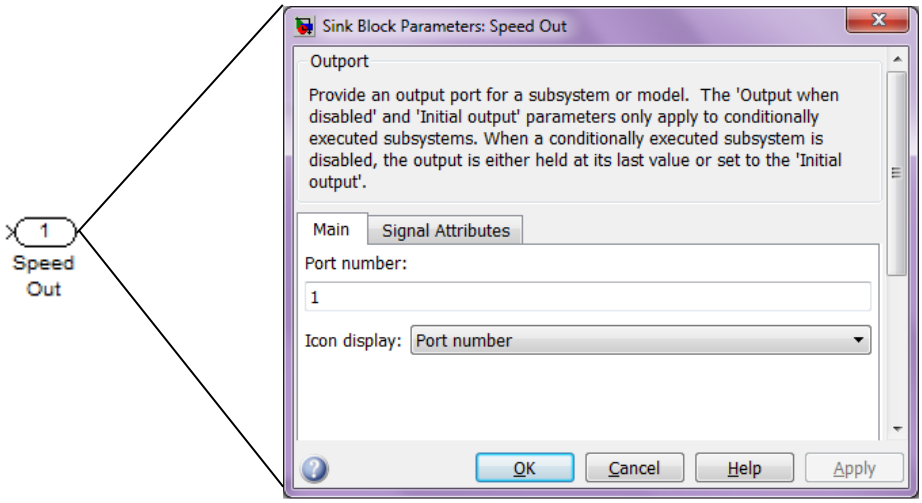

Figure 3.9– "Speed Out" block expanded into the "Outport" function box from *Simulink* used to enable speed data to be used by other subsystems in the model

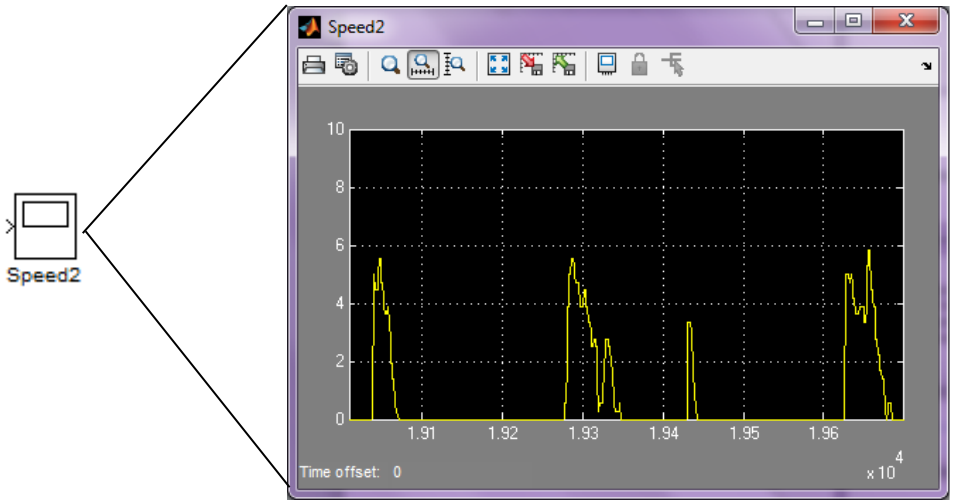

Figure 3.10- "Speed2" block expanded into the "Scope" visualization box from *Simulink* used to follow the input signal behavior along the model

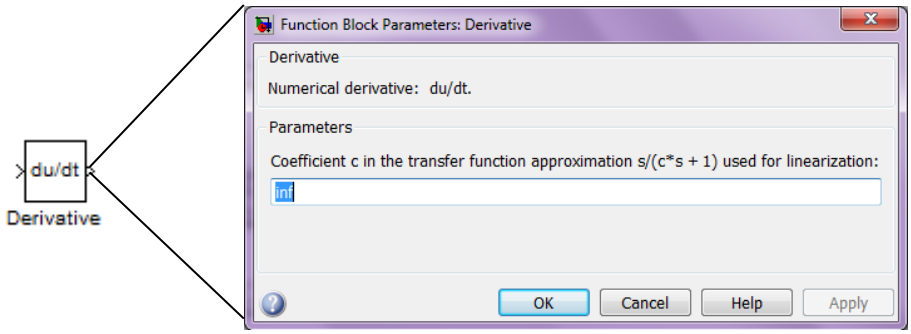

Figure 3.11- "Derivative" block expanded into the "Derivative" function box from *Simulink* used to apply a numerical derivative du/dt, being "u" the input signal "speed"

3.2.2.2 Subsystem 2: Tractive Force

The tractive force subsystem is responsible for handling all calculations related to the forces involved in moving the vehicle forward, whenever promoting resistance to the movement or facilitating it (case of the hill climbing force when the vehicle goes down a slope). This subsystem schematic is presented in Figure 3.12.

The tractive force subsystem has two inputs represented by the "Inport" number 1, accounting for speed and number 2, for acceleration. Every time a signal has to be received from another subsystem, the "Inport" block does the trick. Figure 3.13 shows the "Inport" block "Speed In" expanded into the correspondent *Simulink* function box in order to represent this function category for the whole model, once it appears many times.

Rolling resistance force calculation is one of the functions performed by this subsystem. After receiving the speed signal through the "Speed In" block, this input signal goes to the "Rolling Resistance" block represented by the "Fcn" *Simulink* function box. This box allows the formulation of any mathematical function using the input signal, represented by "u(1)" in the "Expression" field, as observed in Figure 3.14. The "Expression" field in this case is filled with the formulation of the rolling resistance force, expressed in eq. 3.1 and its respective coefficient equation in 3.2.

For the *Simulink* model, the mass of the bus is decomposed in three different parameters: *mb, ms and mp*. It was done so in order to allow modifications in the energy storage device mass that the bus carries and on the number of passengers for evaluation purposes. Thus the bus structure weight is *mb,* the energy storage weight *ms* and the passengers' weight *mp.*

Another function represented in this subsystem is the aerodynamic drag force, which schematic is shown in Figure 3.15. According to equation 3.3, this force is calculated by multiplying the square of the speed (represented by the "u^2" block), the air density (ξ), the aerodynamic drag coefficient (Cw), the vehicle frontal area (A) and further applying the *0.5* factor, being these variables represented by the "aerodynamic drag" block.

Figure 3.16 represents the "v^2" block and its correspondent *Simulink* function box "Math Function". This box allows the choice to use many different mathematical functions, being "square" the chosen one for this case. Figure 3.17 shows the "aerodynamic drag" block represented by the *Simulink* function box "Constant". The field "Constant Value" can either be filled up with a single constant or an expression that represents a constant, such as this case is. At last, Figure 3.18 describes the "Aerodynamic Drag Final" block expanded into

the “Product” function box from *Simulink* used to perform the multiplication of the inputs to the block. The number of inputs is defined in the “Number of Inputs” field.

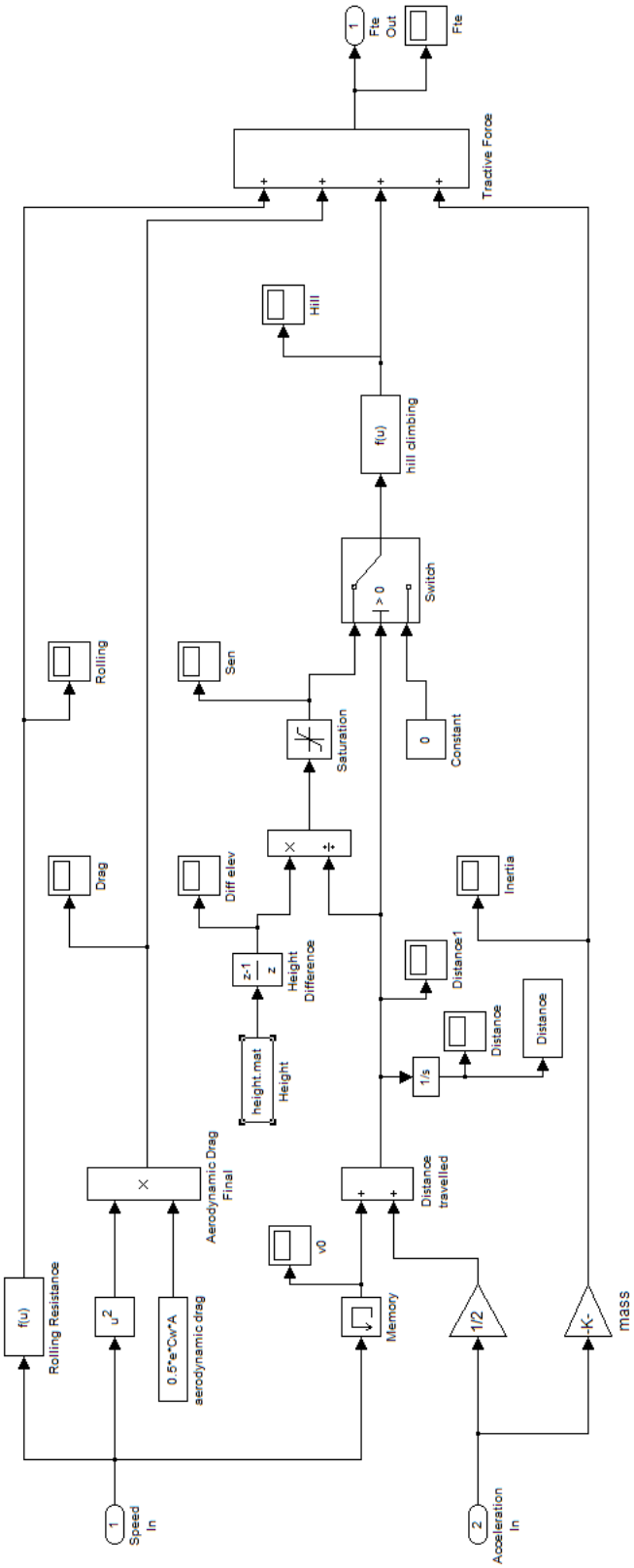

Figure 3.12– Tractive force schematic block in *Simulink*

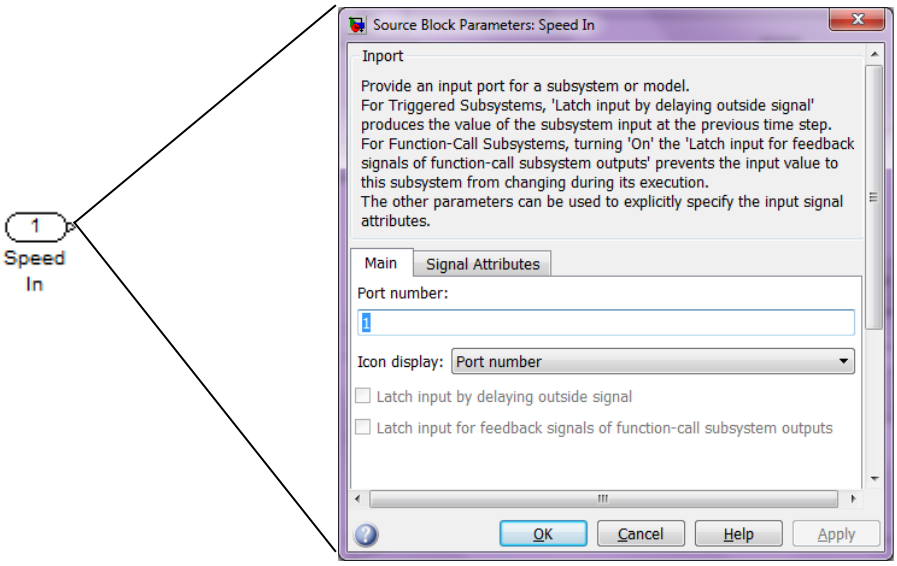

Figure 3.13- "Speed In" block expanded into the "Inport" function box from *Simulink* used to enable the speed signal coming from the "Speed/Acceleration" subsystem to enter the "Tractive Force" subsystem

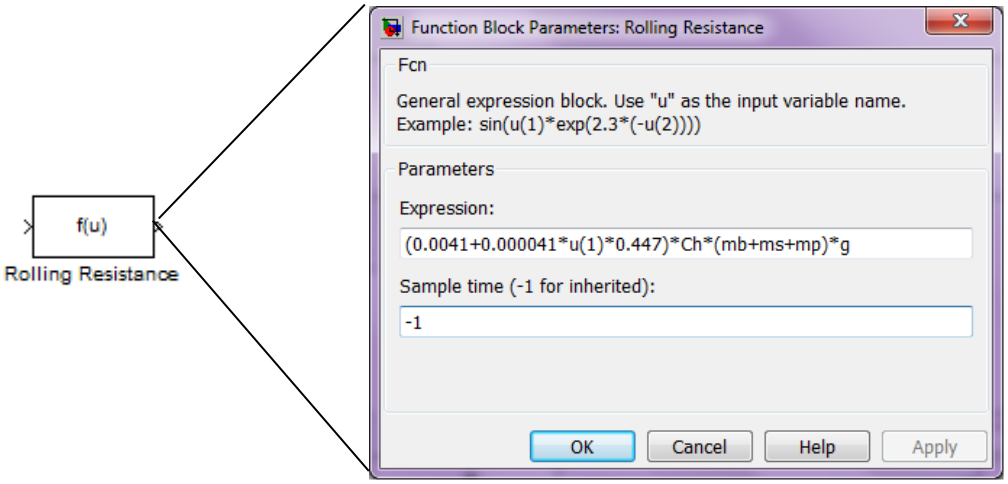

Figure 3.14- "Rolling Resistance" block expanded into the "Fcn" function box from *Simulink* used to apply the mathematical equation representing this force, being "u(1)" the input signal "speed"

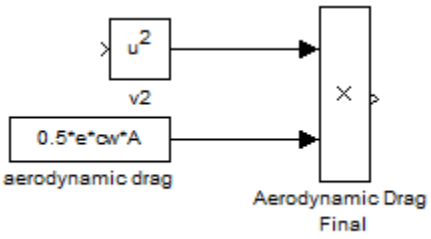

Figure 3.15- Aerodynamic drag force calculation *Simulink* schematic

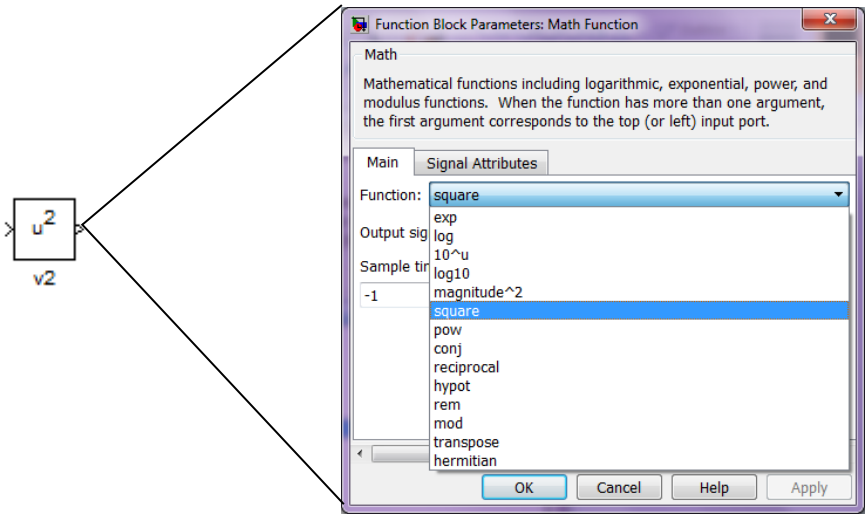

Figure 3.16– "v²" block expanded into the "Math Function" function box from *Simulink* used to apply different mathematical functions to the input signal "speed", being "square" the chosen function

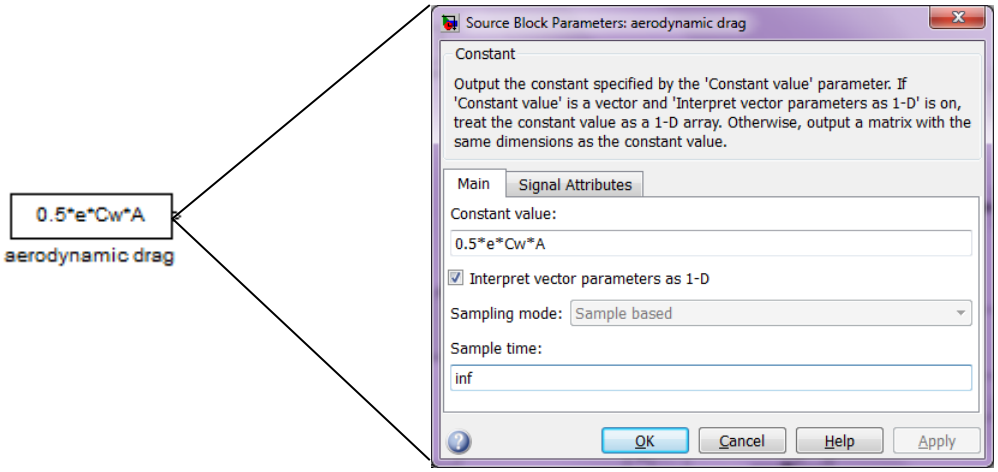

Figure 3.17– "aerodynamic drag" block expanded into the "Constant" function box from *Simulink* used to introduce a constant (or its representative function) to be further used in other calculations

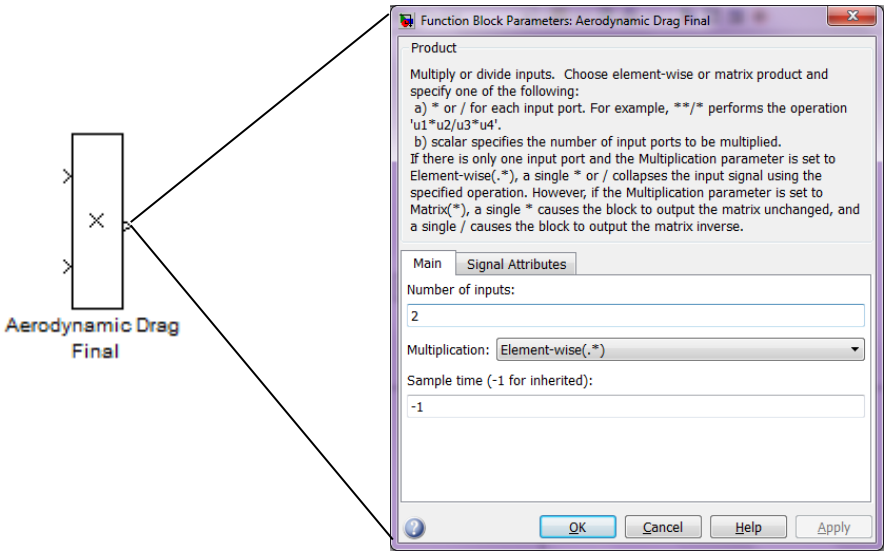

Figure 3.18- "Aerodynamic Drag Final" block expanded into the "Product" function box from *Simulink* used to perform the multiplication of the inputs to the block

The third component of the tractive force is the acceleration force. In *Simulink*, the operation is done by applying the "Gain" block equivalent to the mass of passengers (*mp*) to the input signal "acceleration", represented by the "Inport" block called "Acceleration In". The next operation is to apply the mass factor to the mass of the bus (including the batteries: *mb+ms*), which was done using the "Fcn" box named "Mass Factor". This box contains the code line "*(1.04+0.0025*(u(1)^2))*(mb+ms)*", being its first part responsible for the mass factor expression itself (Eq. 3.8) and *u(1)* accounting for the input signal "Gear" (introduced by the "Inport Gear In"). Figure 3.19 shows the graphical representation of this component in *Simulink*:

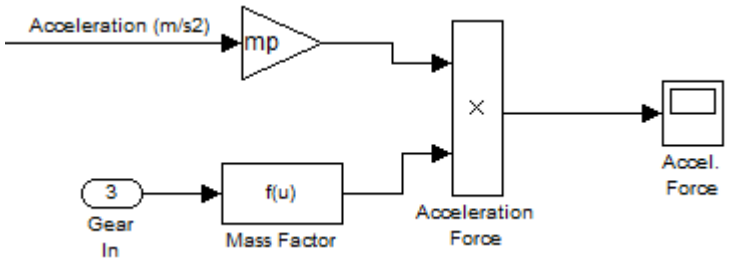

Figure 3.19- Acceleration force calculation *Simulink* schematic

At last there is the calculation of the hill climbing force, which although its equation (3.4) looks pretty simple, it demanded some extra work to be translated into *Simulink*. To begin with, the hill climbing force schematic in *Simulink* can be observed in Figure 3.20.

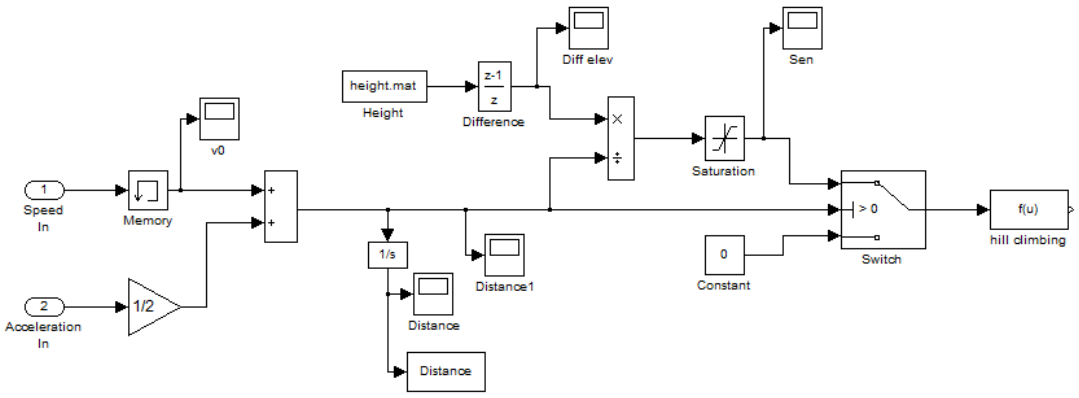

Figure 3.20– Hill climbing force calculation *Simulink* schematic

The main concern in calculating the hill climbing force is to find the sine of the road angle. Since data for altitude come in height values, and not angles, a solution for deducting this angle sine from height had to be found. In this sense, the path followed was applying the basic concept of a trigonometric function, which is: considering a right triangle, the division of the opposite *cathetus* (height) by the hypotenuse (distance travelled) is equal to the sine of the angle ($sin\,\varphi$). Figure 3.21 shows this relationship.

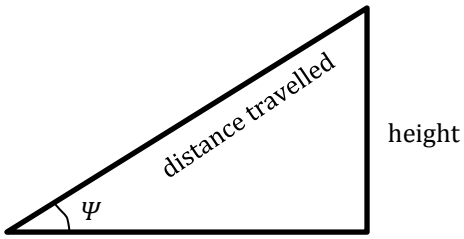

Figure 3.21– The right triangle and its components: concept application to the vehicle hill climbing force calculation

The height data is introduced in the model the same way as speed was in the first presented block: through a *height.mat* file representing height values for each second, making use of the "From file" block. The distance travelled for each second has to be calculated, taking into consideration one of the main kinematics equations presented below:

$$distance = v_0\, t + \frac{1}{2}\, a\, t^2 \qquad 3.28$$

where:

$v_0 =$ initial speed (m/s)

$t =$ time step (s)

Heading back to *Simulink*, the schematic representation of Eq. 3.28 can be observed in Figure 3.22. The two necessary inputs were previously introduced in the beginning of this subchapter, so there was no need to perform this action again. To extract v_0, it was necessary to add a "Memory" block from *Simulink*, which basically applies a one-step delay on the input, being the output its previous input value; the memory block together with its expanded function box window is shown in Figure 3.23.

Because the *time step* variable is always one second, there was no need to add the variable "*t*" to the *Simulink* schematic. At last, a "Gain" function block was applied to the acceleration input signal to account for the factor "1/2" of Eq.3.28, being the final calculation for distance travelled represented by the "Distance travelled" box, performing the sum of the inputs to the block, in this case, both parts of the equation. The number of inputs to the block is defined in the "List of signs", using "+" if the input should be summed up to the other input or "-" if it should be subtracted, as it can be seen in Figure 3.24.

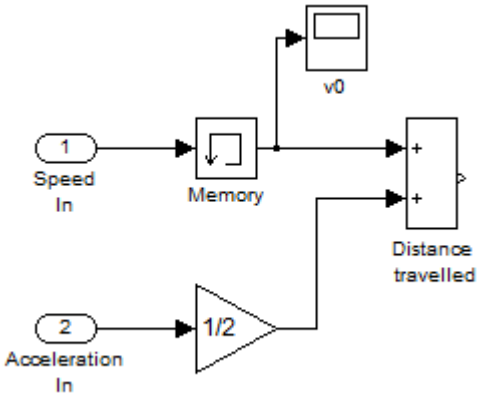

Figure 3.22– Distance travelled calculation *Simulink* schematic

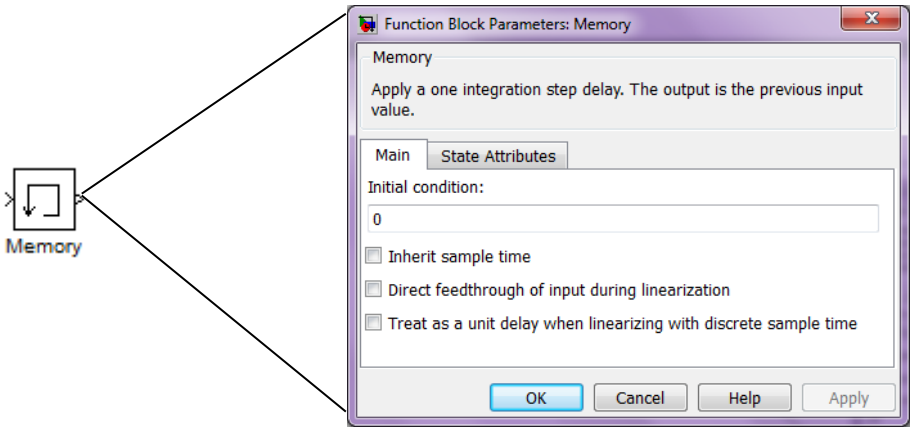

Figure 3.23- "Memory" block expanded into the "Memory" function box from *Simulink* used to apply a one-step delay on the input

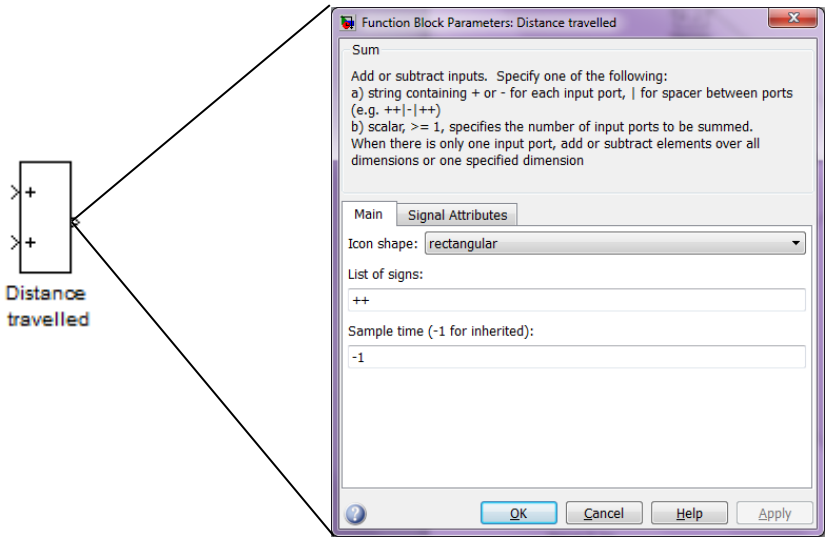

Figure 3.24- "Distance travelled" block expanded into the "Sum" function box from *Simulink* used to perform the sum of the inputs to the block

As previously mentioned, height or elevation data is provided for each second of the bus operation but for effects of calculating the hill climbing force, what is required is the difference between two consecutive elevation points, following the logic for the distance

travelled. To perform this action in *Simulink*, a function block named "Difference" had to be applied to the input signal coming from the file *height.mat* and the characteristics of this block can be observed in Figure 3.25.

Being in possession of the height difference and the distance travelled data, a "Product" function block can be applied to promote the division of the first by the last and the outcome is the sine of the angle. Due to possible inconsistencies in the data (e.g., missed steps in the elevation profile), a saturation of the sine signal is included to assure that the interval for the angle sine ranges between -1 to +1. The "Saturation" function block together with its expanded view is presented in Figure 3.26.

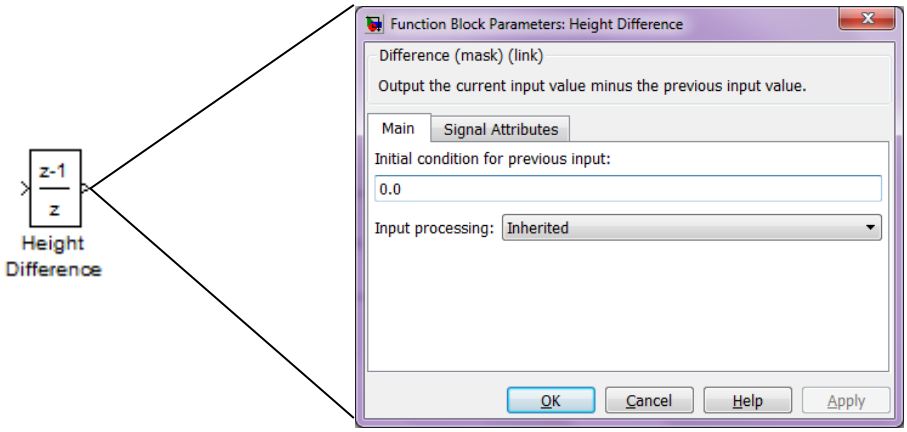

Figure 3.25- "Height Difference" block expanded into the "Difference" function box from *Simulink* used to output the current input value minus the previous input value

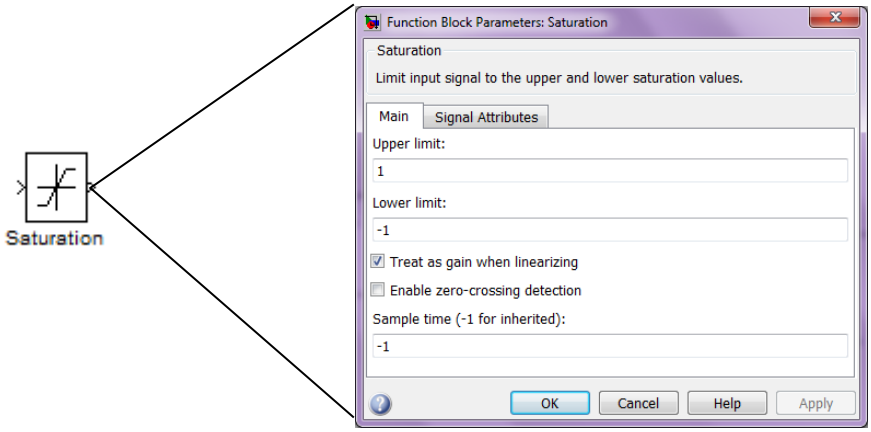

Figure 3.26- "Saturation" block expanded into its corresponded function box from *Simulink* used to saturate the sine signal to the interval of -1 to +1

Whenever the distance travel is zero (vehicle is stopped), an error occurs once it is the denominator of the sine formula, thus resulting in an inexistent output. In order to avoid problems in the calculation of the hill climbing force, the "if" logic had to be used, represented in *Simulink* by the block "Switch", according to Figure 3.27. Therefore whenever "Distance Travelled" (input 2) is greater than 0, the signal passes through input

1 (outcome of the sine calculation). Otherwise the "Switch" block let the signal of input 3 pass, chosen to be the constant 0.

The hill climbing force can be finally calculated. Equation 3.4 is translated to *Simulink* by using the already presented "Fcn" function block (Figure 3.14), filling up its "Expression field" with the code line "*(mb+ms+mp)*g*(u(1))*", being u(1) the input signal represented by the sine of the angle.

At last, the tractive force (F_{te}) is calculated by summing up the signals for rolling resistance, aerodynamic drag, acceleration and hill climbing forces using the "Sum" function block, which is similar to the one from Figure 3.24, except for the "List of signs" field, which is filled up with "*++++*". There is also an "Outport" called "Fte Out" to allow the F_{te} signal to be used by other subsystems.

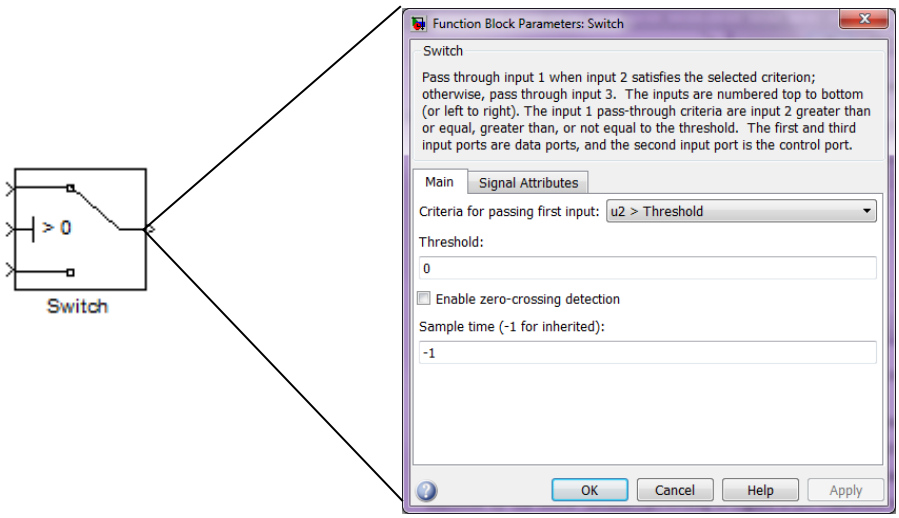

Figure 3.27- "Switch" block expanded into its corresponded function box from *Simulink* used to control the input signal according to input 2 criterion satisfaction

3.2.2.3 Subsystem 3: Gear

The Gear subsystem is responsible for defining the final value for the gear (G) to be considered in the calculations, whenever this parameter is requested. It is relevant to point out that there are two kinds of incoming gears: from the gear box and from the differential. The gear box has two different gear ratios, being the first ratio named "*g1*" and the second ratio, "*g2*". The differential ratio parameter is called "*gd*". The *Simulink* schematic for the Gear subsystem is presented in Figure 3.28.

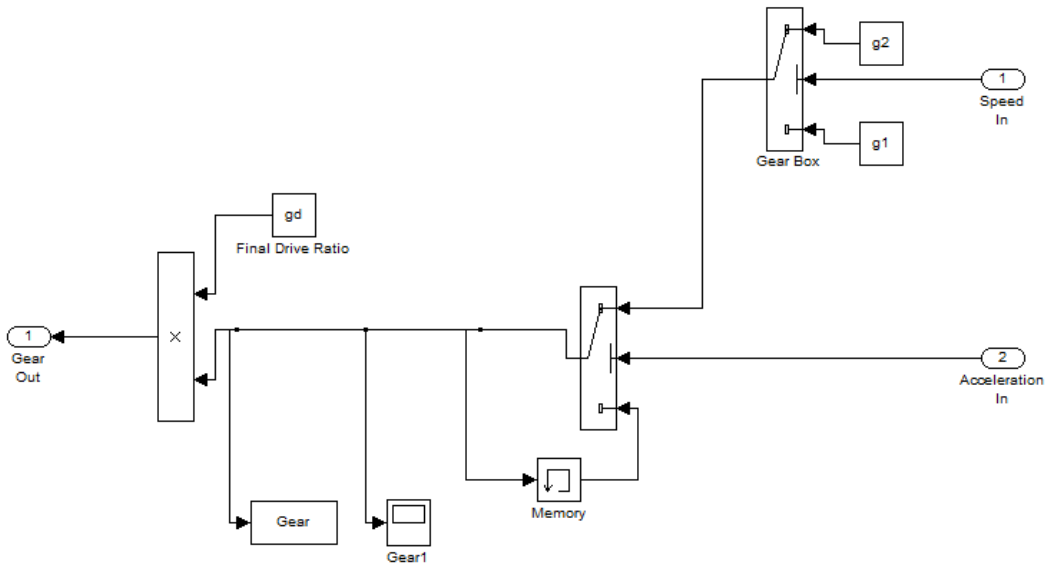

Figure 3.28– Gear subsystem *Simulink* schematic

What dictates whether the gear box ratio to be used is *g1* or *g2* is the speed of the bus, thus a "Switch" block is used, called "Gear Box", to control the gear ratio from the gear box output. Whenever input 2 (speed signal from the "Inport Speed In") is greater than the bus critical speed, *wc*, the output signal belongs to input 1 (*g2*). Otherwise, the signal that passes through the block belongs to input 3 (*g1*). Both *g1* and *g2* are represented in *Simulink* as a "Constant" block.

However, the gear shift modeling presented on the previous paragraph does not work the same way for braking episodes, being restricted to only when the bus accelerates or is in constant acceleration. Whenever the bus is decelerating, the gear remains constant until the bus finally stops (verified in the bus operational data). For this reason, the modeling included another "Switch" function block, having as main parameter the acceleration profile (introduced into this subsystem through the "Inport Acceleration In"). The passing signal through the "Switch" block is controlled in a way that whenever acceleration is equal or greater than 0, the outcome from the "Gear Box" passes through (input 1). Otherwise, input 3 is used, where the gear ratio value from the previous step is held and outputted; this is done by the use of the "Memory" function block (already presented in Figure 3.23).

After defining the gear ratio from the gear box, it should be multiplied by the differential ratio or final drive ratio *gd* to come up with a final value for the gear *G*. The "Product" function block is used, parameterizing it to account for two inputs. The final gear is made available for using in other subsystems through the "Outport Gear Out".

3.2.2.4 Subsystem 4: RPM/ Efficiency Block

The forth subsystem is responsible for handling the calculations to find the motor speed and the motor/controller efficiency, considered together for simplification reasons. Instead of what happened in the already presented subsystems, this block is quite straightforward to the equations involved, namely 3.11 and 3.12. The *Simulink* schematic for this subsystem is presented in Figure 3.29.

There are two input ports, "Gear In" and "Speed In", variables used to the calculation of the motor speed. There is a third component in this calculation and it is represented by a "Constant" block, being the content expressing the equation "*2 π r*". Then, the product of the gear, the speed and a factor of *60* (represented by a "Gain" block) should be performed, dividing the result by the "Constant" block output. The "Product" box performs all these operations and the output is the required motor speed for a certain driving cycle. In order to not run the risk of overpassing the bus technical limitations, a "Saturation" box was added and the interval of saturation is the one defined by the motor supplier: -5000 to 5000 rpm.

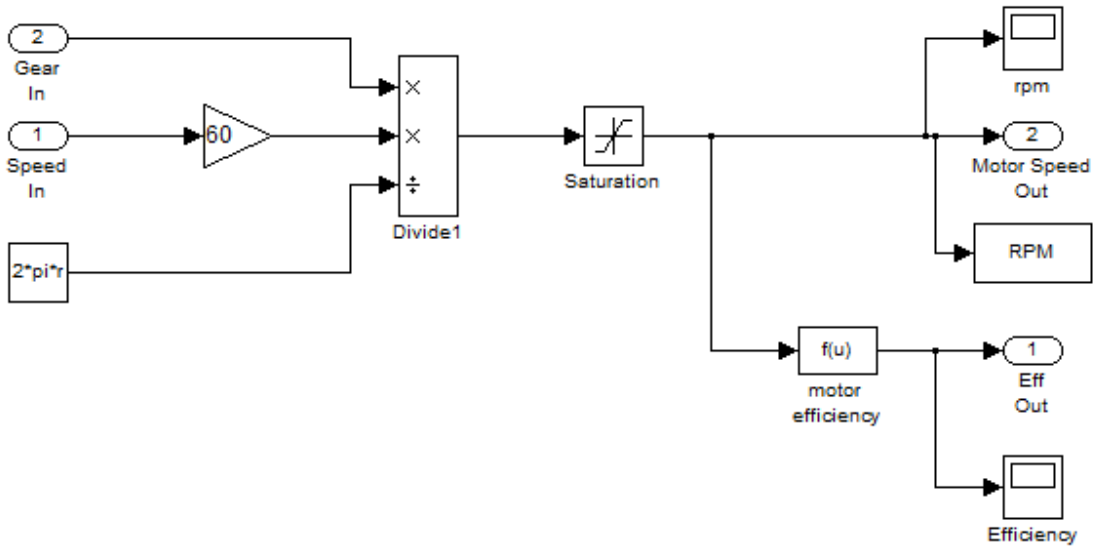

Figure 3.29– RPM/ Efficiency subsystem *Simulink* schematic

The motor efficiency equation has as unique input variable the motor speed, thus it enters a "Fcn" block named "motor efficiency". The code line inside this box resembles the equation presented, as follows: "*(-3*(10^(-8))*(u(1)^2)) + 0.0002*u(1) + 0.638*". Both the motor speed and the motor efficiency have "Outport" called "Motor Speed Out" and "Eff Out", respectively.

3.2.2.5 Subsystem 5: Power

This subsystem is responsible for calculating the required power from the batteries to perform a specific driving cycle and can be observed in Figure 3.30. Similar to the fourth presented subsystem, the equations involved are easily applied in *Simulink*. Equation 3.10 has already shown that to calculate the power disregarding efficiencies (P_{te}), the tractive force F_{te} should be multiplied by speed. *Simulink* performed this operation by using the "Product" block. Both inputs enter this subsystem through two "Inport" named "Fte In" and "Speed In".

For applying the efficiency factor η_m (imported parameter from the previous subsystem through "Inport Eff In"), a "Switch" block had to be used, once the way it is done depends on the P_{te} signal. Whenever $P_{te} > 0$, input one is used where η_m is divided from P_{te}; otherwise, the passing signal belong to input 2, where η_m is multiplied by P_{te}.

The next step in this subsystem is to calculate the power required by the accessories. As previously mentioned in section 3.2.1.7, the most demanding accessories are the air conditioning, the steering pump and the air compressor. The air conditioning can have two possible operating regimens: off, with no consumption and on, requiring 3360 W of power.

Both the steering pump and the air compressor have a minimum requirement of 800 W and 1200 W respectively. These minimum consumptions happen when the bus is in regular operation, i.e. motor is operating and the route is linear (steering pump case) and/or there is no need to use the compressed air (e.g., doors kept closed). In case there is the need of harsh maneuvers, for instance, at sharp turns, the steering pump requirement can get to a maximum of 5500 W of power and for the presence of many episodes of doors opening or the need of braking constantly; the air compressor can require a maximum of also 5500 W.

Therefore the required power from accessories is treated in *Simulink* in two ways: power from the steering pump and air compressor together and power from the air conditioning. In the first case, speed was used to discriminate the power requirements for when the bus is stopped (minimum consumption) or in movement (higher than the minimum and possibly maximum). This is done by the use of a "Switch" block: whenever speed (introduced variable into the subsystem through "Inport Speed In") is equal to zero, input 3 from the "Switch" block is used and the signal that passes through is equivalent to the sum of the minimum requirements for both the steering pump and air compressor (2000 W). For speed values different from zero, input 1 is used and the passed signal is another value in a "Constant" block higher than the minimum. Following the resulting

signal from the "Switch" block, it is added (through the use of a "Sum" block) to the value for the air conditioning power requirement, introduced using also a "Constant" block, concluding the calculation for the accessories power requirement P_{acc}.

P_{acc} signal is added to the P_{mot} signal through a "Sum" block, resulting in the total power required from the batteries P_{bat}. It is then transformed into kW ("Gain" block of "*1/1000*"), once it was in Watts, and further saturated to -150 kW to +150 kW due to technical limitations of the bus. It was created an "Outport" for the P_{bat} variable, called "Power (Pbat) Out".

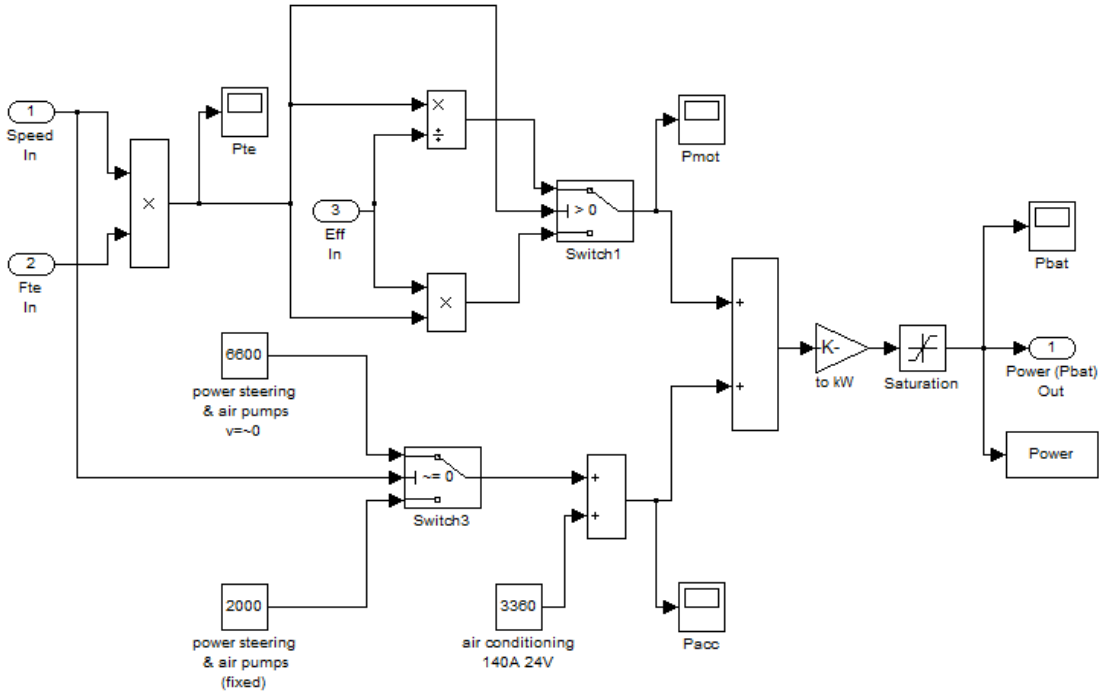

Figure 3.30- Power subsystem *Simulink* schematic

3.2.2.6 Subsystem 6: Torque

Similarly to the power subsystem, the torque is easily calculated in *Simulink*, being the modeling a simple representation of its mathematical equation 3.16. This subsystem is composed of three "Inport": "Pbat In", "Motor Speed In" and "Speed In". It can be observed in the torque calculation equation that the motor speed is a denominator, which means it can never be zero or it would cause a mathematical inconsistency.

To solve this issue, a "Switch" block was used, having the speed as the parameter on its main port: whenever speed is different from zero, the input port number 1 should be used; otherwise, input number 3 is the chosen one. Input port number 1 receives the signal from the motor speed whilst input port number 3 lets a constant number 1 to pass through, represented by the function box "Constant".

Torque equation is represented by the "Torque" block in Figure 3.31, which is the "Product" *Simulink* function box. The first input to this box is P_{bat}, which is converted back to Watts ("Gain" block, "1000"), divided by the motor speed (second input) and also by a factor represented by the code line "*2*π /60*" ("Constant" block on the third input port). The resulting output has its signal saturated; similarly to what happens to the motor speed and power, finishing with the "Outport" called "Torque (N.m) Out". Because this block is close to one of the final scopes, (Performance Scope), "Outport" for the motor speed "RPM out" and power "Pbat (kW) Out" were also created.

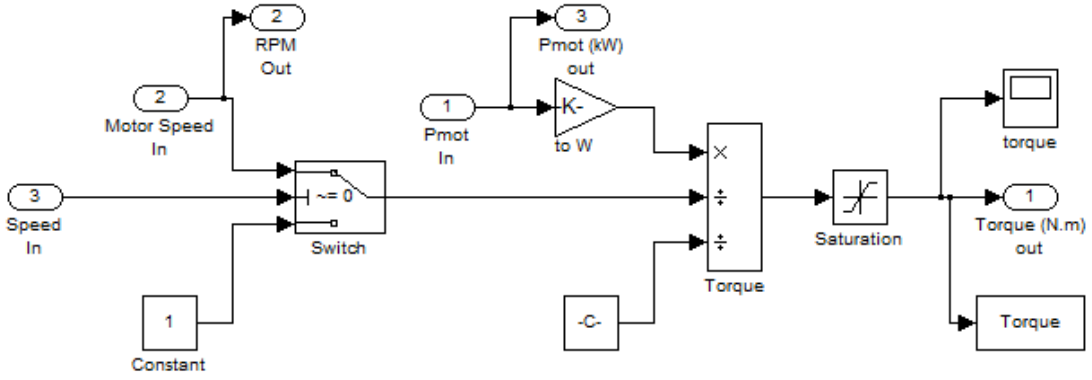

Figure 3.31- Torque subsystem *Simulink* schematic

3.2.2.7 Subsystem 7: Battery

The seventh and last subsystem may be probably the largest, once many of the outcomes are visually presented in the Battery Scope, namely battery current and voltage and the state-of charge; energy consumption is also calculated in here but its visual representation goes to the Performance Scope instead. According to the specific functions this subsystem develops, each one of them is presented separately, starting with the battery current calculation (called Segment 1).

The battery current calculation involves mainly two different equations according to the flow of the current in relation to the battery: 3.19 for current flowing "out" (motoring mode) and 3.23 for current flowing "in" (generator mode). Segment 1 *Simulink* schematic is presented in Figure 3.32.

Power gets into the subsystem through the "Inport Power In" and transformed to Watts by a "Gain" block. This output signal gets into a "Fcn" block called "4RP(d)" containing the line code "*4*R*u(1)*" - being *R* the internal resistance of the battery and "*u(1)*" the input signal to the box - to be further subtracted from "E^2" ("Constant" block containing the nominal voltage "*E*" followed by the "Math Function" block for "$u(1)^2$"). The resulting signal feeds

another "Fcn" block to perform the square root of its input. This output is subtracted by the "*E*" signal in another "Sum" box.

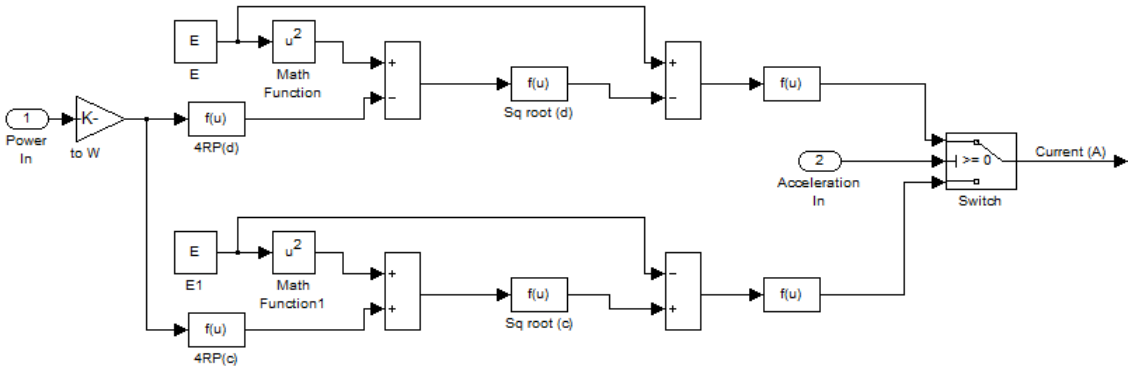

Figure 3.32– Segment 1 of the battery subsystem *Simulink* schematic to represent the calculation of the "preliminary" battery current

Similarly, the battery current for the generator mode uses the same *Simulink* boxes, with differences relying specially in the "Sum" blocks. The first "Sum" block calculates the sum of the "E^2" with the "Fcn" block called "4RP(c)" containing the code line "*4*R*u(1)*" while the second "Sum" block receives a negative "E" value and sums it to the square root of the output signal from the first "Sum" block. In both cases, what is missing is dividing the resulting signal by two times the battery resistance to finish the application of the mentioned equations.

However, it is relevant to point out that not only these functions were performed but also re-defined to accommodate the notation used in the data coming from the real bus. The conventional approach to define battery current signal is: whenever the current leaves the battery, it is considered positive and in episodes of current flowing into the battery, its signal is considered negative.

Data coming from the bus showed that they do not behave according the conventional approach, being "negative" the current flowing out of the batteries and positive whenever flowing in the opposite direction. Therefore, either for the motoring mode or the generator mode, the last "Fcn" block had the "minus" signal included in front of their equations in order to solve the abovementioned issue.

The computerized model encompasses a logic based on the acceleration value to decide whether the signal that passes is from the motoring or the generating branches. This is done by the use of a "Switch" block and the used parameter to perform this decision is acceleration ("Inport Acceleration In"). Whenever acceleration is equal or greater than zero, input number 1 from the "Switch" block is used, allowing the calculated signal from

the motoring mode to be used. In cases when acceleration is negative, input number 3 is used instead, and the calculated signal for the generating mode is passed through the "Switch" block.

Another interesting behavior of the battery current was discovered from the data analysis of the real bus. Whenever the bus decelerates and the speed fells below 2.5 m/s (or 9 km/h), no energy regeneration happened. In other words, the values for battery current in those cases were negative such as those from acceleration periods, instead of the expected positive values. In order to translate this new behavior into the *Simulink* model, a logic schematic had to be added to Segment 1 and is herein called Segment 2; it can be observed in Figure 3.33.

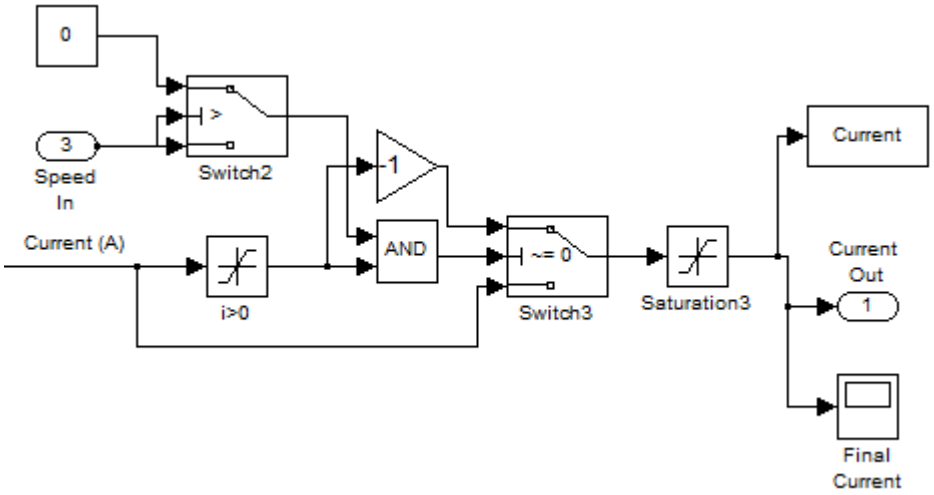

Figure 3.33– Segment 2 of the battery subsystem *Simulink* schematic to represent the behavior of the battery current for speeds lower than 9 km/h

The "heart" of this segment is the "AND" box containing two inputs. Whenever both inputs have valid values (different from zero), the logic output is "1"; otherwise is "0". The "AND" block expanded into the "Logical Operator" function box from *Simulink* is shown in Figure 3.34. The first input to the "AND" block is the outcome of the "Switch2" block, which function is to let pass through speed values whenever lower than 2.5 m/s; otherwise, a "0" is outputted. The second input to the "AND" block is the stream of positive battery current values, being those the outcome of a "Saturation" block parameterized to perform this function (I>0).

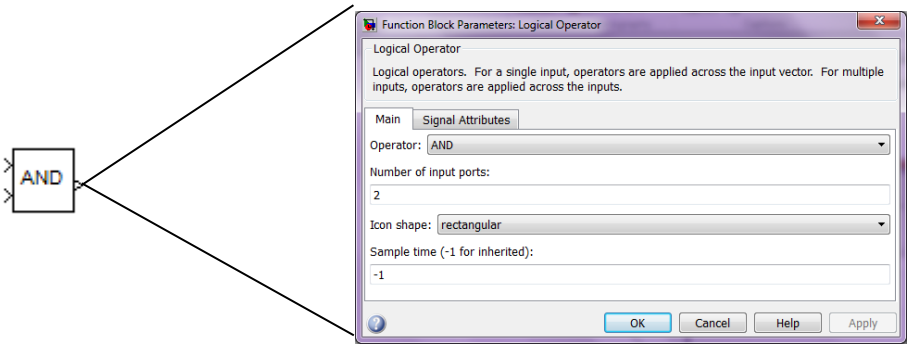

Figure 3.34- "AND" block expanded into the "Logical Operator" function box from *Simulink* used to perform the logical function "*AND*"

Now that battery current values are filtered so that only those belonging to periods where speed is lower than 2.5 m/s represents a valid (equal to 1) output from the "AND" block, it is time to finally compose the final battery current stream. This is accomplished by the "Switch 3" block: whenever the output from the "AND" block is valid (equivalent to 1), the positive battery current string value is multiplied by "-1" ("Gain") and the "Switch3" block outputs this outcome. Otherwise, the regular battery current value is outputted. The resulting signal from the "Switch3" block enters the "Saturation3" block so that battery current stays in the interval of -300 A to 150 A; this interval was defined during the calibration process of this model later in Chapter 5.

The next step in this subsystem is to calculate the battery voltage, being this part of the subsystem called Segment 3, presented in Figure 3.35. Similarly to the battery current calculation of Segment 1, two equations for battery voltage have to be considered: one for episodes where power is greater than 0 (Eq. 3.17) and another for negative power (Eq. 3.22). Thus the "Switch1" block performs this distinction, using the acceleration as its criterion threshold. It allows the signal from its first input to pass whenever acceleration is equivalent or greater than zero and on episodes of negative acceleration, the input from its third port is used.

The signal that gets through the first input of the "Switch1" block results from the "Fcn" block called "Voltage P>0", which code line is "*E-u(1)*R*", whilst the third input to the "Switch1" block is derived from another "Fcn" block called "Voltage P<0", being the function performed by it defined as "*E+u(1)*R*". The resulting signal is the battery voltage behavior that will feed the next segment to be presented (Segment 4).

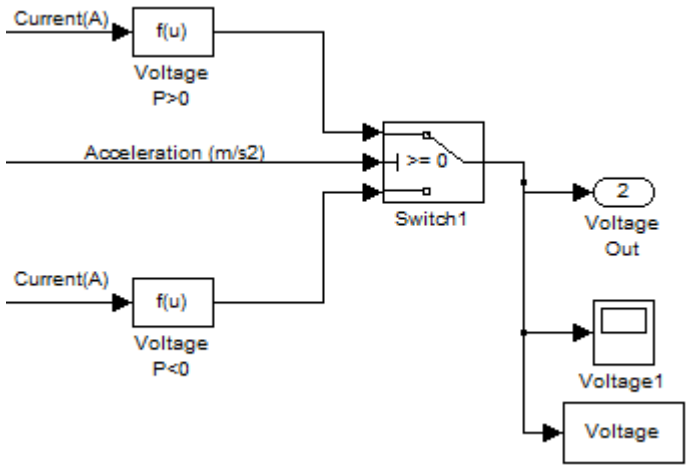

Figure 3.35- Segment 3 of the battery subsystem *Simulink* schematic to represent the calculation of the battery voltage

Segment 4 is responsible for the calculation of the energy consumption and the total energy that was regenerated, as it can be observed in Figure 3.36. This segment receives the values for the battery current from Segment 2 and those for battery voltage from Segment 3. Both signals are multiplied (according to Eq. 3.18) in a "Product" block and follows two different paths. The first branch serves as input to an "Integrator" function box of *Simulink*, which graphic representation expanded into the corresponding source box is shown in Figure 3.37.

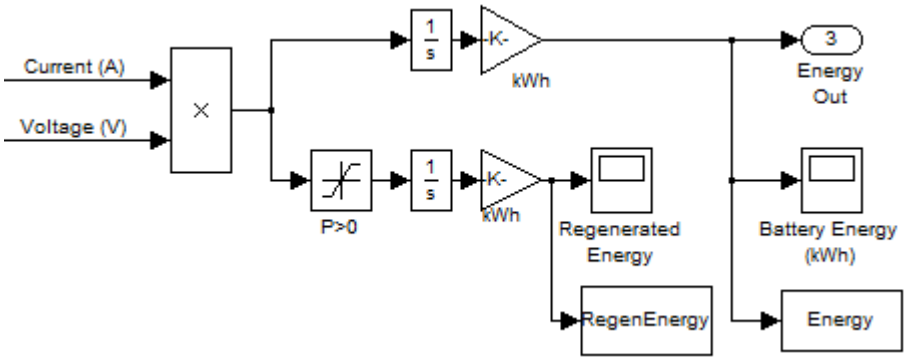

Figure 3.36- Segment 4 of the battery subsystem *Simulink* schematic to represent the calculation of the energy consumption and the regenerated energy

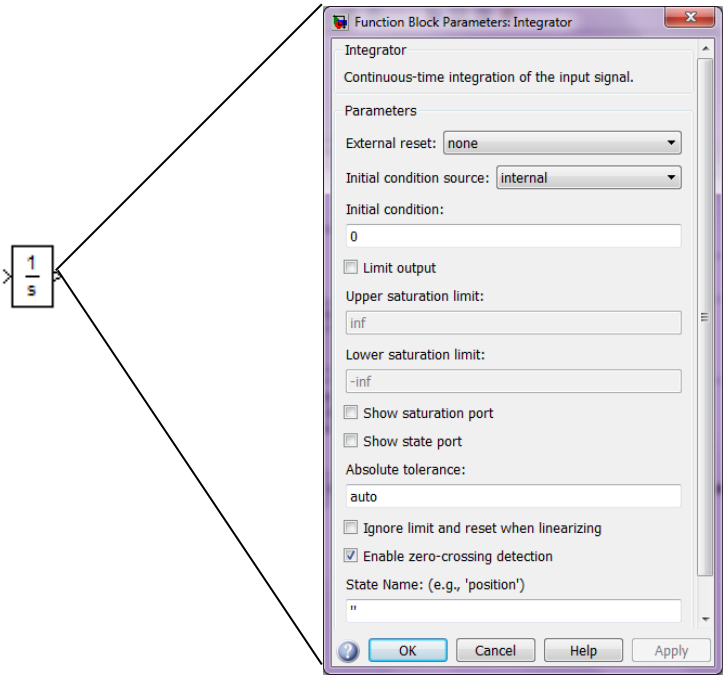

Figure 3.37- "Integrator" block graphic representation and the expanded corresponding function box parameters in *Simulink*

The "Integrator" box performs the numerical integration of the input signal, and its output follows to a "Gain" block, so that it is converted to kWh. Besides that, this block is also responsible for changing the signal of the input, transforming the negative values into positive and vice-versa. This is necessary once the battery current had its signals previously changed to be in accordance to the bus data, as already explained. Thus, the "Gain" block has as representative function "*-1/3600000*".

The second branch goes to the part of the segment responsible for calculating the total amount of energy that was regenerated. In order to do that, the signal is saturated so that only positive values pass through and then the integration happens, following a similar path to the energy consumption calculation.

At last, Segment 5 is responsible for calculating the state-of-charge (SOC) of the battery. Equations 3.20 and 3.21 are applied in *Simulink* in a slightly different manner, as it can be observed in Figure 3.38. The previously calculated current enters in a "Fcn" block, containing the code line "*(u(1)/3600)/Cp*100*", which represents the first equation entirely and part of the second equation. The integration of this signal is performed afterwards ("Integrator" block), and the resulting signal is added up ("Sum" block) to the initial SOC of the battery (defined in a "Constant" function box), so that the resulting signal represents the SOC of the battery in the end of the operation. After describing all the segments involved on the battery subsystem, Figure 3.39 shows the whole *Simulink* schematic for the battery modeling, containing all five segments and their connections.

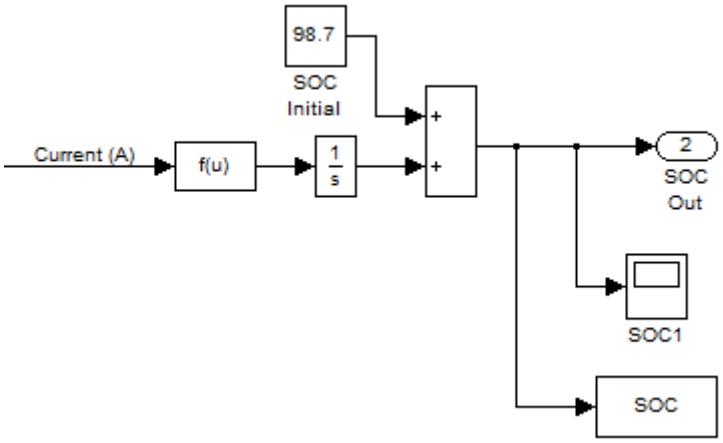

Figure 3.38- Segment 5 of the battery subsystem *Simulink* schematic to represent the calculation of the battery SOC

3.2.2.8 Results presentation

After performing a simulation run, the results are compiled and presented in two different scopes: Battery and Performance. The Battery Scope is responsible for the visual representation of the battery behavior, accounting for the current (A), voltage (V) and SOC (%) behavior curves; whilst the Performance Scope presents the behavior of different performance factors of the bus, namely Energy (kWh), Torque (N.m), Motor Speed (rpm) and Power (kW). Their visual representation in *Simulink* can be observed in Figure 3.40.

3.3 Parameters Definition

After presenting all the mathematical equations involved in the development of the electric bus conceptual model and their implementation in *Simulink*, it is necessary to define the values used for the mentioned parameters. Those values are presented in Table 3.1. The battery parameters are already accounting for their final value that is considering the number of cells in parallel and in series of the battery package.

In *Simulink*, all functions are performed using symbols for those parameters and not their actual values, as observed along this chapter. In this sense, a callback function in the form of a "*Matlab* Code (.m)" file has to be defined, containing all those parameters. Once it done, the *Simulink* model has to be parameterized so that this callback function runs as soon as the simulation starts, by using the option "InitFcn" in the model properties.

Figure 3.41 shows the file developed for this project. By having all parameters defined on a separate file, it guarantees that whenever a certain change is performed in a parameter, all involved equations containing this parameter will consider its correct value.

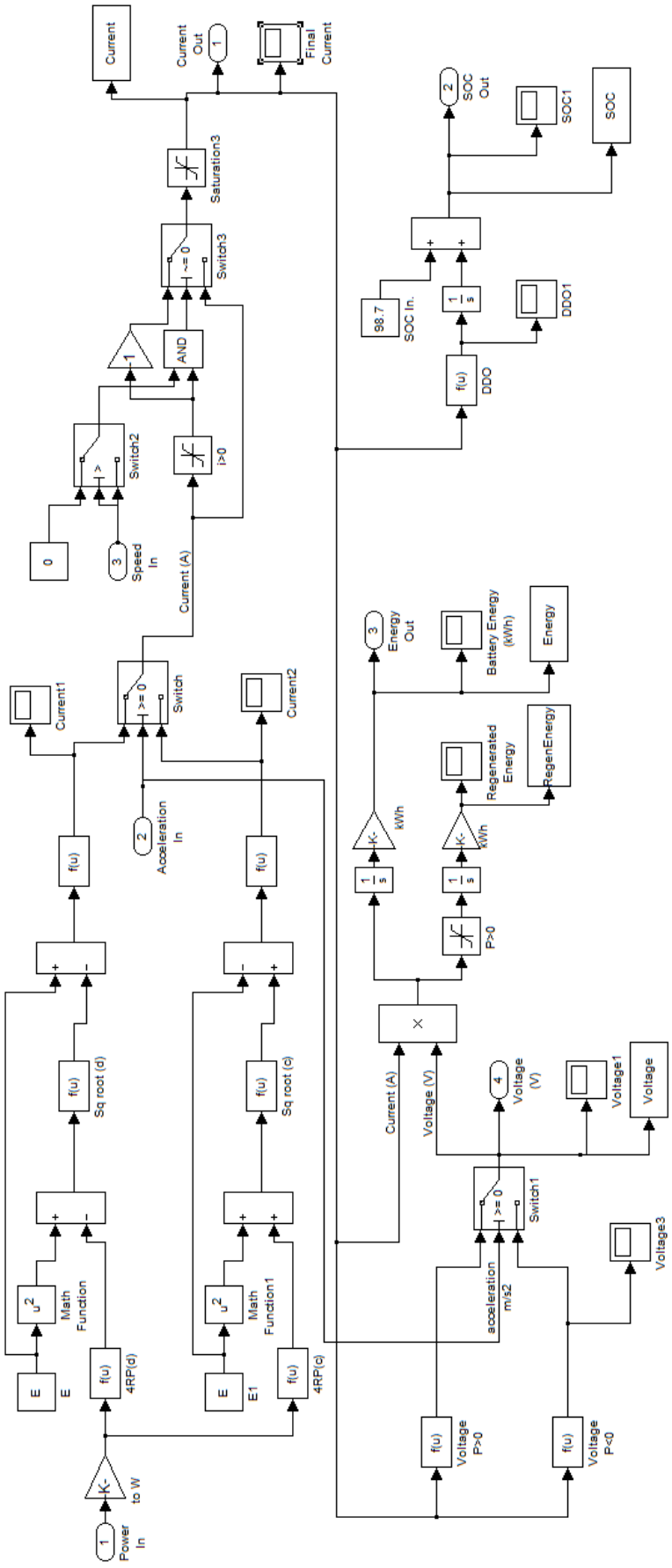

Figure 3.39- Complete battery subsystem schematic representation in *Simulink*

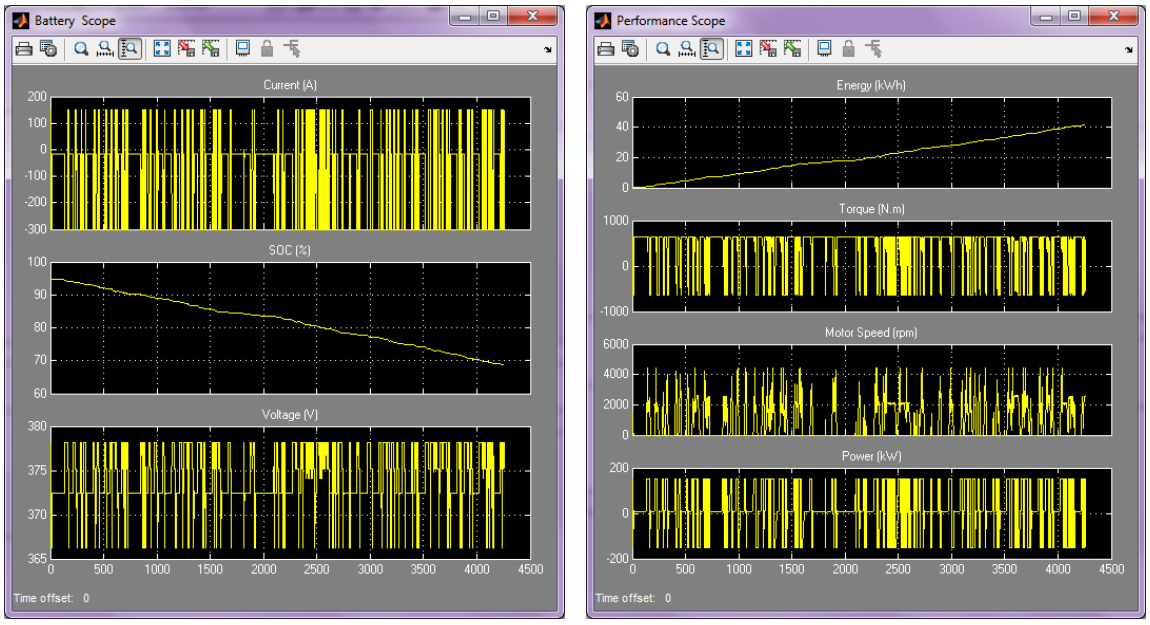

Figure 3.40– Representation for Battery Scope and Performance Scope in *Simulink*

Table 3.1– List of the parameters used in the simulation model

Parameter	**Symbol**	**Value**
Bus Mass	*Mb*	11055 kg
Batteries Mass	*Ms*	1411 kg
Passengers Mass	*Mp*	80 kg – 4581 kg
Road coefficient surface	*Ch*	1.2
Critical speed(Gear shift)	*Wc*	9.58 m/s
Gravity force	*g*	9.81 m/s^2
Aerodynamic drag coefficient	*Cw*	1.17
Air density	*ξ*	1.23 kg/m^3
Vehicle frontal area	*A*	6.5 m^2
Tire radius	*r*	0.548 m
1st Gear ratio	*g1*	3
2nd Gear ratio	*g2*	1
Differential Gear ratio	*gd*	8.83
Battery nominal voltage	*E*	372.2 V
Battery resistance	*R*	0.02
Battery nominal capacity	*Cp*	420 Ah
Number of Cells in Parallel	*np*	140
Number of Cells in Series	*ns*	112

```
%Parameters for electric bus performance

mb = 11055;    %(kg) Mass of the bus, excluding the energy storage device(s)
ms = 1411;     %(kg) Mass of energy storage device(s)
mp = 4581;     %(kg) Mass of the passengers
Ch = 1.2;      % Road coeficient surface
wc = 9.58;     %(m/s)Critical speed/Gear shift
g = 9.80665;   %(m/s2) Gravity force
Cw = 1.17;     % aerodynamic drag coefficient
e = 1.22521;   %(kg/m3) Air density
A = 6.5;       %(m2) Vehicle frontal area
r = 0.548;     %(m) Wheel radius
g1 = 3;        % Gear ratio 1st box
g2 = 1;        % Gear ratio 2nd box
gd = 8.83;     % Gear ratio differential
E = 372.2;     % (V) Battery Nominal Voltage
R = 0.02;      % (ohms) Battery Resistance Discharging
Cp = 420;      %(Ah) Battery Nominal Capacity
```

Figure 3.41– *Matlab* Code (*.m*) file to be used as a callback function for the simulation

3.4 Conclusions

This chapter presented in detail the development of the electric bus conceptual model and its further implementation in the software called *Simulink*. It could be noticed that the conceptual model differs significantly from the computerized model, especially regarding the logic that had to be developed in *Simulink* as a way to mimic the behavior of the bus.

For instance, it could be observed that the attempt to represent the regenerative braking in the computerized model has demanded a complex logic, whereas the conceptual model just dictates that whenever the power is negative than the bus is recovering. From the observations of the real bus data, the simple conceptual model approach did not correctly represent what happens in reality. Similarly to this example, there are others that were thoroughly described in this chapter.

In order to promote a more realistic representation of the performance of the electric bus in the urban environment, it becomes imperative to represent the routes that the bus performs in a traffic simulator. In this sense, the next chapter presents the requirements that a traffic simulator should have, so that it can be integrated to the *Simulink* model. The chosen traffic simulator is presented in detail, together with the used integration framework and the necessary adjustments that had to be done in the *Simulink* model.

Chapter 4

Development of the Simulation Integrated Platform

4.1 Summary

This chapter focuses on the integration of the computerized model of the electric bus, which was developed in the previous chapter with a microscopic traffic simulator. An overview of the latter is provided together with the architecture devised for the integration of both models. The required adaptations and extensions for the integration to work are also described.

4.2 The Traffic Simulation Domain

The previous chapter presented the electric bus simulation model representing the real bus dynamics. By having a matrix of speed versus time and another one of elevation versus time, the *Simulink* model could be run and the performance results analyzed. This worked perfectly well for the calibration and validation of the model, where a pre-defined route was performed by the real bus and data were gathered so as to feed the simulation model, which in return provided results to be compared.

However, the main objective of this thesis is to assess the performance of the bus immersed in the urban context, performing different routes, stopping at bus stops for passengers boarding and alighting, interacting with other vehicles, stopping on traffic lights, etc. In this sense, *Simulink* alone could not provide this level of analysis and this is when traffic simulation comes to scene. This section provides an overview of the different kinds of traffic simulation regarding their level of aggregation.

4.2.1 Macroscopic Simulation

Macroscopic simulation models are at the highest level regarding the aggregation scale of traffic models (depicted in Figure 4.1), being concerned with flow rates and densities, e.g. vehicles/hour on a certain street as a metric for flow rates (May 1990) and vehicles/kilometer as a measure for density (Maerivoet and De Moor 2005). Analogies to

physical phenomena are often used, such as the behavior of gases and liquids flowing; thus differential equations similar to the ones used in such cases are usually applied.

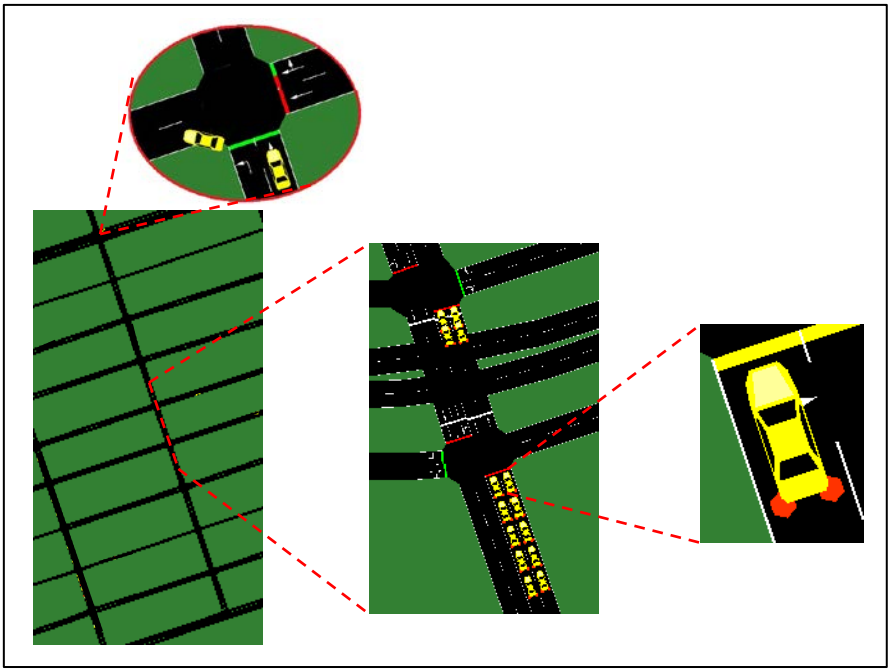

Figure 4.1– The different levels of aggregation for traffic simulation, from left to right: macroscopic, microscopic and nanoscopic; the circle represents the mesoscopic. Adapted from (Krajzewicz et al. 2002).

This kind of traffic simulation is largely used for transportation planning and congestion analysis for large and complex networks. It has been widely spread since large investments on traffic sensors and data collection were made as a way to evaluate traffic flows. The data gathered by these sensors are in the same level of aggregation as macroscopic models are, thus leveraging their development (Burghout 2004).

4.2.2 Mesoscopic Simulation

Mesoscopic simulation models represent a trade-off between the macroscopic and the microscopic simulation models. They no longer analyze traffic as flows and do not go into detail for each vehicle individually. Mesoscopic models have different ways of representing traffic entities.

Leonard et al. (1989) with the *CONTRAM* package were one of the first to approach traffic analysis using a mesoscopic simulation. They conjugate a set of vehicles into packets, supposed to respect the speed of each road they enter. This speed is defined based on the density of that road by the time the "packet" enters: if density is high (lots of traffic in the road), the vehicles speed in the packet is reduced, whilst low densities result in higher speeds. It does not allow microscopic interactions such as lane changes or acceleration/deceleration episodes.

Another interpretation for those "entities" is considered by *DynaMIT* (Ben-Akiva 1996), where vehicles are gathered into cells that control their behavior, such as their speed. The vehicles can either enter or leave a specific cell but never overtake it. A third approach of mesoscopic models is to use a queue-server paradigm, where the street is modeled as a queuing and a running part. The lanes can be modeled individually but usually they are not. Vehicles respect a speed-density function and at the downstream end, a queue-server is transferring the vehicles to connecting roads (Burghout 2004). Some models follow this approach, such as *FASTLANE* (Gawron 1998) and *DYNASMART* (Jayakrishnan et al. 1994).

4.2.3 Microscopic Simulation

Microscopic simulation models tackle some of the inherit disadvantages of the two traffic simulation types previously discussed, especially regarding their low level of detail of vehicles interaction, both between vehicles and between vehicles and the road infrastructure. A certain set of rules governs their behavior, namely acceleration, deceleration, lane change and route choice. Usually, there are three paradigms responsible for the behavior of vehicles in microscopic models: car-following, lane-changing and route-choice models (Burghout 2004).

In short, the car-following model makes a vehicle to follow the behavior of the vehicle in front of it regarding acceleration and deceleration but it also respects for instance the road speed limits and curvature (Kraus et al. 1997). The lane-changing model as the name says regards the decision of the driver to change lanes according to the situation in either the current lane or the destination lane, besides the speed of the vehicle in front (Ben-Akiva et al. 2006). At last, the route-choice models allow the driver to choose which route to take according to its origin and destination, taking into consideration the surrounding traffic and route information along the way (Prashker and Bekhor 2004).

Besides the vehicle behavior regarding other vehicles, microscopic models also account for a detailed representation of traffic components, such as traffic lights and their operation, traffic signs, traffic detectors, etc. Flows and densities are not model variables anymore, as in macroscopic and mesoscopic models but rather result from the vehicles interaction along the simulation. Due to this higher level of detail, microscopic simulation may demand larger processing abilities from the CPU of a commodity computer, making it really demanding and time-consuming for large networks (Burghout 2004). Some of the widely used microscopic simulators are *VISSIM* (Fellendorf 1994), *MITSIMLab* (Ben-Akiva et al. 1997), *AIMSUN* (Barceló et al. 1994) and *PARAMICS* (Smith et al. 1995).

In 2001 the German Aerospace Center (DLR) started the development of the open-source traffic simulation *SUMO* (Simulation of Urban MObility). It consists now of a full-featured package of traffic modeling and routing utilities from various input sources (origin destination matrices, traffic counts, etc.), including also tools for demand generation. In addition, *SUMO* is equipped with the "remote control" interface TraCI (Traffic Control Interface) allowing for adjustments on the simulation online (Behrisch et al. 2011).

4.2.4 Nanoscopic Simulation

Nanoscopic simulation models account for an even finer-grained representation of traffic (Ratrout and Rahman 2009). Nanoscopic models were born from the need to go even further into detailing traffic simulation models. Therefore, nanoscopic models focus on the vehicle individually, either accounting for its dynamics and interaction with others or the driver's behavior (Ni 2003).

Dia and Panwai (2008) have developed an agent-based driver behavior model to be used in nanoscopic simulation so that to allow the modeling in the field of intelligent transportation systems (ITS) and vehicle telematics. Using a similar approach, an extension to the microscopic simulator *DRACULA*[19] (Dynamic Route Assignment Combining User Learning and microsimulAtion) was developed in order to apply agent-based techniques on the modeling of driver behavior (Rossetti et al. 2002; Rossetti and Liu 2005a). The use of autonomous agents to mimic driver behavior allows for a variety of complex analyses, such as assessing the impact of pre-trip information on travel demand and performance of the traffic system (Rossetti and Liu 2005b).

Since one of the possible interpretations for nanoscopic models is the driver's behavior, research on the field of modeling autonomous vehicles also applies in this context. Figueiredo et al. (2009) present an approach to simulate the implementation of autonomous vehicles in the city, studying the interaction between them and with the regular traffic.

4.3 The Integrated Platform

As a way to allow the analysis of the electric bus performance when immersed in the urban environment, another step is required towards the simulation platform development: to integrate the computerized model of the bus developed in *Simulink* with a traffic simulator. Firstly, it is important to define the level of aggregation required for this

[19] (DRACULA 2008)

platform, so as to decide whether to use macroscopic, mesoscopic, microscopic or nanoscopic traffic simulators.

The *Simulink* model by itself can be considered a nanoscopic simulator. It is responsible for simulating the bus behavior in detail according to a specific driving cycle, as explained previously. Therefore, integrating it with another nanoscopic model will not bring any further advantages. Considering that some of the main aspects when analyzing the bus behavior are its interaction with the surrounding traffic, how it is affected by the topology of the route it performs and the design of bus stops to correctly simulate its operation, microscopic models seem to provide the right level of aggregation.

The nanoscopic model of the bus has to be represented by an entity on the microscopic traffic model, preferably of the specific vehicle class "bus". The choice for the microscopic traffic model has also to take into consideration the ease of access to its variables, its application programming interface (API) and the communication protocols used.

Moreover, the integration does not necessarily need to support bi-directional communication capabilities. The traffic simulator should provide the speed profile to the nanoscopic model of the electric bus, so that it performs all calculations but the bus model does not have to return any variables to the traffic simulator. Maybe for further developments it would be necessary, as for the case of using *Simulink* to adjust parameters in real time in the traffic simulator but for the scope of this thesis, this is not required. However, the traffic model should be capable of sending data to *Simulink* while it makes all calculations for each simulation step, and this is an important issue to be addressed.

The integration of the nanoscopic model of the bus with the microscopic traffic simulator was carried out in the form of a Master's thesis in the Laboratory of Artificial Intelligence at FEUP by (Macedo 2013). His thesis focused on distributed simulation, which refers to technologies "that enable a simulation program to execute on a computing system containing multiple processors, such as personal computers, interconnected by a communication network" (Fujimoto 2001). Macedo (2013) implemented this integration using the recent High Level Architecture (HLA) concept. The HLA is a real industry standard developed by *IEEE* which provides the interoperability and reusability of diverse simulation systems.

The next sections of this chapter present an overview of the chosen microscopic traffic simulator and the main required tools for simulating buses on it. In addition, some attention is given to the HLA, primarily its main concepts, framework, and an overall

approach to the work performed for this integration is also presented. The required adaptations to the *Simulink* model to make this integration work are also described.

4.3.1 *SUMO*: Simulation of Urban Mobility

In order to meet the previously defined requirements for the microscopic traffic simulator to be integrated to the *Simulink* model, *SUMO* seemed like a reasonable choice. It consists of many separate programs for different simulation-related tasks and has one graphical user interface called *SUMO*-GUI, being all other programs called from the command line. *SUMO* has a unique advanced feature which is its architecture flexibility, being of relevance for the upcoming integration to *Simulink* (Passos et al. 2011).

In *SUMO,* the level of resolution is modeled with a detailed representation of the traffic dynamics. This approach describes the behavior of the entities that make up the traffic stream as well as their interactions. To define the entity "vehicle", the modeler needs to associate it with an identifier (name), a departure time and assign it a certain route throughout the network. A simulated vehicle can be associated with a type that describes the physical properties of the vehicle and the variables of the kinematic model, such as car, bus, etc. By distinguishing different vehicle types, *SUMO* allows the simulation of public transport or emergency vehicle prioritization at intersections (Krajzewicz et al. 2002).

SUMO supports external control through TraCI (Traffic Control Interface), which is an API that allows the traffic simulation to interact with an external application via a socket connection in runtime. This approach allows the application to retrieve values of simulated objects and to manipulate their behavior. TraCI is composed of three main sets of functions that are related to the information access, the control of the state of objects during the simulation (e.g., speed at each step) and the subscription of determined structure variables (Perrotta et al. 2014). In the next sections, some *SUMO* relevant tools used in this project are presented.

4.3.1.1 Network Import

SUMO roads network can be either generated using a specific tool (*netgen.exe*) or imported from other formats using the *netconvert.exe*. This tool allows importing road networks that comes either from other simulators, such as *VISSIM* and *VISUM*, or also from shapefiles and *OSM* (Open Street Map 2014) . For practical reasons, the *OSM* format is the chosen format to be used in this thesis. It allows easy selection of the intended area of analysis and further refinement/edition using a software such as JOSM (2014).

Once the desired area is extracted from the *OSM* website, a specific script should be run in the command line to make the conversion into the *SUMO* format. For an extracted *OSM* map called "my_file.osm.xml" and the output *SUMO* network to be called "map.net.xml", the script to be written on the command line can be observed in Appendix D – *SUMO* Scripts.

The new "map.net.xml" is composed of the main road network, traffic lights and junctions. The roads have specific speed limits according to their class in the *OSM* but it is customizable in *SUMO* if needed, and so are the traffic lights assignment and regimens. Due to the fact that the *OSM* maps also comprise a wide range of additional polygons such as buildings and rivers, those can be imported by *SUMO* using the *polyconvert.exe* function in the command line. The added polygons are for visual enhancement only, and do not perform any specific function.

4.3.1.2 Public Transport (Bus)

SUMO allows the coding of bus stops and the definition of how much time it is supposed to be stopped at each bus stop. Besides, the route of the bus is defined lane by lane, which means it is done manually using the visualization of the *SUMO* network in *SUMO*-GUI, GUI accounting for graphical user interface (Figure 4.2). All this data are defined in an additional file called "buses.add.xml" and should be called together with the network before running the simulation (more details in section 4.3.1.4). Figure 4.3 shows the "buses.add.xml" file format.

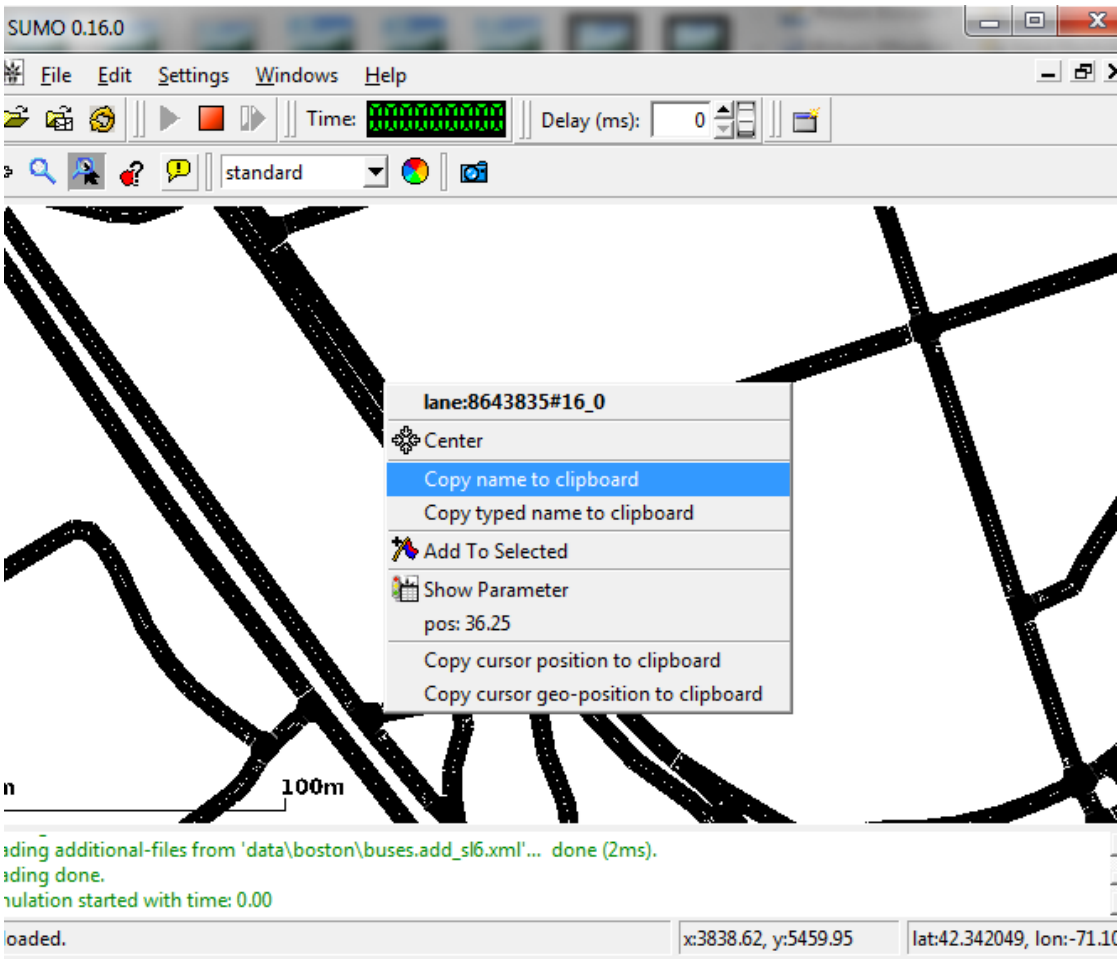

Figure 4.2– *SUMO* GUI and lane visualization for composing the bus route

```
<additional
    <busStop id="busstop1" lane="2/1to1/1_0" startPos="10" endPos="50" lines="100 101 102"/>
    <busStop id="busstop2" lane="1/2to0/2_0" startPos="20" endPos="40" lines="100 101"/>
    <busStop id="busstop3" lane="0/1to0/0_0" startPos="20" endPos="40" lines="100 101 102"/>
    <busStop id="busstop4" lane="1/0to2/0_0" startPos="20" endPos="40" lines="100 101"/>
    <vType id="BUS" accel="2.6" decel="4.5" sigma="0" length="12" minGap="3" maxSpeed="70" color="1,1,0" guiShape="bus"/>

    <vehicle id="0" type="BUS" depart="0" color="1,1,0">
        <route edges="2/0to2/1 2/1to1/1 1/1to1/2 1/2to0/2 0/2to0/1 0/1to0/0 0/0to1/0 1/0to2/0 2/0to2/1"/>
        <stop busStop="busstop1" duration="20"/>
        <stop busStop="busstop2" duration="20"/>
        <stop busStop="busstop3" duration="20"/>
        <stop busStop="busstop4" duration="20"/>
    </vehicle>
</additional>
```

Figure 4.3– Bus coding in *SUMO*: the "*buses.add.xml*" file format

The file starts with the definition of the bus stops, which string is composed of the bus stop "*id*", the name of the lane that the bus stop should be located at "*lane=*", the begin position on the lane "*startPos=*", the end position on the lane "*endPos=*" and the lines of buses that uses this bus stop "lines", being the latter only useful for visualization purposes. The position on the lane can be seen in Figure 4.2 as the parameter "*pos:*".

The "*vtype id*" refers to the class of the vehicle (bus in this case), and it is followed by values for acceleration and deceleration (in m/s^2), the length of the vehicle (in meters), the maximum speed (in m/s) and the color and the shape of the bus to shown up in *SUMO*-GUI.

Sigma is also in this string and accounts for the driver's imperfection, which represents the inability of a driver to maintain a constant speed and is "*0*" by default.

The next section of the file accounts for the definition of the bus route and times at the bus stops. Because it is possible to simulate more than one bus in a single file, the vehicle "*id*" should be defined, being "0" in this example. "*depart=0*" means the bus is starting to run right on the beginning of the simulation. "*route edges=*" accounts for the set of streets (edges) that the bus have to pass by and this is manually defined, being those edges separated by spaces. At last, the string starting with "*stop busStop=*" defines the duration that the bus should stop in each bus stop individually (in seconds).

4.3.1.3 Demand Modeling

After defining the network and the bus routes/operation in this context, traffic modeling should be performed. Firstly, it is important to differentiate a trip from a route. A trip is a vehicle movement from one place to another defined by the starting edge (street), the destination edge, and the departure time. A route is a detailed trip, which means it contains all the edges the vehicle will pass to go from the starting edge to the destination edge. There are several ways to generate routes for *SUMO* but here the focus is on two: randomization and origin/destination (O/D) matrices.

Randomization (*randomTrips.py*) allows the generation of a set of random trips for a given network ("*-n*"), by choosing a source and destination edge either uniformly or weighted based on: the number of lanes that the edge contain (optional "*-l*"), the edge length (optional "*-L*") or both. The outcome (optional "*-o*", which default name is "trips.trips.xml") is an *.xml* file used by another *SUMO* function called *duarouter.exe*, responsible for creating the routes. *duarouter.exe* can be called simultaneously with *randomTrips.py* by adding the optional "*-r*" to the string, followed by the file name for the resulting route file.

The trips are distributed evenly in an interval defined by begin (option "*-b*", default "*0*") and end time (option "*-e*", default "*3600*") in seconds. The number of trips is defined by the repetition rate (option "*-p*", default "*1*") in seconds. An example is presented in Appendix D, where the outcome is already the route file "routes.rou.xml".

Another way of representing the traffic in *SUMO* is through importing O/D matrices using the function *od2trips.exe*. O/D matrices are a way to represent the number of cars that leaves from a certain origin to go to a specific destination within a period of time. It is usually a table where the origins are located on the first column and the destinations are shown on the first row, being the number of trips (cars) located in the crossing cells.

The origins and destinations are usually represented by numbers, being these numbers what *SUMO* understands as "districts". Thus the first step in the process of importing an OD matrix is to tell *SUMO* which area those districts comprise in the network. The steps for translating the districts of an O/D matrix into *SUMO* follow below:

- Once having the *shapefile* of districts involved in the OD matrix, it can be easily converted to a polygon file *.poi* in *SUMO* by running a script presented in Appendix D ("*N*" is the column name on the *shapefile* attribute table that accounts for the district number)
- The next step is to define which edges compose each district. The tool *edgesIndistricts.py* performs this function: having as input the network file and the polygon file of the districts, it outputs an *.xml* containing all edges for each district (called "taz.xml", taz named as "traffic analysis zone"). The "*-w*" is an option accounting for weighing the edges according to its length and number of lanes, increasing the probability of wider and longer lanes to accommodate more cars when generating the routes.

At this point, *SUMO* recognizes the O/D matrix districts and their location in the network, together with data regarding every single edge that composes them. Now, the O/D matrix itself has to be adapted to a format that *SUMO* understands. *SUMO* can understand several formats, being the "O-format" chosen for its simplicity and easy conversion from the conventional *Excel* format, as presented in Figure 4.4. The resulting O/D matrix in the *SUMO* format is a text file that can be called "odmatrix.txt" for future use.

Finally, all the o*d2trips.exe* required input files are defined and a call can be made. It is important to define the beginning "*-b*" and the end "*-e*" of the trips generation according to the period of time that the O/D matrix comprises. In the presented example in Appendix D, the O/D matrix accounts for the traffic of one hour (3600 seconds):

```
$OR;D2
* From-Time  To-Time
0.00 1.00
* Factor
1.00
* some
* additional
* comments
        1   1   0
        1   2   0
        1   3   0.02
        1   4   0.02
        1   5   0.02
```

Figure 4.4- The O-format for the O/D matrix simply lists each origin and each destination together with the amount of cars in one line

The last step is to compute routes, which for the generation of random trips can be done automatically by using the option "*r*" when calling the *randomTrips.py*, but in this case *duarouter.exe* has to be called separately and it may have two different purposes: building routes from the trip file or computing routes during user assignment. In the first case, the *duarouter.exe* computes vehicle routes that may be used by *SUMO* applying the shortest path computation.

For the second case, the *duarouter.exe* is called iteratively, performing the dynamic user assignment (DUA). In order to do that, the function "*duaIterate.py*" has to be called and what it does is to run the *duarouter.exe* and *SUMO* alternating them both, so that the outcome of the previous step serves as input for the next step. The objective is to converge to user equilibrium.

duaIterate.py runs by default 50 steps. If the network is large and the computer does not have adequate processing capacity, it can be really time consuming. However, it is possible to determine the number of steps by adding the option "*-l*" followed by the desired number ("*10*" in the example of Appendix D). Another interesting aspect is that for each step, the resulting route file is computed so as to allow testing those intermediate files even if the whole operation is not yet completed.

4.3.1.4 Configuration File

The design of a configuration file is made necessary when in presence of many "options" to be loaded simultaneously, such as the previously presented road network, traffic and bus operation altogether. This file contains all the wanted parameters to start the simulation at *SUMO* and it is the only required file to effectively do so. A configuration file has as extension "*.sumo*cfg", having as root element "*configuration*". The input options are written as element names:

- *<net-file="map.net.xml/>*: loads the road network;
- *<additional-files value="districts.poi.xml;buses.add.xml"/>*: loads the visualization of the districts and the bus stops, together with route data for the simulation;
- *<route-files value="routes.rou.xml"/>*: loads the cars traffic.

In this configuration file, the time of simulation run is also defined, which in the example presented in Figure 4. refers to the defined period of time of the demand modeling presented earlier (3600 s). This file also allows many processing options to be added, having the example focused on "*<time-to-teleport value="120"/>*", a relevant parameter when working with large networks. This processing option states that whenever there is a vehicle stopped for more than 120 s, it will be teleported and re-inserted in the network in

a further stage, following its pre-defined route. This makes the simulation runs more smoothly and helps preventing complex congestions.

At this point, both the nanoscopic representation of the electric bus in *Simulink* and the microscopic traffic simulator *SUMO* are defined well. The *Simulink* model was extensively discussed in Chapter 3 whereas the main *SUMO* functions and tools were presented in this chapter. The next step in this development process is to integrate both simulators so that it allows the inter-communication between them. The next section presents the high-level architecture (HLA) as the solution to integrate the simulators, advantages in using it and some necessary adaptations in the process.

```
<configuration>

    <input>
        <net-file value="map.net.xml"/>
        <additional-files value="districts.poi.xml;buses.add.xml"/>
        <route-files value="routes.rou.xml"/>
    </input>

    <time>
        <begin value="0"/>
        <end value="3600"/>
    </time>

    <processing>
        <time-to-teleport value="120"/>
    </processing>

</configuration>
```

Figure 4.5– *SUMO* configuration file "*sumo*cfg.xml" for loading several options in *SUMO* simultaneously

4.3.2 The High-Level Architecture Concept

The High-Level Architecture, HLA, is an architecture that enables several simulation systems to work together (interoperate). The systems need to work together to achieve a common goal by exchanging services. HLA also allows the reuse of different systems in new combinations, so that new analysis can be performed (Pitch 2012).

The HLA concept is based on the idea of the distributed simulation approach that no single simulation model can meet alone the requirements of all usages and users. In order to facilitate the aforementioned interoperability and reusability, HLA differentiates between the simulation functionality provided by the members of the distributed simulation and a set of basic services for data exchange, communication and synchronization (Macedo et al. 2013).

4.3.2.1 HLA Architecture and Components

The HLA concept finds a wide applicability through a vast range of simulation application areas such as education, training, analysis, engineering and even entertainment at multiple levels of resolution. These broadly different application areas suggest the variety of requirements that have been taken into account for the development and the ongoing evolution of the HLA standards. Three main components formally define the HLA concept:

- The HLA Framework and Rules Specification summarize a set of rules that ensure the proper interaction of federates in a federation and define the responsibilities of federates and federations (IEEE-Std 2 2010);
- The Object Model Template (OMT) provides the object models that define the information produced or required by a simulation application and for matching definitions among simulations to produce a common data model for mutual interoperation (IEEE-Std 3 2010);
- The Federate Interface Specification describes a generic communication interface that allows simulation models (called federates) to be connected and coordinated, implemented by a Run-Time Infrastructure (RTI). Federates communicate with the RTI using its ambassador (objects that have the methods needed to communicate) as an interface (IEEE-Std 1 2010).

4.3.2.2 The Proposed Architecture

The proposed architecture developed by Macedo (2013) for the integration of the electric bus model in *Simulink* with *SUMO* is shown in Figure 4.6. The first key elements in the proposed architecture to be explained are federates. A federate can be a computer simulation, corresponding to the HLA simulation entities, and is represented by *SUMO* and the *Electric Bus Simulink Model*.

The second functional element is the runtime infrastructure (RTI). RTI is a distributed operating system for the HLA, and provides a set of general-purpose services that support federate-to-federate interactions. It routes messages and data exchange between the *SUMO* and the *EBPS* federates.

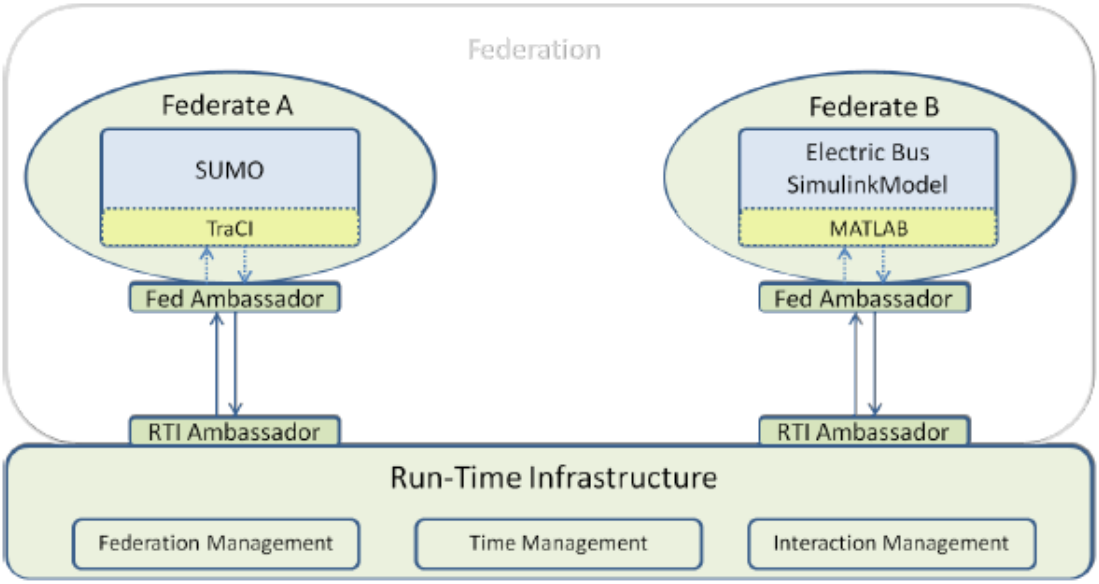

Figure 4.6– The proposed system architecture for the integration of *Simulink* and *SUMO* (Macedo et al. 2013)

The third element is the interface to the RTI, called RTI Ambassador. Its specification provides a standard way for federates to interact with the RTI. It is used whenever RTI services is called to support runtime interactions among federates and to respond to requests from the RTI. This interface is implemented by the chosen RTI: *Pitch pRTI* (Pitch 2012).

The forth element is the Federate Ambassador, accounting for a specific interface that allows the RTI to communicate with the federate. It should be implemented by the federate developer using a code language of choice (*Java* was used). The RTI will provide interactions to federates by performing calls to its Federate Ambassador.

As seen in Figure 4.6, the communication between the "Federate A" ambassador and *SUMO* is performed through *SUMO*'s API TraCI. In a similar way the communication between "Federate B" ambassador and the *Simulink* model is performed through *Matlab*, which was used in this case to perform the function of the *Simulink*'s API.

4.4 Required Adaptations in the *Simulink* Model

When working on the integration process, Macedo (2013) found out a challenge that had to be overcome so that the simulation could run smoothly. On the one hand, *SUMO* is a microscopic traffic simulator that follows a discrete-time simulation of 1-second steps by default. On the other hand, *Simulink* is a continuous-time model. Therefore, modifications to some of its blocks had to be done in order to transform it into a discrete time model.

Every time a continuous-time function block was used in the *Simulink* model, it had to be changed to a discrete block to perform the same function. This happened specifically for two blocks: "Derivative" and "Integrator". The "derivative" block was replaced by the "Difference" block, which was already introduced in section 3.2.1.3 as one of the components for calculating the hill climbing force (Figure 3.25). The "Integrator" block had to be replaced by the "Discrete-Time Integrator" function block, and can be observed in Figure 4.7

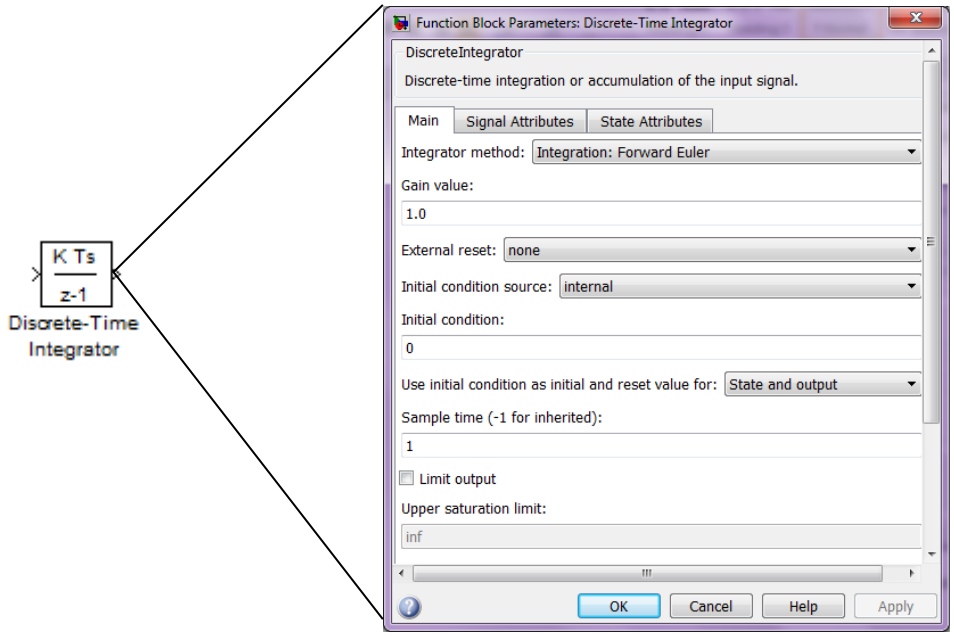

Figure 4.7- "Discrete-Time Integrator" block graphic representation and its expanded corresponding function box parameters in *Simulink*

There is another required adaptation to be implemented in the *Simulink* model related to the inputs and outputs. At a certain point in the development process of this integration, there existed the need to use the *Matlab* function *set_param()* so that it could control the *Simulink* model step-by-step through *Matlab* commands (Macedo et al. 2013). As previously mentioned, *Matlab* served as an API for *Simulink*.

In this sense, all the input and output blocks were replaced by "*MATLAB* S-function" *Simulink* blocks, which are a user-definable, block written using the "*MATLAB* S-Function API". The fields "S-function Name" and "Parameters" should be filled up accordingly. Figure 4.8 depicts an example of this block.

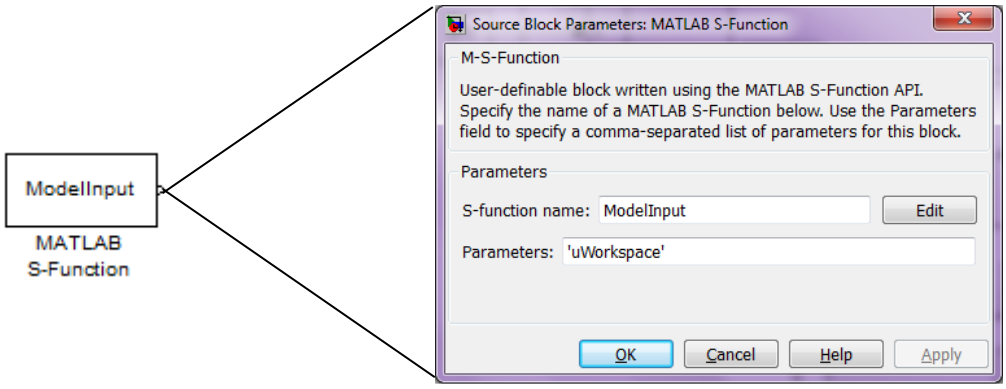

Figure 4.8- "*MATLAB* S-function" box graphic representation and the expanded corresponding function block parameters in *Simulink*

4.5 Simulation Platform Operation

Once the network import is concluded, the route of the bus is defined well, and the traffic is generated either randomly or based in an O/D matrix, the simulation can be performed. In order to do that, the following steps must be performed:

- Start the Pitch RTI;
- Start *SUMO* federate, which is developed as an *Eclipse*[20] project;
- Start *Simulink* Federate, also developed as an *Eclipse* project;
- Run both federates;
- Verify, through the RTI GUI, if the federates connected to the RTI and joined the federation.

The verification in the RTI GUI can be observed in Figure 4.9. It is clear that both federates are connected to the RTI and joined into the federation herein called "Electric Bus in Traffic Simulation".

[20] Eclipse is an Integrated Development Environment (IDE) (Eclipse 2014)

Figure 4.9 – Pitch RTI GUI with connected federates for *SUMO* and the EBPS, joined in the federation "Electric Bus in Traffic Simulation"

4.6 Conclusions

This chapter has presented an overview of traffic simulation, their many different types according to the level of aggregation and the choice of the microscopic simulator to be integrated to the *Simulink* model. It became clear the advantages of using such an integrated platform to perform the electric bus simulations, since route definition to the interaction with the traffic. The platform is able of representing in a realistic and detailed manner the routes that the bus is supposed to perform, which never could be accomplished if only the *Simulink* model would be used.

Some emphasis was given to the description of a set of relevant tools in *SUMO*, as a way to make this work replicable by the scientific community. Moreover, the chapter presented the main aspects of the architecture used to perform the integration, the HLA, together with a summary of main concepts and the applied developed framework. The integration was performed as a Master's thesis in FEUP and all details can be verified in Macedo (2013) and Macedo et al. (2013).

The next chapter focuses on the calibration and validation process of the *Simulink* model. Albeit the adjustments performed on it, they do not impact in the outcome of the model thus the calibration and validation were performed in the original *Simulink* model in standalone mode.

Chapter 5

Simulation Model Calibration and Validation

5.1 Summary

The aim of this chapter is to describe the many calibration and validation techniques in the world of simulation models and identify the most suitable for the specific case of the electric bus model. The chosen methods are applied to this context and the results are analyzed.

5.2 Terms Definition

After the whole process of developing the simulation model, some questions arise: Why should the outputs of a simulation be trusted? Do the mathematical equations correctly represent the target system? And even further, are those equations represented well in the computer programs? In the literature, these problems are commonly related to validation and verification.

It is relevant to take into consideration that validation comprises three sub-categories: data validity, conceptual (or theoretical) validity and operational validity (Sargent 2005; Gass and Thompson 1980). These three are shown as part of the modeling process in Figure 3.1.

Data validity concerns the quality and suitability of the data that is used to build, evaluate and test the model (Sargent 2005). According to Gass and Thompson (1980), the evaluation of data should take into consideration their accuracy, completeness, impartiality and appropriateness. Kleijnen (1995) has a different view about this matter, focusing more on the accurate definition of the system boundaries and attributes rather than on data validity itself. However, he describes the advantages as well as disadvantages of having from scarce to abundant data available, being the latter the case of this project, once data is collected electronically.

When there is an overload of input data, they can promote a more powerful validation process, unless these data go so far back in time that different laws governed the system is analysis. Moreover, knowing when exactly different laws governed the system is itself a validation issue. Another aspect to be taken into consideration is to assure that there are no observation errors, or at least mitigate this possibility the most (Kleijnen 1995).

Conceptual (theoretical) validation is the process of ensuring that the model is an accurate representation of the system itself. However, a conceptual model will never be perfect, as only the "Entity" or the real system itself is (Kleijnen 1995). In other words, the theories and assumptions underlying the conceptual model are correct and the representation of the real system is good enough according to the intended use of the model (Sargent 1984). Theoretical validation can also be seen as the process of guaranteeing that those major stated and implied assumptions which are embodied in the theories underlying the model are well-adapted to the modeled system. The applicability and restrictiveness of these assumptions in relation to the internal and external problem environments should also be evaluated (Gass and Thompson 1980).

Operational validity is probably the most discussed sub-category of validation found in the literature. Sargent (2005) defines it as determining that the model's output behavior has sufficient accuracy for its intended purpose and applicability. It is inherent to the model not to be able to represent infallibly the real-world situation. Similarly, Gass and Thompson (1980) believe that it is concerned with assessing the importance of these errors and divergences upon the actual use of the model.

Another step in Sargent's diagram (Figure 3.1) is Computerized Model Verification, linking the Conceptual Model to the Computerized Model. This process is related to how accurate the conceptual model is translated to the computer model. In other words, to verify that all the mathematical equations are programmed well when implemented in a computer software (Sargent 2005).

An interesting distinction between verification and validation is given by Whitner and Balci (1989). They define validation as "substantiating that the input-output transformation of the model has sufficient accuracy in representing the input-output transformation of the system", while their view of verification is "substantiating that a simulation model is translated from one form into another, during its development life-cycle, with sufficient accuracy". Basically, every time a model is compared to the real system, it is called validation. Verification is more related to building the model right, i.e., with no bugs.

In the end, there are no standards in what concerns either the process of validation and verification or devising a perfect solution for that. According to Barlas and Carpenter (1990): “Model validation is a gradual process of building confidence in the usefulness of a model; validity cannot reveal itself mechanically as a result of some formal algorithms”.

There is a line of thought that says verification and validation will end up being intertwined, once only the "net outcome" of a simulation can be evaluated and it is not possible to address these two issues one by one (Frigg and Hartmann 2012). In the case of this project, the “net outcome” or the results will come from the simulation on the computer model, so it is assumed that the program represents accurately the mathematical equations developed for the conceptual model. Moreover, there is no complex programming involved in this project; therefore the term validation is going to represent verification as well.

Calibration of a system model, on the other hand, is hardly mentioned in the literature of verification and validation (V&V); it is usually approached separately (although it makes sense to be considered part of the validation process). Kleijnen (1995) is one of the few that actually talks about it in his V&V article. He defines calibration as the adjustment of the simulation model parameters to promote a better accuracy between the outputs of the model with the ones of the real system.

Hofmann (2005) believes that “the adjustments done by parameter calibration are necessary because the models are based on abstractions, idealization, and many disputable assumptions. Thus, in order to get trustworthy results from the model, input-output pairs of the model are fine-tuned to input-output samples of the reference system”. He also states that the importance of calibration is controversial, once sometimes the system is not well defined and it is hard to find truly reliable data. However, he believes calibration is essential for many simulation models that need the “classical sense of fine-tuning”.

The Transportation Planning Handbook (Edwards 1992) defines calibration somewhat similarly to Kleijnen as the process of estimating the values of various constants and parameters in the model structure. This process is a trial-and-error effort that seeks the parameter values which have the greatest probability or maximum likelihood of being accurate within acceptable tolerance of error.

Kennedy and O’Hagan (2001) describe the need for calibration for those models in which values for necessary parameters are unknown, and advise that observation of the real

system in specific conditions is crucial for learning about those parameters. They call calibration as the method of fitting the model to the observed data by adjusting those parameters. Once calibration is done, the model may be used to predict behavior for other conditions.

Azcarate et al. (2012) address their modeling problem by defining a set of rules dependent on a set of parameters. In their view, model calibration is characterized by being the process of determining the values of unobservable parameters, constraining model output to replicate observed data.

There are different views for calibration, although they are quite similar between each other. The simulation model in analysis in this work has two unobservable inputs: energy consumption of accessories and number of passengers carried on the bus. The validation process will pass through analyzing the best value (or range of values) for those parameters in order to mimic the real bus behavior based on data collected in its operation for specific events. On the next section, methods of validation are presented.

5.3 Methods of Validation

After defining what validation is, the question that arises is how it is done. It is relevant to say that the methods are related to the operational validity only. Because data is collected electronically and they are recent, and also by knowing the system has not gone through changes in this period of time, these data is considered appropriate for the intended use of the model. In relation to conceptual (theoretical) validity, the author assumes that once operational validation is performed, it will validate the conceptual design of the model.

Operational validation is basically comparing the outcomes of the simulation model with those from the real system, once historical data is fed in the model (Kleijnen 1995). Therefore methods of validation are represented by different technics to compare and analyze those data. Some of these methods require the use of knowledgeable people of the real system, methods not considered for this project. Some are related to visually comparing the time series outputs of the real system with those of the simulation model: outputs are displayed in graphics and subjectively compared against each other. For example, studies to evaluate market tendencies can easily pass through this eyeballing process, once the behavior of the model can be compared to the real system with no numbers attached. For instance, Barlas (1989) presented a system that would only allow subjectively validation, once either the behavior of the system and the simulation model are “highly transient and non-stationary”.

In case it is necessary to perform a more objective analysis of the graphs, different mathematical statistical methods can be used. One of the main statistical methods is confidence intervals, which can be applied over the differences between means, variances, and distributions for each set of experimental conditions. They can be used as the model range of accuracy for model validation. Another method to compare means, variances and distribution is the hypothesis tests, in which the first step is to define the hypothesis: H0 standing for model is valid under the set of experimental conditions for the acceptable range of accuracy and H1 for model is invalid in the aforementioned conditions. This can lead primarily to two types of errors: Type 1, as for rejecting a valid model, and Type 2, as for accepting an invalid model. The probability of having those errors are high so extreme caution is advised when opting for this method of validation.

The abovementioned methods of validation are used whether the real system is composed of observable inputs and outputs only. In case there is at least one unobservable input, it is recommended to apply the sensitivity analysis method. Kleijnen defines sensitivity or "what-if" analysis as the systematic investigation of model outputs when its inputs are subject to drastic changes. Kennedy and O'Hagan (2001) put it in another way, namely identifying the inputs to which the outputs are sensitive or insensitive to. Learning about how a certain input affects outputs and to what extent it happens is crucial for the validation of models.

Frey and Patil (2002) classified methods for sensitivity analysis in three main categories: mathematical, statistical and graphical. Mathematical methods assess sensitivity of a model output to a range of variation of a certain input. They can be really useful in screening the most important inputs and are widely used in verification and validation of models. Statistical methods are about assigning probability distributions to the inputs and analyzing the effect of variance in inputs on the outputs distribution. It is useful for assessing the interaction among various inputs. Graphical methods are about representing sensitivity visually on a graph or chart. Basically they can be applied earlier in the process so as to gain insight into the influence of inputs over outputs, and other methods are used in conjunction or they can complement results for a better visualization.

Each of these three main categories for sensitivity analysis methods can be carried out in many different ways. Frey and Patil in their review have come up with a very good table that summarizes most of the existing methods, describing their applicability, computational issues, way the representation of sensitivity is done and where would they

be best used; this table can be consulted bellow (Table 5.1). In the next section, the chosen method for validating the system model of this thesis is presented.

Table 5.1- Overview of comparison of validation methods (Frey and Patil 2002)

Methods	Applicability	Computational Issues	Representation of Sensitivity	Best Use of Methods
Nominal Range Sensitivity Analysis	Deterministic model.	Need nominal range for each input, potentially time consuming.	Ratios, percentages. Does not include effect of interactions or correlated inputs. Easy to understand.	Key inputs for linear models, verification and validation.
ΔLOR	Deterministic model with output as a probability.	Need nominal range for each input, potentially time consuming.	Ratios, percentages. Does not include effect of interactions or correlated inputs. Easy to understand.	Key inputs for linear models, verification and validation.
Break-Even Analysis	Models used to choose among alternatives.	Complex for model with many decision options and/or more than two inputs, potentially time consuming.	Graphical representation.	Robustness of solution.
AD	Locally differentiable models.	Requires specific software (e.g., ADIFOR).	Local sensitivity measures, such as sensitivity coefficients.	Potential key inputs, verification.
Regression	To results from probabilistic simulation.	Must specify functional form, computation time and value of solution depends on specific techniques used.	R^2, t-ratios for regression coefficients, standard regression coefficients, and others.	Key inputs, joint effect of multiple inputs, verification.
ANOVA (MF)[a]	Probabilistic models.	Time consuming for a large number of inputs with interactions.	F-value, Tukey test coefficients, and others that are calculated at different stages of ANOVA.	Key inputs, joint effect of multiple inputs, verification.
RSM	Any deterministic model.	Developed using a variety of techniques, some require functional forms, others do not; may require extensive runs to generate a calibration data set.	Graphical, evaluation of functional form, method-dependent measures.	Model of models, used with other SA methods to save time.
FAST (MF)	Probabilistic models.	Better with no interactions/higher-order input. Caution against discrete inputs.	Portion of output variance attributable to each input.	Key inputs, including combined effect, verification.
MII (MF)	Probabilistic model.	Complex, no computer code available, time consuming.	Amount of "mutual information" about the output provided by each input, also graphs of intermediate stages.	Key inputs, including combined effect.
Scatter Plots (MF)	Probabilistic model.	Easy, time requirement depends on the number of input/outputs.	Graphical, no quantitative sensitivity.	Verification and validation.

[a] MF = denotes a model-independent approach.

5.4 Electric Bus Simulation Model Validation Method

After going through the whole design of the conceptual model and translating it to the computer model, it is imperative to evaluate the applicability of this model and how realistic is its representation of reality. There is no better way to do that than comparing its behavior with the one from the real bus for specific situations or so-called scenarios. As already mentioned in section 2.3.7, the collection of data is made electronically for lack of

data is certainly not an issue. Moreover, the time lapse of the collected data was chosen such as to guarantee that the real system, aka the bus, has not gone through any changes. To be more specific, the collected data are from the operation of the bus at the Stuttgart airport from June to August of 2014.

5.4.1 Model Calibration

Before validating the model, calibration is necessary for adequate performance. The electric bus model is composed of mathematical formulas in its entirety to account for the bus dynamic behavior, mimicking its real operation. In order to calibrate the model, the bus operator has provided some data about the bus, either regarding fixed parameters (weight, front area, tire radius, etc.), or range of operational parameters, like battery current and voltage behavior. The fixed parameters were already presented in Table 3.1, and are not relevant here. Concerning the operational parameters, they are theoretically restricted to the range of values for battery current and voltage, which can be observed in Table 5.2.

Table 5.2- Range of operation for the real bus battery current and voltage

Variable	**Theoretical range of operation**
Battery Current (in Ampere)	Motoring mode: -500 A Generator mode: 200 A
Battery Voltage (in Volts)	Minimum: 280 V Maximum: 408.8 V Nominal: 358.4 V

It is relevant to state at this point that the negative signal before the value of current in the motoring mode is due to current being drained from the battery, while the positive value for generating mode is for current being returned to the battery as a consequence of regenerative braking. Thus the values presented in Table 5.2 can be interpreted as the limitations of the bus; they can never be lower than the minimum or higher than the maximum thresholds, respectively.

However, when analyzing the collected data from the real bus operation, it could be noticed that the bus hardly gets to these extremes, and this is where calibration does its job: to calibrate those parameters so that the model would mimic the real bus behavior for the chosen scenarios. To start with, data from four different days of operation at the Stuttgart airport were collected. For each day, the bus worked for different time periods and sometimes spending several minutes stopped but always keeping the motor on, thus spending energy.

Data from the bus operation came encrypted for it was necessary to develop a script in *Matlab* to decrypt them (described in Appendix E). After doing that, it was possible to extract the values for battery current (in Ampere) and voltage (in Volts) in a time series format, and evaluate if the ranges in Table 5.2 match the real-life operational range. Because the important issue here is to graphically evaluate the current and voltage behavior, graphs will be presented altogether: Figure 5.1 stands for the battery current behavior for each scenario whereas Figure 5.2 does for battery voltage behavior. Each graph has the date of operation for the collected data and different time ranges can be noticed, as previously explained.

It can be noticed after observing all graphs from that the ranges of battery current operation are quite different from the values presented in Table 5.2. The battery current range is now -300 A to 150 A, instead of the -500 A to 200 A previously defined. This difference plays a very important role in many calculations on the model, for calibrating it to these new maximum and minimum values is crucial for the validation process. Something similar happens when evaluating voltage (Figure 5.2): the real range of operation is much smaller, 355 V to 380 V. However, because voltage is calculated based on current, its behavior and range of operation do not need to be calibrated (through signal saturation as in the case of the battery current), once they would never extrapolate the limitations of the battery previously dictated by the battery current.

Although battery voltage behaves accordingly to its limits, another parameter should be taken into consideration: the nominal voltage. This is calculated based on the supplier's defined nominal voltage for each cell and further multiplied by the number of cells in series that compose the battery pack (as previously explained in Chapter 3). Whenever the bus is stopped, the battery voltage curve shows periods of constant behavior. The value for voltage in these periods is largely due to the nominal voltage value, with a small parcel coming from the battery current in idle times. After evaluating the real system voltage graphs, it can be observed that the value for voltage during those times is slightly superior: around 372.5 V.

Therefore calibration had to be performed firstly on the current boundaries, saturating the signal so that it would be in accordance with the real operational values (-300 A to 150 A). Thus whenever the bus is accelerating, the maximum value for current will be -300 A whereas when braking, the bus could reach a maximum of 150 A. Concerning battery voltage, there was no need to limit its range of operation. The next step will be to define the variables to be validated and the process is described in the next section.

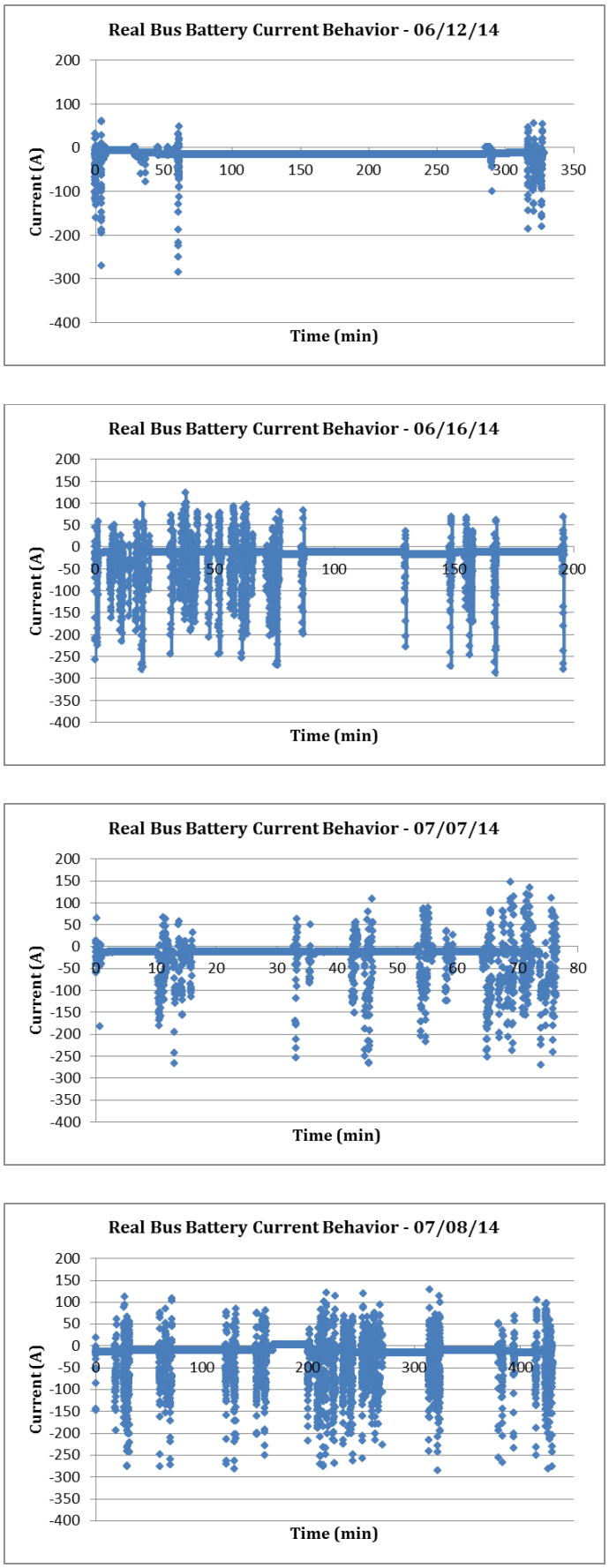

Figure 5.1– Battery current behavior of the real bus operation for different days of operation

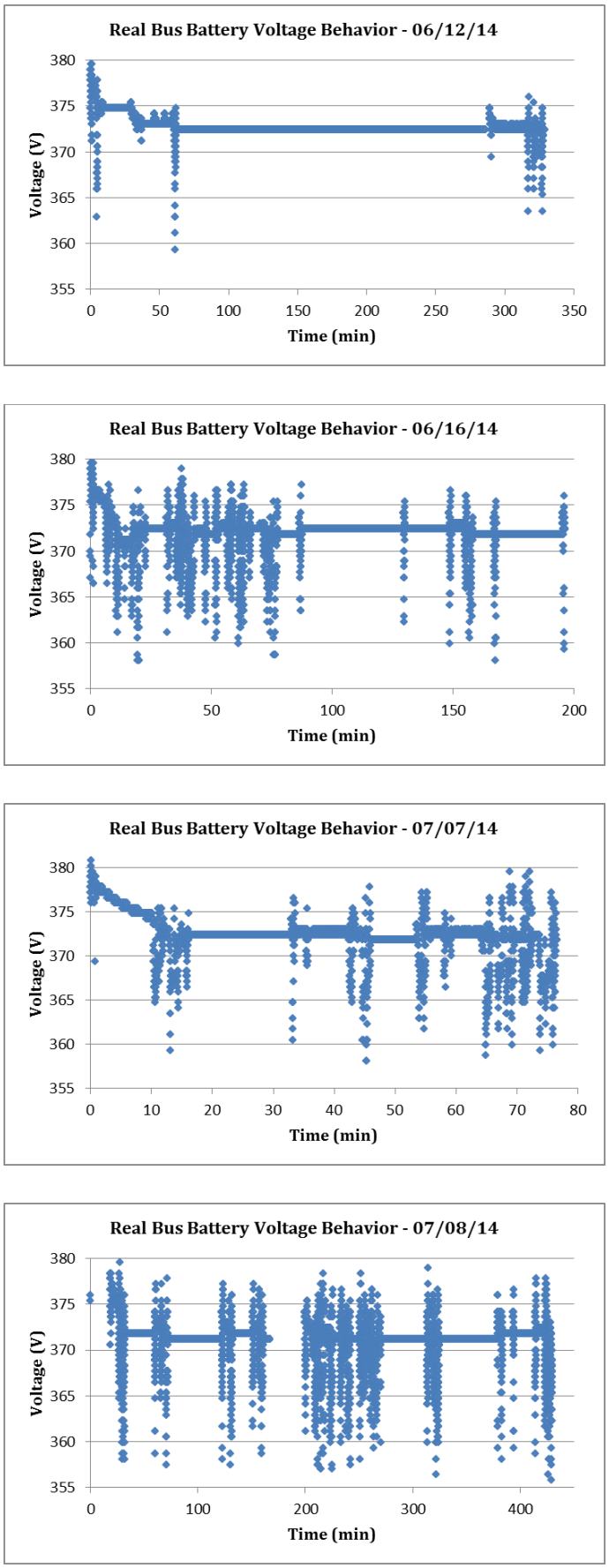

Figure 5.2– Battery voltage behavior of the real bus operation for different days of operation

5.4.2 Model Validation

In the previous subchapter, current and voltage calibration were performed according to real data collected from the bus. Now that the range of operation of both variables in the model is assured to mimic the one from the real world, validation of the model is mandatory. When talking about electric vehicles, the first concern of the majority of people is whether they are going to run out of energy on the batteries in the middle of nowhere. Therefore, two output variables were considered to be the most important to be validated in this context: energy consumption and state-of-charge (SOC) of the batteries.

Before choosing a method for validating the model, it is crucial to define whether unobservable inputs exist or not as it may change the path to be followed. In the real system, there exist three main inputs: speed, accessories and passengers.

Speed is an observable input once its values are electronically collected and it feeds all the main mathematical equations of the model.

Accessories account for the energy consumption of anything but the electric motor, namely the power steering, the air compressor, the air conditioning, lights, smaller electrical systems, etc. They represent a smaller portion of the energy consumption of the system but still generate some impact on performance.

Due to the fact that the data collection was performed during summer time and at an airport, where clients' satisfaction is the paramount goal, it was considered that the air conditioning system was turned on during the whole operation of the bus. In this sense, this variable will not be used on the sensitivity analysis; only the power steering and the air compressor are discriminated, once together with the air conditioning they represent almost 100% of energy consumption from accessories. Their behavior is considered to be similar: if the bus is idle their values go to a minimum. If the bus operates more intensely, e.g. with harsh maneuvers, both parameters increase.

At last, the number of passengers that board on or alight from the bus can also be considered an unobservable input, once the only way of counting it is "manually" for the bus is not equipped with a scale. For both inputs, the range of operation is well-established and is crucial for the validation process. These inputs can be observed in Table 5.3.

Table 5.3- Range of variation of the unobservable inputs: power consumed in accessories and total weight of the passengers carried

Input variable	**Range of operation**
Power consumed in accessories (kW)	Power steering: 0.8 – 5.5 kW Air compressor: 1.2 – 5.5 kW
Total weight of the passengers (kg)	80 – 4581 kg

Due to the existence of two unobservable inputs, the choice of the validation technique is restricted, and once the range of variation for those inputs are well-known, the technique that makes more sense to be applied is sensitivity analysis. As described in the early session of this chapter, sensitivity analysis will allow the model to be valid for a range of possible values for the unobservable inputs; the impacts on the chosen outputs due to the changes on those inputs will be evaluated.

The first step on the sensitivity analysis process is to define baseline values for both unobservable inputs. By doing that, baseline outputs are also defined for each scenario and variations on them are evaluated as the process of changing the input variables continues. Those baseline values were defined as the average of the range of variation for each variable and can be seen in Table 5.4.

Table 5.4– Defined baseline values for the unobservable inputs: power consumed in accessories and total weight of the passengers

Input variable	**Baseline values**
Power consumed in accessories (kW)	Power steering: 3.2 kW Air compressor: 3.4 kW Total: 6.6 kW
Total weight of the passengers (kg)	2333 kg

The next step is to run the simulation with the baseline values for the variables presented in Table 5.4 and access the behavior of both selected outputs in comparison to the real system's: energy consumption and SOC. Hence values for the unobservable inputs will be modified one at a time, and their impacts on the energy consumption and SOC will be evaluated accordingly; this process will be performed for the same four scenarios used on the calibration process.

The variation in the input variables was performed in a systematic way. The weight of passengers was firstly held constant (in its baseline value) and the accessories were adjusted to their minimum possible value and then to their maximum value. On a later stage, the value of accessories remained as their baseline and the weight of passengers varied from the equivalent of an empty bus (only the driver aboard) to a full-capacity bus.

The different variation tests on the inputs can be observed in Table 5.5. It is important to state that those inputs were purposely varied individually, in order to assess their sole impact on the outputs.

Table 5.5– Definition of the unobservable inputs values to perform sensitivity analysis

Input variable	Test 1	Test 2	Test 3	Test 4
Power consumed in accessories (kW)	2 kW	11 kW	6.6 kW	6.6 kW
Total weight of the passengers (kg)	2333 kg	2333 kg	80 kg	4581 kg

The presentation of the results will not be based on each of the four scenarios, but in the tests that were made, together with the baseline. In this sense, it is possible to perform a better evaluation of the impacts of each input variation in the outputs.

5.4.2.1 Sensitivity Analysis – Energy Consumption

The first output to be analyzed is the energy consumption, which is calculated by multiplying the current and voltage at each time step and further integrating this result in time. It is relevant to say that these data are collected in a time stamp of 1 second, thus the considered time step is one second. The analysis is held in two ways: graphically and through percentage. Graphs allow evaluation through the behavior of the curve in relation to the real system. And because in the case of this variable the final value is of great importance, once it summarizes all the energy consumption after the whole operation, percentages in relation to the real system of the final values of every test were also calculated and evaluated.

For each of the four scenarios, five graphs were developed: baseline, test 1, test 2, test 3 and test 4; each graph has the curve for the real system in order to facilitate the comparison. The graphs are compiled not for scenarios relative to the days of operation but for baseline and tests, e.g., the first set of graphs to be evaluated is for the baseline case, and they can be observed in Figure 5.3. The blue line is related to the real system and the red to the simulation result.

It is clear that the graphs are quite similar in what concerns being a growing curve over time, which was expected once this variable is a result of an integration procedure. The second characteristic to be observed is the behavior of those curves, not only because they grow synchronously but also because they have similar behavior, apart from some cases where they deviate slightly from the real system at a certain point. In order to quantify how this deviation affected the final mark for energy consumption, percentages were

calculated and can be consulted in Table 5.6; the absolute values for final energy consumption are also presented.

Table 5.6- Energy consumption values and their percentage deviation from the real system for baseline cases

Scenarios	**June12th,2014**	**June16th,2014**	**July 7th, 2014**	**July 8th, 2014**
Real System (kWh)	31.1 kWh	25.0 kWh	10.7 kWh	48.5 kWh
Baseline (kWh)	31.0 kWh	26.4 kWh	11.6 kWh	51.4 kWh
Baseline (%)	-0.21%	5.76%	8.40%	6.09%

Except for the case of June 12th, which had an insignificant deviation, all the other three cases had positive deviations ranging from 5.5% to 8.5%. This can be explained by assuming that the input variable values in June 12th are closer to the reality of that day than in the other occasions, meaning the bus ran with half of its full capacity and the route was composed of some harsh turns.

Having presented the baseline graphs and percentages, it is time to evaluate the impacts of changes in input variables on the energy consumption when compared to this baseline. Firstly, it will be analyzed the impact of the accessories in contrast to the weight of passengers when reducing their values from the ones stipulated for the baseline (test 1 and test 3). Because all the graphs for energy consumption for test 1 and test 3 had a very similar behavior to those of Figure 5.3, it was decided to present only the percentages of variation on the energy consumption final mark for each test, which can be observed in Table 5.7.

By taking a careful look at this table, it is clear the reduction in the required power for the accessories has a greater impact on the bus energy consumption. While the difference on the overall consumption promoted by the reduction of the weight associated with passengers (half-capacity bus to one passenger) was less than 2% in all cases, the reduction in the power required by accessories (from 6.6 kW to 2.0 kW) accounts for an average of 4% decrease, representing double of the impact.

Table 5.7- Energy consumption values and their percentage deviation from baseline for test 1 and test 3

Scenarios	**June12th, 2014**	**June16th, 2014**	**July 7th, 2014**	**July 8th, 2014**
Baseline (kWh)	31.0 kWh	26.4 kWh	11.6 kWh	51.4 kWh
Test 1 (kWh)	30.8 kWh	25.3 kWh	11.0 kWh	49.5 kWh
Difference	-0.73%	-4.14%	-4.97%	-3.77%
Test 3 (kWh)	30.8 kWh	26.0 kWh	11.3 kWh	50.7 kWh
Difference	-0.48%	-1.71%	-1.87%	-1.38%

Next step is to provide the same numbers and analysis for the tests where the unobservable inputs suffer an increase: test 2 sensitive to accessories increase and test 4 to passenger increase. Table 5.8 summarizes the values for the energy consumption of the bus in tests 2 and 4, presenting the baseline value for reference.

Table 5.8- Energy consumption values and their percentage deviation from baseline for Test 1 and Test 3

Scenarios	**June12th,2014**	**June16th, 2014**	**July 7th, 2014**	**July 8th, 2014**
Baseline (kWh)	31.0 kWh	26.4 kWh	11.6 kWh	51.4 kWh
Test 2 (kWh)	31.2 kWh	27.5 kWh	12.1 kWh	53.3 kWh
Difference	0.69%	4.17%	4.76%	3.61%
Test 4 (kWh)	31.1 kWh	26.8 kWh	11.7 kWh	52.0 kWh
Difference	0.40%	1.53%	1.60%	1.15%

Similarly to what happened in test 1 and test 3, energy consumption coming from accessories had a greater impact than the one promoted by the number of passengers. Percentages of the accessories when increasing their required power from 6.6 kW to 11 kW represent in some cases three times as much impact when compared to increasing the weight of passengers from a half- to a full-capacity bus. Summarizing, it is clear that energy consumption of accessories plays a major role in what concerns energy consumption of the whole bus when directly compared to the number of passengers carried (or their consequently weight). The next subchapter demonstrates a similar analysis to the unobservable variable state-of-charge of the batteries.

5.4.2.2 Sensitivity Analysis – State-of-Charge (SOC)

The second output to be analyzed is the state-of-charge of the batteries, which is calculated based on the current and the nominal capacity of the battery, as already described in section 3.2.1.8. At this point, it should be brought into attention that the frequency of these specific collected data in the real system is random, which means that the signal is updated on a random time step. Due to this fact, some inconsistencies occur on the data, such as the repetition of a same value for several steps, which is further updated to three units less (e.g., step 100 inputs the value “95” and step 101 inputs “92”). In order to solve this issue, some actions had to be taken in order to fine-tune the data, namely:

- Hold the first input of a certain value and delete the consecutive ones that are equivalent to it;
- Delete inputs in which the value is zero.

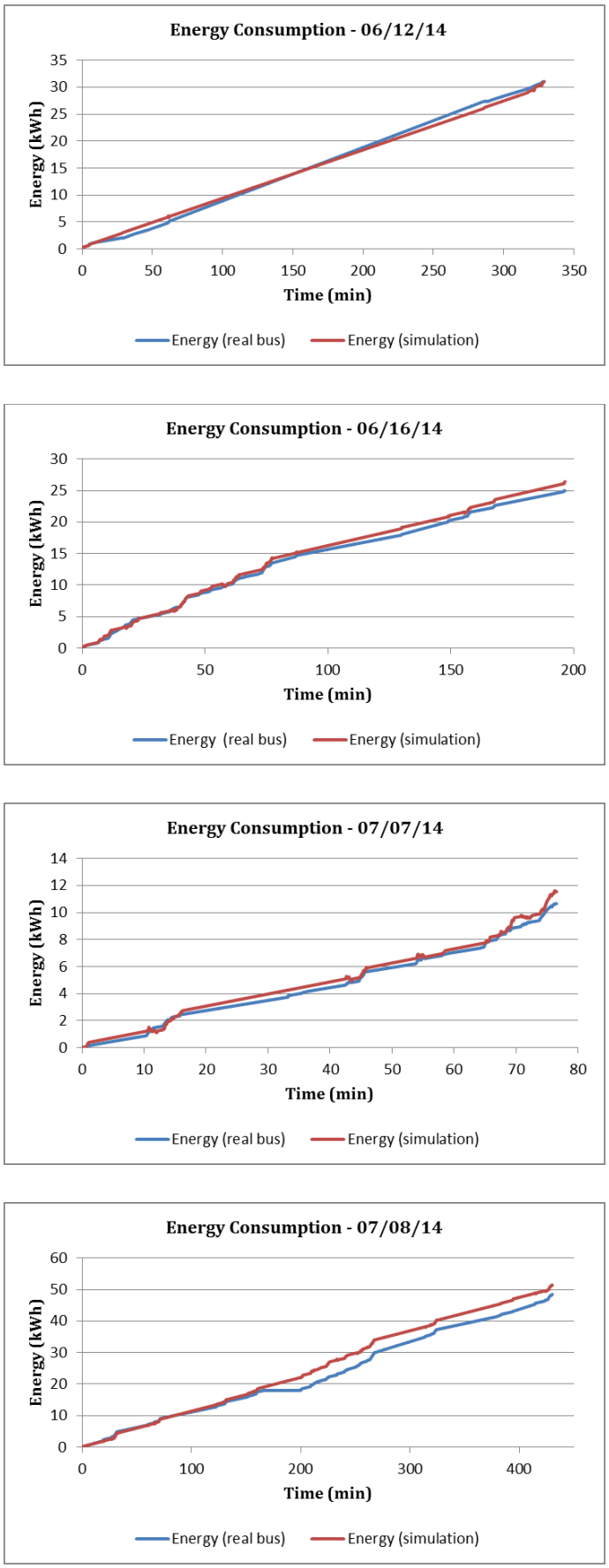

Figure 5.3- Energy consumption comparative graphs for the baseline case of the different days of operation

The main objective in applying such actions is to have a nice linear regression equation, respecting the behavior of the curve. If either the repeated values or the zeros were left on the data stream, the linear regression would be wrongly deviated. The graphs are composed of blue markers for the real system inputs, a dotted black line for the linear regression trend line, and a red line for the simulation output. Following what was done in the previous subchapter, the analysis is held in graphs and numbers, once the final value is also of great importance. Five graphs were plotted for each of the four scenarios, namely the baseline, test 1, test 2, test 3 and test 4; the baseline graphs are presented in Figure 5.4.

The graphs are quite similar in what concerns being a descending curve along time, which was expected once this variable is supposed to decrease as current is being applied. The second characteristic to be observed is the behavior of those curves, where in most of the cases, the inclination of the linear regression and the red lines are similar, except for the case of June 12th, where the observed deviation is larger. In order to quantify how this deviation affected the final mark for the SOC, percentages were calculated and can be checked in Table 5.9; the absolute values for the final SOC are also presented. Again, except for the case of June 12th, all other three cases had quite insignificant deviations from the real values, ranging from -0.2% to -1.4%.

Table 5.9- SOC values and their percentage deviation from the real system for baseline cases

Scenarios	**June12th,2014**	**June16th,2014**	**July 7th, 2014**	**July 8th, 2014**
Real System (%)	90.4%	82.0%	91.8%	68.2%
Baseline values (%)	78.9%	81.9%	91.5%	67.2%
Difference (%)	-12.7%	-0.24%	-0.40%	-1.39%

After defining the baseline values, it is time to start the sensitivity analysis of the unobservable inputs: energy consumption of accessories and number of passengers. Mimicking what was developed for the energy consumption case, the first analysis is held on the decrease of the values for power from accessories and number of passengers (according to Table 5.5), as a way to evaluate the impact on the SOC. The outcomes of the simulation can be checked in Table 5.10.

Table 5.10– State-of-charge values and their percentage deviation from baseline for test 1 and test 3

Scenarios	**June 12th, 2014**	**June 16th, 2014**	**July 7th, 2014**	**July 8th, 2014**
Baseline (kWh)	78.9%	81.8%	91.5%	67.2%
Test 1 (kWh)	78.8%	81.1%	91.1%	66.1%
Difference	-0.17%	-0.86%	-0.38%	-1.76%
Test 3 (kWh)	78.8%	81.5%	91.3%	66.9%
Difference	-0.10%	-0.32%	-0.13%	-0.56%

Although the overall impact of the decrease of those variables was small, the required power from accessories seemed to impact more on SOC, following the behavior observed in energy consumption. While the weight of passengers never had an impact over -1%, accessories had examples in which this difference raised close to -2%. In order to access the impact of the increase of those variables, a similar approach was taken, where tests 2 and 4 are presented in Table 5.11.

Table 5.11- SOC values and their percentage deviation from the real system for Test 2 and Test 4 when compared to the baseline

Scenarios	**June 12th, 2014**	**June 16th, 2014**	**July 7th, 2014**	**July 8th, 2014**
Baseline	78.9%	81.8%	91.5%	67.2%
Test 2	79.0%	82.5%	91.8%	68.5%
Difference	0.18%	0.85%	0.40%	1.84%
Test 4	79.0%	82.0%	91.6%	67.7%
Difference	0.12%	0.36%	0.15%	0.68%

Similarly to what was observed with the decrease in the unobservable variables, the variations in energy consumption of accessories are greater than the ones observed for a full-capacity bus. In the first case, the variation has gotten closer to 2% while in the latter, the highest value was nearly 0.7%.

The overall conclusion of this sensitivity analysis is that neither the accessories energy consumption nor the weight of the passengers plays a central role in what concerns the global energy consumption of the bus and consequently its SOC; the greatest impact observed was around 5%. For a bus that weighs 15 tons, a power of 11 kW consumed in accessories or the weight of around 50 people do not seem to affect much its performance.

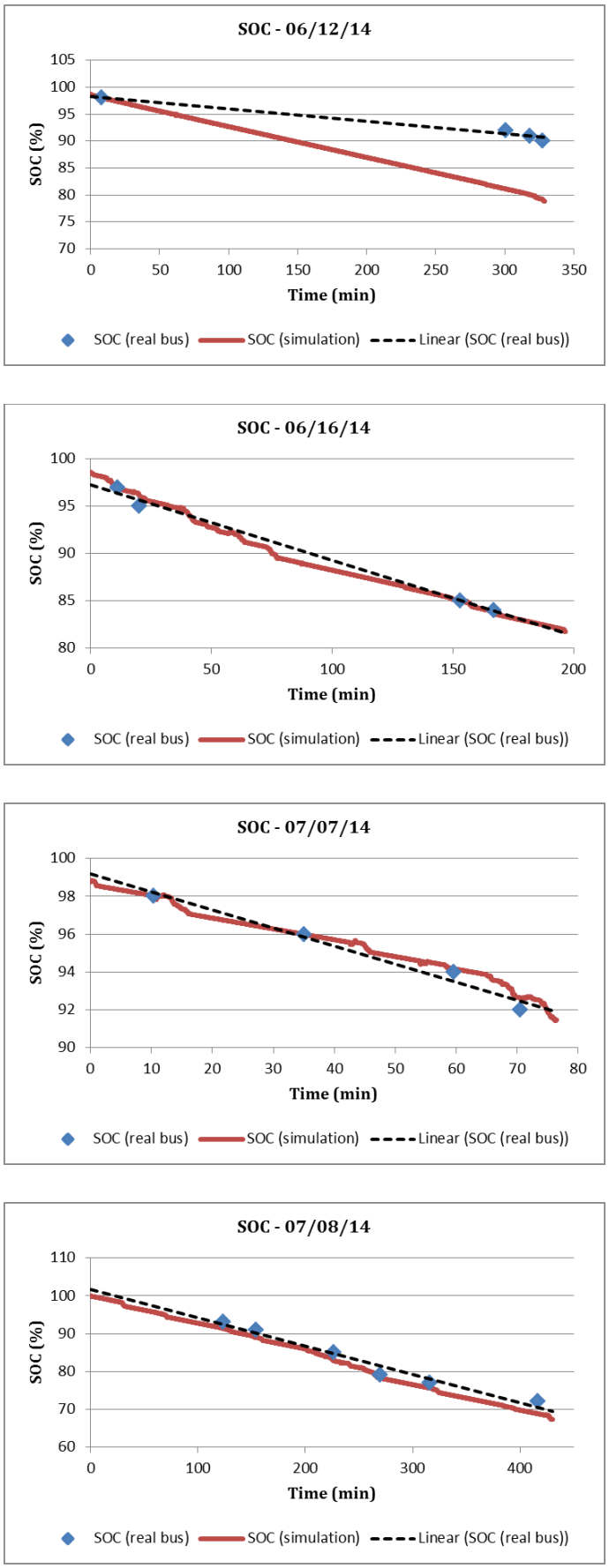

Figure 5.4- State-of-charge comparative graphs for the baseline case of the different days of operation

5.4.2.3 The Baseline Value Redefinition

A baseline case was previously defined to compose the scenarios for the sensitivity analysis and because the objective was only to evaluate the impacts of changes in the inputs on the overall energy consumption and SOC, not much attention was given to those inputs. As a final step in the validation process of this simulation model, it is proposed an evaluation of which of the studied scenarios (baseline itself, tests 1 to 4) best represents the behavior of the real bus. In order to do that, the outcome of the simulation was compared to the outcome of the real system for the energy consumption on each of the four days. The percentages were graphically represented in radar charts, which are an intuitive way to compare those percentages. The charts can be observed in Figure 5.5.

Figure 5.5 shows fairly clearly that test 1 presented the smallest deviation from the real system on each of the four days. All markers in test 1 point out to a less than 3% deviation while most of the other tests, baseline included, reached up much higher values. Therefore from this point on, test 1 is the new baseline and all further simulations will be performed with its variable values, unless data is available regarding them.

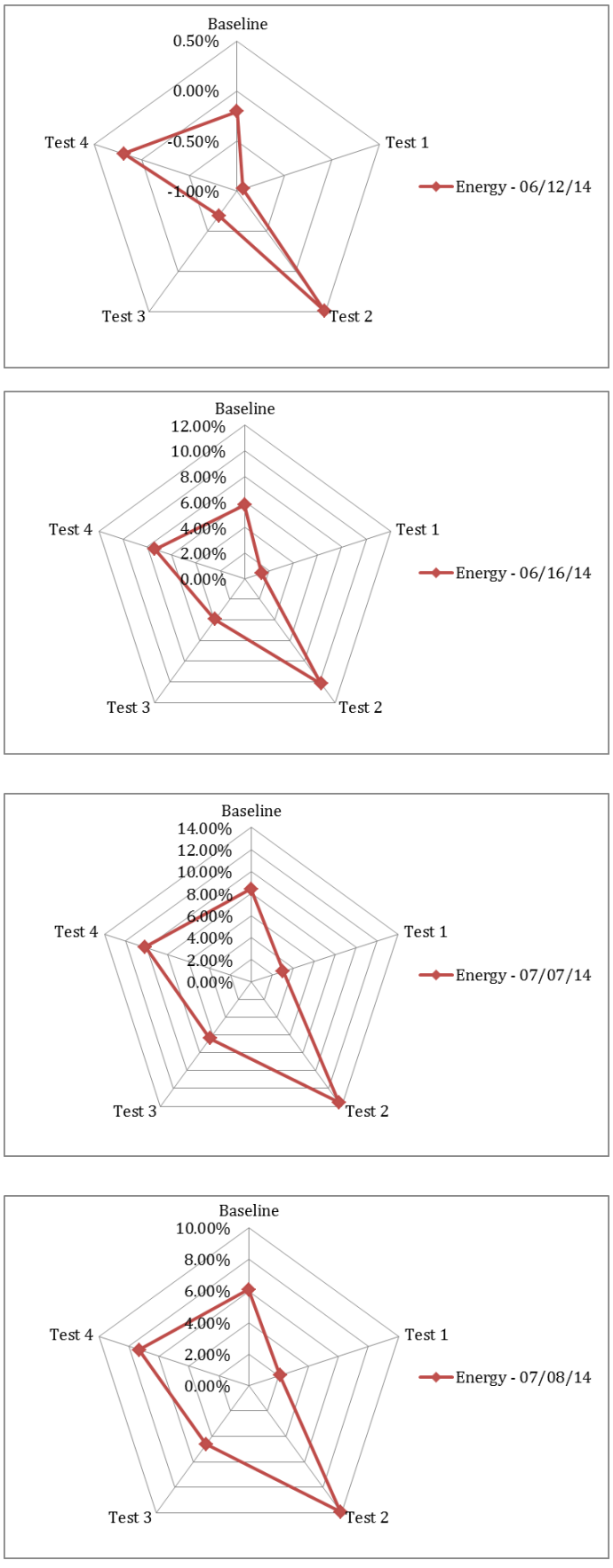

Figure 5.5- Comparative radar charts for energy consumption deviation from the real system

5.5 Conclusions

Calibration and validation processes for simulation models are not simple. They require extensive knowledge of the model, its inputs, outputs - whether observable or not -, and many other details that are specific to the model in analysis. In this chapter, a process for validating and calibrating the *Simulink* model of the electric bus was performed. Calibration was carried out on the battery electric current and voltage variation ranges, and further extended to the voltage nominal value.

Once calibration was performed, many validation methods were described and one of them was chosen based on a really simple fact: there exist unobservable variable inputs. When this is the case, the methods are limited to a few and the choice was to use sensitivity analysis. Sensitivity analysis was performed on the two variables that represent the unobservable inputs: accessory energy consumption and weight of passengers carried. None of those inputs seemed to play a relevant role in the global energy consumption of the bus or in the state-of-charge of batteries.

The sensitivity analysis served as a major role, where the defined baseline was not the best option as a baseline *per se*. The last part of the chapter was dedicated to finding the best values for the unobservable variables based on the tests performed during the sensitivity analysis. It came up to a conclusion where test 1 had the best markers and the values for the variables used on it will be considered for all future simulations, assuming there is no known data for them.

The next chapter presents the case studies performed with the electric bus integrated simulation platform. The first case study performed is about the performance on three real existing Portuguese bus routes regarding the impact that the topology of each route has on the performance of the bus. The second is about the impact of driver's behavior on the electric bus performance, and is setup in Porto. The other case study is about the implementation of the electric buses in Boston, involving a real O/D matrix to account for the circulating traffic.

Chapter 6

Case Studies on the Integrated Simulation Platform

6.1 Summary

In this chapter, some case studies performed with the integrated simulation platform are presented. For the first Portuguese case, an analysis is held regarding energy consumed and generated for three different real bus routes in Porto. The second focuses on the driver's behavior and its impact on performance. A third case study was held in the context of the implementation of the BRT (Bus Rapid Transit) system in the Greater Boston, which involves the electric bus performance analysis for a complete fleet. In the end, a holistic analysis is performed considering a whole day of operation for an electric bus in Boston.

6.2 Portuguese Case Study 1: Analysis of Three Routes Scenarios

The first case study performed with the developed simulation platform was performed on Portuguese scenarios, more specifically in the city of Porto. Porto is served in terms of transportation primarily by the public entity STCP (*Sociedade de Transportes Colectivos do Porto*)[21], which provided the necessary data to make those simulations possible. Porto is known by its irregular topography, either related to its narrow streets, sharp turns or elevation profile, as it can be observed in Figure 6.1.

Porto case studies focus on analysis held for three different STCP routes, namely lines 401, 204, and 602. Line 401 is characterized for having a demanding topography to be performed, being a small urban route composed by many differences in elevation and harsh turns. Line 204 is a regular urban route, though straighter than line 401. Line 602 is an inter-urban route, longer than the others and accounting for bigger distances between stops, and also fewer traffic lights in some parts of the route (Perrotta et al. 2014). Table 6.1 summarizes those main characteristics of those routes, accounting for their number of stops and extension as well.

[21] www.stcp.pt (STCP 2014)

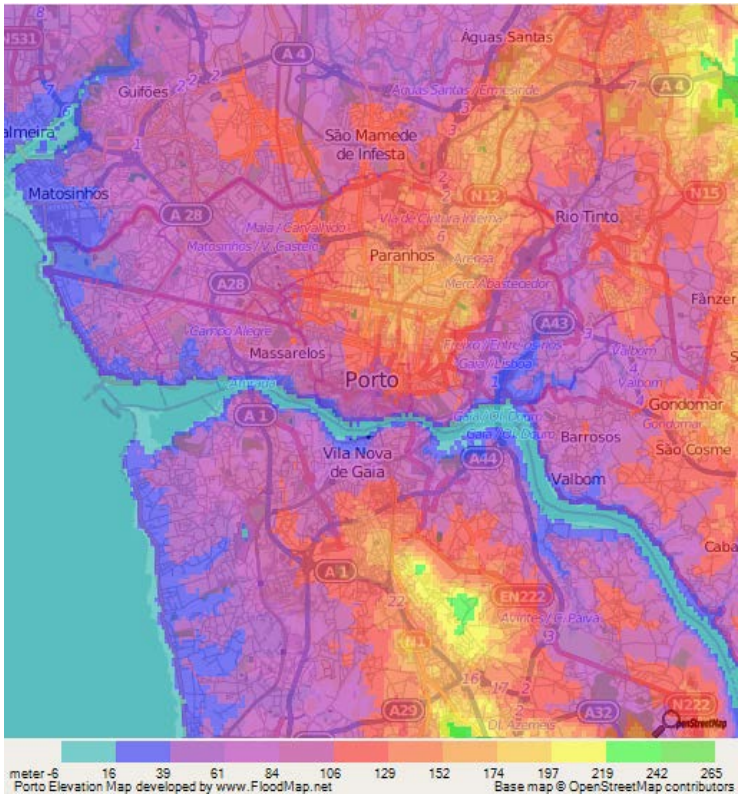

Figure 6.1– Porto elevation map (Floodmap 2014)

Table 6.1– Porto bus routes characteristics

Bus lines	Type	Stops (nº)	Size (km)
401	Demanding topography	26	8
204	Urban	38	12
602	Inter-urban	55	19

In addition, Figure 6.2 depicts each route on a map alongside their elevation profile plots. In order to define these routes, data was collected and further made available by STCP. These data comprised the geographic coordinates of bus stops for each of the three routes, which made them essential to perform the elevation profile definition. As a way to extract elevation data from latitude and longitude, a tool developed in LIACC at FEUP was used. This tool is basically an *.html* script that works as a web crawler, systematically browsing pre-determined Internet webpages to collect elevation values for each latitude/longitude point.

6.2.1 Objectives

This case study has as primary objective the comparison of the electric bus performance for the three routes presented concerning energy consumption and the amount of regenerated energy. Due to the peculiar nature of the routes especially regarding their different sizes, the energy consumption parameter is analyzed in kilometers. In addition,

the regenerated energy is approached from its percentage amount in relation to the overall consumption.

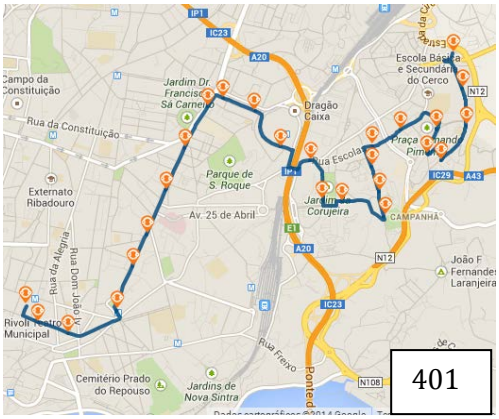

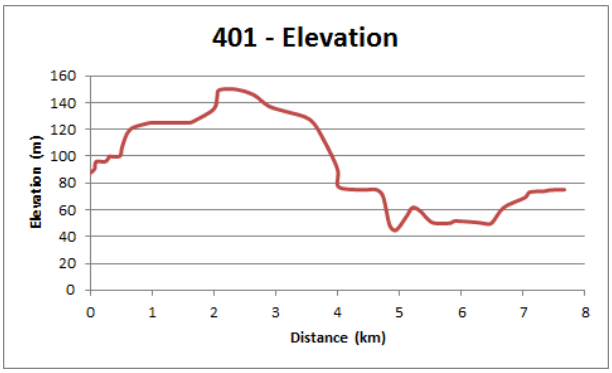

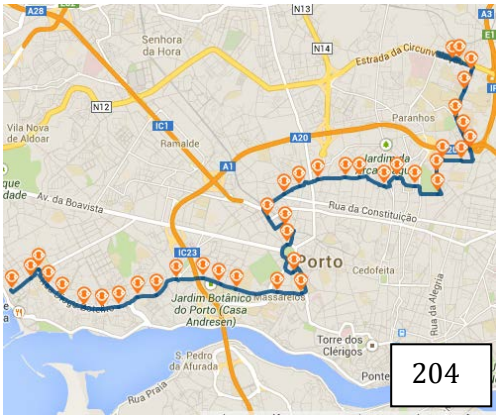

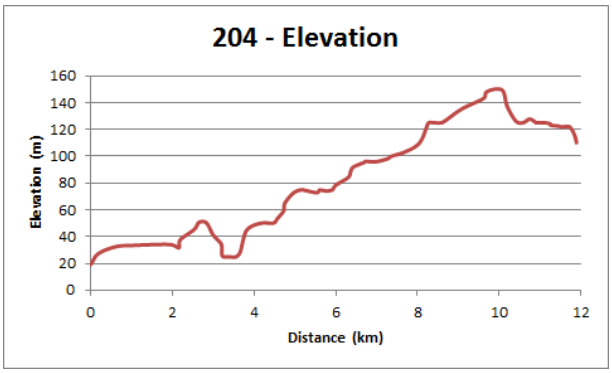

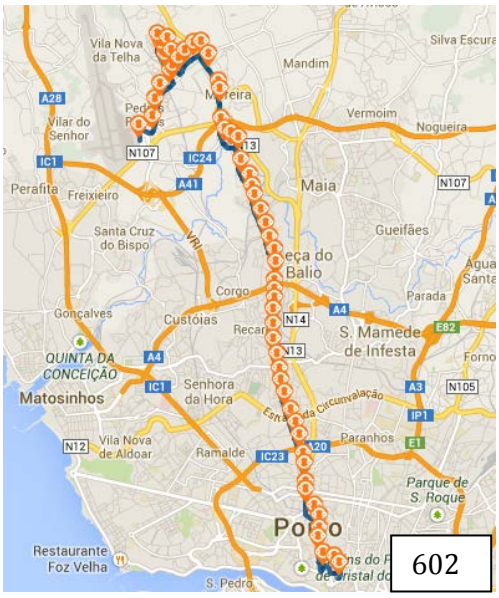

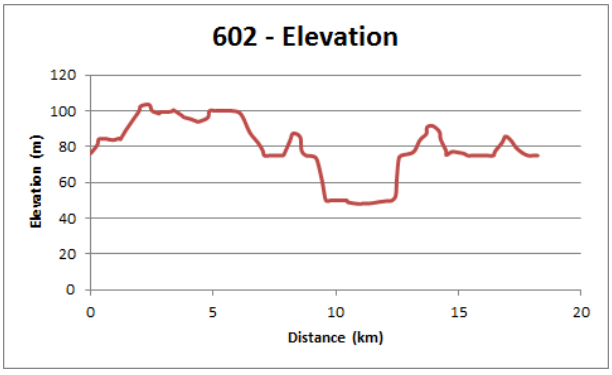

Figure 6.2– Graphical representation of the three Porto bus lines and their elevation profile

6.2.2 Simulation Setup

So far, the three Portuguese routes were presented, together with their main characteristics. This serves as basis for the simulation setup, which is composed of area

definition, demand model and route coding in *SUMO*. At this point, it is relevant to mention that an ideal traffic flow is considered, which means that the buses performed on free-flow roads. This decision was necessary once the objective is to evaluate the impact of the route topography and stops distribution on the electric bus, and not the influence of traffic congestion. Therefore, no detailed demand modeling was required.

For each of the three routes, a specific area definition and its posterior conversion to *SUMO* format is handled, as well as route coding, manually performed on top of the imported map. Moreover, the bus stops and the time that the bus actually arrives at each stop are also coded for each route scenario.

6.2.2.1 Line 401 Coding

The first coded route concerns line 401, which happens to be the smallest among the three. The area where this route is contained was extracted from *Open Street Maps*, to be later imported to *SUMO*, being illustrated in Figure 6.3.

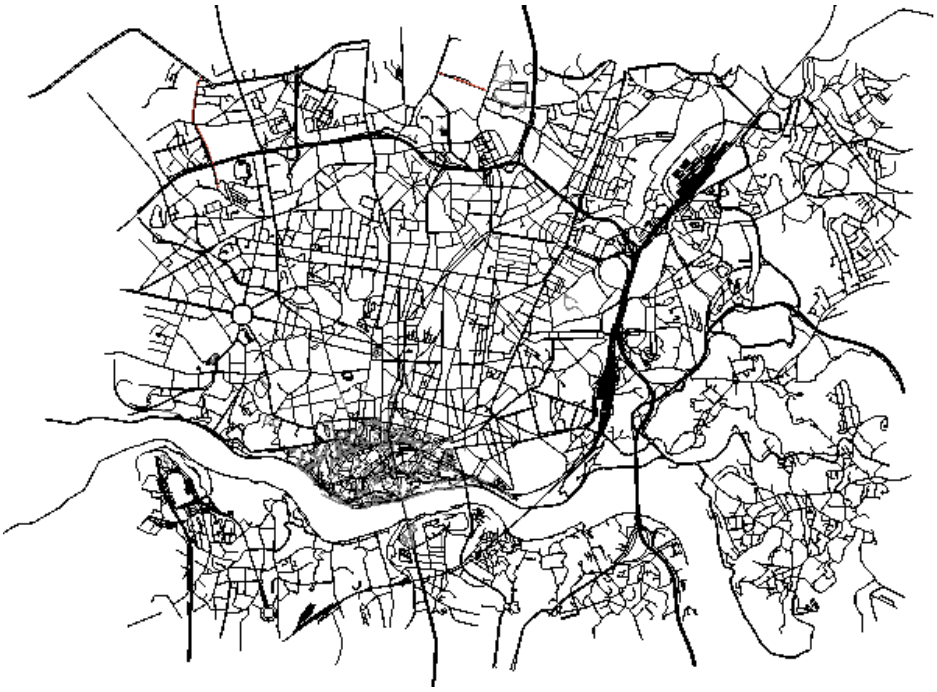

Figure 6.3- *SUMO* representation of the map for coding route of line 401.

Once the map is imported into *SUMO*, the route can be coded. The coding process was explained in detail in the previous chapter but basically each street the bus passes by have to be manually defined in the *SUMO* code. After that, the bus stops have to be defined in order, according to the bus direction (chosen to be clockwise).

The bus performs full stops at every bus stop. Moreover, due to the fact that there is no data available for the number of passengers that board on the bus, it was stipulated that this time is 20 seconds. The route information, bus stops and time at bus stops are defined

in a file called "buses.add.xml" and can be observed in Appendix F. This file also contains parameters for the bus, such as acceleration, deceleration and maximum speed allowed.

The data provided by *STCP* contained, besides the geographical coordinates of the route, the speed of the bus. Based on that, the average values for acceleration/deceleration were calculated: 1.5 m/s^2. Regarding the maximum speed, it is considered the value regulated for urban areas in Portugal: 60 km/h. The "buses.add.xml" and the imported map files have to be called simultaneously by the simulation platform. This can be achieved by defining a configuration file (*.cfg*) containing them both in its content.

6.2.2.2 Line 204 Coding

Line 204 is the next to be coded, which represents a straighter urban route when compared to line 401. The approach is similar to that applied to line 401, where the area definition was performed in *Open Street Maps* and the resulting map imported into *SUMO* (Figure 6.4). Once having the map in *SUMO*, the route could be coded, together with the bus stops and the time that the bus stays stopped at each one of them; again 20 seconds per stop is considered.

Figure 6.4- *SUMO* representation of the map for coding the 204 route

Similarly, all route data are compiled in a file "buses.add.xml" (Appendix G), as well as are the values for acceleration/ deceleration and maximum speed. Acceleration and deceleration were found analogous to the 401 (calculated from the speed in the *STCP* data), and are both 1.5 m/s^2. The maximum allowed speed is also the regulated value of 60 km/h, and the *.cfg* file is coded to account for both the map and the bus route definition.

6.2.2.3 Line 602 Coding

Line 602 is the longest of the three, being an inter-urban route and as such having longer distances between stops. The map was extracted from *Open Street Maps* as well and then imported into *SUMO*, whose visualization is presented in Figure 6.5. The "buses.add.xml" file (Appendix H) contains all the data for the route and also for the bus operation, being the acceleration/deceleration rates 1.7 m/s^2 (inferred from the speed data of the *STCP* file) and the maximum allowed speed, namely 60 km/h. It is good to reinforce that the time the bus has to stop for passengers to board/alight is also 20 seconds. A *.cfg* file was set up containing the *SUMO* network map and the bus route definition.

6.2.3 Results and Discussion

Simulations were performed for the analysis of the three mentioned routes. The focus of the collected data was energy consumption and energy regenerated in braking episodes (or due to "down-the-hill" movement). The higher this recovery, the more efficient is the performance.

The first analyzed parameter is the amount of consumed energy per kilometer. Once the routes are really different among them, the absolute values of consumed energy would not mean much. Line 602 was the one that spent the least amount of energy per kilometer performed, thus being used to normalize the parameter. The other two bus lines are compared on a percentage basis, as it can be observed in Figure 6.6.

It is worth highlighting that line 602's route is characterized by an inter-urban itinerary that is primarily straight, whereas line 401 represents the smallest among them and has the least number of bus stops. However, it possesses a demanding topography of harsh turns and shorter distances between bus stops, making the bus perform many acceleration episodes in short periods of time. Therefore, the route of line 401 consumed a similar amount of energy per kilometer compared to line 602.

Line 204, on the other hand, had the highest amount of energy consumed per kilometer. This is perfectly understandable from the point of view of its elevation profile, accounting for a smooth yet constant up-the-hill route. In addition, this route is also composed of some harsh turns along the way, contributing for its higher energy consumption.

Figure 6.5- *SUMO* representation of the map for coding route 602

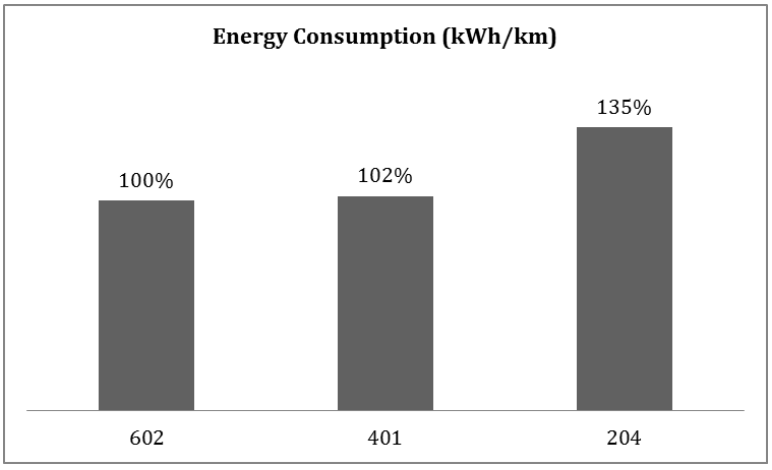

Figure 6.6- Comparative analysis of the consumed energy for the three routes

The next analyzed parameter is the percentage amount of regenerated energy in relation to the total energy consumption for each route; its graphical representation can be observed in Figure 6.7. This regeneration can happen either in braking episodes or

whenever the bus is going down a hill. Line 204 consumed the highest amount of energy per kilometer and this is partly due to the fact that it was the line that recovered less energy during its operation: around 38% of its overall energy consumption.

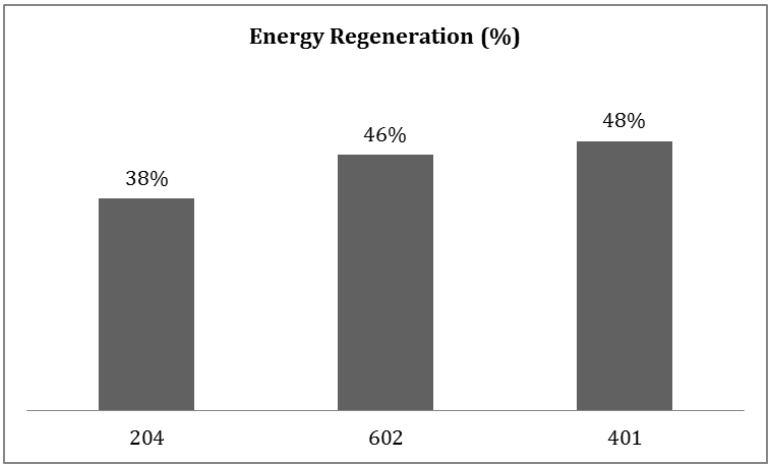

Figure 6.7– Comparative analysis of the regenerated energy to the total energy consumption for each route

On the other hand, routes from lines 602 and 401 had a better energy recovery performance, being their values 46% and 48% of their total energy consumption, respectively. In the case of line 401, the route is composed of a steep descent from Km 2 to Km 5, which greatly contributes for its energy regeneration. For line 602, the reason why it had high values for regeneration can be due to the bus being able to perform at rated and constant speed, not having to stop so frequently and thus impacting positively on its performance.

6.3 Portuguese Case Study 2: The Driver's Behavior Analysis

When talking about the operation efficiency of internal combustion vehicles, there is one factor that plays an important role on the fuel consumption: driver's behavior, which can be aggressive or regular. In the literature of driving behavior, there are usually three types of aggressive driving: verbal or physical aggression, negative emotions (such as anger) and risk-taking (Dula and Ballard 2003). The one that matters for this analysis is the latter: risk taking.

The risk-taking category includes behaviors such as speeding up, running red lights, maneuvering without signaling, and frequent lane changing; it also comprises the dangers from lapses of attention while driving, typical for those who use the cell phone, eat, drink, smoke, or adjust the radio. Those behaviors can happen even in the absence of negative emotion or intent to harm (Dula and Geller 2003).

Generally, this type of behavior has implications on fuel consumption (for internal combustion vehicles) or energy consumption (for electric vehicles), once it is characterized for the opposite behavior of the so-called eco(logical)-driving. An ecological strategy is to anticipate what is happening ahead, and drive in a way to minimize acceleration and braking, and also running at the optimal speed (Kamal et al. 2009). In other words, it may be represented by a soft driving, especially restricting acceleration rates (Miyatake et al. 2011).

6.3.1 Objectives

The implications of risk taking attitudes of a driver towards the energy consumption of electric buses when compared to regular drivers are analyzed in this case study. The parameter used to differentiate one from another is the absolute value used for the acceleration and deceleration rates, once they impact directly on the speed profile of the bus and consequently on all the calculations performed (Perrotta et al. 2013).

6.3.2 Simulation Setup

A random route was modeled in *SUMO*, considering as base reference the region of Aliados Av., in the city of Porto, Portugal. The modeling method adopted is similar to the case previously presented, with the extra characteristic of having a picture as a layer on top of the *SUMO* network. On this route, 10 bus stops were defined and it was assumed that the bus would stop 20 seconds at each one of them. Stops at red traffic lights were also considered, and random vehicle traffic was generated. Moreover, the battery initial state-of-charge (SOC) is established at 95%.

The region of *Aliados* Av. in *SUMO* format can be observed in Figure 6.8, with the aforementioned extra-feature of the real map on top of the network. Since this is a high-density area, it was considered that the bus ran full of passengers and, to provide them with comfort, the ventilation system was on.

For calculation purposes four scenarios were set up, varying the acceleration and/or deceleration rates, as it can be observed in Table 6.2. It is relevant to point out that none of these values surpasses the technical restrictions of the electric bus. The simulation was then performed four times for the exact same route, accounting for the different scenarios.

Figure 6.8- Aliados Av. region network in *SUMO*, with a top-layer of a real map

Table 6.2- Acceleration/ Deceleration rates for simulation

Scenario	Acceleration (m/s^2)	Deceleration (m/s^2)
a05d05	0.5	0.5
a1d05	1.0	0.5
a05d1	0.5	1.0
a1d1	1.0	1.0

6.3.3 Results and Discussion

After running the simulation for all four scenarios, two parameters were collected and analyzed: the amount of energy spent and recovered. Although the simulation results are on a time scale, for this analysis, only the final value of the parameters were considered, once it is the result of a numerical integration, as such the only that matters. Therefore, those values were put in parallel for each scenario and the resulting column graph can be observed in Figure 6.9. Based on this graphic, analyses are made according to the impact of changes in acceleration and/or deceleration.

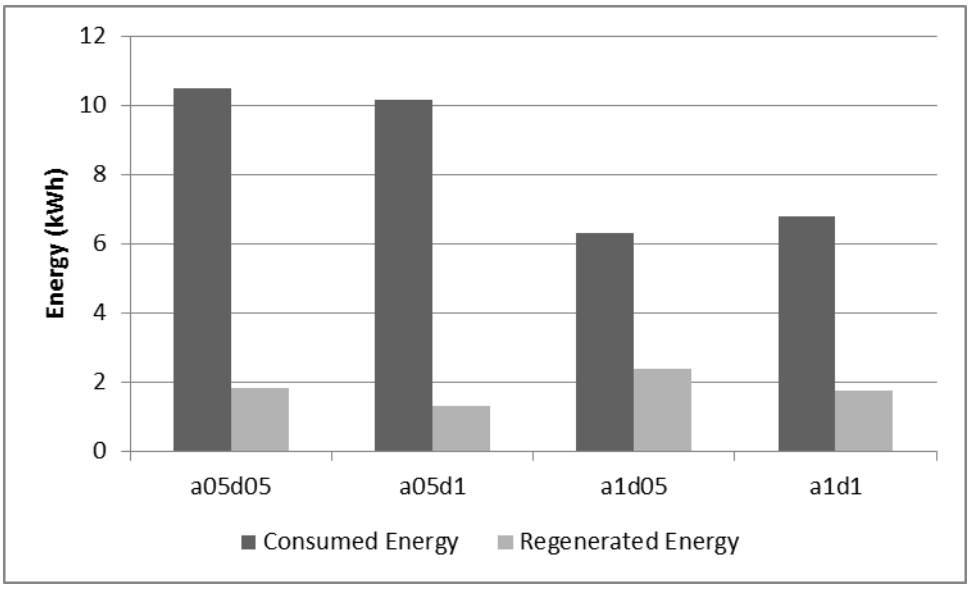

Figure 6.9– Comparative graph on the consumed and regenerated energy for all four scenarios

The first analysis is on the impact of the deceleration rate increase on the energy consumption and regeneration. For the first two scenarios, it is clear from the graphic that the higher the deceleration rate, the lower is the regenerated energy, although in this case, this did not impact much on the overall energy consumption. For the last two scenarios, the regenerated energy was also lower with the increase of the deceleration rate, and in this case, the energy consumption was higher.

On the other hand, the evaluation of the increase in the acceleration rate over those parameters shows different results: the higher the acceleration rate, the lower the energy consumption and the higher its regeneration. This can be explained by the way the simulation model calculates the gear value, which is based on a specific speed. Once this speed is achieved, the gear is shifted and its value goes from 3 to 1. This reduction impacts greatly on the calculations of energy, as it could be noticed. In real life, gear shift is programmed in a controller, and it may happen before or after this speed is reached.

In this sense, due to the higher value of acceleration, the right speed for the gear to be shifted is reached sooner, thus making the energy consumption lower. However, the deceleration rate impacts greatly on the consumption – whenever the driver pays attention to the traffic and plans his actions, much more energy can be saved, which in the end will impact on the overall energy consumption anyway.

6.4 Boston Case Study: the BRT Implementation

According to Levinson et al. (2003), BRT systems are “an integrated system of facilities, services and amenities that collectively improve the speed, reliability, and identity of bus

transit". It provides greater operating flexibility and potentially lower investments and operating costs, besides being a catalyst for cities redevelopment. BRT systems have some really special operational aspects that make them a lot different from regular buses, such as being controlled by a central office, making it possible for the BRT system to be classified as an intelligent transportation system (Deng and Nelson 2012). This allows real-time traveler information at stations and on vehicles, besides controlling and scheduling the vehicle itself and driver assistance.

Another characteristic of the operability of BRT systems is the use of a dedicated lane or at least its own right-of-way (ROW) in some section, providing a more reliable and efficient means of transportation, raising the average speed and reducing the amount of time that the users spend on commuting (Wright and Hook 2007). Usually, these lanes have a specific signalization, either by colors or physical markers. They also have greater distances between stations, which also contributes to a better performance of the system, once the bus can reach its rated speed and keep the average high.

The concept of BRT has emerged in Latin America in the 1970s, where planners have to develop an inexpensive system to accommodate their ever-growing demand. In this sense, one of the reference models when talking about BRT systems is Curitiba (Brazil), which has implemented their first corridor in 1974, bringing major benefits to the city. Another successful implementation was held in Bogotá (Colombia) later in 2000, where after some years have achieved impressive results in travel time savings, passenger satisfaction and reduction of emissions (Deng and Nelson 2011).

Boston has a history regarding the implementation of such systems. The next subchapter presents the Urban Ring project, which is a complex plan on the development of a circumferential transportation route to satisfy nearby areas and to complement the already existent radial transportation system. Later, the re-definition of the western-half of the Urban Ring, the Diamond Ring, is also presented, as well as the Silver Line Gateway project, whose objective is to provide a high-quality service for Chelsea and East Boston.

6.4.1 Objectives

This case study is designed to analyze the BRT fleet performance when running in the corridor. Performance parameters are collected for buses entering the network at different times during the morning peak. The main idea is to evaluate the difference on performance according to the increase in traffic volume, especially regarding average speed, time to complete the route and state-of-charge of the batteries in the end, as well as consumed and regenerated energy.

6.4.2 Urban Ring

The Urban Ring was a proposed major new bus rapid transit (BRT) system that would run in a circle through dense areas of the Greater Boston. Concepts for a circumferential transit line date back to the 1960s. The project would supplement the highly radial existing transit network, generating significant travel time savings and freeing capacity in the downtown rail network. The Urban Ring project map can be observed in Figure 6.10. The legend on this map concerns the rights of way for each part of the route, which are not going to be considered for simulation purposes.

In 1995, the Massachusetts Bay Transportation Authority (MBTA) – one of the main operators of public transport in Greater Boston - started a Major Investment Study, completed in early 2001. It identified the Urban Ring corridor and destinations for service, proposing a three-phase implementation strategy. In October 2001, a review of the proposed project was performed, generating the Draft Environmental Impact Report (DEIR). This review included citizens' opinion for a broad engagement of the Urban Ring project.

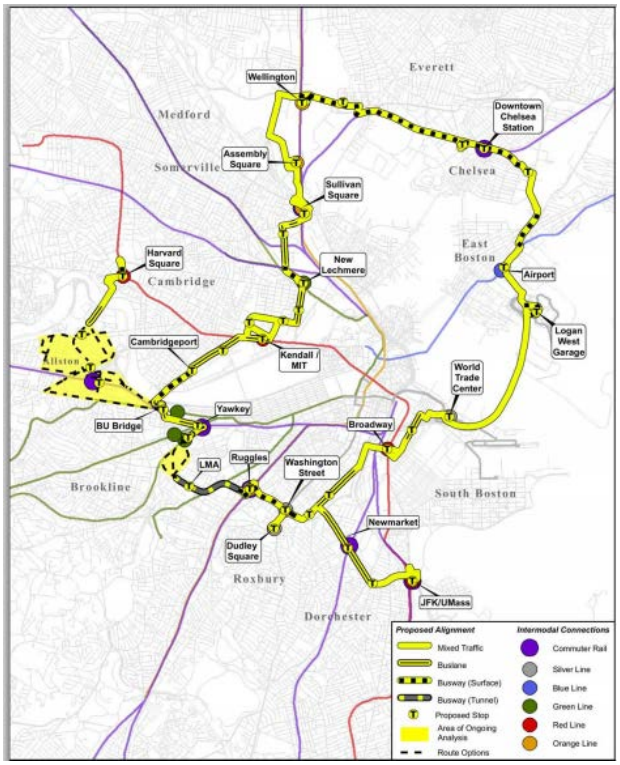

Figure 6.10– The Boston Urban Ring original alignment graphical representation (EOT and FTA 2008)

In November 2008, the Draft Environmental Impact Statement (DEIS) was developed and a revision to the DEIR for Phase 2 was made (originating the RDEIR – revised DEIR), to meet both state and federal review requirements. For this stage of the environmental process, a Locally Preferred Alternative (LPA) was selected, including preliminary designs

for alignment and stations. It is expected that the Urban Ring will improve transit access of more than 218,000 people by offering more direct connections. The combined RDEIR/DEIS report is the latest step in a decades-long planning process for public transit improvements in the Urban Ring corridor and can be consulted elsewhere (EOT and FTA 2008).

6.4.3 BRT Workshop and the Diamond Ring

In the fall of 2013, students from the Massachusetts Institute of Technology (MIT) and the Pontifical Catholic University of Chile collaborated on the design of BRT corridors. Working in cross-disciplinary teams of architects, designers, engineers, and planners, they expanded the concept of BRT, considering its potential not only as a mode of transportation, but also as a mechanism for driving innovations in urban design, development, and governance (Stewart and Figueroa 2014).

As part of the workshop, the students worked in Chile's corridor called *Gran Avenida* and on the Boston corridor, more specifically in the western half of the Urban Ring, which was rebranded to the "Diamond Ring". For the purpose of this thesis, the outcome of the analysis on the Diamond Ring is of great importance, as some adjustments to the original Urban Ring alignment were made. Those adjustments are considered for the route modeling in *SUMO* to further evaluate the electric bus in this context. The Diamond Ring alignment and its stops can be observed in Figure 6.11.

6.4.4 Silver Line Gateway Project

The Silver Line is established since 2002 comprising four routes. The Silver Line Gateway is the most recent development, whose purpose is connecting the South Station – located downtown and also a terminal for other three Silver Line routes - to Chelsea and East Boston. This project addresses the identified transit access needs of the corridor, while promoting economic development for these communities.

In Chelsea, there is the greatest proportion of transit-dependent residents in Greater Boston and the most densely populated residential neighborhoods outside of the City of Boston. The extension of the Silver Line to satisfy this area represents a much needed transit alternative. The proposed Silver Line Gateway will provide a new BRT route, and will operate in addition to the existing Silver Line routes. It will utilize existing Silver Line infrastructure and overlay existing service whenever possible (MassDot 2014). The alignment of the Silver Line Gateway and the stops are presented in Figure 6.12.

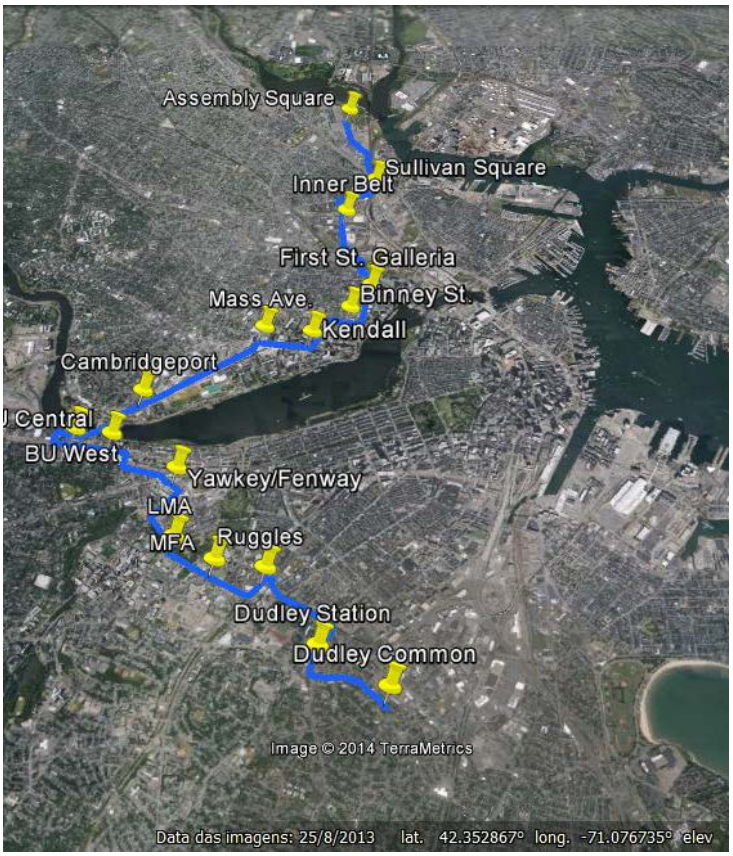

Figure 6.11– The Diamond Ring alignment: a new approach to the western half of the Urban Ring

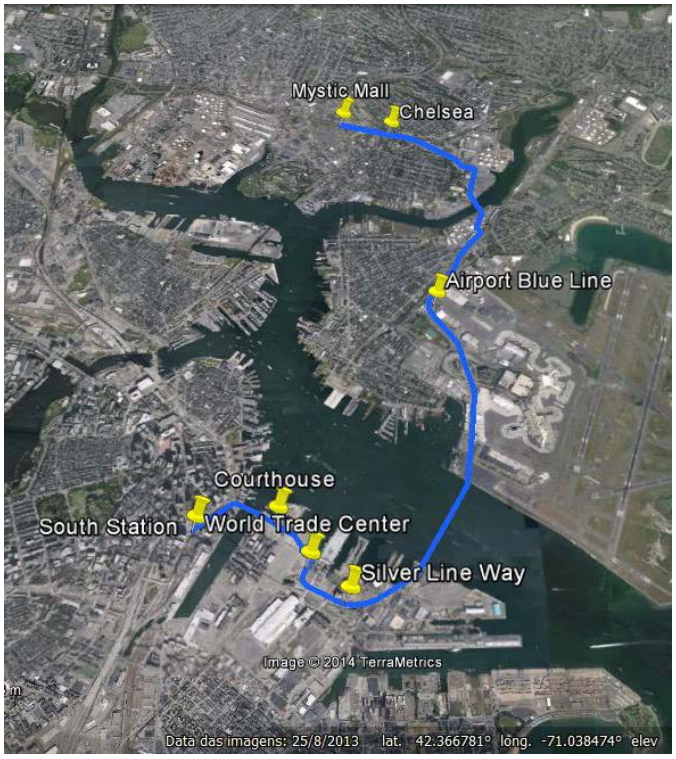

Figure 6.12- The Silver Line Gateway graphical representation

6.4.5 Simulation Setup

So far, three of the Boston BRT projects were presented, responsible for assessing public transportation needs of an ever-growing population. In order to analyze the behavior of the electric bus in this context, the simulation is divided into three different routes:

- The Diamond Ring, accounting for the western-half of the original Urban Ring;
- The Urban Ring eastern-half;
- The Silver Line Gateway.

Those three routes are comprised within the area of the Greater Boston, for the map area extracted from the *OSM* is unique. Moreover, the demand model is also unique and thus these two topics are approached only once. The resulting map generation and demand model work for all three routes.

6.4.5.1 Area Definition

Some edition on the map was required, especially regarding traffic lights. The original extracted map only had the traffic lights coded for downtown Boston, which implied in the coding of more than a thousand extra traffic lights by hand in *JOSM*. Figure 6.13 shows an example of coding traffic lights in *JOSM*.

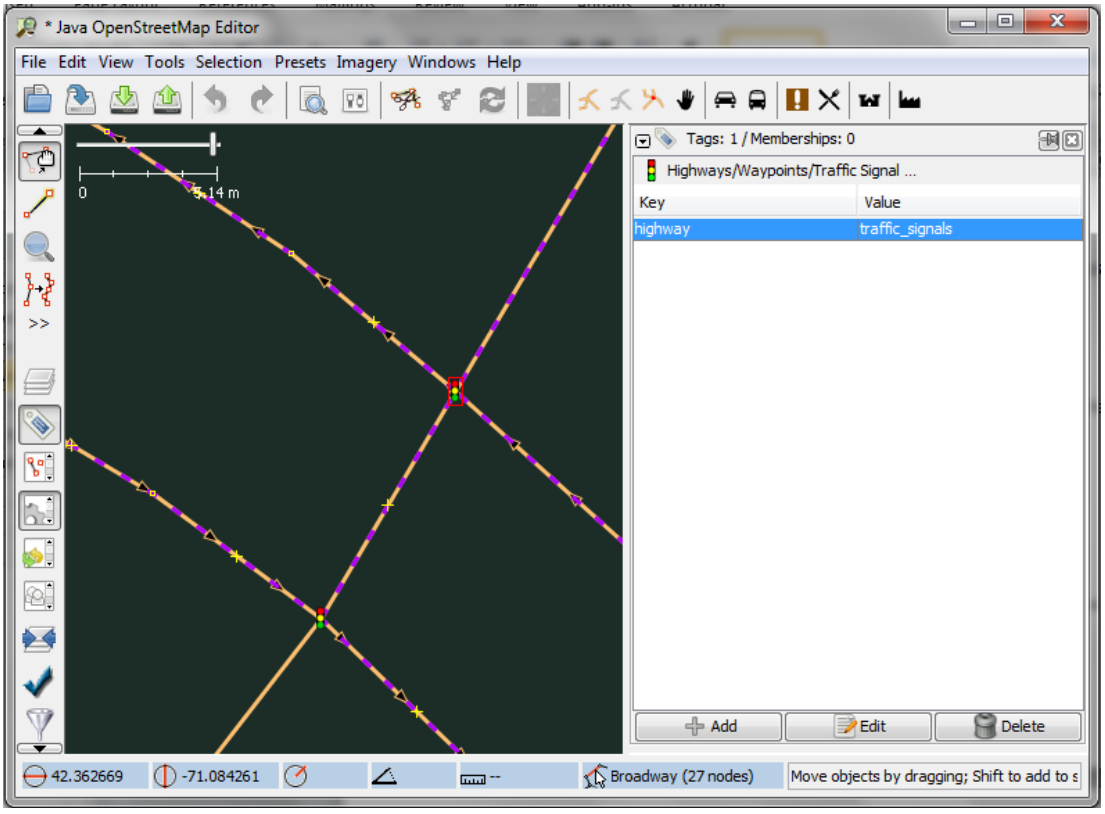

Figure 6.13– Traffic light coding in *JOSM*: example for one intersection

Once the traffic lights were added for the whole network, specific editing regarding new developments proposed for the Diamond Ring were performed. The first one was the connection to the Grand Junction, which is a deactivated rail line that will be used for the BRT route, and can be observed as the red arrow in Figure 6.14. The Grand Junction also had to have its parameter changed from "*rail*" to a regular street, so as to allow the bus to run on it. It can be noted in the picture by the line in gray connected to the red arrow instead of the characteristic dashed line for the typical rail representation in *JOSM*.

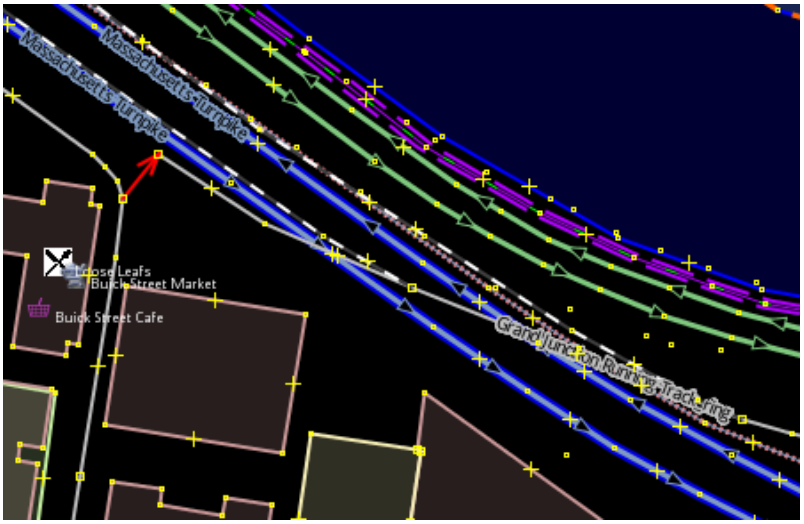

Figure 6.14– The newly created street connection (in red) to the Grand Junction in *JOSM*

Another alteration on the map regards the creation of a by-pass street at Kendal Square close to the "Galaxy: Earth Sphere Park" to improve transit in the area. It provides a direct connection between the Main Street and the Third Street and can be observed in Figure 6.15 represented by the red arrow.

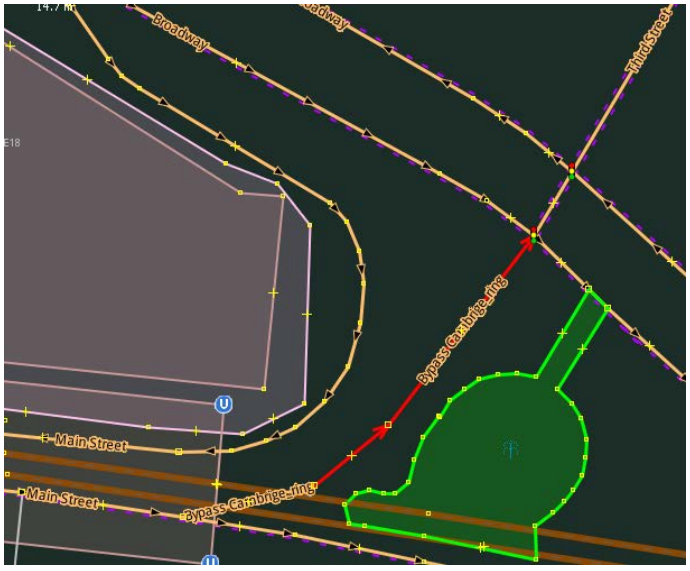

Figure 6.15- The newly created "Bypass Cambridge_ring" (in red) at *JOSM*

At last, a third addition to the original map had to be performed. It accounts for the creation of a bridge nearby the Lechmere Station, providing a straight connection to the Inner Belt Road, thus saving commuting time. This new bridge can be observed in Figure 6.16 as the red arrow.

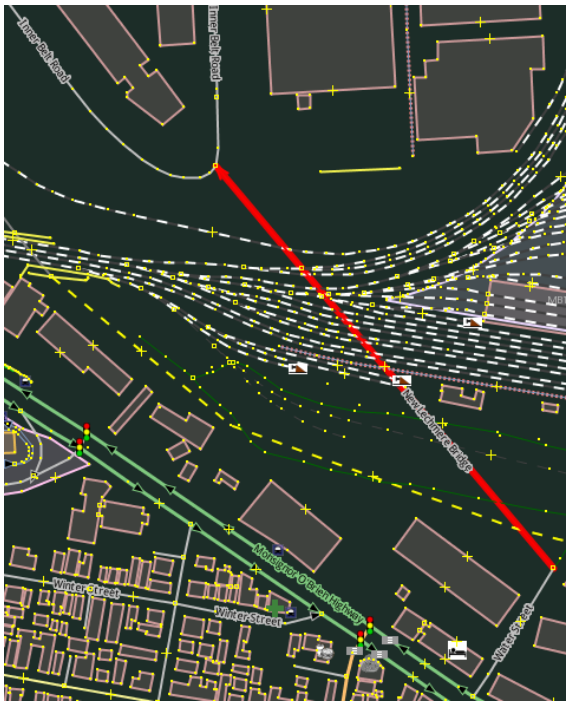

Figure 6.16– The newly created "New Lechmere Bridge" (in red) in *JOSM*

Those were the three major changes regarding new developments for the bus route. Other minor changes were also made, such as changes on parameters from railway to street. The eastern-half of the Urban Ring encompasses the use of some abandoned rail lines as routes for the BRT, and as such those parameters in *JOSM* had to be changed so as to allow the coded bus route to use those new streets. Once all changes were modeled, the *OSM* map was ready to be converted into the *SUMO* format; its visual representation can be observed in Figure 6.17. Once the map is in the *SUMO* format, the demand for the traffic behavior can be modeled.

6.4.5.2 Demand Modeling

Demand can be modeled in two ways: generating random traffic or generating traffic based on a real O/D matrix. Due to a partnership with the Department of Urban Studies at MIT (Massachusetts Institute of Technology), the demand could be generated based on real data (Murga 2014) and used in this thesis. Because MIT works with some different traffic simulation software, being this specific department used to working with *CUBE* (Citilabs 2014), some actions had to be taken, especially regarding the definition of the exact area in CUBE corresponding to the one defined in *SUMO*.

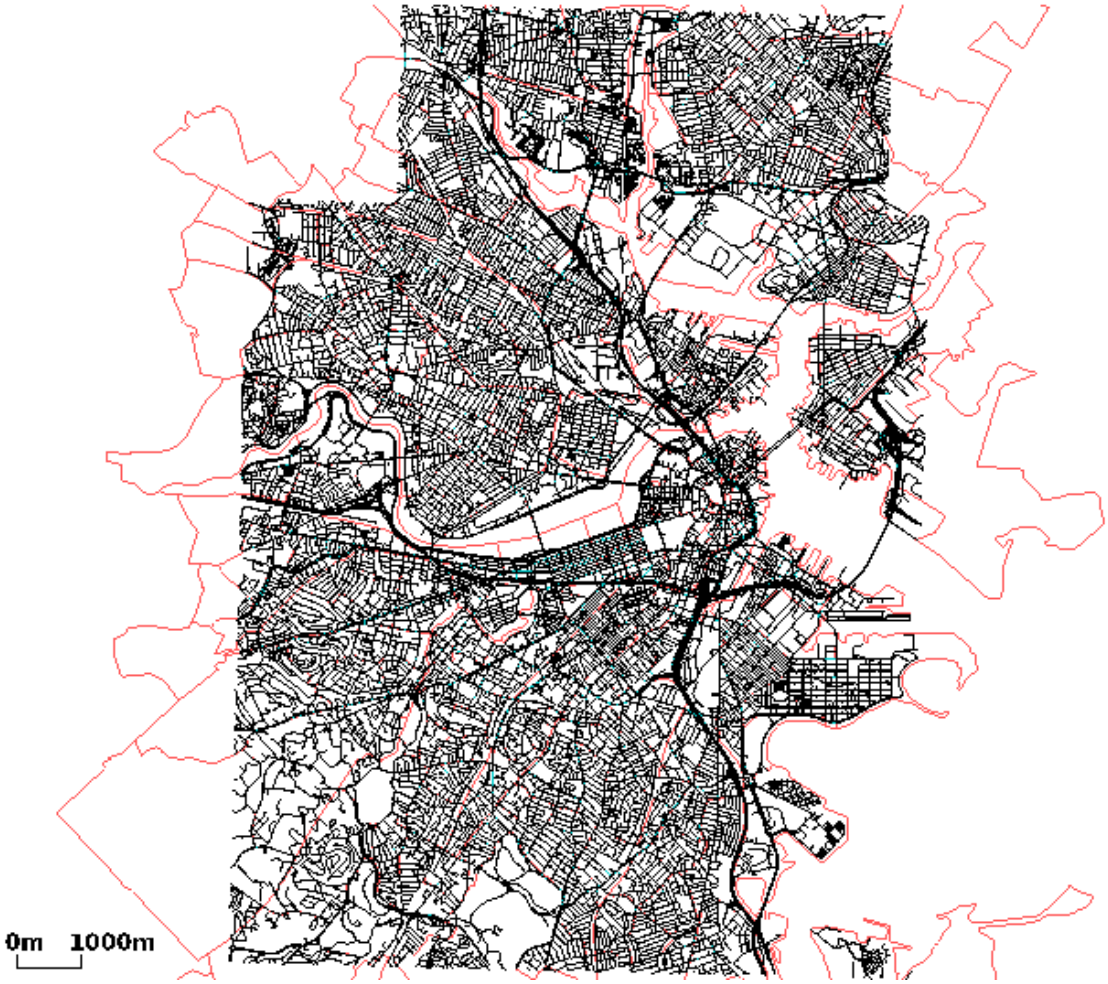

Figure 6.17– Converted Boston network map in *SUMO* GUI (red lines represent the districts)

The first action was to define exactly which TAZs (traffic assignment zones) the *SUMO* network comprises and share them with the MIT team. This dictated the boundaries definition in the CUBE model so as to allow the generation of the new centroids and then the simulation O/D matrix for this subarea (the CUBE model encompasses a much larger area). The simulation matrix is derived from the so-called planning O/D matrix, which represents the real trips performed in the CUBE original area.

Figure 6.18 shows the Boston network containing the generated centroids (blue dots); the red dots represent the roads that cross the subarea boundary, accounting for any traffic coming from outside of the subarea. Moreover, the three previously defined BRT routes were also coded and the established headway for each one was ten minutes during the period of analysis: morning peak (7.00 am to 9.30 am). This allowed the estimation of the bus boarding at the terminals stops. Once the area is defined and the routes are coded, the simulation was run in *CUBE*. Some real intense congestion has aroused, thus being necessary to perform iterations pursuing user-equilibrium and a more realistic O/D matrix.

The generation of the simulation O/D matrix can bring some issues, especially spillbacks on the new centroids at the boundaries due to the higher amount of vehicles from outside the area of analysis. These spillbacks negatively impact route assignment and the results of the simulation O/D matrix (Jha et al. 2004), as the MIT team could notice. The resulting simulation O/D matrix is a 701x701 matrix in *.csv* format. Each origin and destination is represented by a number, being this either the original TAZ number (blue dots in the map) or a created one for the roads at the boundary.

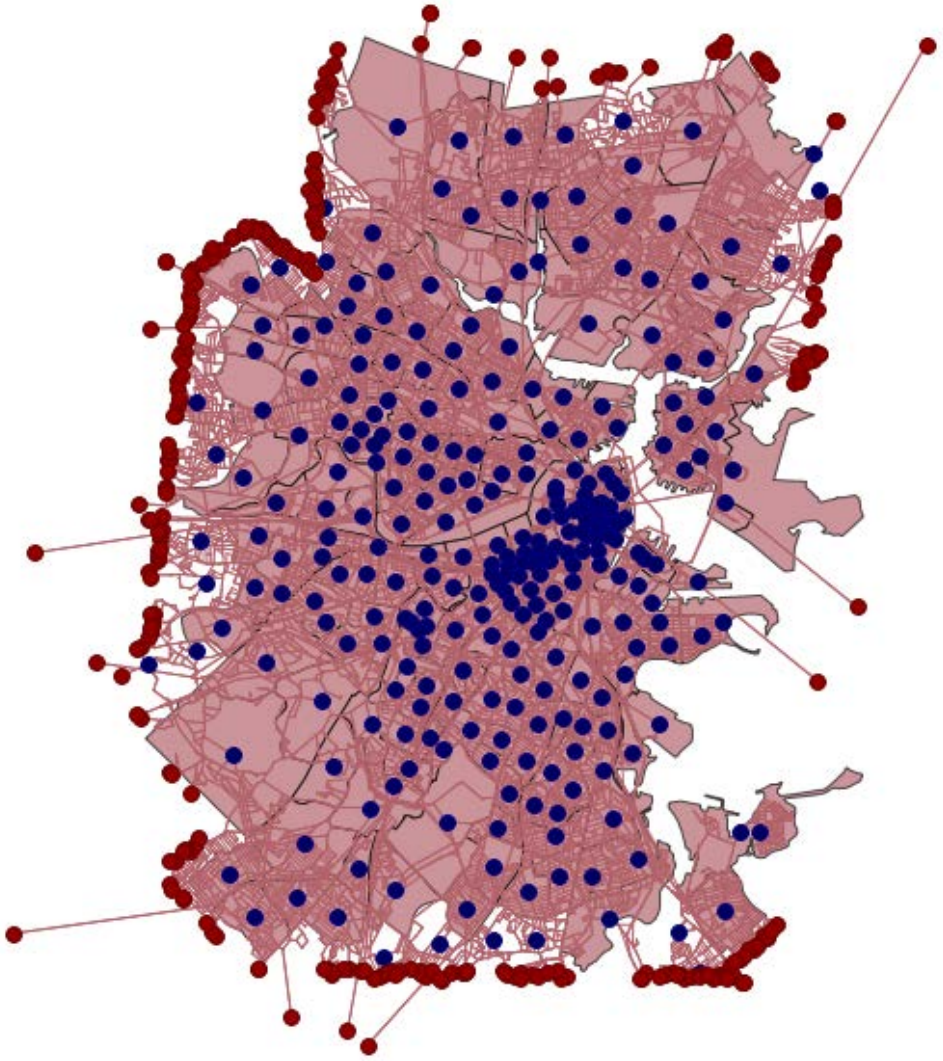

Figure 6.18– Boston area and the centroids in CUBE: the blue dots represent the centroids and the red dots account for the roads that cross the subarea boundaries

Before converting this simulation O/D matrix to the *SUMO* format, some adjustments are required, especially concerning the 274 generated boundary nodes (red dots in Figure 6.18). Due to the fact that they are not real TAZs, *SUMO* would not recognize any traffic coming from or going to them. The most efficient way of solving this issue is to assign their demand to the nearest centroid, which may bring issues such as congestion whenever

many boundaries nodes are assigned to a single centroid. In any case, this was the procedure taken and the new O/D matrix is a 255x255.

Once the final O/D matrix is defined, it could be converted into the *SUMO* format, following the steps of section 4.3.1.3. Recapitulating some concepts, an O/D matrix accounts for the number of cars (trips) that leaves an origin to reach a destination in a certain period of time. The route that the car is going to take to reach its destination is assigned by *SUMO*, which applies the shortest-path algorithm. Due to the high number of trips involved and the necessary adjustments to the boundary nodes, this simple way of assigning routes generated many points of huge congestion in the network.

Those congestion points are located closer to the boundaries, not affecting directly the BRT routes. However, those vehicles did not have the chance to approach the corridor, thus creating the false illusion of a clear route. Therefore, the dynamic-user assignment tool was used, as an attempt to address those issues by generating a better distribution of the traffic and as such promoted the necessary alleviation of those congested intersections.

6.4.5.3 Diamond Ring Coding

The Diamond Ring is the new alignment of the western-half of the original Urban Ring proposed by students during a workshop after a profound analysis of social context and needs. In order to code it in *SUMO*, two steps are required besides the already performed map importing and demand modeling. The first is the definition of the route lane-by-lane and the second is coding the bus stops position; section 4.3.1.2 had provided more details on how to perform those tasks in *SUMO*.

In addition, the time the bus is going to stop at each bus stop has also to be defined, which for the terminals (Dudley Common in this case) can be inferred by the number of people boarding. For the others, it is important to differentiate the intermodal stops from the regular ones. Intermodal stops usually involve more passengers to board on the bus, either due to transport connections from other modes of transportation or to the fact of being inherently larger and centrally located.

TPB (2013) presents a study on BRT travel time estimation and suggests a 2-minute stop at larger intermodal stops, a 1-minute stop at smaller intermodal stops and a 15-second one at standard stops. This approach seems quite conservative, especially for the intermodal stations but it provides some allowance for the potential presence of bicycle

users, ramp deployments, and other unpredictable events. Those times were estimated assuming a pre-fare collection and the possibility of boarding through both doors.

The proposed route for the Diamond Ring coded in *SUMO* leaves Dudley Common stop, on the bottom part of the ring, and rides until Assembly Square, which is the farthest to the North station. The 17 bus stops involved in the Diamond Ring (and their connections to other transportation modes) are as follows:

- Dudley Common;
- Dudley Station (connection with Silver Line);
- Ruggles (Intermodal with Green Line/ Orange Line and Commuter Rail [Franklin, Needham, Providence]);
- MFA (Intermodal with Green Line);
- LMA;
- Yawkey (Intermodal with Commuter Rail);
- BU West;
- BU East;
- Cambridgeport;
- Massachusetts Ave / MIT;
- Kendall Square (Intermodal with Red Line);
- Binney St;
- First St / Galleria;
- Lechmere (Intermodal with Green Line);
- Inner Belt;
- Sullivan Square (Intermodal with Commuter Orange Line);
- Assembly Square (Intermodal with Orange Line).

After coding the bus stops location, some parameters for the bus operation have to be defined and can be observed in Table 6.3.

All these parameters and this route headway are set in the "buses.add_ring_west.xml" file, responsible for compiling all the specific bus parameters. This file can be consulted in more detail in Appendix I. The required final step before running the simulation is to define de configuration file (*.cfg*). It comprises the files to be loaded simultaneously in order to run the simulation. For this case, it is the network, the demand and the bus files. "Time to teleport" was also configured in this file in the processing options. This allows vehicles that got stuck in a certain intersection to be removed from the network and then re-inserted along their route. This is especially relevant to larger traffic demands, where

an intersection blockage may have profound impacts in the network dynamics. The considered "time to teleport" in this case is 120 s.

Table 6.3- Diamond Ring: bus operational parameters

Parameter	Value
Acceleration rate	0.7 m/s^2
Deceleration rate	1.0 m/s^2
Maximum allowed speed	17 m/s (60 km/h)
Time at regular bus stops	15 s
Time at large intermodal stops (Ruggles)	120 s (2 min)
Time at other intermodal stops	60 s (1 min)
Time at Dudley Common stop	120 s (2 min)

6.4.5.4 Urban Ring Coding

The Urban Ring is a proposed circumferential transportation system to satisfy an existing demand that cannot take advantage from the current radius system in the Greater Boston area. In the original project, the eastern-half of the Urban Ring had two different BRT lines, being the JFK/UMass and Newmarket stops in Figure 6.19 served by a specific BRT service and the remaining by another. In order to avoid creating different routes, the coding in *SUMO* for this route has suffered a slightly different change, as it can be seen in Figure 6.19. This new proposal provides a more direct and efficient route and the connections to several other transportation services.

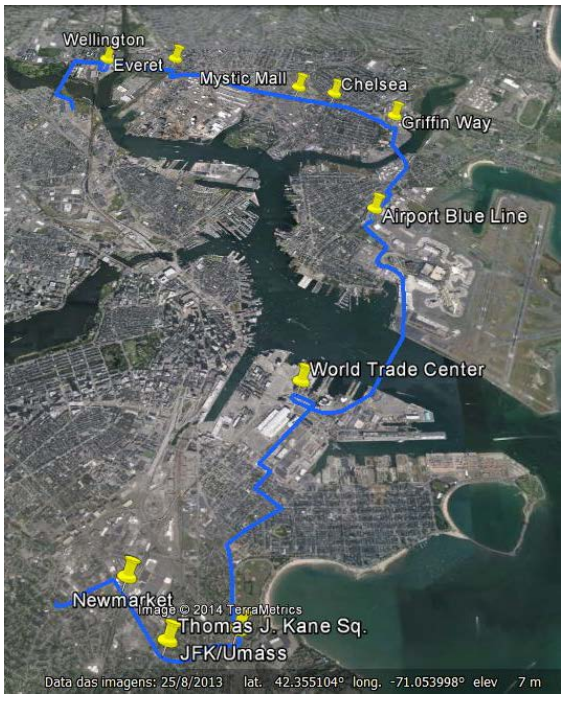

Figure 6.19– The new alignment of the eastern half of the Urban Ring

Similarly to the Diamond Ring, the Urban Ring route/bus stop coding is made on top of the previously defined map, and the demand traffic model uses the same O/D matrix. For the Urban Ring stops, they are coded according to the LPA report, except for the eliminated Broadway stop and the addition of the Thomas J. Kane Square stop, due to the mentioned changes to the route. Considering this route as a continuation of the Diamond Ring, respecting the clockwise direction, its stops are as follows:

- Assembly Square (Intermodal with Orange Line);
- Wellington (Intermodal with Orange Line);
- Everett;
- Mystic Mall;
- Chelsea (Intermodal with Commuter Rail ([Newburyport/Rockport]);
- Griffin Way;
- Airport Blue Line (Intermodal with Blue Line);
- World Trade Center (connection with Silver Line);
- JFK/UMass (Intermodal with Red Line and Commuter Rail [Greenbush, Kingston/ Plymoulth and Middleborough/Lakeville]);
- Thomas J. Kane Square;
- Newmarket (Intermodal with Commuter Rail [Fairmount and Franklin]);
- Dudley Common.

The parameters for the bus (acceleration/ deceleration rates and maximum speed allowed) have been set similarly to the Diamond Ring's; also in general, the assumptions for time at regular bus stops (15 s) and intermodals' (60 s) are the same, being JFK/UMass considered the only large intermodal station, thus requiring the bus to stop for *120 s*. The exceptions go to Assembly Square, Wellington, and Dudley Common, where the number of people boarding is small and 15 s were considered. Those bus parameters and headway are compiled in the "buses.add_ring_east.xml" file, presented in Appendix J. The "*.cfg*" file follows the same format as the Diamond Ring's regarding parameters and processing options.

6.4.5.5 Silver Line Gateway Coding

The Silver Line Gateway coding follows the previously defined steps for both the Diamond Ring and the Urban Ring coding. Its alignment is presented in Figure 6.12 and its stops are as follows:

- Chelsea (Intermodal with Commuter Rail ([Newburyport/Rockport]);
- Griffin Way;
- Airport Blue Line (Intermodal with Blue Line);

- Silver Line Way (connection with other Silver Lines);
- World Trade Center (connection with other Silver Lines);
- Courthouse (connection with other Silver Lines);
- South Station (Intermodal with intercity trains, the Orange Line and several commuter rail lines).

Some of the stops are also used by the Urban Ring but time at stops is considered slightly different. Based on the boarding data, 60 s was used for Chelsea and 120 s for Griffin Way. For the remaining stops, it was assumed 15 s, once the number of boarding is irrelevant. It is needless to say that the bus parameters are the same and together with headway are compiled on a file called "buses.add_sl6.xml" (Appendix K); moreover, the .cfg file is also similar to the presented for both previous cases.

6.4.6 Results and Discussion

Once the simulation set-up was performed for three different routes, the results and discussion is equally divided, being analyzed for each case individually: the Diamond Ring is analyzed first, followed by the east-half of the Urban Ring and further the Silver Line Gateway. Later, a broader analysis is held on the implementation of possible conjugation of routes as for a regular day of operation.

6.4.6.1 Diamond Ring

Starting with the Diamond Ring, the simulation was run considering headway of 10 minutes, totalizing 15 buses being simulated simultaneously. Data were collected for buses leaving Dudley Common at steps 0 s, 1800 s, 3600 s, 5400 s and 7200 s. The analysis is held with the objective of evaluating the influence of the surrounding traffic on the performance parameters after completing the route, namely: average speed (m/s), time (min), consumed and regenerated energy (kWh) and state-of-charge (SOC, in %).

In this sense, a sample of 5 buses was chosen for the analysis, having different departure times throughout the morning peak. The buses were named according to the simulation step they leave the terminal, and this is valid for all three routes (Diamond Ring, Urban Ring and SL6); their IDs can be observed in Table 6.4.

The graphics presented in Figure 6.20 show that the traffic peak occurs around 8.00 am, once the bus that leaves Dudley Common at this time (s3600) develops the lower average speed (3.3 m/s), thus taking 26% more time than the first bus in the morning (74 min instead of 59 min) to get to the final destination at Assembly Square. The buses ID are presented in the x-axis.

Table 6.4- Buses identification (ID) name for the analysis of the BRT routes (Diamond Ring, Urban Ring and SL6) according to the time they leave the terminal

Bus ID	Simulation step (s)	Morning Hour
s0	0	7.00 AM
s1800	1800	7.30 AM
s3600	3600	8.00 AM
s5400	5400	8.30 AM
s7200	7200	9.00 AM

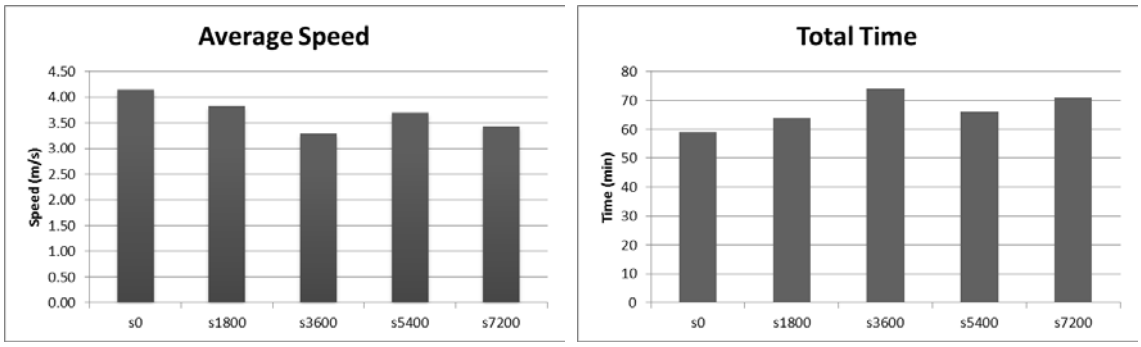

Figure 6.20– Diamond Ring: Average speed in m/s and total time in minutes for five buses during the morning peak

Regarding the energy consumption, the bus leaving at 8.00 am (s3600) not only developed the lowest average speed and spent more time to get to the final destination, but also consumed up to 18% more energy when compared to the s0 bus. As a consequence, this bus finished the route with less energy in the batteries, having a SOC of 67%. Figure 6.21 shows the SOC for all five buses and Figure 6.22 presents the consumed and regenerated energy, being the latter relatively constant in all cases, accounting for 25% of the total energy spent.

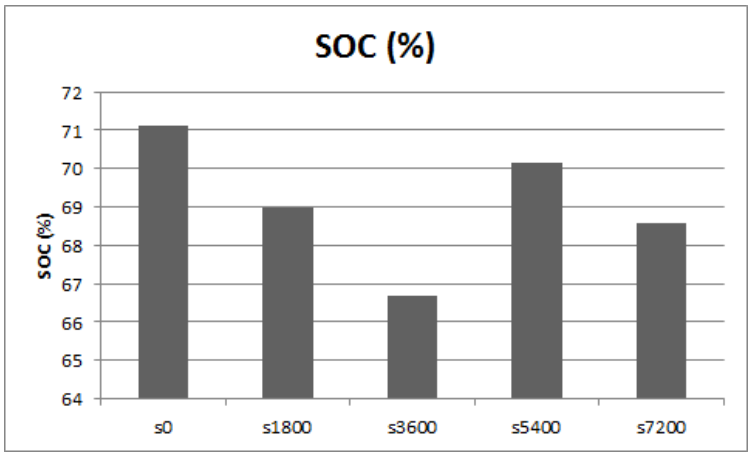

Figure 6.21– Diamond Ring: SOC in % for five buses during the morning peak

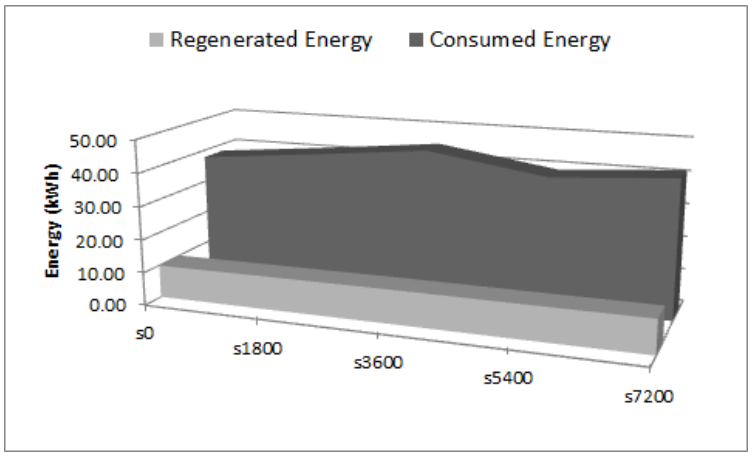

Figure 6.22– Diamond Ring: Consumed and regenerated energy in kWh for five buses during the morning peak

6.4.6.2 Urban Ring

Considering headway of 10 minutes, the simulation for the eastern-half of the Urban Ring was run for 15 buses and data were collected regarding buses leaving at instants 0 s, 1800 s, 3600 s, 5400 s and 7200 s, similarly to what was done for the Diamond Ring analysis. The buses ID are also defined according to Table 6.4. The comparative graphics representing the average speed and the time spent to finish the route can be observed in Figure 6.23.

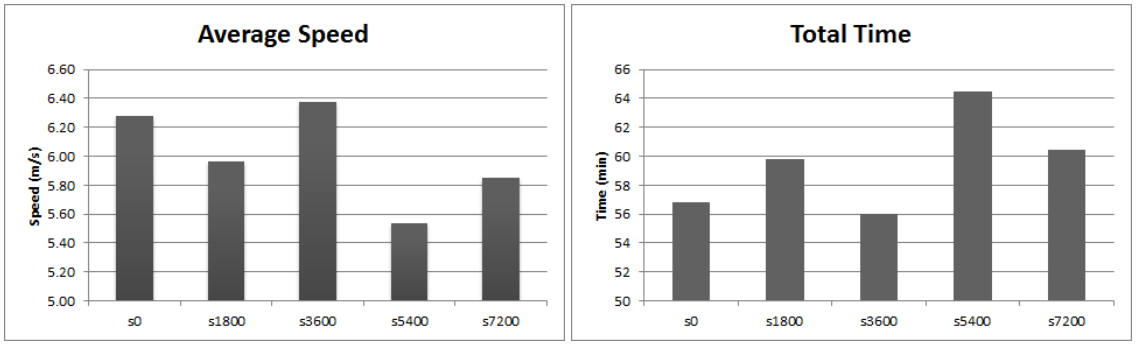

Figure 6.23- Urban Ring: Average speed in m/s and total time in minutes for five buses during the morning peak

It is curious to see that the impact of traffic is different in the eastern-half of the Urban Ring when compared to the Diamond Ring, once the bus leaving at instant 3600 s was the one which performed the best in the first case, having the highest average speed and thus taking the least amount of time to get to the final stop. However, it is relevant to highlight that a large part of this route passes by old railways to be converted into street for the bus, avoiding the traffic that takes the regular main streets.

The worst performance belongs to the bus that left the terminal at instant 5400 s, thus having the lowest average speed and spending the highest amount of time to perform the route. Nevertheless, in a general way the performance of the five buses did not differ much

from each other, being the largest observed difference on time around 15% higher and on average speed around 15% lower (comparison data belonging to buses leaving at instants 3600 s and 5400 s).

The other analyzed parameters are related to the SOC of the buses after finishing the entire route and also to the consumed and regenerated energy, as it can be observed in Figure 6.24 and Figure 6.25, respectively. The final SOC ranged from 67% (s1800 and s5400) to 71% (s0). The poor performance of the bus s5400 was already expected, once it took the longest to reach the destination and developed the lowest average speed. Surprisingly, the bus s1800 had a very similar final SOC value, despite performing better regarding the two first parameters. Being the SOC a consequence of the consumed and regenerated energy, their behavior regarding both parameters was accordingly.

In an attempt to justify the unexpected poorer performance of bus s1800, the speed profile of all the buses was evaluated. It seems that the speed profile for bus s1800 has a large period of time where a constant low speed is maintained, whereas none of the other buses suffer from the same behavior. This impacts greatly on the energy consumption and regeneration, somewhat similar to what happened in the Portuguese case study of the driver's behavior (lower acceleration rates leading to higher energy consumption), though not enough to make this bus take the longest to perform the route or develop the lowest average speed. This mentioned period of time can be seen from 30 to 34 minutes in the speed profile presented in Figure 6.26.

In addition, all the buses have recovered around 30% of their overall energy consumption, being again the s1800 and s5400 the worst performers with 30% and the others with 33% of energy recovery.

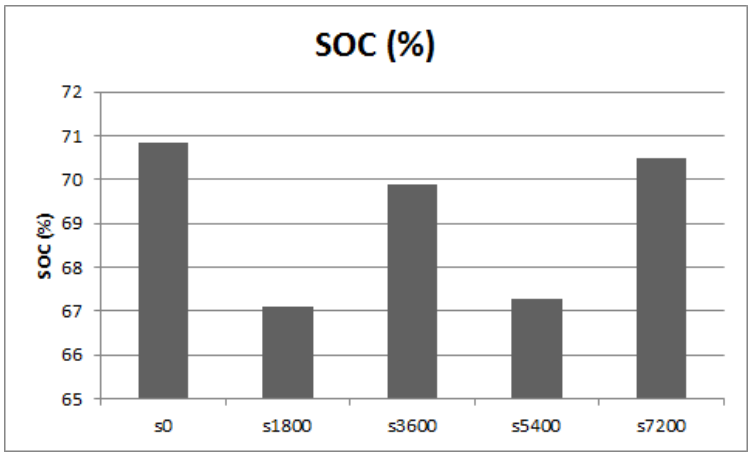

Figure 6.24- Urban Ring: SOC in % for five buses during the morning peak

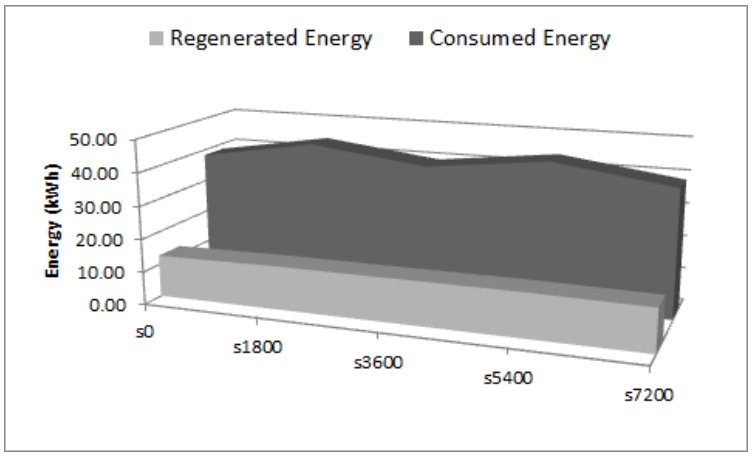

Figure 6.25- Urban Ring: Consumed and regenerated energy in kWh for five buses during the morning peak

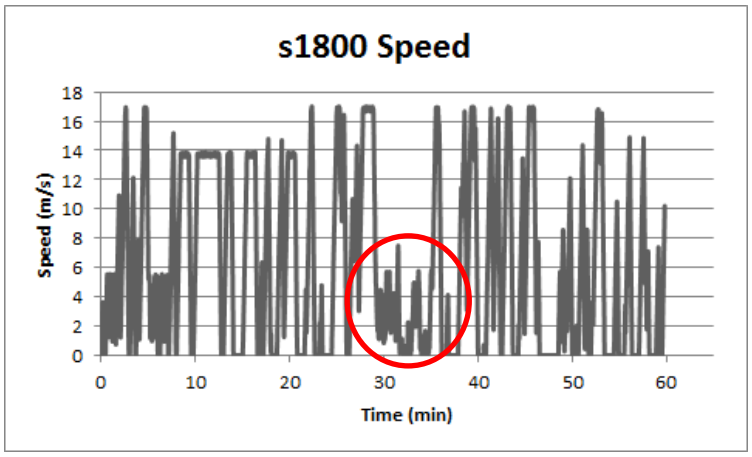

Figure 6.26- Urban Ring: Bus s1800 speed profile and the demarcated low-speed time period

6.4.6.3 Silver Line Gateway

For the analysis of the Silver Line Gateway (SL6), the same 10-minute headway was considered, being the buses identified according to the instant they leave the origin: s0, s2800, s3600, s5400 and s7200 (Table 6.4). As previously described, the SL6 has a smaller route compared to the other two and its beginning is similar to the Urban Ring's. However, the buses performance differs greatly, being clearly the s7200 the worst performer regarding average speed and total time to run the route, as it can be observed in Figure 6.27.

Bus s7200 seems to have been impacted greatly by the traffic, spending 60% more time to perform the route and developing an average speed 40% lower when compared to the best performer: the s0 bus. Consequently, the s7200 final SOC in the end of the route is 15% lower, which leads to a very high energy consumption (twice as much s0) and lower energy recovery (half the others, around 15% of its overall energy consumption). The graphs showing the SOC and the energy consumed/recovered for all buses can be observed in Figure 6.28 and Figure 6.29, respectively.

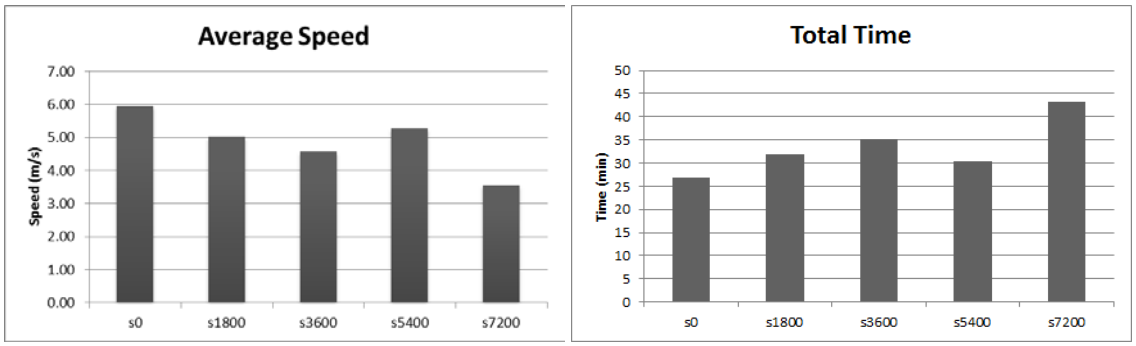

Figure 6.27- Silver Line Gateway: Average speed in m/s and total time in minutes for five buses during the morning peak

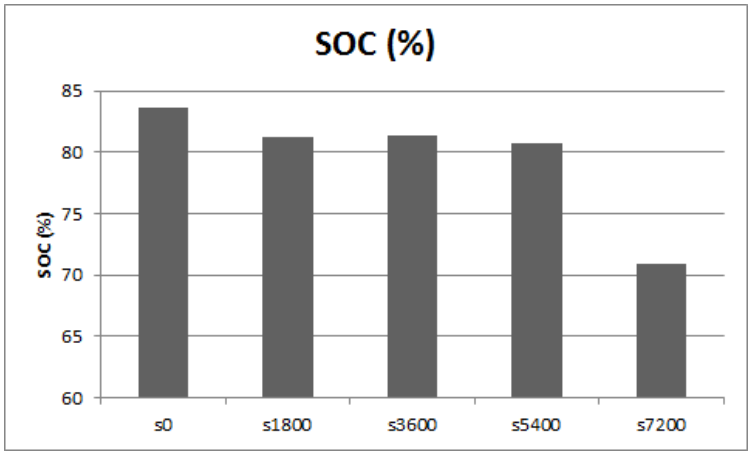

Figure 6.28- Silver Line Gateway: SOC in % for five buses during the morning peak

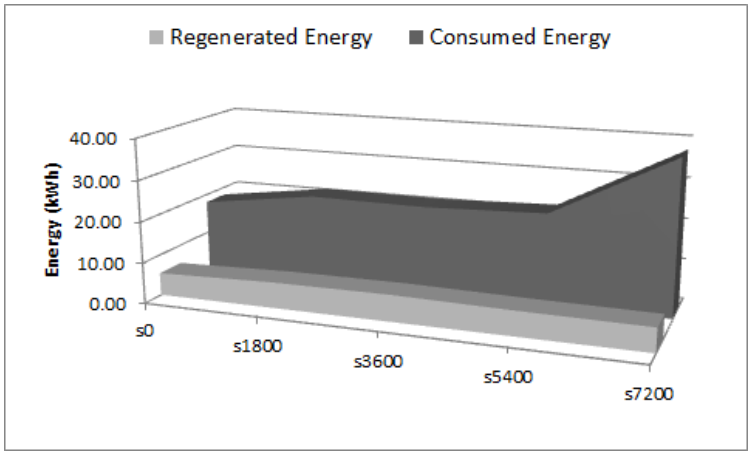

Figure 6.29- Silver Line Gateway: Consumed and regenerated energy in kWh for five buses during the morning peak

By following the behavior of the bus during the simulation, it could be observed that the s7200 was caught in the middle of an intense traffic around Chelsea area, where it developed low speeds to leave the Griffin Way stop and get to the Eastern Avenue. Therefore, the bus developed a really low speed for a large period of time (approximately 10 minutes), as it can be observed in its speed profile presented in Figure 6.30. It is believed that this was the cause for the poor performance of this specific bus.

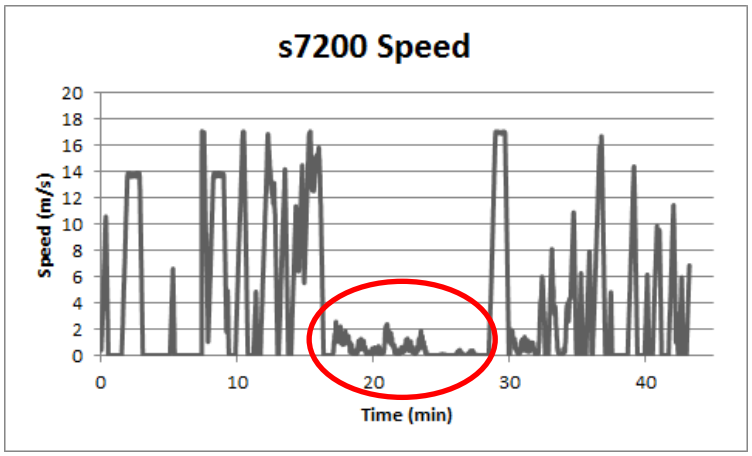

Figure 6.30- Silver Line Gateway: Bus s7200 speed profile and the demarcated low-speed time period

6.4.6.4 Implementation of Electric BRT Buses

More than just evaluating the performance of each bus, it is interesting to notice the impact that a dense traffic have on the performance parameters. This information is of great importance to the public transportation operators, not only to make a better schedule for their buses but also for planning the batteries recharge when using electric buses. In this sense, this section objective is to plan an electric bus schedule on a regular operation day.

Considering a scenario where a bus starts its journey at Dudley Common and follows the Diamond Ring route, further performing the eastern-half of the Urban Ring. Aspects like the time it leaves Dudley Common, the number of passengers to board and alight, and the amount of traffic on the streets influence the energy consumption of the bus, as it could already be seen in the previous case studies. For this broader analysis, some simulation results are used as baseline.

For a more robust analysis, it was considered the worst case scenario of energy consumption, which is around 45 kWh to perform either the Diamond Ring or the Urban Ring. It was already shown that it represents 28% (e.g., the s3600 bus of the Diamond Ring finished its route with a SOC of 67%, being the initial SOC 95%) of the total energy that the batteries can carry, thus resulting in a rate of approximately 0.63% for each kWh of consumed energy. Based on this parameter, Table 6.5 presents a schedule for one whole day of operation, assuming the bus leaves from Dudley Common terminal at 7.00 am and finishes its operational day at 10.30 pm at Assembly Square; both terminals are equipped with a fast-charge station and also have a bus depot for overnight stay. The table also presents the SOC once the bus arrives at the specific station.

In summary, the bus can perform three routes before the need to recharge, so two strategic fast-recharges must be considered in order to make the bus circulate during all day. In order to preserve the battery health, a regular slow-charge is necessary and it is strategically located during the night, at the bus depot. In case this bus depot only exists at Dudley Common, once the bus started its operation there, then it should stop a little earlier at 9.30 pm and then go to the overnight recharge.

Table 6.5- Schedule for an electric BRT bus for a whole day of operation in Boston, presenting the SOC at each terminal and also two possibilities for the overnight recharge

	7am	**8am**	**9am**	**10:30am**	**10:30am-1:30pm**
Assembly Square		72%		16%	**Fast Recharge**
Dudley Common	100%		44%		
	1:30pm	**2:30pm**	**3:30pm**	**4:30pm**	**4:30pm-7:30pm**
Assembly Square	100%		44%		
Dudley Common		72%		16%	**Fast Recharge**
First Option: Bus Depot at Assembly Square					
	7:30pm	**8:30pm**	**9:30pm**	**10:30pm**	**10:30pm-6:30am**
Assembly Square		72%		16%	**Slow Recharge**
Dudley Common	100%		44%		
Second Option: Bus Depot only at Dudley Common					
	7:30pm	**8:30pm**	**9:30pm**	**9:30pm-6:30am**	
Assembly Square		72%			
Dudley Common	100%		44%	**Slow Recharge**	

This schedule example can be extended for all the buses composing the fleet, and should be adjusted according to the time of the day, due to the differences in the performance. It makes sense to use the bus that performed the Diamond Ring to continue to the eastern-half of the Urban Ring, once the terminal station of the first is the start station of the second. If it was considered that this bus would continue the operation by performing the SL6 route, then it would spend an unnecessary amount of energy just to get to Chelsea stop (SL6 start stop).

Bus operators have their means to increase performance and consequently reduce costs when scheduling the routes the bus is supposed to perform on a day. In this sense, so as for the electric buses to be implemented, they should also consider the strategic fast recharges as part of their algorithms, and plan the best possible way the routes the bus should perform. It is important to mention that it was purposely not considered the ultra-fast recharges at the stops, once the coded bus is not equipped with such a technology.

6.5 Conclusions

This chapter presented three main case studies, each of them focusing on specific aspects of electric bus operations. The first two case studies were set up in Porto area, one analyzing the impacts of the route and the other the driver's attitude influence on the electric bus performance. It could be observed that the topography of the route (linearity and elevation profile) plays a major role in the energy consumption of the bus, together with the distance between stops. For the driver's behavior, planning ahead the braking episodes can impact greatly on the amount of recovered energy in regenerative braking. However, a higher acceleration seemed to make the bus spend less energy to perform the route, which can be explained by the way the simulation platform interprets gear ratio and may not be as realistic as expected.

The third case study was focused on three future BRT routes to be implemented in Boston, and the simulation was held taking into consideration a real O/D matrix provided by MIT. Besides analyzing the electric bus performance in this context, the main objective was to assess the impact of traffic on this performance, evaluating the extra energy the bus may spend due to traffic conditions. The electric bus was differently impacted by traffic density for the analyzed three routes, and the ones that are composed of more alternative parts (e.g. converted rail lines) to main streets had better performance parameters. Later, a holistic analysis was made regarding a schedule for an electric bus performing the Diamond Ring followed by the eastern-half of the Urban Ring during a day operation, where strategic fast-charges were considered, ending with an overnight slow-charge at the bus depot.

Chapter 7

Conclusions

7.1 Main Findings

This thesis proposal was ambitious, once its outcome is supposed to change the perception people have about electric buses. Electric vehicles in a general way are associated with fear: fear of not having enough energy on the batteries for a trip, fear of not having enough available charging stations on the streets, fear of the durability of batteries and their appropriate disposal, once such large battery packs are expensive, and not common in the everyday life. All these fears are perfectly understandable: electric vehicles are a new technology when compared to regular internal combustion engine vehicles.

However, when referring to electric buses instead of electric private cars, all those fears are not supposed to impact this much. Buses have fixed routes, fixed operation schedules and terminals. This means that the same way routes are programmed for a whole day operation, so can the batteries' energy be. Bus routes can be planned for a day operation in a way so as to make the most use of the energy contained in the batteries and to schedule when and for how long they should recharge.

In this sense, this thesis presents an electric bus simulation platform, where a mathematical model of the bus dynamic behavior is implemented in the *Simulink* software, which in turn is interfaced with the traffic simulator *SUMO* using the high-level architecture (*HLA*) standard from *IEEE*. This platform allows the simulation of the bus performing any route, besides allowing the inclusion of the bus stops and traffic interactions, such as performed in the case studies.

The developed simulation integrated platform was calibrated and validated based on data collected from the real bus operation. For instance, the battery current range was calibrated taking into account these data, once the theoretical range of operation was

different from the real one. Moreover, a sensitivity analysis was performed on some parameters, as a way to make the platform valid for a range of their values.

The platform was tested in many scenarios, both Portuguese (Porto) and American (Boston). For the Portuguese scenarios, two different analyses were held. The first one was about comparing the performance of the bus in three completely different routes from the Porto buses operator *STCP*, differing in size, topographic profile and number of stops. Once the objective was to evaluate the impact of the route profile on performance, no car traffic was used. The consumed energy was compared per kilometer of route, and it was found that the route that consumed more energy per kilometer was the urban route 204, which was not the one containing more turns but rather a steady elevation in a certain point, which impacted on this result. It was also found that it had the worse energy recovery percentage, which can also be attributed to its elevation profile.

On the other hand, the other two analyzed routes had a similar performance, despite being completely different from each other. The smallest urban route 401 is composed of many turns and an interesting elevation profile, having more negative than positive slopes, while the 602 is a very linear interurban route and is almost plan. Consequently, both had equivalent energy consumption per kilometer and regeneration rate. However, for route 401, the regeneration was somewhat higher due to various descents along the itinerary, while the better performance of route 602 compared to 204 can be ascribed to the fact that the stops are farther away from each other and the bus can operate at rated speed for longer.

The other Portuguese case study was developed to evaluate a completely different aspect: impact of a risk-taking driver compared to regular ones. The used parameters to make this differentiation were acceleration and deceleration rates, where the higher these values, the more risk-taking the driver. The scenario was built in the region of Aliados, in Porto, where the bus performed a made-up route composed of ten bus stops; in addition, it was considered the interaction with random traffic.

The results have shown that the deceleration rate has a big impact on the recovered energy, indirectly affecting the overall energy consumption: the higher the deceleration rate, the lesser the amount of recovered energy. This makes total sense once a better energy recovery is achieved in longer and controlled braking episodes, thus planning actions about braking episodes can make the bus recover much more energy.

For the acceleration rate, the results were different: for higher values of acceleration, the bus has consumed less energy to finish the route. Although this may seem counterintuitive, results can be justified by the fact that the simulation platform does not account for a dynamic representation of the gear shift by shifting gear once the bus reaches a certain speed. Therefore, the higher the acceleration, the faster it achieves the required speed then changing the gear. The gear ratio for the second gear is one-third the value for the first gear, thus impacting positively on the bus energy consumption. In the real bus, the gear shift is programmed in the controller, and it can be done in a way that no matter how hard the accelerator pedal is pressed, the shift will only change when the controller commands it to.

The American case studies were developed in a way to evaluate the impacts of the traffic on a whole bus fleet during the morning peak. The scenario was set in Boston, where three different routes were coded in *SUMO*; such routes making part of future plans for the city. Moreover, due to the importance of traffic for this case, a real origin/destination (O/D) matrix was used (representing traffic from 7.00 am to 9.30 am), thanks to the partnership established with the Department of Urban Studies from MIT, which provided the data.

For the first analyzed route, the Diamond Ring, the simulation was run for the planned headway of 10 minutes, totaling 15 buses. The analysis was held comparing the performance of 5 buses, which left the terminal at steps 0 s, 1800 s (30 minutes), 3600 s (1 hour), 5400 s (1.5 hour) and 7200 s (2 hours). It could be noticed that the most intense traffic was achieved in the middle of the morning peak, once the bus that left the terminal at instant 3600 s took longer to reach the final station (74 minutes) and had the lower average speed (3.3 m/s). On the other hand, the first bus in the morning performed better, as expected once there was not much traffic.

Besides having a lower average speed and taking longer to get to the final station, the bus leaving at step 3600 s consumed 18% more energy than the first one, ending the route with 67% of energy in the batteries while the first one ended it with 71%. This case was great to have a perception of the impact of traffic on the electric bus performance, providing tools for operators to schedule other routes this bus is supposed to perform in a day operation accordingly. Certainly, this schedule will differ from the first bus that left the terminal, once its performance was completely different.

For the other two analyzed routes, the eastern-half or the Urban Ring and the Silver Line Gateway (SL6), a similar simulation set-up was taken into consideration. The impact of the traffic was somewhat different, especially because both routes are composed of major

"alternative" paths, avoiding main streets, and thus buses performed similarly. However, the s7200 bus of SL6 route has performed really poorly, taking 60% more time to finish the route when compared to the best-performer, s0, and consuming twice more energy. This was justified by the 10-minute period of a developed low speed due to traffic density in the Chelsea area. After those analyses, a schedule was presented for a whole day operation of an electric bus performing the Diamond Ring followed by the Urban Ring (closing the circumferential route), considering strategic fast-recharges during the day.

All the presented cases were useful to provide insights into the electric bus operation and performance. The gained insights are extremely important to build a deeper knowledge about this mode of operation, and to demonstrate that the developed platform may serve as a useful tool for bus operators to know in detail the performance of an electric bus in their cities, allowing them to plan their routes accordingly.

Table 7.1 summarizes the case studies performed, giving an appropriate interpretation for the results and suggesting possible strategies to be taken (e.g., by bus operators) accordingly. This table shows how an important and robust tool this platform can be for bus operators, transit planners and practitioners. It is known that internal combustion engine (ICE) buses have fewer problems with autonomy. Usually, the bus can perform any route during a whole day operation without the concern of running out of fuel. However, the negative impact it causes on the environment and the ever-growing emissions control rules appeal for bus operators to search for a cleaner transportation and the electric buses fit in this scenario perfectly.

The performed case studies were intentionally developed in order to have a holistic approach over the bus operation, analyzing from its performance according to the route to the driver behavior and traffic impact. It was demonstrated that the electric bus can perform really similarly to ICE buses, either in speed or in time to travel a route. Also, once the adequate route schedule is assigned, the energy in the batteries are used in an optimized way, allowing bus operators to consider electric buses as an important part of their fleet.

7.2 Key Contributions

The integrated simulation platform developed in this thesis has its origins on the identification of a scientific gap after performing a literature review on electric vehicle simulators. It was shown that most simulators rely on existing standard driving cycles, not allowing for the correct representation of the route in terms of topographic profile, bus

stops and interaction with traffic. For electric buses, they are of great importance on the evaluation of their performance, once they require a more detailed approach on the energy it spends.

Table 7.1 – Case Studies Summary: Results interpretation and possible decisions

Case Studies	**Evaluation Purpose**	**Results Interpretation**	**Possible Strategies/Decisions**
Three Routes Analysis	Impact of route topographic profile and bus stops distribution	- Positive inclination: higher energy consumption - Negative inclination: higher energy recovery - Larger distance between stops: smaller energy consumption	- Distribute the rotes according to their topographic profile - Do not assign demanding routes (steep inclinations, lots of turns) one after the other - Plan the routes as such they are somehow balanced regarding topographic profile
Driver's Behavior Analysis	Impact of a driver's (un)planned actions	- Higher deceleration rates: smaller energy recovery - Higher acceleration rates: smaller energy consumption	- Provide training for the bus drivers to plan ahead of time their acceleration and braking episodes - Program the bus controller to "punish" higher acceleration rates, allowing the gear shift to occur faster for those that accelerate slower
Bus Fleet Analysis	Impact of Traffic	- Denser traffic: smaller average speed, more time to complete the route, higher energy consumption and consequently less energy in the batteries in the end	- Buses should have their routes scheduled differently according to the time of the day - Buses that get more traffic should be assigned "lighter" routes to be performed afterwards, or should have partial charging scheduled during the day, or increased autonomy

It is expected that this simulation platform will serve as a powerful decision tool, especially for bus operators, as a way to build confidence over electric buses. The platform has demonstrated that the performance of electric buses is similar to ICEs', and that with the adequate route schedule, there is no reason to worry about their limited autonomy. Implementing electric buses in a city is a matter of operation, of learning how to work with them and to adapt to their requirements. In summary, the key contributions of this thesis are:

- Electric bus mathematical model: a complex electric bus mathematical model was devised. It accounts for the representation of the forces that impact the bus movement and the battery model. This model uses speed as it main input and all variables are defined on a separate sheet, allowing for the simulation of other electric vehicle models by changing those variables. The outcome of this model is the performance parameters: power, torque, motor speed, consumed and regenerated energy, and SOC.
- *Simulink* model: the previously developed mathematical model was implemented in the *Simulink* software. Besides containing the aforementioned mathematical equations explaining bus dynamics and the battery model, the *Simulink* implementation encompasses all the required logics for the bus to perform realistically. Therefore, this model takes into account the real bus operation, which could not be expressed in the mathematical model alone.
- *SUMO* traffic simulator: the integration of the *Simulink* model to the traffic simulator *SUMO* has provided a much more realistic representation of the routes the bus is supposed to perform. More than just analyzing the electric bus based on a certain speed profile, the electric bus in *SUMO* reacts to surrounding traffic, to the traffic lights, to the bus stops and to the elevation profile of routes.
- The simulation platform as a decision-support tool: the performed case studies have demonstrated how powerful this simulation platform is for decision-making, such as shown in Table 7.1. The performance parameters resulting from it can be used for a variety of analyses and one of its most important outcomes is the conclusion that the implementation of electric buses should be seen as an opportunity more than a threat.

7.3 Further Development

So far in the chapter, it is clear that the developed simulation platform has many positive aspects and represents really well the bus operations, once it is validated based on real data. The platform answers well the proposed research questions, establishing its role as a robust tool for decision-making; however, it also presents some limitations. Figure 7.1 presents a summary of both strengths and weaknesses identified.

Based on the identified weaknesses, those should be addressed in further developments. The first one is the acceleration profile of the bus, which is dictated by the chosen values for acceleration and deceleration defined in *SUMO*. The simulation of buses in *SUMO* is held according to a pre-specified file that includes the route it performs, the bus stops along the route and the time the bus is expected to arrive at each bus stop. This file also defines the acceleration and deceleration rates for the bus, thus overriding the natural evolution of the bus speed, normally dictated by its motor.

A further development would be to simulate a regular acceleration of the bus in *Simulink*, making it interactively and on-line with *SUMO*, so that the values in the *SUMO* file for acceleration and deceleration are instead override. In this sense, once the simulation starts, the defined route in *SUMO* is performed according to the acceleration behavior that *Simulink* provides. Then *SUMO* would send the developed speed back to *Simulink* according to the traffic interactions throughout the route, performing the calculations as they currently are.

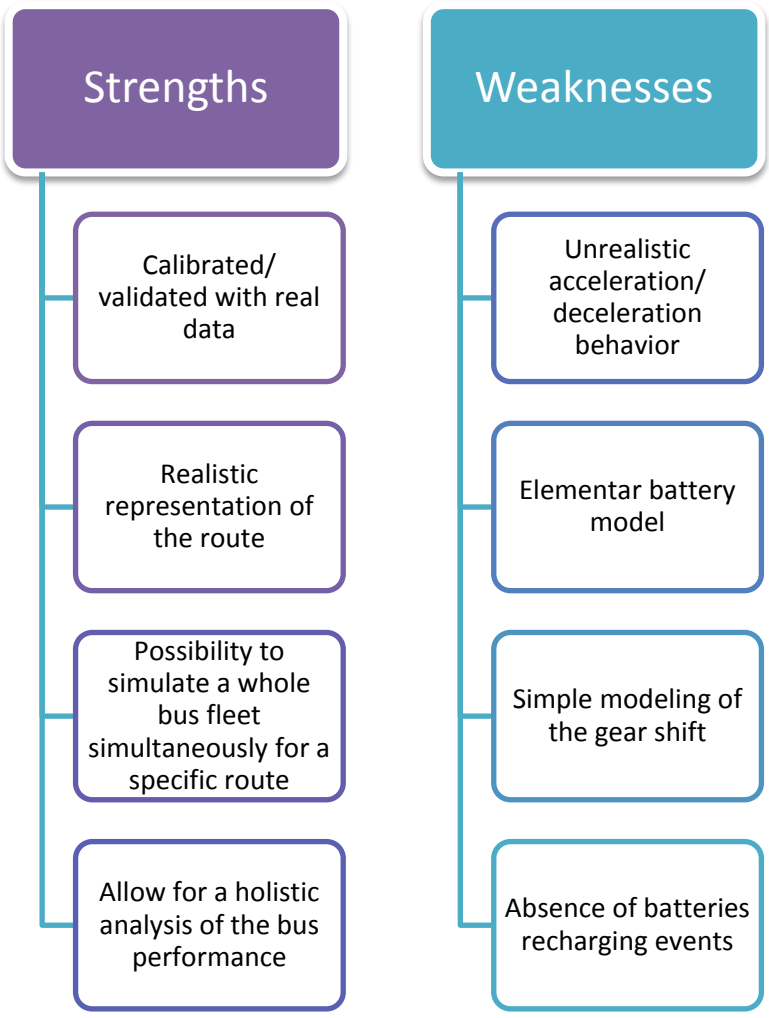

Figure 7.1- The simulation platform strengths and weaknesses

Another interesting development would be to perform a more realistic model of the batteries behavior. The developed model does not account for the dynamic behavior of the batteries, in terms of temperature and SOC impact on performance, for example. In this way, the extracted curves for battery current and voltage somewhat differ from the real curves, although the final energy consumption values (derived from the multiplication of current and voltage) are fairly similar.

A third useful aspect that could be improved on the developed platform is related to the gear shift. As mentioned earlier on in this chapter, the gear shift is performed taking into consideration the achievement of a certain speed value, which means that the faster this value is reached, the faster the gear is shifted. Lower gear ratio implies more energy consumption as it represents the beginning of the bus movement overcoming inertia.

When the acceleration is performed intensely, it is expected that the vehicle spends more energy due to the extra power demanded from the motor. However, the case study has shown lower energy consumption for higher acceleration rates, contradicting this behavior. A possible reason to justify this behavior is the way the gear shift is performed in the platform, where the faster the speed is reached, the faster the gear is shifted. In this sense, a further development in the platform would consider a more realistic approach to gear shift, modeling the way an automatic gear shift is performed.

The last listed aspect as a weakness is to consider the batteries recharging events. This is of main importance for a more optimized operation of the bus, to ideally schedule the recharge events along the day (if needed). However, this would imply in a really large amount of extra work, and it was decided not to be considered in the scope of this thesis.

7.4 Future Work

Besides the further developments listed to overcome identified weaknesses, this work allows for other projects to be developed stemming from this thesis. Some ideas are:

- Develop an extension to *SUMO*, where a bus route can be loaded automatically according to a set of geographic coordinates, and not manually as is. . Some work has been started so as to allow procedural scenario construction in SUMO simulations crawling data from repositories such as OSM (Gonçalves et al. 2015);
- Extend *SUMO* to account for three-dimensional maps and send these data at each step of the simulation to *Simulink*, so that it considers elevation data automatically. Automatic Vehicle Localization (AVL) systems have been developed to use GPS data to

improve digital maps and can be used in this direction (Freitas et al. 2009; Freitas et al. 2010);

- Develop simulation agents to act as the bus drivers, allowing a more complex simulation regarding their attitudes when reacting to traffic, for example. Recent efforts to model driver behavior and improve Advanced Driver Assistance Systems (ADAS) combine concepts such as peer-designed agents and serious games (Goncalves et al. 2012; Rossetti et al. 2013). This approach can greatly help gain insight into drivers' anxiety and improve driving styles towards a more efficient use of electric vehicles;
- Simulate the bus passengers in *SUMO*, so that the bus can stop for a designated period of time according to the number of passengers boarding and alighting. Integrating agent-based demand models representing transit commuters (Rossetti et al. 2002) and activity-based approaches (Rossetti and Liu 2005) are to be explored in this way;
- Make *SUMO* to send these simulated data of bus passengers to *Simulink*, and *make Simulink* react to it by changing the load carried on the bus accordingly. This will imply further improvements to the HLA integration presented in this work (Macedo 2013; Macedo et al. 2013);
- Simulate the recharging stations and recharging events, allowing a more realistic representation of the bus operation. Such operational aspects of electric mobility are to be investigated on the basis of more contemporary approaches to simulating transportation systems through agent-based Artificial Transportation Systems (ATS) (Rossetti et al. 2011);
- Integrate more than one instance of the *Simulink* bus simulator to *SUMO*, so that different routes can be simulated at the same time. Cloud computing and simulation-as-a-service are also in the agenda to extend the HLA integration platform (Macedo 2013; Macedo et al. 2013) so as to allow lager and more complex networks to be modeled and simulated.

References

ABB, 2014a. “ABB and Volvo form global partnership for electric and hybrid bus fast-charging.” *ABB Press Release*. http://www.abb.com/cawp/seitp202/6ce621212d3e502ac1257d1c002eb875.aspx [Accessed November 25, 2014].

ABB, 2014b. “ABB Website.” http://www.abb.com/ [Accessed November 25, 2014].

ABB, 2013. “Large-capacity, flash-charging, battery-powered pilot bus takes to the street.” http://www.abb.com/cawp/seitp202/9315e568e4c6a1f8c1257b7400302fcd.aspx [Accessed December 30, 2014].

Adelaide City Concil, 2012. “Tindo - The World’s First Solar Electric Bus.” In *Informative Media*. Adelaide.

Altairnano, 2014. “Altairnano Webiste.” http://www.altairnano.com/ [Accessed November 24, 2014].

Anhui Ankai Automobile Company Ltd., 2014. “Anhui Ankai Automobile Company Ltd.” http://www.jac-buscn.com/8-new-energy-bus.html [Accessed November 23, 2014].

Aowey, 2014. “Shanghai Aowei Technology Development Co.” http://www.aowei.com/en/aboutus.php [Accessed November 25, 2014].

Azcarate, C., Mallor, F. and Barado, J., 2012. “Calibration of a decision-making process in a simulation model by a bicriteria optimization problem.” In *Proceedings Title: Proceedings of the 2012 Winter Simulation Conference (WSC)*. IEEE, pp. 1–10. doi:10.1109/WSC.2012.6465078 .

Barceló, J., Ferrer, J.L. and Grau, R., 1994. *Report: AIMSUN2 and the GETRAM simulation environment*, Universitat Politecnica de Catalunya. Barcelona.

Barlas, Y., 1989. “Multiple tests for validation of system dynamics type of simulation models.” *European Journal of Operational Research*, 42(1), pp.59–87. doi:10.1016/0377-2217(89)90059-3 .

Barlas, Y. and Carpenter, S., 1990. “Philosophical roots of model validation : two paradigms.” *System Dynamics Review*, 6(2), pp.148–166.

Barz, S., 2009. “A zero-emission bus tours California, Toyota flirts with ethanol, and more green auto news.” http://grist.org/article/green-light-all-up-in-my-bus-ness/ [Accessed November 24, 2014].

Behrisch, M., Bieker, L., Erdmann, J. and Krajzewicz, D., 2011. “SUMO – Simulation of Urban MObility.” In *SIMUL 2011 : The Third International Conference on Advances in System Simulation*. pp. 63–68.

Ben-Akiva, M., 1996. *Development of a deployable real-time dynamic traffic assignment system, Task D Interim report: analytical developments for DTA system*, Cambridge (MA).

Ben-Akiva, M., Choudhury, C. and Toledo, T., 2006. "Lane Changing Models." In *Proceedings of the International Symposium of Transport Simulation*. Lausanne, Switzerland.

Ben-Akiva, M.E., Koutsopoulos, H.N., Mishalani, R.G. and Yang, Q., 1997. "Simulation Laboratory for Evaluating Dynamic Traffic Management Systems." *Journal of Transportation Engineering*, 123(4), pp.283–289. doi:10.1061/(ASCE)0733-947X(1997)123:4(283) .

Blackburn, S., 2005. *The Oxford Dictionary of Philosophy*, Oxford University Press, UK.

Bombardier Transportation, 2014. "Bombardier Website." http://www.bombardier.com/ [Accessed November 25, 2014].

Burghout, W., 2004. *Hybrid microscopic-mesoscopic traffic simulation*. PhD Diss., Royal Institute of Technology.

BusinessWire, 2012. "City of Windsor First in North America to Launch BYD Environmentally-Friendly Electric Buses." http://www.businesswire.com/news/home/20120504006182/en/City-Windsor-North-America-Launch-BYD-Environmentally-Friendly#.VHNYBvmsVik [Accessed November 24, 2014].

Butler, K.L., Ehsani, M. and Kamath, P., 1999. "A Matlab-based modeling and simulation package for electric and hybrid electric vehicle design." *IEEE Transactions on Vehicular Technology*, 48(6), pp.1770–1778. doi:10.1109/25.806769 .

BYD, 2014. "BYD Unveils World's Largest Battery Electric Vehicle." http://www.byd.com/news/news-256.html [Accessed November 24, 2014].

BYD, 2013a. "BYD wins Schiphol contract: 35 pure electric buses for airside services." http://www.byd.com/news/news-169.html [Accessed November 24, 2014].

BYD, 2013b. "Netherlands Launch All-Electric Bus Service." http://www.byd.com/na/news/news-157.html [Accessed November 24, 2014].

BYD - Build Your Dreams, 2014. "BYD Website." http://www.byd.com/ [Accessed November 23, 2014].

CaetanoBus, 2011a. "Apresentação do Autocarro Eléctrico Caetano 2500EL." http://www.caetanobus.pt/ [Accessed November 26, 2014].

CaetanoBus, 2011b. "CaetanoBus Inicia a Segunda Fase de Testes do Eeléctrico 2500EL." http://www.caetanobus.pt/ [Accessed November 26, 2014].

CaetanoBus, 2009. "eCobus -100% Electric Bus." In *CaetanoBus Confidential Material*. Porto.

Camagni, R., 2002. “Urban mobility and urban form: the social and environmental costs of different patterns of urban expansion.” *Ecological Economics*, 40(2), pp.199–216. doi:10.1016/S0921-8009(01)00254-3 .

Campana, M., 2014. “Autocarro eléctrico suíço carrega em 15 segundos.” *PC Guia*, p.20, July 1.

Cerqueira, J., 2014. “Solaris. Estreia Urbino elétrico na Alemanha.” *Turbo Oficina Pesados*, pp.54–55, May 1.

Chen, M., Member, S. and Rinc, G.A., 2006. “Accurate Electrical Battery Model Capable of Predicting Runtime and I – V Performance.” *Energy Conversion, IEEE Transactions on*, 21(2), pp.504–511. doi:10.1109/TEC.2006.874229 .

Chinabuses, 2012. “Ankai electric bus operation mileage breaks 110,000 km.” http://www.chinabuses.org/news/2012/0229/article_5040.html [Accessed November 23, 2014].

Chinabuses, 2014. “Ankai Makes a New Splash in the New Energy E-Era.” http://www.chinabuses.org/news/2014/1021/article_8477.html [Accessed November 23, 2014].

Choi, U., 2012. “Commercial operation of ultra low floor electric bus for Seoul city route.” In *2012 IEEE Vehicle Power and Propulsion Conference*. Seoul, Korea: Ieee, pp. 1128–1133. doi:10.1109/VPPC.2012.6422619 .

Cikanek, S.R. and Bailey, K.E., 2002. “Regenerative braking system for a hybrid electric vehicle.” In *Proceedings of the 2002 American Control Conference (IEEE Cat. No.CH37301)*. American Automatic Control Council, pp. 3129–3134. doi:10.1109/ACC.2002.1025270 .

Citilabs, 2014. “Cube Simulator.”

Clean Technica, 2013. “Adelaide creates world’s first solar-powered public transport system.” http://reneweconomy.com.au/2013/adelaide-creates-worlds-first-solar-powered-public-transport-system-32530 [Accessed November 25, 2014].

Courtenay, P., 2014. “What is a tram?” http://www.thetrams.co.uk/whatisatram.php [Accessed November 21, 2014].

Crippen, A., 2008. “Warren Buffett Invests In Chinese Company Developing ‘Green’ Cars.” http://www.cnbc.com/id/26916857#. [Accessed November 24, 2014].

Delicado, C., 2013. “CaetanoBus. A inovação em autocarros.” *Pesados, August 1*, pp.28–31.

Deng, T. and Nelson, J.D., 2011. “Recent Developments in Bus Rapid Transit: A Review of the Literature.” *Transport Reviews*, 31(1), pp.69–96. doi:10.1080/01441647.2010.492455 .

Deng, T. and Nelson, J.D., 2012. “The perception of Bus Rapid Transit: a passenger survey from Beijing Southern Axis BRT Line 1.” *Transportation Planning and Technology*, 35(2), pp.201–219. doi:10.1080/03081060.2011.651885 .

Dia, H. and Panwai, S., 2008. "Nanoscopic Traffic Simulation: Enhanced Models of Driver Behavior for ITS and Telematics Simulations." In *3rd International Symposium on Transport Simulation*. Gold Coast, Australia: Monash University.

DRACULA, 2008. "Dynamic Route Assignment Combining User Learning and microsimulAtion." http://www.its.leeds.ac.uk/software/dracula/ [Accessed January 13, 2015].

Dula, C.S. and Ballard, M.E., 2003. "Development and Evaluation of a Measure of Dangerous, Aggressive, Negative Emotional, and Risky Driving1." *Journal of Applied Social Psychology*, 33(2), pp.263–282. doi:10.1111/j.1559-1816.2003.tb01896.x .

Dula, C.S. and Geller, E.S., 2003. "Risky, aggressive, or emotional driving: Addressing the need for consistent communication in research." *Journal of Safety Research*, 34(5), pp.559–566. doi:10.1016/j.jsr.2003.03.004 .

Eclipse, 2014. "Eclipse." www.eclipse.org [Accessed January 6, 2015].

EcoLocalizer, 2013. "Adelaide Creates World's First Solar-Powered Public Transit System." http://ecolocalizer.com/2013/09/04/adelaide-has-worlds-first-solar-powered-public-transport-system/ [Accessed December 30, 2014].

Edwards, J.D. ed., 1992. *Transportation Planning Handbook* 1st ed., Prentice Hall Professional Technical Reference.

Efacec, 2014. "Efacec." http://www.efacec.pt/ [Accessed November 26, 2014].

Ehsani, M., Rahman, K.M. and Toliyat, H. a., 1997. "Propulsion system design of electric and hybrid vehicles." *IEEE Transactions on Industrial Electronics*, 44(1), pp.19–27. doi:10.1109/41.557495 .

EOT and FTA, 2008. *Circumferential Transportation Improvements in the Urban Ring Corridor; Urban Ring Phase 2*, Massachusetts.

EPFL, 2014. "Ecole polytechnique fédérale de Lausanne." http://www.epfl.ch/ [Accessed November 25, 2014].

European Comission, 2014. *Progress Report: Towards Achieving the Kyoto and EU 2020 Objectives*,

Eurostat, 2014. "Greenhouse gas emissions by sector (source: EEA)." http://epp.eurostat.ec.europa.eu/tgm/refreshTableAction.do?tab=table&plugin=1&pcode=tsdcc210&language=en [Accessed December 9, 2014].

Federal Transit Administration, 2010. *Public Transportation's Role in Responding to Climate Change*,

Fellendorf, M., 1994. "VISSIM: A microscopic Simulation Tool to Evaluate Actuated Signal Control including Bus Priority." In *Technical Paper, Session 32 at the 64th ite Annual Meeting*. Dallas, pp. 1–9.

Figueiredo, M.C., Rossetti, R.J.F., Braga, R.A.M. and Reis, L.P., 2009. "An approach to simulate autonomous vehicles in urban traffic scenarios." *Intelligent Transportation*

Systems, 2009. ITSC '09. 12th International IEEE Conference on, pp.1–6. doi:10.1109/ITSC.2009.5309524 .

Floodmap, 2014. "Porto Elevation Map." http://www.floodmap.net/Elevation/ElevationMap/?gi=2735943 [Accessed November 16, 2014].

Freitas, T.R.M., Coelho, A. and Rossetti, R.J.F., 2010. "Correcting routing information through GPS data processing." *13th International IEEE Conference on Intelligent Transportation Systems*, pp.706–711. doi:10.1109/ITSC.2010.5624996 .

Freitas, T.R.M., Coelho, A. and Rossetti, R.J.F., 2009. "Improving digital maps through GPS data processing." *2009 12th International IEEE Conference on Intelligent Transportation Systems*, pp.1–6. doi:10.1109/ITSC.2009.5309537 .

Frey, H.C. and Patil, S.R., 2002. "Identification and Review of Sensitivity Analysis Methods." *Risk Analysis*, 22(3), pp.553–578. doi:10.1111/0272-4332.00039 .

Frigg, R. and Hartmann, S., 2012. "Models in Science" E. N. Zalta, ed. *The Stanford Encyclopedia of Philosophy (Fall 2012)*, p.28.

Fujimoto, R.M., 2001. "Parallel and distributed simulation systems." In *Proceeding of the 2001 Winter Simulation Conference*. IEEE, pp. 147–157. doi:10.1109/WSC.2001.977259 .

Gao, D.W., Mi, C. and Emadi, A., 2007. "Modeling and Simulation of Electric and Hybrid Vehicles." *Proceedings of the IEEE*, 95(4), pp.729–745. doi:10.1109/JPROC.2006.890127 .

Gass, S.I. and Thompson, B.W., 1980. "Letter to the Editor—Guidelines for Model Evaluation: An Abridged Version of the U.S. General Accounting Office Exposure Draft." *Operations Research*, 28(2), pp.431–439. doi:10.1287/opre.28.2.431 .

Gawron, C., 1998. *Simulation-Based Traffic Assignment; Computing User Equilibria in Large Street Networks*. PhD Diss., University of Cologne.

Gillespie, T.D., 1992. *Fundamentals of Vehicle Dynamics*, Society of Automotive Engineers, Inc.

Goncalves, J., Rossetti, R.J.F. and Olaverri-Monreal, C., 2012. "IC-DEEP: A serious games based application to assess the ergonomics of in-vehicle information systems." In *Intelligent Transportation Systems (ITSC), 2012 15th International IEEE Conference on*. pp. 1809–1814. doi:10.1109/ITSC.2012.6338828 .

Gonçalves, J.S. V, Jacob, J., Rossetti, R.J.., Coelho, A. and Rodrigues, R., 2015. "An Integrated Framework for Mobile-Based ADAS Simulation." In M. Behrisch & M. Weber, eds. *Modeling Mobility with Open Data, Lecture Notes in Mobility*. Switzerland: Springer International Publishing.

Grbovi, P.J., Member, S., Delarue, P., Le, P. and Member, M., 2011. "Modelling and Control of the Ultra-Capacitor Based Regenerative Controlled Electric Drives." *Industrial Electronics, IEEE Transactions on*, 58(8), pp.3471–3484. doi:10.1109/TIE.2010.2087290 .

Gruber, M., 2013. *How a bus manufacturer prepares for future demand. Report: Solaris Bus & Coach S.A.*, Barcelona.

Hamilton, T., 2009. "Next Stop : Ultracapacitor Buses." *Technology Review - MIT. October 19*, pp.1–2.

Hankuk, 2014. "Hankuk Fiber Group." http://www.fiber-x.com/en/ [Accessed January 7, 2015].

HHI, 2014. "Hyndai Heavy Industries." http://english.hhi.co.kr/main/ [Accessed January 7, 2015].

Hofmann, M., 2005. "On the Complexity of Parameter Calibration in Simulation Models." *JDMS*, 2(4), pp.217–226.

Høyer, K.G., 2008. "The history of alternative fuels in transportation: The case of electric and hybrid cars." *Utilities Policy*, 16(2), pp.63–71. doi:10.1016/j.jup.2007.11.001 .

Hsu, F., 2006. "Muni trolleybus wires at Haight & Divisadero, San Francisco, California." http://en.wikipedia.org/wiki/Trolleybuses_in_San_Francisco#mediaviewer/File:Muni_trolleybus_wires_at_Haight.jpg [Accessed December 30, 2014].

Huang, J., Yang, S., Liang, Q. and Gai, X., 2008. "Research on improving energy regeneration efficiency of super-capacitors electric bus." *2008 IEEE Vehicle Power and Propulsion Conference*, pp.1–5. doi:10.1109/VPPC.2008.4677638 .

Hutchinson, 2005. "Simon Fraser University." *Boston Trolleybus Photos 5*. http://www.sfu.ca/person/dearmond/chain/Boston_photos-5.htm [Accessed November 22, 2014].

Hyundai, 2011. "Hyundai To Showcase New Thinking At The 2011 Seoul Motor Show." http://globalpr.hyundai.com/prCenter/news/newsView.do?dID=1170 [Accessed November 23, 2014].

IEEE-Std 1, 2010. *IEEE Standard for Modeling and Simulation (M & S) High Level Architecture (HLA) — Federate Interface Specification*, IEEE Computer Society.

IEEE-Std 2, 2010. *IEEE Standard for Modeling and Simulation (M & S) High Level Architecture (HLA) — Framework and Rules*, IEEE Computer Society.

IEEE-Std 3, 2010. *IEEE Standard for Modeling and Simulation (M & S) High Level Architecture (HLA) — Object Model Template Specification*, IEEE Computer Society.

Iglesias, R., Lago, A., Nogueiras, A., Marcos, J., Quintans, C., Moure, M.J. and Valdés, M.D., 2012. "Modelado y Simulación de una Batería de Ion-Litio Comercial Multicelda." In *Seminario Anual de Automática, Electrónica Industrial e Instrumentación (SAAEI 2012)*. pp. 464–469.

Jandt, F., 2010. "Finding a Spark." *Mass Transit, April/ May*, XXXVI(3).

Jayakrishnan, R., Mahmassani, H.S. and Hu, T.-Y., 1994. "An evaluation tool for advanced traffic information and management systems in urban networks." *Transportation*

Research Part C: Emerging Technologies, 2(3), pp.129–147. doi:10.1016/0968-090X(94)90005-1 .

Jha, M., Gopalan, G., Garms, A., Mahanti, B., Toledo, T. and Ben-Akiva, M., 2004. "Development and Calibration of a Large-Scale Microscopic Traffic Simulation Model." *Transportation Research Record*, 1876(1), pp.121–131. doi:10.3141/1876-13 .

Jinrui, N., Zhifu, W. and Qinglian, R., 2006. "Simulation and Analysis of Performance of a Pure Electric Vehicle with a Super-capacitor." *2006 IEEE Vehicle Power and Propulsion Conference*, pp.1–6. doi:10.1109/VPPC.2006.364349 .

JOSM, 2014. "JOSM." https://josm.openstreetmap.de/ [Accessed November 4, 2014].

Kamal, M., Mukai, M., Murata, J. and Kawabe, T., 2009. "Development of Ecological Driving Assist System Model Predictive Approach in Vehicle Control." In *16th ITS World Congress and Exhibition on Intelligent Transport Systems and Services*. Stockholm, pp. 1–11.

Kennedy, M.C. and O'Hagan, A., 2001. "Bayesian calibration of computer models." *Journal of the Royal Statistical Society: Series B (Statistical Methodology)*, 63(3), pp.425–464. doi:10.1111/1467-9868.00294 .

Kleijnen, J.P.C., 1995. "Verification and validation of simulation models." *European Journal of Operational Research*, 82(1), pp.145–162. doi:10.1016/0377-2217(94)00016-6 .

Knowledge of London, 2014. "The London Omnibus." http://www.knowledgeoflondon.com/buses.html [Accessed November 22, 2014].

Kokkinogenis, Z., Monteiro, N., Rossetti, R.J.F., Bazzan, A.L.C. and Campos, P., 2014. "Policy and incentive designs evaluation: A social-oriented framework for Artificial Transportation Systems." *17th International IEEE Conference on Intelligent Transportation Systems (ITSC)*, pp.151–156. doi:10.1109/ITSC.2014.6957682 .

Kooser, A., 2014. "Battery-topped electric buses flash charge in 15 seconds." http://www.cnet.com/news/battery-topped-electric-buses-flash-charge-in-15-seconds/ [Accessed November 25, 2014].

KoreaTimes, 2010. "Hyundai Motor employees try a prototype of the firm's electric." http://www.koreatimes.co.kr/www/news/biz/2014/07/258_68104.html [Accessed December 30, 2014].

Krajzewicz, D., Hertkorn, G., Wagner, P. and Rössel, C., 2002. "SUMO (Simulation of Urban MObility); An open-source traffic simulation Car-Driver Model." In *4th Middle East Symposium on Simulation and Modelling (MESM2002)*. Sharjah / United Arab Emirates: SCS European Publishing House, pp. 183–187.

Kraus, S., Wagner, P. and Gawron, C., 1997. "Metastable States in a Microscopic Model of Traffic Flow." *Physical Review E*, 55(304), pp.55–97. doi:10.1103/PhysRevE.55.5597 .

Larminie, J. and Lowry, J., 2003. *Electric Vehicle Technology Explained*, West Sussex: John Wiley & Sons, Ltd.

Lee, J., 2005. *Rotating Inertia Impact on Propulsion and Regenerative Braking for Electric Motor Driven Vehicles*. MSc Diss., State University.

Leonard, D.R., Gower, P. and Taylor, N.B., 1989. "CONTRAM: structure of the model." *Research report - Transport and Road Research Laboratory*, (178).

Levinson, H.S., Zimmerman, S., Clinger, J. and Gast, J., 2003. "Bus Rapid Transit." *Transportation Research Board*.

Lin, C., Filipi, Z., Wang, Y., Louca, L., Peng, H., Assanis, D. and Stein, J., 2001. *Integrated , Feed-Forward Hybrid Electric Vehicle Simulation in SIMULINK and its Use for Power Management Studies*,

Linden, D. and Reddy, T.B., 2002. *Handbook of Batteries* 3rd ed., McGraw-Hill.

Loveday, E., 2011a. "BYD to supply city of Frankfurt with three electric eBUS-12s." http://green.autoblog.com/2011/06/18/byd-to-supply-city-of-frankfurt-with-3-electric-ebus-12s/ [Accessed November 24, 2014].

Loveday, E., 2011b. "Report: Electric bus catches fire in Shanghai." http://green.autoblog.com/2011/07/22/report-electric-bus-catches-fire-in-shanghai/ [Accessed November 23, 2014].

Loveday, E., 2010. "Seoul's commercial electric bus fleet hits the road." http://green.autoblog.com/2010/12/29/seouls-electric-bus-fleet-namasan/ [Accessed November 23, 2014].

Macedo, J., 2013. *An Integrated Framework for Multi-Paradigm Traffic Simulation*. MSc Diss., University of Porto.

Macedo, J., Kokkinogenis, Z., Soares, G., Perrotta, D. and Rossetti, R.J.F., 2013. "A HLA-based multi-resolution approach to simulating electric vehicles in simulink and SUMO." *16th International IEEE Conference on Intelligent Transportation Systems (ITSC 2013)*, pp.2367–2372. doi:10.1109/ITSC.2013.6728581 .

Maerivoet, S. and De Moor, B., 2005. "Traffic Flow Theory." , 32(0). arxiv.org/abs/physics/0507126v1.

Maia, R., Silva, M., Araújo, R. and Nunes, U., 2011. "Electric Vehicle Simulator for Energy Consumption Studies in Electric Mobility Systems." In *2011 IEEE Forum on Integrated and Sustainable Transportation Systems*. Vienna, pp. 227–232. doi:10.1109/FISTS.2011.5973655 .

Manière, F., 2011. "Premiers omnibus à Nantes." *Premiers omnibus à Nantes*. http://www.herodote.net/10_aout_1826-evenement-18260810.php [Accessed November 23, 2014].

Market Street Railway, 2014. "Streetcar, Cable Car: What's the difference?" http://www.streetcar.org/wheels-motion/difference/ [Accessed November 21, 2014].

MassDot, 2014. *Report: Silver Line Gateway*. Massachusetts: Massachusetts Department of Transportation.

Mathworks, 2012. “MATLAB and Statistics Toolbox Release 2012b.”

May, A.D., 1990. *Traffic Flows Fundamentals*, New Jersey: Englewood Cliffs, N.J.: Prentice Hall, 1990.

Van Mierlo, J., 2004. “Models of energy sources for EV and HEV: fuel cells, batteries, ultracapacitors, flywheels and engine-generators.” *Journal of Power Sources*, 128(1), pp.76–89. doi:10.1016/j.jpowsour.2003.09.048 .

Miyatake, M., Kuriyama, M. and Takeda, Y., 2011. “Theoretical study on eco-driving technique for an Electric Vehicle considering traffic signals.” In *2011 IEEE Ninth International Conference on Power Electronics and Drive Systems*. IEEE, pp. 733–738. doi:10.1109/PEDS.2011.6147334 .

Moura, C., 2014. “CaetanoBus lança autocarro urbano elétrico em 2015.” *Transportes em revista*. http://www.transportesemrevista.com/Default.aspx?tabid=210&language=pt-PT&id=35823 [Accessed November 26, 2014].

Moura, C., 2013. “Salvador Caetano e Siemens desenvolvem eCobus.” *Transportes em revista*. http://www.transportesemrevista.com/Default.aspx?tabid=210&language=pt-PT&id=10842 [Accessed November 26, 2014].

Murga, M., 2014. “1.254 Transportation Modeling.” In *Civil Eng, DUSP – MIT*.

New York Transit Museum, 2014. “History of Public Transportation in New York City.” http://www.transitmuseumeducation.org/trc/background [Accessed November 26, 2014].

Ni, D., 2003. “2DSIM: A prototype of nanoscopic traffic simulation.” *IEEE IV2003 Intelligent Vehicles Symposium*, pp.47–52. doi:10.1109/IVS.2003.1212881 .

Open Street Map, 2014. “Open Street Map.” https://www.openstreetmap.org [Accessed December 2, 2014].

Passos, L.S., Rossetti, R.J.F. and Kokkinogenis, Z., 2011. “Towards the next-generation traffic simulation tools: a first appraisal.” In *Information Systems and Technologies (CISTI), 2011 6th Iberian Conference on*. Chaves, Portugal, pp. 1–6.

Perrotta, D., Macedo, J.L., Rossetti, R.J.., Afonso, J.L., Kokkinogenis, Z. and Ribeiro, B., 2014. “Driver Attitude and Its Influence on the Energy Waste of Electric Buses.” In M. Behrisch, D. Krajzewicz, & M. Weber, eds. *Simulation of Urban Mobility SE - 8*. Lecture Notes in Computer Science. Springer Berlin Heidelberg, pp. 99–108. doi:10.1007/978-3-662-45079-6_8 .

Perrotta, D., Macedo, J.L., Rossetti, R.J.., Sousa, J.F. de, Kokkinogenis, Z., Ribeiro, B. and Afonso, J.L., 2014. “Route Planning for Electric Buses: A Case Study in Oporto.” *Procedia - Social and Behavioral Sciences*, 111, pp.1004–1014. doi:10.1016/j.sbspro.2014.01.135 .

Perrotta, D., Macedo, J.L., Rossetti, R.J.F., Afonso, J.L., Kikkinogenis, Z. and Ribeiro, B., 2013. "Driver ' s Attitude and its Influence on the Energy Waste of Electric Buses." In *1st SUMO User Conference 2013*. Berlin - Adlershof, pp. 103–107.

Pierre, M., Jemelin, C. and Louvet, N., 2011. "Driving an electric vehicle. A sociological analysis on pioneer users." *Energy Efficiency*, 4(4), pp.511–522. doi:10.1007/s12053-011-9123-9 .

Pitch, 2012. "The HLA Tutorial: A Practical Guide for Developing Fistributed Simulations." , p.5.

Pourbaix, J., 2012. "Towards a Smart Future for Cities." *Journeys*, (May), pp.7–13.

Prashker, J.N. and Bekhor, S., 2004. "Route Choice Models Used in the Stochastic User Equilibrium Problem: A Review." *Transport Reviews*, 24(4), pp.437–463. doi:10.1080/0144164042000181707 .

Proterra, 2014. "Proterra." http://www.proterra.com/index.php [Accessed November 24, 2014].

Ratrout, N.T. and Rahman, S.M., 2009. "A Comparative Analysis of Currently Used Microscopic and Macroscopic Traffic Simulation Software." *The Arabian Journal for Science and Engineering*, 34(1B), pp.121–133.

RealLi Research, 2012. "BYD's All-electric Buses Will Run in Finland." http://www.realli.org/newsdetail.php?id=310 [Accessed November 24, 2014].

Research India, 2010. *Report: New Electric Technology Buses in Shanghay*,

Rodrigue, J.-P., 2014. "Urban Mobility." *The Geography of Transport Systems*. http://people.hofstra.edu/geotrans/index.html [Accessed November 22, 2014].

Rossetti, R.J.., Bordini, R.H., Bazzan, A.L.., Bampi, S., Liu, R. and Vliet, D. Van, 2002. "Using BDI agents to improve driver modelling in a commuter scenario." *Transportation Research Part C: Emerging Technologies*, 10(5-6), pp.373–398. doi:10.1016/S0968-090X(02)00027-X .

Rossetti, R.J.. and Liu, R., 2005a. "A Dynamic Network Simulation Model Based on Multi-Agent Systems." In F. Klügl, A. Bazzan, & S. Ossowski, eds. *Applications of Agent Technology in Traffic and Transportation SE - 12*. Whitestein Series in Software Agent Technologies. Birkhäuser Basel, pp. 181–192. doi:10.1007/3-7643-7363-6_12 .

Rossetti, R.J.. and Liu, R., 2005b. "An Agent-Based Approach to Assess Drivers' Interaction with Pre-Trip Information Systems." *Journal of Intelligent Transportation Systems*, 9(1), pp.1–10. doi:10.1080/15472450590912529 .

Rossetti, R.J.F., Almeida, J.E., Kokkinogenis, Z. and Goncalves, J., 2013. "Playing Transportation Seriously: Applications of Serious Games to Artificial Transportation Systems." *Intelligent Systems, IEEE*, 28(4), pp.107–112. doi:10.1109/MIS.2013.113 .

Rossetti, R.J.F. and Liu, R., 2005. "Activity-based analysis of travel demand using cognitive agents." In H. Timmermans, ed. *Progress in Activity-Based Analysis*. Oxford: Elsevier, pp. 139–160.

Rossetti, R.J.F., Liu, R., Cybis, H.B.B. and Bampi, S., 2002. "A multi-agent demand model." In *Proceedings of the 13th Mini-Euro Conference and The 9th Meeting of the Euro Working Group Transportation*. pp. 193–198.

Rossetti, R.J.F., Liu, R. and Tang, S., 2011. "Guest Editorial Special Issue on Artificial Transportation Systems and Simulation." *IEEE Transactions on Intelligent Transportation Systems*, 12(2), pp.309–312. doi:10.1109/TITS.2011.2143770 .

Sargent, R.G., 1984. "A tutorial on validation and verification of simulation models." *1988 Winter Simulation Conference Proceedings*, (315), pp.33–39. doi:10.1109/WSC.1988.716122 .

Sargent, R.G., 2005. "Verification and Validation of Simulation Models." In *Proceedings of the Winter Simulation Conference, 2005.* IEEE, pp. 130–143. doi:10.1109/WSC.2005.1574246 .

Servant, L., 1996. "L'automobile dans la ville." *Cahiers du IAURIF, nº 114*.

Siemens, 2013. "Salvador Caetano e Siemens desenvolvem primeiro autocarro 100% elétrico para aeroportos." https://www.swe.siemens.com/portugal/web_nwa/pt/PortalInternet/QuemSomos/negocios/ic/mol/noticias-eventos/noticias/Pages/SalvadorCaetanoeSiemensdesenvolvem.aspx [Accessed December 30, 2014].

Siemens, 2014. "Siemens." http://www.siemens.com/history/en/innovations/transportation.htm#toc-2 [Accessed November 21, 2014].

Siemens Portugal, 2014. "Siemens Portugal." http://www.siemens.com/answers/pt/pt/ [Accessed November 26, 2014].

Sinautec, 2014. "Sinautec Automobile Technologies L.L.C." http://www.sinautecus.com/index.html [Accessed November 25, 2014].

Singh, T., 2010. "South Korea Unveils World's First Commerical Electric Bus." http://inhabitat.com/south-korea-unveils-worlds-first-commerical-electric-bus/ [Accessed November 22, 2014].

Smith, M., Duncan, G. and Druitt, S., 1995. "PARAMICS: microscopic traffic simulation for congestion management." In *Dynamic Control of Strategic Inter-Urban Road Networks, IEE Colloquium on1995*. London, pp. 8/1 – 8/3. doi:10.1049/ic:19950249 .

Solaris Bus & Coach SA., 2014. "Group Urbino electric." http://www.solarisbus.com/vehicles_group/urbino-electric [Accessed November 25, 2014].

Solaris Bus & Coach SA., 2011. "Solaris Urbino Electric." http://www.omnibusarchiv.de/include.php?path=content&mode=print&contentid=922 [Accessed November 25, 2014].

STCP, 2014. "STCP - Sociedade de Transportes Colectivos do Porto, SA." http://www.stcp.pt [Accessed November 16, 2014].

Stewart, A. and Figueroa, C., 2014. "Designing Bus Rapid Transit Oriented Development." http://brtod.net/ [Accessed November 7, 2014].

The International Council of Clean Transportations, 2013. *European Vehicle Market Statistics Pocketbook 2013*,

Times, C.C., 2012. "Shenzhen, China Launches the World's Largest Electric Vehicle Fleet." http://www.chinabuses.org/news/2012/0613/article_5484.html [Accessed November 24, 2014].

TOSA, 2014. "TOSA2013." http://www.tosa2013.com/#/tosa2013 [Accessed November 25, 2014].

TPB, M.A.T.P.B., 2013. *Madison BRT Transit Corridor Study; Proposed BRT Travel Time Estimation Approach*, Madison, USA.

Transport News Brief, 2013. "Chinese electric buses enter service in London." http://www.transportnewsbrief.co.uk/bus-and-coach/chinese-elelectric-buses-enter-service-london/ [Accessed November 24, 2014].

transportweekly, 2014. "Solaris Urbino electric - the customer's choice." http://www.transportweekly.com/pages/en/news/articles/108034/ [Accessed November 25, 2014].

Turbo Oficina Pesados, 2014. "Volvo e ABB . Aposta nos autocarros elétricos." *Turbo Oficina Pesados, September 1*, p.62.

Unger, N., Bond, T.C., Wang, J.S., Koch, D.M., Menon, S., Shindell, D.T. and Bauer, S., 2010. "Attribution of climate forcing to economic sectors." *Proceedings of the National Academy of Sciences of the United States of America*, 107(8), pp.3382–7. doi:10.1073/pnas.0906548107 .

UQM Technologies, 2014. "UQM Technologies." http://uqm.com/products/full-electric/prototype/commercial-vehicles/ [Accessed November 24, 2014].

URS, 2010. *Report: Streetcar Technology Assessment*, North Carolina.

Veasey, C., 2014. "What is a Trolleybus?" http://www.trolleybus.net/subhtml/trams-trolleybuses.htm [Accessed November 21, 2014].

Velez, A., 2011. "Eléctrico para o mundo." *Turbo*, pp.78–79, May 1.

Veolia Transport Finland Oy, 2014. "Veolia." http://www.veolia-transport.fi/ [Accessed November 24, 2014].

Volvo, 2013. "Volvo launches noiseless electric buses in Gothenburg." *Volvo press release, June 17*.

Volvo Group, 2014. "Volvo Group." http://www.volvogroup.com [Accessed November 25, 2014].

Westbrook, M.H., 2001. *The Electric Car: Development and Future of Battery, Hybrid and Fuel-Cell Cars*, Warrendale, PA, USA: Society of Automotive Engineers, Inc.

Whitner, R.B. and Balci, O., 1989. "Guidelines For Selecting And Using Simulation Model Verification Techniques." In *1989 Winter Simulation Conference Proceedings*. IEEE, pp. 559–568. doi:10.1109/WSC.1989.718728 .

Wicks, F. and Donnelly, K., 1997. "Modeling Regenerative Braking and Storage for Vehicles." *Energy Conversion Engineering Conference, 1997. IECEC-97, Proceedings of the 32nd Intersociety*, pp.2030–2035.

Wong, J.Y., 2008. *Theory of Ground Vehicles* 4th ed., John Wiley & Sons Ltd.

Wright, L. and Hook, W., 2007. *Bus Rapid Transit Planning Guide* 3rd editio., New York: Institute of Transportation & Development Policy.

Xiaohua, Z., Haitao, M., Xing, X., Qingnian, W. and Rules, A.P.M., 2008. "Parameter design for power train and performance simulation of electrical city bus." *2008 IEEE Vehicle Power and Propulsion Conference*, pp.1–5. doi:10.1109/VPPC.2008.4677713 .

Xu, C., 2011. "Design and simulation of the power-train system for an electric vehicle." *2011 2nd International Conference on Artificial Intelligence, Management Science and Electronic Commerce (AIMSEC)*, pp.3868–3871. doi:10.1109/AIMSEC.2011.6010059 .

Yin, J., 2007. "Ankai Electric Buses to Support Beijing Olympics." http://www.chinabuses.com/english/news/0710/08001.htm [Accessed November 23, 2014].

Yoney, D., 2010. "Proterra sells electric buses, fast-chargers to Foothill Transit." http://green.autoblog.com/2010/09/11/proterra-sells-electric-buses-fast-chargers-to-foothill-transit/ [Accessed November 24, 2014].

Yu, J., Wang, J., Liang, G. and Li, D., 2012. "Pure electric vehicle driving system parameter matching in motor higher efficiency interval." *2012 International Conference on Systems and Informatics (ICSAI2012)*, (Icsai), pp.594–597. doi:10.1109/ICSAI.2012.6223068 .

Yueqing Ruihua Cabinet & Whole Set Equipment Co. Ltd., 2014. "Yueqing Ruihua." http://www.cnruihua.com.cn/ [Accessed November 23, 2014].

Zebra Technologies, 2014. "Zebra Technologies." https://www.zebra.com/us/en/products-services/accessories/batteries.html [Accessed November 25, 2014].

Appendices

Appendix A - UQM PowerPhase® 150 Datasheet Extract

HPM150 Brushless PM Motor/Generator		
Dimensions		
Length	9.49 in	241 mm
Diameter	15.94 in	405 mm
Weight	200 lb	91 kg
Performance		
Motoring power (peak)	200 hp	150 kW
Motoring torque (peak)	480 lbf·ft	650 N·m
Regeneration power (peak)	200 hp	150 kW
Regeneration torque (peak)	480 lbf·ft	650 N·m
Maximum speed	5000 RPM	
Power density	1.00 hp/lb	1.65 kW/kg

Appendix B – UQM PowerPhase® 150 System

Efficiency Maps Motoring Mode

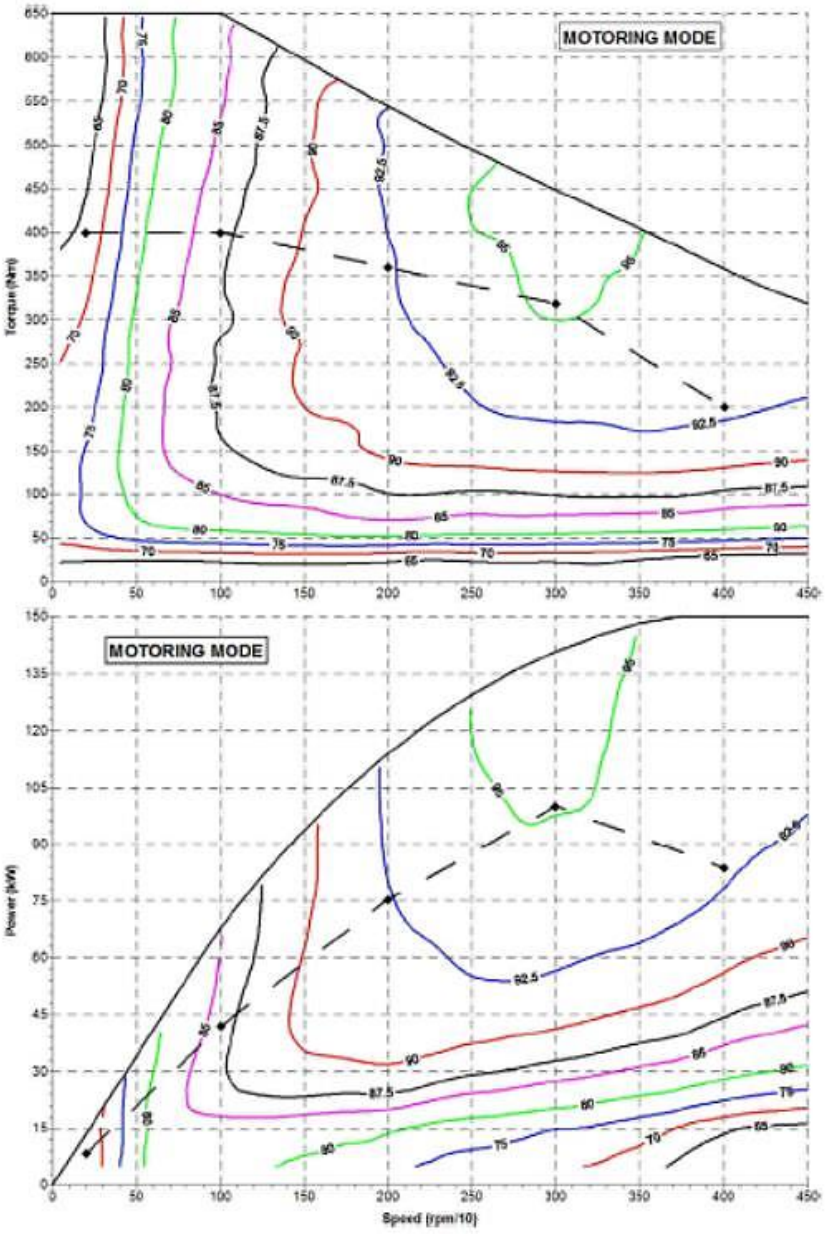

Appendix C - Shenzhen Free TechnologyCo., Ltd

LiFePO4 Battery Cell Specification

Item	Specification
model	26650
Typical capacity	3050mAh@ 0.3 C5A Discharge
Minimum capacity	3000mAh@ 0.3 C5A Discharge
Nominal voltage	3.2V
Internal impendance (Max, at 1000Hz.)	≤25mΩ
Max Charging voltage	3.65V
Dischargingcut-offvoltage	2.0V
Max charging current	1 C_5A
Maxcontinuous discharging current	4 C_5A
Max instant peak value discharging current	8 C_5A
weight	Less than 90g
Charge method	Standard charge：0.3 C_5A×5hrs Rapid charge： 0.5 C_5A×3hrs.
Operating temperature	Charge：0°C ~ 45°C 32°F～113°F Discharge：-20°C ~ 60°C -4°F～149°F Storage temperature : -20℃～45℃；-4°F～113°F

Appendix D – *SUMO* Scripts

- To convert a osm file into *SUMO* format:

netconvert.exe --osm-files my_file.osm.xml -o map.net.xml

- To generate random trips:

randomTrips.py -n map.net.xml -L –l –r routes.rou.xml

- To create a polygon file of districts (TAZs):

polyconvert.exe -n map.net.xml --shapefile.id-column "N" -o districts.poi.xml

- To associate *SUMO* map file to the district file:

edgesInDistricts.py -n map.net.xml,districts.poi.xml -w -o district.taz.xml

- To generate trips from a real O/D matrix:

od2trips.exe –n district.taz.xml -d odmatrix.txt -o trips.trips.xml -b 0 -e 3600

- To generate routes from a trip file:

*duarouter.exe -n map.net.xml -d district.taz.xml -t trips.trips.xml -o routes.rou.xml -b 0 -e 360*0

- To apply dynamic user assignment while generating routes:

duaIterate.py -n map.net.xml -t trips.trips.xml -l 10

Appendix E - Data decoding: *Matlab* Script

All the available data for the operation of the bus is collected electronically. Some of these data come in absolute values, such as the state-of-charge of the batteries; others come encrypted, like the electrical current and voltage and demands unencrypting before it can be useful. Therefore a script was developed in *MATLAB* so that these data can become legible for further uses.

Battery current and voltage data come as a single input composed of ten characters. In order to unencrypt it, the following steps should be taken:

1. Transform the number into hexadecimal, which turns it into an eight-character number where the first two bytes represents the current and the other two, the voltage;
2. Invert the first two bytes, transforming it into a two's complement (if negative);
3. Convert back to decimal to have the current value;
4. Invert the other two bytes;
5. Convert back to decimal to have the voltage value.

These steps had to be translated to *Matlab* so that unencrypting would become simple and fast. Once done, the data can be easily uploaded to *Matlab* so that the script runs over it and generates the final values for those parameters. For explanation purposes, the table containing these data is called *BatIV* and should be firstly imported do *Matlab*.

Starting with the number 1 of the steps, in order to convert the parameter to hexadecimal, the code bellow should be applied over the imported table:

```
Hexa = dec2hex(BatIV);
```

The process of inverting the bytes is performed after applying the following codes:

```
firstbyte = hexa (:,[1 2]);

secondbyte = hexa (:,[3 4]);

currenthexa = [secondbyte firstbyte];
```

In case the current is positive, which happens if the first digit is 1, then the signal should be converted back to decimal and divided by 10 to get to the final value, as follows:

currenthexadec = hex2dec (currenthexa);

currentpositive = currenthexadec/10;

If current is negative, then it should be converted back to decimal to be further transformed into a 16-bit binary:

currenthexadec = hex2dec (currenthexa);

currentbin = dec2bin (currenthexadec,16);

At this point, this number is a two's complement and should be treated accordingly. Firstly, the first digit should be removed and further compiled; the outcome should be transformed from char to cell array:

currentbin1 = currentbin (:,2:end);

currentbin2 = cellstr(currentbin1);

cdig_sig = currentbin (:,1);

cdig_sig1 = cellstr(cdig_sig);

The next step is to inverse the binary. In order to do that, these coded should be used:

newStr = regexprep(currentbin2,'1','a');

newStr1 = regexprep(newStr,'0','b');

invert = regexprep(newStr1,'a','0');

invert1 = regexprep(invert,'b','1');

After the inversion, the outcome should be converted back to decimal and sum 1 unity:

invert1_d = bin2dec (invert1);

cvalue_d = invert1_d + 1;

The absolute value is defined at this point. In order to have the signal following this value, the compiled cell string cdig_sig1 should pass through a process where "1" is replaced by "-" and "0" by "+". The outcome should be further transformed into char:

csig = regexprep(cdig_sig1,'1','-');

cSig = regexprep(csig,'0','+');

cSig1 = char (cSig);

Now that the final absolute value for current and the signal following it are both defined, the final value can be composed by:

cvalue_d1 = num2str (cvalue_d);

cfinal = [cSig1 cvalue_d1];

cfinal1 = str2num (cfinal);

currentfinal = cfinal1/10;

For the composition of the voltage value, the process is the same as the one applied for positive values of current. This script is simple and does not demand much memory from the computer, for it makes the unencrypting process efficient.

Appendix F – Line 401 *buses.add.xml* file

```
<additional xmlns:xsi="http://www.w3.org/2001/XMLSchema-instance"
xsi:noNamespaceSchemaLocation="http://sumo.sf.net/xsd/additional_file.xsd">
    <busStop id="BLAM2" lane="112465238_0" startPos="60" endPos="75" lines="401"/>
    <busStop id="SCAT1" lane="20672084#1_0" startPos="50" endPos="65" lines="401"/>
    <busStop id="PDR" lane="20672084#2_0" startPos="60" endPos="75" lines="401"/>
    <busStop id="C24A1" lane="36268629_0" startPos="45" endPos="60" lines="401"/>
    <busStop id="NAVE1" lane="14328502#1_0" startPos="25" endPos="40" lines="401"/>
    <busStop id="BL4" lane="14328519#4_0" startPos="60" endPos="75" lines="401"/>
    <busStop id="ESR1" lane="14328519#10_0" startPos="90" endPos="105" lines="401"/>
    <busStop id="SCRP5" lane="14328519#16_0" startPos="45" endPos="60" lines="401"/>
    <busStop id="MAV1" lane="159959892#7_0" startPos="20" endPos="35" lines="401"/>
    <busStop id="AANT3" lane="34976568#0_0" startPos="55" endPos="70" lines="401"/>
    <busStop id="DCVT1" lane="34976568#1_0" startPos="205" endPos="220" lines="401"/>
    <busStop id="EDRG1" lane="35043629#1_0" startPos="120" endPos="135" lines="401"/>
    <busStop id="CRJ1" lane="-35168581#1_0" startPos="120" endPos="135" lines="401"/>
    <busStop id="PCRJ1" lane="35416640#2_0" startPos="210" endPos="225" lines="401"/>
    <busStop id="FSNT1" lane="-94481884_0" startPos="15" endPos="30" lines="401"/>
    <busStop id="ICAM2" lane="35443473#1_0" startPos="35" endPos="50" lines="401"/>
    <busStop id="MCAM2" lane="35443473#3_0" startPos="35" endPos="50" lines="401"/>
    <busStop id="BFAL2" lane="35443473#4_0" startPos="65" endPos="80" lines="401"/>
    <busStop id="FALC" lane="10384313#1_0" startPos="5" endPos="20" lines="401"/>
    <busStop id="CRT2" lane="95127168#0_0" startPos="65" endPos="80" lines="401"/>
    <busStop id="PREG" lane="14143474#5_0" startPos="15" endPos="30" lines="401"/>
    <busStop id="CPTO" lane="141435143#0_0" startPos="30" endPos="45" lines="401"/>
    <busStop id="PSG" lane="14143517#5_0" startPos="25" endPos="40" lines="401"/>
    <busStop id="VFNZ2" lane="141435176#9_0" startPos="100" endPos="115" lines="401"/>
    <busStop id="RCP2" lane="141435176#12_0" startPos="220" endPos="235" lines="401"/>
    <busStop id="SR3" lane="13799659#1_0" startPos="40" endPos="55" lines="401"/>
    <vType id="BUS" accel="1.5" decel="1.5" sigma="0.5" length="12" minGap="3" maxSpeed="17"
    color="1,1,0" guiShape="bus/city"/>

    <vehicle id="0" type="BUS" depart="0" color="1,1,0">
        <route edges="112465238 20672084#0 20672084#1 20672084#2 20672084#3 14328357#0
        14328357#1 14328357#2 14328611#1 36268629 13716336#0 13716336#1 13716336#2
        14328502#0 14328502#1 14328502#2 14328519#0 14328519#1 14328519#2 14328519#3
        14328519#4 14328519#5 14328519#6 14328519#7 14328519#8 14328519#9 14328519#10
        14328519#11 14328519#12 14328519#13 14328519#14 14328519#15 14328519#16 14328519#17
        159959892#0 159959892#1 159959892#2 159959892#3 159959892#4 159959892#5 159959892#6
        159959892#7 34976568#0 34976568#1 34976568#2 34976568#3 35043629#0 35043629#1
        35043629#2 35043631 -35168581#2 -35168581#1 103844310 35416640#2 35416640#3
        35416640#4 35416640#5 35416640#6 -94481884 -94481886 20560006i#0 -205599876
        -94481885 35443473#1 35443473#2 35443473#3 35443473#4 35443473#5 10384313#0
        10384313#1 95127163 95127168#0 95127168#1 95127168#2 95127168#3 161124046
        14143474#0 14143474#1 14143474#2 14143474#3 14143474#4 14143474#5 14143474#6
        141435143#0 141435143#1 141435176#4 141435176#5 141435176#6 141435176#7 141435176#8
        14143517#9 141435176#10 141435176#11 141435176#12 141435176#13 13799659#1"/>
        <stop busStop="BLAM2" duration="20"/>
        <stop busStop="SCAT1" duration="20"/>
        <stop busStop="PDR" duration="20"/>
        <stop busStop="C24A1" duration="20"/>
        <stop busStop="NAVE1" duration="20"/>
        <stop busStop="BL4" duration="20"/>
        <stop busStop="ESR1" duration="20"/>
        <stop busStop="SCRP5" duration="20"/>
        <stop busStop="MAV1" duration="20"/>
        <stop busStop="AANT3" duration="20"/>
        <stop busStop="DCVT1" duration="20"/>
        <stop busStop="EDRG1" duration="20"/>
        <stop busStop="CRJ1" duration="20"/>
        <stop busStop="PCRJ1" duration="20"/>
        <stop busStop="FSNT1" duration="20"/>
        <stop busStop="ICAM2" duration="20"/>
        <stop busStop="MCAM2" duration="20"/>
        <stop busStop="BFAL2" duration="20"/>
        <stop busStop="FALC" duration="20"/>
        <stop busStop="CRT2" duration="20"/>
        <stop busStop="PREG" duration="20"/>
        <stop busStop="CPTO" duration="20"/>
        <stop busStop="PSG" duration="20"/>
        <stop busStop="VFNZ2" duration="20"/>
        <stop busStop="RCP2" duration="20"/>
        <stop busStop="SR3" duration="20"/>
    </vehicle>
</additional>
```

Appendix G – Line 204 *buses.add.xml* file

```
<additional xmlns:xsi="http://www.w3.org/2001/XMLSchema-instance"
xsi:noNamespaceSchemaLocation="http://sumo.sf.net/xsd/additional_file.xsd">
    <busStop id="RFAR" lane="21271266#0_0" startPos="8" endPos="23" lines="204"/>
    <busStop id="DTTR" lane="3683604#0_0" startPos="60" endPos="75" lines="204"/>
    <busStop id="MF22" lane="-10505840#0_0" startPos="5" endPos="20" lines="204"/>
    <busStop id="UC2" lane="207634487#1_0" startPos="60" endPos="75" lines="204"/>
    <busStop id="PCL2" lane="207634487#7_0" startPos="10" endPos="25" lines="204"/>
    <busStop id="TRR4" lane="207634487#10_0" startPos="110" endPos="125" lines="204"/>
    <busStop id="PT2" lane="-207634512#1_0" startPos="25" endPos="40" lines="204"/>
    <busStop id="PG2" lane="-167487362#13_0" startPos="145" endPos="160" lines="204"/>
    <busStop id="PLUN2" lane="-167487362#2_0" startPos="15" endPos="30" lines="204"/>
    <busStop id="PLM2" lane="-167487362#0_0" startPos="15" endPos="30" lines="204"/>
    <busStop id="LRD2" lane="167487378_0" startPos="20" endPos="35" lines="204"/>
    <busStop id="JB2" lane="-128363658#7_0" startPos="20" endPos="35" lines="204"/>
    <busStop id="CART2" lane="-128363658#5_0" startPos="35" endPos="50" lines="204"/>
    <busStop id="PLNT2" lane="-128363658#2_0" startPos="20" endPos="35" lines="204"/>
    <busStop id="JM2" lane="-207634523#1_0" startPos="20" endPos="35" lines="204"/>
    <busStop id="PRG1" lane="207634492_0" startPos="60" endPos="75" lines="204"/>
    <busStop id="BS1" lane="128245297_0" startPos="120" endPos="135" lines="204"/>
    <busStop id="BCM2" lane="13714214_0" startPos="35" endPos="50" lines="204"/>
    <busStop id="GRC1" lane="21952796#5_0" startPos="85" endPos="100" lines="204"/>
    <busStop id="CVI4" lane="21952797#1_0" startPos="35" endPos="50" lines="204"/>
    <busStop id="NAT2" lane="-35475028_0" startPos="100" endPos="120" lines="204"/>
    <busStop id="BVLH3" lane="3960795#1_0" startPos="65" endPos="80" lines="204"/>
    <busStop id="SV92" lane="3960795#4_0" startPos="45" endPos="60" lines="204"/>
    <busStop id="VHM3" lane="3960795#10_0" startPos="25" endPos="40" lines="204"/>
    <busStop id="ACN1" lane="3656181#0_0" startPos="15" endPos="30" lines="204"/>
    <busStop id="FG3" lane="3656181#1_0" startPos="135" endPos="150" lines="204"/>
    <busStop id="CVLO2" lane="3091286#0_0" startPos="20" endPos="35" lines="204"/>
    <busStop id="BJ1" lane="3091286#2_0" startPos="20" endPos="35" lines="204"/>
    <busStop id="ACST2" lane="3091286#1_0" startPos="65" endPos="80" lines="204"/>
    <busStop id="AVC1" lane="3464474#0_0" startPos="60" endPos="75" lines="204"/>
    <busStop id="AUL1" lane="3462825#0_0" startPos="15" endPos="30" lines="204"/>
    <busStop id="SAL1" lane="3462825#5_0" startPos="5" endPos="20" lines="204"/>
    <busStop id="CUTE3" lane="206843931_0" startPos="115" endPos="130" lines="204"/>
    <busStop id="MLAR1" lane="3507850#3_0" startPos="10" endPos="25" lines="204"/>
    <busStop id="FEP2" lane="3514552#0_0" startPos="100" endPos="115" lines="204"/>
    <busStop id="FEUP1" lane="3514552#4_0" startPos="20" endPos="35" lines="204"/>
    <busStop id="ESED1" lane="3514552#4_0" startPos="310" endPos="325" lines="204"/>
    <busStop id="HSJ10" lane="212708425#3_0" startPos="15" endPos="30" lines="204"/>

    <vType id="BUS" accel="1.5" decel="1.5" sigma="0.5" length="12" minGap="3" maxSpeed="17"
    color="1,1,0" guiShape="bus/city"/>

    <vehicle id="0" type="BUS" depart="0" color="1,1,0">
        <route edges="21271266#0 212712662#1 212706764 -207719852 36836048#0 3683604#1
        35203145#0 35203145#1 35203138 207634506#0 207634506#1 -10505840#2 -10505840#1
        -10505840#0 207634502#0 207634502#1 207634487#0 207634487#1 207634487#2 207634487#3
        207634487#4 207634487#5 207634487#6 207634487#7 207634487#8 207634487#9 207634487#10
        207634487#11 207634486#0 207634486#1 -207634512#1 -207634512#0 -167487362#13
        -167487362#12 -167487362#11 -167487362#10 -167487362#9 -167487362#8 -167487362#7
        -167487362#6 -167487362#5 -167487362#4 -167487362#3 -167487362#2 -167487362#1
        -167487362#0 13799864 13800268#0 13800268#1 167487378 -128363658#8 -128363658#7
        -128363658#6 -128363658#5 -128363658#4 -128363658#3 -128363658#2 -128363658#1
        -128363658#0 128363659#0 128363659#1 128363659#2 128363659#3 -207634523#1
        -207634523#0 36836223 212706765 207634497#0 207634497#1 207634492 167487372#0
        167487372#1 167487372#2 167487370#0 167487370#1 128245298 128245297 189908449#0
        189908449#1 189908449#2 189908449#3 13714214 21952796#0 21952796#1 21952796#2
        21952796#3 21952796#4 21952796#5 209436199 21952797#0 21952797#1 21952797#2
        212706763 193149514 -35475028 3960795#0 3960795#1 3960795#2 3960795#3 3960795#4
        3960795#5 3960795#6 3960795#7 3960795#8 3960795#9 3960795#10 3960795#11
        39608490#0 39608490#1 3656181#0 3656181#1 212708374 3091286#0 3091286#1
        3091286#2 3091286#0 3091286#1 212708372 3464474#0 3464474#1 3464474#2
        3462825#0 3462825#1 3462825#2 3462825#3 3462825#4 3462825#5 3462825#6
        3462825#7 206843929 206843931 35078502 3507850#0 3507850#1 3507850#2 3507850#3
        3507850#4 3507850#5 3507850#6 3514552#0 3514552#1 3514552#2 3514552#3
        3514552#4 3514552#5 35997762 212708425#0 212708425#1 212708425#2 212708425#3"/>
```

```
        189908449#1 189908449#2 189908449#3 13714214 21952968#0 21952968#1 21952968#2
        21952968#3 21952968#4 21952968#5 209436199 21952970#0 21952970#1 21952970#2
        212706763 193149514 -35475028 3960795 6#0 3960795 6#1 3960795 6#2 3960795 6#3 3960795 6#4
        3960795 6#5 3960795 6#6 396079 56#7 3960795 6#8 3960795 6#9 3960795 6#10 3960795 6#11
        3960849 0#0 3960849 0#1 365618 16#0 365618 16#1 212708374 3091286 1#0 3091286 1#1
        3091286 1#2 3091286 7#0 3091286 7#1 212708372 34644746#0 34644746#1 34644746#2
        34628257#0 34628257#1 34628257#2 34628257#3 34628257#4 34628257#5 34628257#6
        34628257#7 206843929 206843931 35078502 35078501#0 35078501#1 35078501#2 35078501#3
        35078501#4 35078501#5 35078501#6 35145521#0 35145521#1 35145521#2 35145521#3
        35145521#4 35145521#5 35997762 212708425#0 212708425#1 212708425#2 212708425#3"/>
        <stop busStop="RFAR" duration="20"/>
        <stop busStop="DTTR" duration="20"/>
        <stop busStop="MFZ2" duration="20"/>
        <stop busStop="UC2" duration="20"/>
        <stop busStop="PCL2" duration="20"/>
        <stop busStop="TRR4" duration="20"/>
        <stop busStop="PT2" duration="20"/>
        <stop busStop="PG2" duration="20"/>
        <stop busStop="PLUN2" duration="20"/>
        <stop busStop="PLM2" duration="20"/>
        <stop busStop="LRD2" duration="20"/>
        <stop busStop="JB2" duration="20"/>
        <stop busStop="CART2" duration="20"/>
        <stop busStop="PLNT2" duration="20"/>
        <stop busStop="JM2" duration="20"/>
        <stop busStop="PRG1" duration="20"/>
        <stop busStop="BS1" duration="20"/>
        <stop busStop="BCM2" duration="20"/>
        <stop busStop="GRC1" duration="20"/>
        <stop busStop="CVI4" duration="20"/>
        <stop busStop="NAT2" duration="20"/>
        <stop busStop="BVLH3" duration="20"/>
        <stop busStop="SVP2" duration="20"/>
        <stop busStop="VFM3" duration="20"/>
        <stop busStop="ACN1" duration="20"/>
        <stop busStop="FG3" duration="20"/>
        <stop busStop="CVLO2" duration="20"/>
        <stop busStop="BJ1" duration="20"/>
        <stop busStop="ACST2" duration="20"/>
        <stop busStop="AVC1" duration="20"/>
        <stop busStop="AUL1" duration="20"/>
        <stop busStop="SAL1" duration="20"/>
        <stop busStop="OUTE3" duration="20"/>
        <stop busStop="MLAR1" duration="20"/>
        <stop busStop="FEP2" duration="20"/>
        <stop busStop="FEUP1" duration="20"/>
        <stop busStop="ESED1" duration="20"/>
        <stop busStop="ESJ10" duration="20"/>
    </vehicle>
</additional>
```

Appendix H – Line 602 *buses.add.xml* file

```
<additional xmlns:xsi="http://www.w3.org/2001/XMLSchema-instance"
xsi:noNamespaceSchemaLocation="http://sumo.sf.net/xsd/additional_file.xsd">
    <busStop id="CORD1" lane="14326487#1_0" startPos="56" endPos="70" lines="602"/>
    <busStop id="CMO" lane="3468379#2_0" startPos="28" endPos="40" lines="602"/>
    <busStop id="HSA3" lane="14326733#2_0" startPos="25" endPos="40" lines="602"/>
    <busStop id="MATR1" lane="836705$2_0" startPos="70" endPos="85" lines="602"/>
    <busStop id="TRH1" lane="3468315#0_0" startPos="87" endPos="103" lines="602"/>
    <busStop id="CVA2" lane="128246659_0" startPos="6" endPos="16" lines="602"/>
    <busStop id="CMIC1" lane="128133836_0" startPos="170" endPos="192" lines="602"/>
    <busStop id="CZV1" lane="3965434$5_0" startPos="16" endPos="26" lines="602"/>
    <busStop id="CVI1" lane="3965409#0_0" startPos="115" endPos="130" lines="602"/>
    <busStop id="HPRT1" lane="13715015#1_0" startPos="38" endPos="52" lines="602"/>
    <busStop id="CI21" lane="1371484$2_0" startPos="90" endPos="103" lines="602"/>
    <busStop id="PPR1" lane="1371484$4_0" startPos="191" endPos="202" lines="602"/>
    <busStop id="SRPT" lane="1371484$8_0" startPos="112" endPos="125" lines="602"/>
    <busStop id="MTB3" lane="2700984#3_0" startPos="55" endPos="66" lines="602"/>
    <busStop id="CSXB1" lane="2700984#5_0" startPos="30" endPos="45" lines="602"/>
    <busStop id="FGT1" lane="2700984#6_0" startPos="201" endPos="215" lines="602"/>
    <busStop id="CSXN1" lane="2700984#7_0" startPos="95" endPos="106" lines="602"/>
    <busStop id="PLG1" lane="2700984#11_0" startPos="40" endPos="58" lines="602"/>
    <busStop id="VFK1" lane="2700984#14_0" startPos="107" endPos="127" lines="602"/>
    <busStop id="FAP1" lane="2700984#14_0" startPos="434" endPos="444" lines="602"/>
    <busStop id="RSUL1" lane="2700984#16_0" startPos="161" endPos="171" lines="602"/>
    <busStop id="RBX1" lane="2700984#17_0" startPos="125" endPos="135" lines="602"/>
    <busStop id="RNOR1" lane="2700984#17_0" startPos="372" endPos="382" lines="602"/>
    <busStop id="GSUL1" lane="35917687#1_0" startPos="75" endPos="90" lines="602"/>
    <busStop id="EVLB1" lane="35917687#2_0" startPos="285" endPos="300" lines="602"/>
    <busStop id="GNOR1" lane="160766782_0" startPos="335" endPos="350" lines="602"/>
    <busStop id="REAR1" lane="160766782_0" startPos="575" endPos="590" lines="602"/>
    <busStop id="ARJ1" lane="160765782_0" startPos="575" endPos="590" lines="602"/>
    <busStop id="PTH1" lane="160773753#3_0" startPos="195" endPos="210" lines="602"/>
    <busStop id="CTIO1" lane="160773753#4_0" startPos="300" endPos="315" lines="602"/>
    <busStop id="MNSO1" lane="160773753#4_0" startPos="500" endPos="515" lines="602"/>
    <busStop id="MGDE1" lane="160773753#4_0" startPos="970" endPos="985" lines="602"/>
    <busStop id="STL1" lane="160773753#5_0" startPos="465" endPos="480" lines="602"/>
    <busStop id="PTM1" lane="160773753#5_0" startPos="585" endPos="600" lines="602"/>
    <busStop id="RL1" lane="41116145#1_0" startPos="2" endPos="12" lines="602"/>
    <busStop id="QTM1" lane="41116145#3_0" startPos="35" endPos="50" lines="602"/>
    <busStop id="RAL3" lane="168970793#0_0" startPos="10" endPos="25" lines="602"/>
    <busStop id="PDM3" lane="168970793#3_0" startPos="40" endPos="55" lines="602"/>
    <busStop id="MMAI2" lane="168970794#2_0" startPos="50" endPos="65" lines="602"/>
    <busStop id="VIVA1" lane="168970794#2_0" startPos="375" endPos="390" lines="602"/>
    <busStop id="GUD1" lane="2560648#3_0" startPos="20" endPos="35" lines="602"/>
    <busStop id="CZG1" lane="2560648#3_0" startPos="330" endPos="345" lines="602"/>
    <busStop id="R51" lane="51228957#0_0" startPos="65" endPos="80" lines="602"/>
    <busStop id="R7N1" lane="51228957#1_0" startPos="25" endPos="40" lines="602"/>
    <busStop id="R15" lane="51228957#6_0" startPos="40" endPos="55" lines="602"/>
    <busStop id="R1" lane="4063524$4_0" startPos="40" endPos="55" lines="602"/>
    <busStop id="R10" lane="4063524$6_0" startPos="60" endPos="75" lines="602"/>
    <busStop id="R7P1" lane="4063524$9_0" startPos="10" endPos="25" lines="602"/>
    <busStop id="CDR1" lane="4063524$10_0" startPos="145" endPos="160" lines="602"/>
    <busStop id="PRUE1" lane="2560648$11_0" startPos="105" endPos="120" lines="602"/>
    <busStop id="DACH1" lane="2560648$17_0" startPos="30" endPos="45" lines="602"/>
    <busStop id="FRA1" lane="2152306$2_0" startPos="5" endPos="15" lines="602"/>
    <busStop id="PRU3" lane="9972210$1_0" startPos="170" endPos="185" lines="602"/>
    <busStop id="AEPT1" lane="163123398#1_0" startPos="250" endPos="265" lines="602"/>
    <vType id="BUS" accel="1.7" decel="1.7" sigma="0.5" length="12" minGap="3" maxSpeed="17"
    color="1,1,0" guiShape="bus/city"/>

    <vehicle id="0" type="BUS" depart="0" color="1,1,0">
        <route edges="14326487#1 21530197#0 21530197#1 21696809#0 21696809#1 3468379#0
        3468379#1 3468379#2 3468379#3 3468379#4 3468379#5 28193881 14326733#0
        14326733#1 14326733#2 218021069 836705$0 836705$1 836705$2 8367073 3468315#0
        3468315#1 128246659 128246660#0 128246660#1 128133836 3965434$0 3965434$1
        3965434$2 3965434$3 3965434$4 3965434$5 3965434$6 3965434$7 3965434$8
        3965434$9 3965409#0 3965409#1 1371501$0 1371501$1 1371484$0 1371484$1
        1371484$2 1371484$3 1371484$4 1371484$5 1371484$6 1371484$7 1371484$8
        1371484$9 1371484$10 2700984#0 2700984#1 2700984#2 2700984#3 2700984#4
        2700984#5 2700984#6 2700984#7 2700984#8 2700984#9 2700984#10 2700984#11
        2700984#12 2700984#13 2700984#14 2700984#15 2700984#16 2700984#17 2700984#18
        2700984#19 168970837 35917687#0 35917687#1 35917687#2 35917687#3 160766782
        160766784 160773753#0 160773753#1 160773753#2 160773753#3 160773753#4 160773753#5
        160773753#6 40861125 160773750 41116145#0 41116145#1 41116145#2 41116145#3
        41116145#4 41116145#5 41116143 30323572#0 168970804#1 168970800 168970801 26719817#2
        26719817#3 168970791 168970793#0 168970793#1 168970793#2 168970793#3 168970793#4
        168970792 168970794#0 168970794#1 168970794#2 215230645#1 168970788#0 168970788#1
        2560648#0 2560648#1 2560648#2 2560648#3 2560648#4 51228957#0 51228957#1
        51228957#2 51228957#3 51228957#4 51228957#5 51228957#6 51228957#7 4063524$4" />
```

```
            406352488#5 406352488#6 406352488#7 406352488#8 406352488#9 406352488#10 25606487#11
            25606487#12 25606487#13 25606487#14 25606487#15 25606487#16 25606487#17 25606487#18
            25606487#19 25606487#20 215230642#0 215230642#1 215230642#2 215230642#3 215230642#4
            99722109#0 99722109#1 25606442#1 25606442#2 25606442#3 25606442#4 25606442#5
            26310260#0 26310260#1 26310260#2 26310260#3 163123398#0 163123398#1"/>
            <stop busStop="COORD1" duration="20"/>
            <stop busStop="CMO" duration="20"/>
            <stop busStop="HHA3" duration="20"/>
            <stop busStop="MATR1" duration="20"/>
            <stop busStop="TRH1" duration="20"/>
            <stop busStop="CVA2" duration="20"/>
            <stop busStop="CMIC1" duration="20"/>
            <stop busStop="CEV1" duration="20"/>
            <stop busStop="CVI1" duration="20"/>
            <stop busStop="HPRT1" duration="20"/>
            <stop busStop="CI21" duration="20"/>
            <stop busStop="PPR1" duration="20"/>
            <stop busStop="SRPT" duration="20"/>
            <stop busStop="MTB3" duration="20"/>
            <stop busStop="CSXS1" duration="20"/>
            <stop busStop="PGT1" duration="20"/>
            <stop busStop="CSXN1" duration="20"/>
            <stop busStop="PLG1" duration="20"/>
            <stop busStop="VFR1" duration="20"/>
            <stop busStop="FAP1" duration="20"/>
            <stop busStop="RSULI" duration="20"/>
            <stop busStop="RBX1" duration="20"/>
            <stop busStop="RNOR1" duration="20"/>
            <stop busStop="GSULI" duration="20"/>
            <stop busStop="BVLB1" duration="20"/>
            <stop busStop="GNOR1" duration="20"/>
            <stop busStop="REAR1" duration="20"/>
            <stop busStop="ARJ1" duration="20"/>
            <stop busStop="PTH1" duration="20"/>
            <stop busStop="CTIO1" duration="20"/>
            <stop busStop="MNSO1" duration="20"/>
            <stop busStop="MGDE1" duration="20"/>
            <stop busStop="STL1" duration="20"/>
            <stop busStop="PTM1" duration="20"/>
            <stop busStop="RL1" duration="20"/>
            <stop busStop="QTM1" duration="20"/>
            <stop busStop="RAL3" duration="20"/>
            <stop busStop="PDM3" duration="20"/>
            <stop busStop="MMAI2" duration="20"/>
            <stop busStop="VIVA1" duration="20"/>
            <stop busStop="GUD1" duration="20"/>
            <stop busStop="CZG1" duration="20"/>
            <stop busStop="R51" duration="20"/>
            <stop busStop="R7N1" duration="20"/>
            <stop busStop="R15" duration="20"/>
            <stop busStop="R1" duration="20"/>
            <stop busStop="R10" duration="20"/>
            <stop busStop="R7P1" duration="20"/>
            <stop busStop="CDR1" duration="20"/>
            <stop busStop="PRUE1" duration="20"/>
            <stop busStop="DACM1" duration="20"/>
            <stop busStop="FRA1" duration="20"/>
            <stop busStop="PRU3" duration="20"/>
            <stop busStop="AEPT1" duration="20"/>

    </vehicle>
</additional>
```

Appendix I – Diamond Ring *buses.add_ring_west.*xml file

```
<additional xmlns:xsi="http://www.w3.org/2001/XMLSchema-instance"
xsi:noNamespaceSchemaLocation="http://sumo.sf.net/xsd/additional_file.xsd">
    <busStop id="Dudley Common" lane="-8636702#8_0" startPos="15" endPos="30" lines="BRT"/>
    <busStop id="Dudley Station" lane="8651092#1_0" startPos="25" endPos="40" lines="BRT"/>
    <busStop id="Ruggles" lane="88625310_0" startPos="10" endPos="25" lines="BRT"/>
    <busStop id="MFA" lane="-8639965#1_0" startPos="110" endPos="125" lines="BRT"/>
    <busStop id="LMA" lane="-8732587O#0_0" startPos="10" endPos="25" lines="BRT"/>
    <busStop id="Yawkey/Fenway" lane="-90757431#1_0" startPos="75" endPos="90" lines="BRT"/>
    <busStop id="BU Central" lane="240745677#10_0" startPos="40" endPos="55" lines="BRT"/>
    <busStop id="BU West" lane="8646654#1_0" startPos="50" endPos="65" lines="BRT"/>
    <busStop id="Cambridgeport" lane="-90758563#3_0" startPos="10" endPos="25" lines="BRT"/>
    <busStop id="Mass Ave" lane="138749269#16_0" startPos="10" endPos="25" lines="BRT"/>
    <busStop id="Kendal" lane="23945793S#4_0" startPos="25" endPos="40" lines="BRT"/>
    <busStop id="Binney St" lane="28632018#4_0" startPos="80" endPos="95" lines="BRT"/>
    <busStop id="First St Galleria" lane="138749249#5_0" startPos="25" endPos="40" lines=
    "BRT"/>
    <busStop id="Lechemere" lane="138749249#12_0" startPos="35" endPos="50" lines="BRT"/>
    <busStop id="Inner Belt" lane="82329810#7_0" startPos="35" endPos="50" lines="BRT"/>
    <busStop id="Sullivan Square" lane="51811519#1_0" startPos="30" endPos="45" lines="BRT"/>
    <busStop id="Assembly Square" lane="942908S#2_0" startPos="20" endPos="35" lines="BRT"/>

    <vType id="BUS" accel="0.7" decel="1.0" sigma="0.5" length="12" minGap="3" maxSpeed="17"
    color="1,1,0" guiShape="bus"/>

    <vehicle id="163507" type="BUS" depart="0" color="1,1,0">
        <route edges="-8636702#8 -8636702#7 -8636702#6 -8636702#5 -8636702#4 -8636702#3
        -8636702#2 -8636702#1 -8636702#0 8651092#0 8651092#1 8648388#2 11688490O#5
        11688490O#6 11688490O#7 11688490O#8 11688490O#9 -779118 11688490l#0 11688490l#1
        11688490l#2 88299077 -8639115#2 -8639115#1 -8639115#0 8639374#2 88625310 8639184
        8639372#1 8639372#2 -8639965#8 -8639965#7 -8639965#6 -8639965#5 -8639965#4
        -8639965#3 -8639965#2 -8639965#1 -8639965#0 -8647969#5 -8647969#4 -8647969#3
        -8647969#2 -8647969#1 -8647969#0 -8732587O#2 -8732587O#1 -8732587O#0 8638023#0
        8638023#1 8638023#2 8638023#3 8651961#3 8651961#4 8643835#15 8643835#16 8643835#17
        8643835#18 8643835#19 8649816#0 8649816#2 8649816#3 -90757431#1 -90757431#0
        8642453#0 8642453#1 8651294#0 8651294#1 41743615#0 41743615#1 -48917526 -93120171
        -43100845 -48917525 -8814884 240745677#9 240745677#10 8648572 196203198#0
        196203198#1 196203198#2 196203198#3 196203219 8646654#0 8646654#1 8648038#2 8647165
        -779096 -34951026#2 -34951026#1 -34951026#0 -44234973 150052472 150052475 -89881955
        -89881954 -90758563#4 -90758563#3 -90758563#2 -90758563#1 -90758563#0 -90758565
        -779098 138749269#16 23945793S#0 23945793S#2 23945793S#3 23945793S#4 -779074 -779072
        -779070 8615409#1 8615409#2 8615409#4 8615409#5 28632018#4 28632018#5 138749249#1
        138749249#2 138749249#3 138749249#4 138749249#5 138749249#6 138749249#7 138749249#8
        138749249#9 138749249#10 138749249#11 138749249#12 33795680#30 33795680#31
        33795680#32 139184291#0 139184291#1 8604813#1 8604813#2 8615774 -779116 942907O#3
        942982S#0 942982S#1 942982S#2 82329825 82329819 82329823 82329810#0 82329810#1
        82329810#2 82329810#3 82329810#6 82329810#7 8605205#12 8605205#13 8651189#0
        8651189#2 8651189#3 8651189#4 82332100 51811519#0 51811519#1 80676218 8646720#6
        138525020#2 80676225 8651331 138525022 132174875 132174849 132174879 80676224
        51811524 95843690 8647620#0 8647620#1 8647620#2 8647620#3 82332101 51811523#0
        942936S#1 216374586 942908S#0 942908S#1 942908S#2 942908S#3"/>
        <stop busStop="Dudley Common" duration="120"/>
        <stop busStop="Dudley Station" duration="60"/>
        <stop busStop="Ruggles" duration="120"/>
        <stop busStop="MFA" duration="60"/>
        <stop busStop="LMA" duration="15"/>
        <stop busStop="Yawkey/Fenway" duration="60"/>
        <stop busStop="BU Central" duration="15"/>
        <stop busStop="BU West" duration="15"/>
        <stop busStop="Cambridgeport" duration="15"/>
        <stop busStop="Mass Ave" duration="15"/>
        <stop busStop="Kendal" duration="60"/>
        <stop busStop="Binney St" duration="15"/>
        <stop busStop="First St Galleria" duration="15"/>
        <stop busStop="Lechemere" duration="60"/>
        <stop busStop="Inner Belt" duration="15"/>
        <stop busStop="Sullivan Square" duration="60"/>
        <stop busStop="Assembly Square" duration="60"/>
    </vehicle>
```

Appendix J – Urban Ring *buses.add_ring_east.xml* file

```
<additional xmlns:xsi="http://www.w3.org/2001/XMLSchema-instance"
xsi:noNamespaceSchemaLocation="http://sumo.sf.net/xsd/additional_file.xsd">
    <busStop id="Assembly Square" lane="942908#2_0" startPos="20" endPos="35" lines="BRT"/>
    <busStop id="Wellington" lane="903908$4_0" startPos="30" endPos="45" lines="BRT"/>
    <busStop id="Everet" lane="-779094_0" startPos="715" endPos="730" lines="BRT"/>
    <busStop id="Mystic Mall" lane="93276296_0" startPos="650" endPos="665" lines="BRT"/>
    <busStop id="Chelsea" lane="-779088_0" startPos="165" endPos="180" lines="BRT"/>
    <busStop id="Griffin Way" lane="8617228_0" startPos="300" endPos="315" lines="BRT"/>
    <busStop id="Airport Blue Line" lane="-196932477#1_0" startPos="25" endPos="40" lines=
    "BRT"/>
    <busStop id="World Trade Center" lane="236579256#0_0" startPos="15" endPos="30" lines=
    "BRT"/>
    <busStop id="JFK/Umass" lane="215752970#1_0" startPos="15" endPos="30" lines="BRT"/>
    <busStop id="Thomas J. Kane Sq." lane="-8644673#0_0" startPos="80" endPos="95" lines=
    "BRT"/>
    <busStop id="Newmarket" lane="8650867#10_0" startPos="5" endPos="20" lines="BRT"/>
    <busStop id="Dudley Common" lane="-8636702#8_0" startPos="15" endPos="30" lines="BRT"/>

    <vType id="BUS" accel="0.7" decel="1.0" sigma="0.5" length="12" minGap="3" maxSpeed="17"
    color="0,0,1" guiShape="bus"/>

    <vehicle id="163537" type="BUS" depart="0" color="0,0,1">
        <route edges="942908#2 942908#3 942908#4 44142848 -9330582#1 90205634 437918 6#7
        9038805 85327578 216555896#0 216555896#3 85173088#0 85173088#1 9038956 9038628#1
        903862 8#2 903862 8#3 903862 8#4 48807694 48807696 48807692#0 9038241 9330650 2#0
        9330650 2#1 9039085#0 9039085#1 9039085#2 9039085#3 9039085#4 9039085#5 9039085#6
        9038242#0 9038242#1 93306502#1 93306502#2 85107228#0 85107228#1 85107237 --779114
        --779112 --779110 --779090 --779108 --779106 --779094 --779092 --779104 --779102
        -779100 50526448 50526447#0 50526447#1 93276296 -779128 -779088 -779086 8617228
        -861719 1#3 -861719 1#2 -861719 1#1 -861719 1#0 861724 1#0 861724 1#1 -195779437
        -93276300#15 --779078 -779076#0 -779076#1 --779080 -8648069#2 -8648069#1 -864806 9#0
        8648225#0 8648225#1 8648225#2 19640118 7#0 19640118 7#1 -196932477#1 -8648723#1
        -8648723#0 8646235 52093580 -196537067 8652549 236579304 236579311 236579306 8646004
        8651364 8651350 8640564 8647303 8650546#0 8650546#1 236579256#0 236579256#1
        236579256#2 51812124#0 51812124#1 -8648759 -48983955 -48983956 -8651083 -865226 9#1
        -865226 9#0 -8650396 -28615812#1 -28615812#0 864796 4#2 -28615836#5 -28615836#4
        -28615836#3 -28615836#2 -28615836#1 -28615836#0 28640407#4 28640407#5 2864040 7#6
        -864217 4#4 -864217 4#3 -864217 4#2 -864217 4#1 -864217 4#0 -864967 8#16 -864967 8#15
        -8649678#14 -8649678#12 -8649678#11 -8649678#10 -8649678#9 -8649678#8 -8649678#7
        8648389#7 8648389#9 8648215#1 8645270#0 8645270#1 8645270#2 8645270#3 8645270#4
        216275097#0 216275097#1 216275097#2 865156 1#2 8641809 215752970#1 865169 0#1
        865169 0#2 865169 0#3 865169 0#4 865169 0#5 -8644673#2 -8644673#1 -8644673#0 865086 7#0
        865086 7#2 865086 7#3 865086 7#7 865086 7#9 865086 7#10 865086 7#12 865086 7#13 865086 7#14
        -865220 7#9 -865220 7#8 -865220 7#7 -865220 7#6 -865220 7#5 -865220 7#4 -865220 7#3
        -865220 7#2 -865220 7#1 -8636702#12 -8636702#11 8649341 -8636702#8"/>
        <stop busStop="Assembly Square" duration="15"/>
        <stop busStop="Wellington" duration="15"/>
        <stop busStop="Everet" duration="15"/>
        <stop busStop="Mystic Mall" duration="15"/>
        <stop busStop="Chelsea" duration="60"/>
        <stop busStop="Griffin Way" duration="15"/>
        <stop busStop="Airport Blue Line" duration="60"/>
        <stop busStop="World Trade Center" duration="60"/>
        <stop busStop="JFK/Umass" duration="120"/>
        <stop busStop="Thomas J. Kane Sq." duration="15"/>
        <stop busStop="Newmarket" duration="60"/>
        <stop busStop="Dudley Common" duration="15"/>
    </vehicle>
```

Appendix K – SL6 *buses.add_sl6.xml* file

```
<additional xmlns:xsi="http://www.w3.org/2001/XMLSchema-instance"
xsi:noNamespaceSchemaLocation="http://sumo.sf.net/xsd/additional_file.xsd">
    <busStop id="Chelsea" lane="-779088_0" startPos="165" endPos="180" lines="BRT"/>
    <busStop id="Griffin Way" lane="8617228_0" startPos="300" endPos="315" lines="BRT"/>
    <busStop id="Airport Blue Line" lane="-196932477#1_0" startPos="25" endPos="40" lines=
    "BRT"/>
    <busStop id="Silver Line Way" lane="8640564_0" startPos="165" endPos="180" lines="BRT"/>
    <busStop id="World Trade Center" lane="-8649529_0" startPos="15" endPos="30" lines="BRT"/>
    <busStop id="Courthouse" lane="-8652555#0_0" startPos="230" endPos="245" lines="BRT"/>
    <busStop id="South Station" lane="187589422#0_0" startPos="20" endPos="35" lines="BRT"/>

    <vType id="BUS" accel="0.7" decel="1.0" sigma="0.5" length="12" minGap="3" maxSpeed="17"
    color="1,1,0" guiShape="bus"/>

    <vehicle id="163567" type="BUS" depart="0" color="1,1,0">
        <route edges="-779088 -779086 8617228 -8617191#3 -8617191#2 -8617191#1 -8617191#0
        8617241#0 8617241#1 -195779437 -93276300#15 --779078 -779076#0 -779076#1 --779080
        -8648069#2 -8648069#1 -8648069#0 8648225#0 8648225#1 8648225#2 19640118 7#0
        19640118 7#1 -196932477#1 -8648723#1 -8648723#0 8646235 52093580 -196537067 8652549
        236579304 236579311 236579306 8646004 8651364 8651350 8640564 8647303 8650546#0
        8650483#0 -8649529 -8650370#0 -8644890 -8652555#1 -8652555#0 -85891007 -85891024
        -85890979 -48982055#1 -48982055#0 8642027 8640122#0 8640122#1 8640122#2 8638390#0
        8638390#1 8638390#2 187589422#0"/>
        <stop busStop="Chelsea" duration="60"/>
        <stop busStop="Griffin Way" duration="120"/>
        <stop busStop="Airport Blue Line" duration="15"/>
        <stop busStop="Silver Line Way" duration="15"/>
        <stop busStop="World Trade Center" duration="15"/>
        <stop busStop="Courthouse" duration="15"/>
        <stop busStop="South Station" duration="15"/>
    </vehicle>
```